LI
LABORATORY INVESTIGATION
THE BASIC AND TRANSLATIONAL PATHOLOGY RESEARCH JOURNAL
VOLUME 100 | SUPPLEMENT 1 | MARCH 2020

# ABSTRACTS

## GENITOURINARY PATHOLOGY (860-1046)

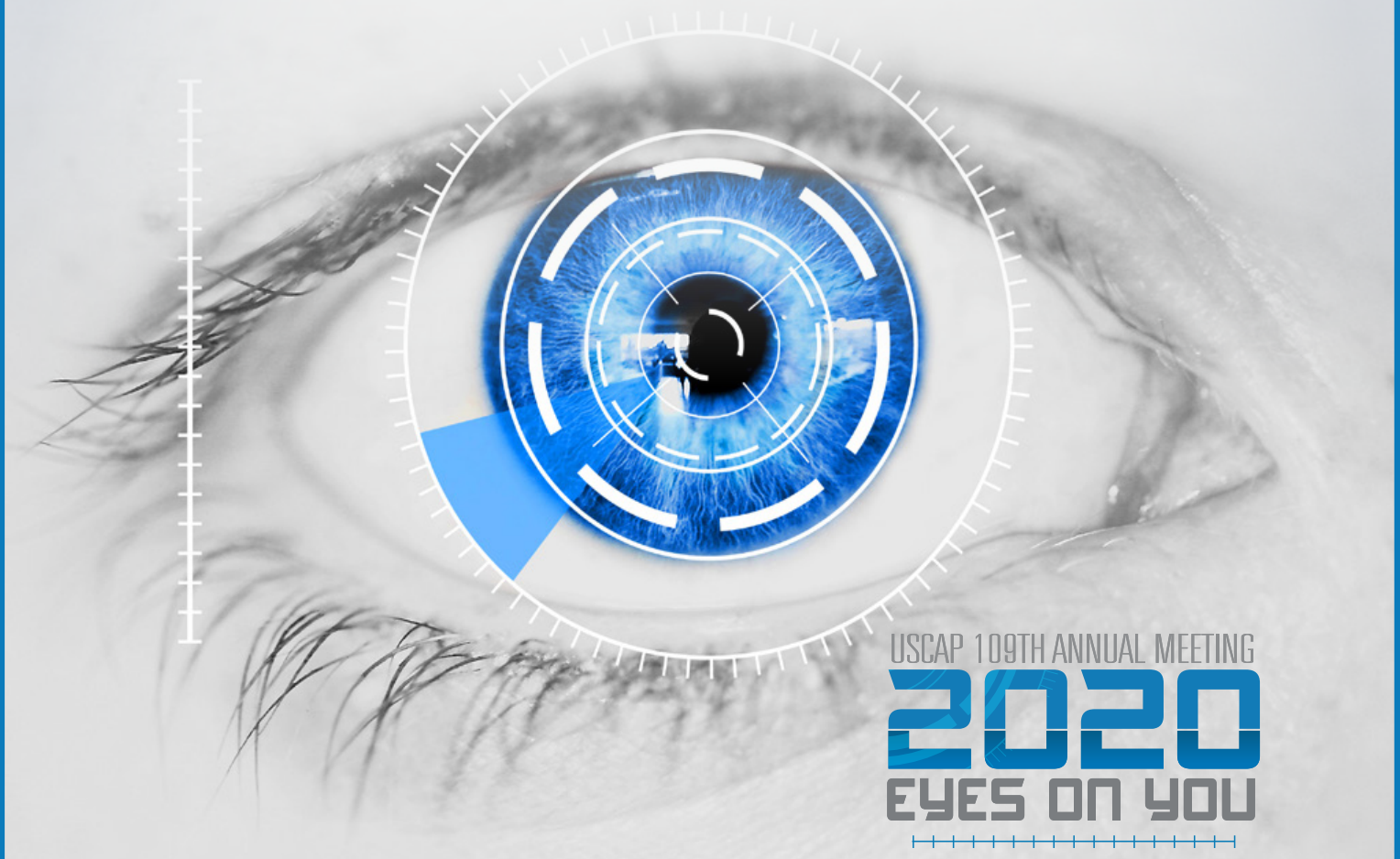


FEBRUARY 29-MARCH 5, 2020

LOS ANGELES CONVENTION CENTER
LOS ANGELES, CALIFORNIA

Published by
SPRINGER NATURE
www.ModernPathology.org

USCAP Creating a Better Pathologist
AN OFFICIAL JOURNAL OF THE UNITED STATES AND CANADIAN ACADEMY OF PATHOLOGY

## EDUCATION COMMITTEE

**Jason L. Hornick**, Chair

**Rhonda K. Yantiss,** Chair, Abstract Review Board and Assignment Committee

**Laura W. Lamps**, Chair, CME Subcommittee

**Steven D. Billings**, Interactive Microscopy Subcommittee

**Raja R. Seethala**, Short Course Coordinator

**Ilan Weinreb**, Subcommittee for Unique Live Course Offerings

**David B. Kaminsky** (Ex-Officio)

**Zubair Baloch**
**Daniel Brat**
**Ashley M. Cimino-Mathews**
**James R. Cook**
**Sarah Dry**
**William C. Faquin**
**Yuri Fedoriw**
**Karen Fritchie**
**Lakshmi Priya Kunju**
**Anna Marie Mulligan**
**Rish K. Pai**
**David Papke,** Pathologist-in-Training
**Vinita Parkash**
**Carlos Parra-Herran**
**Anil V. Parwani**
**Rajiv M. Patel**
**Deepa T. Patil**
**Lynette M. Sholl**
**Nicholas A. Zoumberos,** Pathologist-in-Training

## ABSTRACT REVIEW BOARD

**Benjamin Adam**
**Narasimhan Agaram**
**Rouba Ali-Fehmi**
**Ghassan Allo**
**Isabel Alvarado-Cabrero**
**Catalina Amador**
**Roberto Barrios**
**Rohit Bhargava**
**Jennifer Boland**
**Alain Borczuk**
**Elena Brachtel**
**Marilyn Bui**
**Eric Burks**
**Shelley Caltharp**
**Barbara Centeno**
**Joanna Chan**
**Jennifer Chapman**
**Hui Chen**
**Beth Clark**
**James Conner**
**Alejandro Contreras**
**Claudiu Cotta**
**Jennifer Cotter**
**Sonika Dahiya**
**Farbod Darvishian**
**Jessica Davis**
**Heather Dawson**
**Elizabeth Demicco**
**Katie Dennis**
**Anand Dighe**
**Suzanne Dintzis**
**Michelle Downes**
**Andrew Evans**
**Michael Feely**
**Dennis Firchau**
**Gregory Fishbein**
**Andrew Folpe**
**Larissa Furtado**
**Billie Fyfe-Kirschner**
**Giovanna Giannico**
**Anthony Gill**
**Paula Ginter**
**Tamara Giorgadze**
**Purva Gopal**
**Anuradha Gopalan**
**Abha Goyal**
**Rondell Graham**
**Alejandro Gru**
**Nilesh Gupta**
**Mamta Gupta**
**Gillian Hale**
**Suntrea Hammer**
**Malini Harigopal**
**Douglas Hartman**
**John Higgins**
**Mai Hoang**
**Mojgan Hosseini**
**Aaron Huber**
**Peter Illei**
**Doina Ivan**
**Wei Jiang**
**Vickie Jo**
**Kirk Jones**
**Neerja Kambham**
**Chiah Sui Kao**
**Dipti Karamchandani**
**Darcy Kerr**
**Ashraf Khan**
**Francesca Khani**
**Rebecca King**
**Veronica Klepeis**
**Gregor Krings**
**Asangi Kumarapeli**
**Alvaro Laga**
**Steven Lagana**
**Keith Lai**
**Michael Lee**
**Cheng-Han Lee**
**Madelyn Lew**
**Zaibo Li**
**Faqian Li**
**Ying Li**
**Haiyan Liu**
**Xiuli Liu**
**Yen-Chun Liu**
**Lesley Lomo**
**Tamara Lotan**
**Anthony Magliocco**
**Kruti Maniar**
**Emily Mason**
**David McClintock**
**Bruce McManus**
**David Meredith**
**Anne Mills**
**Neda Moatamed**
**Sara Monaco**
**Atis Muehlenbachs**
**Bita Naini**
**Dianna Ng**
**Tony Ng**
**Michiya Nishino**
**Scott Owens**
**Jacqueline Parai**
**Yan Peng**
**Manju Prasad**
**Peter Pytel**
**Stephen Raab**
**Joseph Rabban**
**Stanley Radio**
**Emad Rakha**
**Preetha Ramalingam**
**Priya Rao**
**Robyn Reed**
**Michelle Reid**
**Natasha Rekhtman**
**Jordan Reynolds**
**Michael Rivera**
**Andres Roma**
**Avi Rosenberg**
**Esther Rossi**
**Peter Sadow**
**Steven Salvatore**
**Souzan Sanati**
**Anjali Saqi**
**Jeanne Shen**
**Jiaqi Shi**
**Gabriel Sica**
**Alexa Siddon**
**Deepika Sirohi**
**Kalliopi Siziopikou**
**Sara Szabo**
**Julie Teruya-Feldstein**
**Khin Thway**
**Rashmi Tondon**
**Jose Torrealba**
**Andrew Turk**
**Evi Vakiani**
**Christopher VandenBussche**
**Paul VanderLaan**
**Olga Weinberg**
**Sara Wobker**
**Shaofeng Yan**
**Anjana Yeldandi**
**Akihiko Yoshida**
**Gloria Young**
**Minghao Zhong**
**Yaolin Zhou**
**Hongfa Zhu**
**Debra Zynger**

To cite abstracts in this publication, please use the following format: **Author A, Author B, Author C, et al. Abstract title (abs#). In "File Title."** ***Laboratory Investigation*** **2020; 100 (suppl 1): page#**

## 860 De Novo Neuroendocrine Transdifferentiation in Primary Prostate Cancer - A Phenotype Associated with Advanced Clinico-Pathologic Features and Aggressive Outcome

Eman Abdulfatah[1], Zachery Reichert[2], Arul Chinnaiyan[3], Rahul Mannan[4], Xiaoming (Mindy) Wang[2], Sethuramasundaram Pitchiaya[4], Saravana Dhanasekaran[2], Chandan Kumar-Sinha[2], Jeffrey Montgomery[2], Alon Weizer[2], Brent Hollenbeck[2], Joshi Alumkal[2], Samuel Kaffenberger[2], Ganesh Palapattu[2], Matthew Davenport[2], Todd Morgan[2], Daniel Spratt[2], Aaron Udager[5], Rohit Mehra[2]

*[1]Grosse Pointe Farms, MI, [2]University of Michigan, Ann Arbor, MI, [3]Plymouth, MI, [4]Michigan Medicine, University of Michigan, Ann Arbor, MI, [5]University of Michigan Medical School, Ann Arbor, MI*

**Disclosures:** Eman Abdulfatah: None; Zachery Reichert: None; Arul Chinnaiyan: None; Rahul Mannan: None; Xiaoming (Mindy) Wang: None; Sethuramasundaram Pitchiaya: None; Saravana Dhanasekaran: None; Chandan Kumar-Sinha: None; Jeffrey Montgomery: None; Alon Weizer: None; Brent Hollenbeck: None; Joshi Alumkal: None; Samuel Kaffenberger: None; Ganesh Palapattu: None; Matthew Davenport: None; Todd Morgan: None; Daniel Spratt: None; Aaron Udager: None; Rohit Mehra: None

**Background:** Blocking androgen receptor is the main therapeutic target in advanced and metastatic prostate cancer (PCa). However, a subset of patients relapse and develop androgen-independent and aggressive forms of PCa. Androgen deprivation therapy (ADT) may induce transdifferentiation of PCa cells to neuroendocrine-like tumor cells resulting in resistance to therapy, disease progression and poor outcomes. While PCa neuroendocrine transdifferentiation(NETD) after ADT has been well described, NETD occurring in a de novo setting is understudied. Herein, we report a series of de novo NETD in untreated high-grade PCa.

**Design:** Treatment naïve patients with primary PCa with NETD between 2013-2019 were identified. H&E slides were reviewed by 2 GU pathologists to evaluate morphologic features. Cases with lack of conventional small cell carcinoma(SCC) features were included. IHC stains for PSA, NKX3.1, Chromogranin, Synaptophysin, Cyclin D1, RB1 and Ki67 were performed. Radiology, treatment and follow-up data were reviewed.

**Results:** Fourteen patients were included(9 biopsies, 3 transurethral resection, 2 prostatectomy). High-grade PCa with focal acinar features was identified, reminiscent of Gleason scores 9 or 10. Additionally, areas showed sheets of tumor cells with deep amphophilic/basophilic cytoplasm, enlarged hyperchromatic nuclei with granular chromatin and inconspicuous nucleoli with high mitotic activity. IHC showed the neoplastic cells to express patchy NKX3.1(8/14), Synaptophysin(7/14),Chromogranin(8/14) with negative PSA(10/14). RB1 showed loss of expression(8/14), cyclin D1 showed reduced expression(13/14) and Ki67 showed high-proliferative index(14/14). Adverse radiologic findings(extraprostatic extension and seminal vesicle invasion) were identified in most cases. Metastasis was documented in 5 patients. Two patients died of the disease. Treatment included ADT alone, ADT followed by docetaxel, carboplatin-based chemotherapy and radiation therapy. Both patients on ADT and 3 of 4 who received ADT followed by docetaxol showed undetectable PSA, while those who received carboplatin and etoposide showed progression.

**Conclusions:** PCa with NETD exhibit high-grade nuclei, lack of prominent nucleoli, high mitotic activity, reduced PSA expression with high Ki67 and functional inactivation of RB1 pathway, suggesting transdifferentiation from androgen-driven to more proliferative-driven phenotype. While the majority of these tumors are seen in patients with history of PCa post ADT, de novo cases can occur.

## 861 ALK Rearrangements are Highly Prevalent in Pseudosarcomatous Myofibroblastic Proliferations of the Urinary Bladder

Andres Acosta[1], Paola Dal Cin[2], Michelle Hirsch[2], Christopher Fletcher[2], Vickie Jo[1]

*[1]Brigham and Women's Hospital, Harvard Medical School, Boston, MA, [2]Brigham and Women's Hospital, Boston, MA*

**Disclosures:** Andres Acosta: None; Paola Dal Cin: None; Michelle Hirsch: None; Christopher Fletcher: None; Vickie Jo: *Employee*, Merck and Co

**Background:** Pseudosarcomatous myofibroblastic proliferation (PMP) is a descriptive term used to designate a group of genitourinary (mostly bladder) lesions of uncertain nosology. PMP is somewhat morphologically heterogenous, spanning a spectrum that includes post-operative spindle cell nodules and lesions showing morphologic overlap with inflammatory myofibroblastic tumors (IMT). The latter, however, show significant clinical and histologic differences with classic IMTs of soft tissue or other visceral sites. An inconsistent association with *ALK* rearrangement has been reported in PMPs, ranging from 0% to 60%. Furthermore, ROS expression has not been evaluated in PMPs. In this study, a systematic histopathologic review was conducted on 29 PMPs of the bladder, with ROS IHC and *ALK* FISH performed on a subset of cases.

**Design:** 29 PMPs with available FFPE whole-tissue sections were identified in consultation archives, all with known ALK IHC status. ROS IHC was performed using monoclonal rabbit antibodies (clone D4D6, Cell Signaling Technology (CST), Danvers, MA) and Signalstain boost IHC detection method (CST) after antigen retrieval at pH8 and 125°C for 30 seconds. FISH was performed using the LSI break-apart *ALK* probe (Abbot Molecular, Des Plaines, Illinois) following standard protocols.

**Results:** The study cohort included 19 men and 10 women, with median age 47 years (range 12-81). Microscopically, tumors showed variable degrees of cellularity and mitotic activity (median 4 mitoses/10 hpf, range 0-24). Infiltrative borders and foci of necrosis were frequent, seen in 48% (14/29) and 38% (11/29) of cases, respectively. By IHC, 20/29 (69%) cases were positive for ALK (3 focal, 17 diffuse or multifocal), 95% (18/19) positive for SMA, 97% (28/29) positive for desmin, and 72% (13/18) positive for keratins. ROS IHC was consistently negative (0/28). FISH performed on 20 PMPs that were ALK-positive by IHC detected *ALK* rearrangements in 90% (18/20) cases.

**Conclusions:** *ALK* rearrangements are frequent in PMPs, although not in all cases that were ALK-positive by IHC. These results suggest that a large subset of PMPs may be ALK-driven. Given the significant clinicopathologic differences between classic IMTs and PMPs, PMPs likely still warrant classification as a distinct clinicopathologic entity. Further molecular characterization of these cases is underway.

## 862 Langerhans Cell Histiocytosis Occurring in a Renal Cell Carcinoma is a Neoplastic Process: Clinicopathologic and Molecular Study of Five Cases

Abbas Agaimy[1], Michael Bonert[2], Asghar Naqvi[2], Chunjie Wang[3], Ondrej Hes[4], Kiril Trpkov[5], Ian Gibson[6], Arndt Hartmann[7]
*[1]Universitätsklinikum Erlangen, Germany, Erlangen, Germany, [2]McMaster University, Hamilton, ON, [3]Saskatoon City Hospital, Saskatoon, SK, [4]Biopticka laborator s.r.o., Plzen, Plzensky kraj, Czech Republic, [5]University of Calgary, Calgary, AB, [6]University of Manitoba, Winnipeg, AB, [7]Institut fur Pathologie, Erlangen, Germany*

**Disclosures:** Abbas Agaimy: None; Michael Bonert: None; Asghar Naqvi: None; Chunjie Wang: None; Ondrej Hes: None; Kiril Trpkov: None; Ian Gibson: None; Arndt Hartmann: None

**Background:** Langerhans cell histiocytosis (LCH) is a rare proliferative histiocytic disorder composed of Langerhans cells admixed with reactive mononuclear and granulocytic cells, with predominance of eosinophils. LCH is accepted as a neoplasm, driven in most cases by oncogenic RAS/RAF/MEK/ERK pathway mutations. Clinically, LCH may present as unifocal, multifocal-unisystemic, or multifocal-multisystemic disease. Children are most often affected, and adults and elderly are only rarely affected. Urinary system involvement is rare in multisystemic disease.

**Design:** We present five patients, who presented with LCH within an underlying clear cell (ccRCC; n=4) or clear cell papillary (ccPRCC; n=1) renal cell carcinoma (RCC). All patients were identified prospectively in our routine and consultation files from 2013 to 2018. In addition to the clinicopathological analysis, we examined microdissected LCH lesions for *BRAF* mutations using pyrosequencing and/or RT-PCR methods.

**Results:** The patients included three females and two males, with median age of 54 years (range: 39 to 73). None had a history of LCH or other LCH manifestations at time of RCC diagnosis. All tumors involved the left kidney, had a median size of 2.5 cm (range, 1.8-8.3) and were treated by partial (4), or radical (1) nephrectomy. The RCC showed at least focal gross cystic changes and were low-grade (WHO/ISUP grade 1-2). LCH foci were limited to only few high-power fields (< 2mm$^2$) in four cases and occupied almost the entire 2 cm RCC nodule in the ccPRCC case. No LCH manifestations were detected in the normal kidney or in perinephric fat. Immunohistochemistry confirmed the Langerhans cell phenotype by immunoreactivity for S-100, CD1a & langerin, and negative staining for pankeratin. Pyrosequencing and RT-PCR of microdissected LCH DNA revealed V600E *BRAF* mutation in all cases. Review of the literature was done and we found only three similar cases published since 1980; none was examined for *BRAF* mutation.

Figure 1 - 862

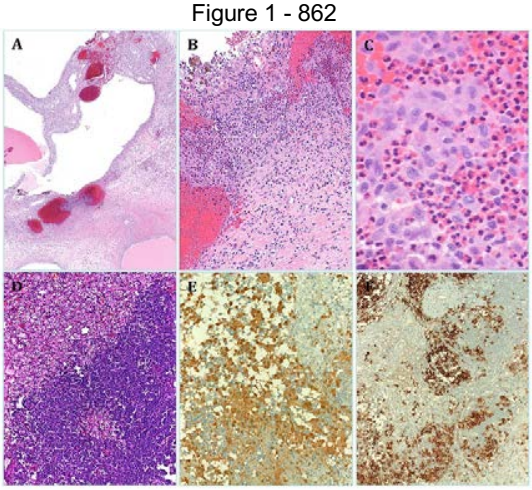


**A, B, C**: ccRCC with solid and cystic areas associated with multiple hemorrahgic LCH foci (note prominent eosinophils). **D**: This eosinophil-poor LCH focus closely mimicked high-grade transformation. Strong expression of S100 (**E**) and CD1a (**F**).

**Conclusions:** This is the first study that illustrates and analyzes the morphologic and genetic features of LCH within RCC. Identification of five cases in 5 years possibly suggests under-recognition of this condition. If unrecognized, LCH may erroneously lead in some RCC cases to a diagnosis of dedifferentiation or high-grade transformation. Finally, the detection of BRAF mutations confirms that LCH is indeed a neoplasm, and excludes the possibility that this is a reactive lesion.

## 863 Clear Cell Carcinoma of the Urethra: A Comprehensive Genomic Profiling Study

Talal Ahmad[1], Julia Elvin[2], Douglas Lin[2], James Corines[3], Jo-Anne Vergilio[2], Keith Killian[2], Erik Williams[4], Natalie Danziger[5], James Haberberger[6], Julie Tse[4], Shakti Ramkissoon[6], Eric Severson[6], Amanda Hemmerich[6], Naomi Lynn Ferguson[6], Claire Edgerly[6], Daniel Duncan[6], Richard Huang[7], Jon Chung[2], Russell Madison[2], Siraj Ali[8], Venkataprasanth Reddy[2], Kimberly McGregor[2], Jeffrey Ross[3]
*[1]Upstate Medical University, Liverpool, NY, [2]Foundation Medicine, Inc., Cambridge, MA, [3]Upstate Medical University, Syracuse, NY, [4]Boston, MA, [5]Foundation Medicine, Inc., Somerville, MA, [6]Foundation Medicine, Inc., Morrisville, NC, [7]Foundation Medicine, Inc., Cary, NC, [8]Cambridge, MA*

**Disclosures:** Talal Ahmad: None; Julia Elvin: *Employee*, Foundation Medicine, Inc; *Employee*, Hoffman La Roche; Douglas Lin: *Employee*, Foundation Medicine; James Corines: None; Jo-Anne Vergilio: *Employee*, Foundation Medicine, Inc; *Employee*, Foundation Medicine, Inc; Keith Killian: *Employee*, FMI; Erik Williams: *Stock Ownership*, F. HoffmanLa Roche, Ltd.; *Employee*, Foundation Medicine, Inc.; Natalie Danziger: *Employee*, Foundation Medicine Incorporated; James Haberberger: *Employee*, Foundation Medicine Inc.; Julie Tse: *Employee*, Foundation Medicine, Inc.; *Consultant*, Pathology Watch, LLC.; Shakti Ramkissoon: *Employee*, Foundation Medicine/Roche; Eric Severson: *Employee*, Foundation Medicine; Amanda Hemmerich: *Employee*, Foundation Medicine, Inc; Naomi Lynn Ferguson: *Employee*, Foundation Medicine; Claire Edgerly: *Employee*, Foundation Medicine, Inc.; Daniel Duncan: *Employee*, Foundation Medicine; Richard Huang: *Employee*, Roche/Foundation Medicine; Jon Chung: *Employee*, Foundation Medicine; *Stock Ownership*, Roche; Russell Madison: *Employee*, Foundation Medicine; *Stock Ownership*, Roche; Siraj Ali: *Employee*, Foundation Medicine; *Advisory Board Member*, Incysus therapeutics; *Consultant*, Takeda; Venkataprasanth Reddy: *Employee*, Foundation Medicine; Kimberly McGregor: *Employee*, Foundation Medicine; Jeffrey Ross: *Employee*, Foundation Medicine

**Background:** Clear cell carcinoma of the urethra (UCCC) is an uncommon malignancy predominantly occurring in women associated with a wide variety of clinical outcomes. The following study is the first comprehensive genomic profiling (CGP) evaluation of this rare tumor.

**Design:** Comprehensive genomic profiling (CGP) was performed on FFPE samples from 12 cases of UCCC. Tumor mutational burden (TMB) was determined on 0.8 to 1.1 Mbp of sequenced DNA and microsatellite instability (MSI) was determined on 114 loci. PD-L1 expression in tumor cells (Dako 22C3) was measured by IHC.

**Results:** There were 11 (92%) female and 1 (8%) male patients in this UCCC cohort. The median age was 64 years (range 41 to 72 years). All (100%) of cases were clinically advanced and 10 (83%) had documented metastatic disease at the time of sequencing. The primary tumor was used for CGP in 5 (42%) cases; a metastasis biopsy was used in 7 (58%) cases including lung (2 cases), bladder (2 cases) and bone, cervix and lymph node (1 case each). IHC staining was uniformly positive for PAX-8, HNF1b and CK7, uniformly negative for CK20, WT-1, p63, napsin and ER/PR and variably positive for racemase, p53 and vimentin. There were 3.7 genomic alterations (GA) per case. The most frequent potentially actionable GA included activating mutations in *PIK3CA* (4 cases; 33%) and *PTCH1* (1 case; 8%), inactivating mutation in *TSC2* (1 case, 8%) and amplifications of *EGFR* (1 case; 8%) and *MET* (1 case; 8%). All (100%) of the UCCC were MSI stable and had a median TMB of 5 mutations/MB (range 0 to 9.6 mutations/Mb). There were no (0%) UCCC with a TMB $\geq$ 20 mutations/Mb. Only 1 UCCC case had PD-L1 expression measured by IHC which was negative.

**Conclusions:** CGP of UCCC reveals frequent potentially targetable GA in the MTOR Pathway (*PIK3CA* and *TSC2*) as well as potential kinase targetable GA in genes such as *EGFR, PTCH1* and *MET*. Absence of MSI High, high TMB or know PD-L1 expression indicates that clinically advanced UCCC may not be responsive to immunotherapy regimens. Further study of UCCC in mechanism driven clinical trials appears warranted.

## 864 Renal Cell Carcinomas with TFE3 Gene Fusion: Report of 85 cases with TFE3 Fusion Status Confirmed by Fluorescence In Situ Hybridization (FISH)

Mahmut Akgul[1], Liang Cheng[1], David Grignon[1], John Eble[1], Muhammad Idrees[1]
*[1]Indiana University School of Medicine, Indianapolis, IN*

**Disclosures:** Mahmut Akgul: None; Liang Cheng: None; David Grignon: None; John Eble: None; Muhammad Idrees: None

**Background:** Renal cell carcinomas associated with TFE3 gene fusion (XP11.2) account for the majority of Microphthalmia Transcription Factor (MIT) family translocation renal cell carcinomas (TFE3 RCC). It is a crucial diagnostic differential in the evaluation of renal epithelial neoplasms. TFE3 RCC exhibits heterogeneous morphology and immunohistochemical profile. We evaluated clinicopathologic features, biomarker expression characteristics, and FISH analysis from a large single institutional cohort.

**Design:** We included TFE3-RCC diagnosed between January 2010 – August 2019 with the diagnosis confirmed by FISH analysis. Gender, age, procedure type, nuclear grade, tumor size, tumor stage, and lymph node/distant metastasis were recorded. Immunohistochemical (IHC) expression of TFE3 was graded as positive, negative, or equivocal (i.e. positive expression in both tumor cells and non-neoplastic renal tubules). Other immunohistochemical markers were reported as positive or negative.

**Results:** There was slight male predominance (M/F = 45/40) and the median age was 53 (range 11-82). International Society of Urologic Pathology/World Health Organization nuclear grade was 4 in 16/85 cases (19%). At the time of the diagnosis, lymph node and distant metastases were seen in 10 (12%) and 11 (13%) patients, respectively. (See Table 1). TFE3 IHC was available in 82/85 cases, and was positive in 68 (82%), negative in 5 (6%) and equivocal in 10 (12%). Pancytokeratin was negative in 20/64 (31%) cases. Consistently positive markers were AMACR (57/64), CD10 (62/69), and vimentin (63/76). On the other hand, CK7, Cathepsin K, Melan A, and HMB45 were negative in majority of cases (61/78, 50/71, 39/50, and 29/34; respectively).

| | TFE3 FISH Positive Case |
|---|---|
| General Characteristics | |
| Male n(%) | 45(53%) |
| Female n(%) | 40(47%) |
| Total | 85(100%) |
| Age | |
| Median (Range) | 53(11-82) |
| Age≤18 | 2(3%) |
| Age≤50 years n(%) | 38 (33%) |
| Age >50 years n(%) | 57 (67%) |
| | |
| Procedure | |
| Biopsy n(%) | 5(6%) |
| Partial Nephrectomy n(%) | 27(32%) |
| Radical Nephrectomy n(%) | 53(62%) |
| | |
| ISUP/WHO Nuclear Grade 4 | 16(19%) |
| Rhabdoid | 5(6%) |
| Sarcomatoid | 9(11%) |
| Bizarre Pleomorphism | 4(5%) |
| | |
| Tumor Size | |
| Median (Range) | 6.1(1-27) |
| ≤4 cm | 22(29%) |
| >4 - 7≤ cm | 26(34%) |
| >7 - 10≤ cm | 19(24%) |
| >10 cm | 10(13%) |
| Total | 77 |
| | |
| AJCC 8th Edition T-Category | |
| 1a | 20(26%) |
| 1b | 16(21%) |
| 2a | 3(3.5%) |
| 2b | 4(6%) |
| 3a | 26(35) |
| 3b | 3(3.5%) |
| 3c | 1(1.5%) |
| 4 | 3(3.5%) |
| Total | 76 |
| | |
| Lymph Node Metastasis | 10(12%) |
| | |
| Distant Metastasis | 11(13%) |

**Conclusions:** Despite remarkable morphologic heterogeneity, several markers show consistent immunoexpression in FISH confirmed TFE3 translocation carcinomas including positive expression of TFE3, AMACR, CD10, and vimentin; and negative expression of CK7, Cathepsin K, Melan A, and HMB45.

## 865 Recurrent KRAS Mutation is an Early Event in the Development of Papillary Renal Neoplasm with Reverse Polarity

Khaleel Al-Obaidy[1], John Eble[1], Liang Cheng[1], Mehdi Nassiri[2], Sean Williamson[3], Muhammad Idrees[1], David Grignon[1]
*[1]Indiana University School of Medicine, Indianapolis, IN, [2]IUPUI, Indianapolis, IN, [3]Henry Ford Health System, Detroit, MI*

**Disclosures:** Khaleel Al-Obaidy: None; John Eble: None; Liang Cheng: None; Mehdi Nassiri: None; Sean Williamson: None; Muhammad Idrees: None; David Grignon: None

**Background:** Papillary renal neoplasm with reverse polarity is a recently proposed distinct renal tumor. In addition to its unique morphologic and immunohistochemical features, a recent study showed that these tumors represent the only kidney tumor with recurrent *KRAS* mutation.

**Design:** We reviewed a series of 177 previously retrieved cases of end stage kidneys at Indiana University for incidentally found non-mass forming papillary renal neoplasms with reverse polarity, using the same criteria suggested by Al-Obaidy et al. The tumors were composed of papillary or tubulopapillary architecture covered by a single layer of eosinophilic cells with finely granular eosinophilic cytoplasm and apically located round nuclei with inconspicuous nucleoli. No intracellular hemosiderin, psammoma bodies, mitotic figures, necrosis, or clusters of foamy macrophages should be present. Immunohistochemical staining (GATA-3, AMACR and vimentin) and polymerase chain reaction (PCR) for *KRAS* mutations was performed.

**Results:** The cohort consisted of 8 cases from 7 patients, 4 were males and 4 were females, with an age range of 42-75 years (mean, 57 years, median 60 years) and a size range of 1-3 mm. All cases were positive for GATA-3 immunostain. AMACR and vimentin immunostains were performed on one and both were negative (Figure 1). Of the 8 cases identified, only 3 had successful PCR analysis (neoplasm sizes 3 mm). These were identified in 2 patients (one with bilateral neoplasms). *KRAS* mutations were present in all 3 neoplasms and were clustered in exon 2—codon 12: c.35 G>T (n = 2) or c.34 G>T (n = 1) resulting in p.Gly12Val and p.Gly12Cys alterations, respectively. An attempt to analyze the remaining 5 cases failed to detect any mutations, most likely due to the small size (1 mm), and a high likelihood of tissue loss with deeper sectioning despite microdissection attempts. One lesion with a *KRAS* mutation had an associated acquired cystic diseases associated renal cell carcinoma; that was negative for *KRAS* mutation.

Figure 1 - 865

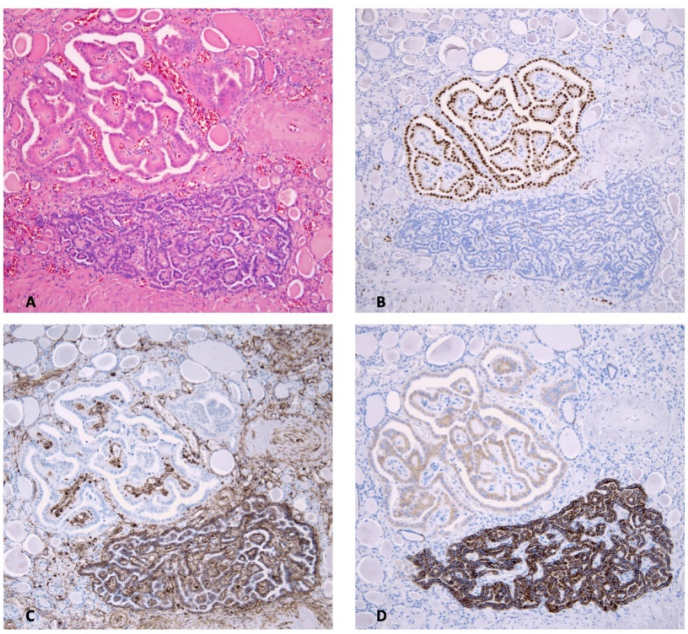


Figure 1: A. Representative histologic image of a non-mass forming papillary renal neoplasm with reverse polarity, and usual papillary adenoma (upper and lower part of image). B-D, Papillary renal neoplasm with reverse polarity stains positive for GATA-3 and negative for vimentin. AMACR immunostaining showing only weak immunostaining, while usual papillary adenoma is negative for GATA-3, and positive for vimentin and AMACR, respectively.

**Conclusions:** The presence of *KRAS* mutations in small, clinically undetectable lesions provides a unique supportive finding to this proposed entity. In contrast to the size criteria used to define the clinical course of papillary adenoma vs carcinoma, the terminology "papillary renal neoplasms with reverse polarity" is recommended for all lesions identified regardless of the size as this study finds *KRAS* mutation to be an early event in their pathogenesis.

## 866 EWSR1-PATZ1 Gene Fusion in Thyroid-Like Follicular Renal Cell Carcinoma: A Novel Molecular Finding

Khaleel Al-Obaidy[1], John Eble[1], Liang Cheng[1], Mehdi Nassiri[2], Muhammad Idrees[1], David Grignon[1]
*[1]Indiana University School of Medicine, Indianapolis, IN, [2]IUPUI, Indianapolis, IN*

**Disclosures:** Khaleel Al-Obaidy: None; John Eble: None; Liang Cheng: None; Mehdi Nassiri: None; Muhammad Idrees: None; David Grignon: None

**Background:** *EWSR1* rearrangements is classically found in small round blue cell tumors, most commonly, *EWSR1-ETS* and *EWSR1-WT1* gene fusions. The advances in genetic understanding have led to recognition of distinct tumor entities while supporting the distinct nature of others. In recent years, rare fusion partners have been identified. *EWSR1-PATZ1* is a rare fusion partner that described in few cases of sarcomas and rare cases of glioneuronal tumor. Thyroid-like follicular renal cell carcinoma is a rare renal tumor and considered a provisional entity in the current WHO classification of kidney tumors. The tumors resemble thyroid follicles histologically; however, they stain negative for TTF-1 and thyroglobulin, while are positive for PAX-8, CK7, CK19 and to a lesser extent, AMACR. Herein, we report a novel molecular finding in this entity.

**Design:** Five thyroid-like follicular renal cell carcinomas diagnosed at Indiana University were identified. SMAD4 immunostaining was performed on 4 tumors. Two had sufficient material for molecular testing. A targeted next generation sequencing (NGS) for DNA mutation and RNA gene fusion was performed on unstained sections obtained from formalin-fixed paraffin embedded tissues. This was followed by *EWSR1* gene fusion testing by fluorescence in situ hybridization (FISH).

**Results:** The cohort comprised 5 patients (cases 1, 2 and 3 were included in a previously published abstract [Mod Pathol 32(S2): 7-8; abstract no. 785.]), all were females (n=5, 100%). The mean and median ages were 37 and 40 years, respectively (range 19-58 years) (Table 1). SMAD4 immunostaining was performed on 4 tumors and was positive in all. Two tumors (tumors 2 and 3) had sufficient material for molecular testing. RNA gene fusion identified *EWSR1-PATZ1* gene fusion in both tested tumors. These 2 tumors also were positive for *EWSR1* gene rearrangement by FISH. No significant pathogenic mutations were identified by DNA next generation sequencing.

**Table 1: A summary of the clinicopathologic findings in patients with Thyroid-like follicular renal cell carcinoma**

| | procedure | Age | Gender | Size (mm) | Laterality | P-stage | Recurrence/ Metastasis | Significant History | Gene fusion |
|---|---|---|---|---|---|---|---|---|---|
| 1 | Partial Nephrectomy | 58 | F | 40 | Right | pT1a | N | Hypertension | *EWSR1-PATZ1* |
| 2 | Partial Nephrectomy | 40 | F | 56 | Left | pT3a | N | | *EWSR1-PATZ1* |
| 3 | Partial Nephrectomy | 25 | F | 38 | Right | pT1a | N | Slight enlargement over 7 years | Not tested |
| 4 | Nephrectomy | 42 | F | 8 | Left | pT1a | - | Family history of Hereditary leiomyomatosis and renal cell cancer syndrome | Not tested |
| 5 | Renal biopsy | 19 | F | 11 | Right | pT1a | - | Treated acute lymphoblastic leukemia | Not tested |

**Conclusions:** Overall, our study identifies for the first time a novel gene fusion involving the *EWSR1* (*EWSR1-PATZ1*) in a tumor that is morphologically and immunohistochemically different from the small round blue cell tumor family. This finding adds support to it's the designation of thyroid follicular carcinoma-like renal cell carcinoma as a unique entity, although confirmation in additional cases is required.

## 867 Hepatoid Yolk Sac Tumor (HYST), Hepatocellular Carcinoma (HCC) and Hepatocytic Teratoma (HT): A Morphologic and Immunohistochemical (IHC) Study of 31 Cases

Khaleel Al-Obaidy[1], Sean Williamson[2], Fatimah Alruwaii[1], Muhammad Idrees[1], Thomas Ulbright[1]
*[1]Indiana University School of Medicine, Indianapolis, IN, [2]Henry Ford Health System, Detroit, MI*

**Disclosures:** Khaleel Al-Obaidy: None; Sean Williamson: None; Fatimah Alruwaii: None; Muhammad Idrees: None; Thomas Ulbright: None

**Background:** YST is known for its multiple patterns, which assist in its diagnosis. Purely hepatoid differentiation is rare, consisting of nests and cords of cells with abundant, eosinophilic to clear cytoplasm, well-defined cell borders, and round nuclei with prominent nucleoli. It is usually seen in metastases of patients with late recurrence, often years after orchiectomy, which complicates its recognition. Additionally, hepatocytic differentiation is a rare aspect of teratoma; it requires separation from HYST, and both should be distinguished from *de novo* HCC. We therefore investigated the morphologic and IHC features of these entities.

**Design:** We retrieved 12 metastatic HYSTs (representing >90% of the tumor), 17 HCCs and 2 HTs (Figures 1-3, respectively) from tissue archives. Hematoxylin and eosin stained slides were reviewed to confirm each diagnosis. 4 µm-thick sections were stained with antibodies against SALL4, CK7, CK19, CDX2, glypican-3, arginase, HepPar-1, and villin in a Dako automated instrument.

**Results:** The median and mean age of patients with HYST was 36 years (range, 20-63). 3 presented with metastatic disease and 9 recurred at a median of 10 years (range, 2-24) after initial diagnosis. The tumors formed trabeculae and cords, occasional gland-like structures, and had frequent basement membrane deposits. SALL4 (100%), glypican-3 (100%), CK19 (85%), CDX2 (85%) and villin (75%) were prominently positive; HepPar-1 stained rare single tumor cells (70%) and arginase was infrequently reactive (26%) (patchy in 1 and rare cells in 4). In HCC, HepPar-1 (94%) and arginase (82%) were diffusely positive, whereas glypican-3 (35%) and villin (12%) were less common. SALL4, CK19 and CDX2 were negative. HTs formed sheets of hepatocytes with abortive ducts and portal triads (Figure 1). The hepatocytes stained positively for glypican-3, arginase, and HepPar-1 (2/2). Villin was positive in 1. CK7 (1/2) and CK19 (2/2) highlighted ductular formation. SALL4 and CDX-2 were negative (0/2).

Figure 1 - 867

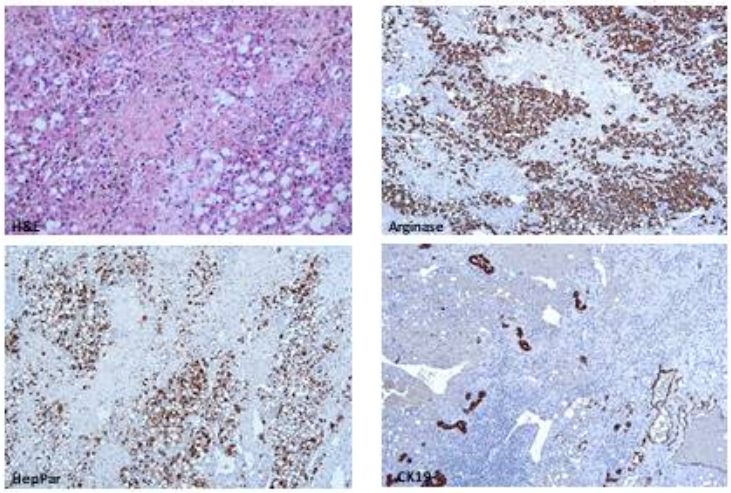


**Conclusions:** In summary, SALL4, glypican-3, CDX2, and CK19 are sensitive markers for HYST, as is widely scattered single cell reactivity with HepPar-1. SALL4, CK19 and CDX2 positivity are specific in the differential with HCC, as are prominent intercellular basement membrane deposits. HTs show more consistent staining for arginase and HepPar-1 than HYST; they lack SALL4, contrasting with HYST.

## 868 How Important is the Routine Use of p16 Immunohistochemistry in the Diagnosis of Pre-invasive Penile Cancer Lesions? An Evaluation of the Cases Seen at a Large Tertiary Referral Centre Between 2016-2018

Duncan Alexander[1], Arie Parnharn[2], Pedro Oliveira[3]
*[1]University of Manchester Medical School, Manchester, Greater Manchester, United Kingdom, [2]Department of Urology The Christie NHS Foundation Trust, Manchester, Greater Manchester, United Kingdom, [3]The Christie Hospital NHS Foundation Trust, Manchester, Lancashire, United Kingdom*

**Disclosures:** Duncan Alexander: None; Arie Parnharn: None; Pedro Oliveira: None

**Background:** HPV profile of penile in-situ lesions (PeIN) is important for diagnostic accuracy, prognostic considerations, and epidemiological study. The surrogate biomarker p16 is an accepted method of determining High-risk HPV (HR-HPV) status via immunohistochemistry (IHC), and is used worldwide in cervical pathology. However, in PeIN, p16 has been performed on a case by case scenario and is dependent on the pathologist. Herein we analyse a large series of cases evaluated at The Christie Hospital (CH) for the last 3 years, where routine p16 IHC was performed in order to assess the practical relevance of its use.

**Design:** All new cases of PeIN from 2016-2018 that were diagnosed/referred to CH were identified. At CH these cases were classified according to the WHO 2016 Classification of Undifferentiated and Differentiated PeIN. In 65 cases the original diagnosis was made externally, and the original reports and slides reviewed for evidence of p16 staining. Discrepancies between the original and the revised diagnoses were assessed and the value of p16 in the diagnostic interpretation evaluated.

**Results:** In 84.6% of the cases, the original diagnosis didn't follow the WHO 2016 terminology, encompassing multiple terminologies (e.g. Dysplasia NOS, In Situ SCC, PeIN NOS). At CH, p16 was performed/reviewed in 140 cases; in one case, no paraffin block was available,

and in five cases no request was made. Of the 65 cases referred for review, p16 IHC was available in 11 (16.9%). Of the remaining 54 cases, p16 IHC requested at CH showed positivity in 47. Overall, 87.7% of the cases referred had strong association with HPV aetiology, based on p16 IHC. In three cases, a major discrepancy in diagnosis was identified: one case with a benign diagnosis, and two with low grade dysplasia that later proved to be undifferentiated PeIN, with all three cases showing strong p16 positivity. A trend towards increasing use of p16 IHC from the referral hospitals was however observed from 2016 (8%) to 2019 (31%).

**Conclusions:** The large discrepancy in p16 staining between different hospitals and the high rate of 'missed' p16-positive cases is worrying, and warrants the introduction of guidelines to standardise this practice. Understanding HR-HPV related aetiology in these lesions is potentially relevant, not only in terms of treatment options (e.g. Imiquimod therapy), but also from a public health perspective to support strategies to reduce the burden of HPV-associated disease (such as male HPV immunisation programmes).

## 869 Histopathologic Features of Prostate Cancer in Patients Who Underwent Seminal Vesicle-Sparing Radical Prostatectomy: A Novel Surgical Approach

Mohamed Alhamar[1], Oudai Hassan[1], Akshay Sood[1], Sohrab Arora[1], Wooju Jeong[1], Sean Williamson[1], Mani Menon[1], Nilesh Gupta[1]
*[1]Henry Ford Health System, Detroit, MI*

**Disclosures:** Mohamed Alhamar: None; Oudai Hassan: None; Akshay Sood: None; Sohrab Arora: None; Wooju Jeong: None; Sean Williamson: None; Mani Menon: None; Nilesh Gupta: None

**Background:** Incontinence and erectile dysfunction are common complications of radical prostatectomy (RP). Seminal vesicle (SV) involvement is found in 5-23% of RP, frequently with grade group (GG) 3-5. At our institution a novel seminal vesicle-sparing approach (SVSRP) has been introduced, with preservation of either one or both seminal SVs in a select group of patients to improve functional outcomes. Here we report on the surgical pathology findings on SVSRP.

**Design:** All SVSRP were reported by a specialist genitourinary pathologist. Detailed pathologic findings including grade, tumor size, number of tumor nodules, margin status, and pathologic stage were studied.

**Results:** Specimens from 33 patients were studied with median age of 63 (range 51-80). In the diagnostic biopsy, 7 were Grade Group (GG) 1, 16 GG2, 6 GG3, 2 GG4, 1 GG5, and 1 not applicable (post hormonal therapy). Median number of biopsies taken was 12 (6-36) and median number positive biopsies was 3 (1-11). Half (16/33, 48%) had frozen section (FS) evaluation of the SV. Almost all (32/33) had bilateral sparing of SV, whereas in one FS of the SV base was positive and unilateral sparing of SV was performed. Median tumor percentage was 6% (1-30%). A dominant tumor nodule (DN) was identified in 31/33 (94%), whereas 2 had scattered microscopic tumor foci. Median size of the DN was 21 mm (11-30) and median number of secondary nodule(s) was 1 (1-6). Median GG of the DN was 2 (1-5). Positive margin was present in 20/33 (60%). However, only one (3%) had positive margin at the site of SVSRP. Median linear extent of positive margin was 3.5 mm (1-20 mm). Lymphovascular invasion was present in 2/33 (6%), 1/33 (3%) had bladder neck invasion, 1/33 (3%) had lymph node metastasis, 15/33 (45%) had extraprostatic extension, and 4/33 (12%) showed intraductal carcinoma. The case with positive margin at the SVSRP site was the case with unilateral (left) SV sparing. (Table).

| SVSRP Data | Cases | Percentage of cases |
|---|---|---|
| **GG on diagnostic biopsy(s)** | | |
| 1 | 7/33 | 22% |
| 2 | 16/33 | 49% |
| 3 | 6/33 | 19% |
| 4 | 2/33 | 6% |
| 5 | 1/33 | 3% |
| Hormonal therapy | 1/33 | 3% |
| **SVSRP GG** | | |
| 1 | 2/33 | 6% |
| 2 | 16/33 | 49% |
| 3 | 12/33 | 36% |
| 4 | 0/33 | 0% |
| 5 | 2/33 | 6% |
| Hormonal therapy | 1/33 | 3% |
| **Surgical margins** | | |
| Positive | 20/33 | 60% |
| Negative | 13/33 | 40% |
| **Location of positive margins** | | |
| Radical | 19/20 | 95% |
| SVSRP site | 0/20 | 0% |
| Both (Radical & SVSRP site) | 1/20 | 5% |
| **Gleason pattern at positive margin** | | |
| Pattern 3 | 9/20 | 45% |
| Pattern 4 or 5 | 11/20 | 55% |
| **Extent of positive margin** | | |
| < 3 mm | 9/20 | 45% |
| ≥ 3 mm | 11/20 | 55% |
| **Clinically significant secondary nodules** | | |
| GG1 | 13/26 | 50% |
| GG2 to GG5 | 13/26 | 50% |
| **TNM Stage** | | |
| pT2 | 18/33 | 55% |
| pT3a | 13/33 | 39% |
| pT3b | 2/33 | 6% |

**Conclusions:** SVSRP is a promising surgical approach which may offer early return of continence compared to RP while allowing resection of clinically significant tumor. Although 60% of our cases had positive margins, only one case with aggressive disease had positive margin at the SVSRP site. The rest would have had positive margins with a conventional RP. Further refinement of selection criteria with additional pre-op or intra-op biopsies of the seminal vesicles may help to improve oncologic control in this surgical approach.

## 870 Precision Prostatectomy: Analysis of Surgical Pathology Findings of a Promising and Novel Surgical Approach for Patients with Low to Intermediate-Risk Prostate Cancer

Mohamed Alhamar[1], Nilesh Gupta[1], Oluwayomi Oyedeji[1], Kathryn Hogan[1], Akshay Sood[1], Sohrab Arora[1], Daniel Schultz[1], Wooju Jeong[1], Sean Williamson[1], Mani Menon[1], Oudai Hassan[1]
*[1]Henry Ford Health System, Detroit, MI*

**Disclosures:** Mohamed Alhamar: None; Nilesh Gupta: None; Oluwayomi Oyedeji: None; Kathryn Hogan: None; Akshay Sood: None; Sohrab Arora: None; Daniel Schultz: None; Wooju Jeong: None; Sean Williamson: None; Mani Menon: None; Oudai Hassan: None

**Background:** Precision Prostatectomy (PP) is a novel surgical approach introduced at our institution to treat low to intermediate-risk prostate cancer. It includes radical resection of the dominant nodule (DN) side, with preservation of neurovascular bundle, capsule, & 5–10 mm of prostatic tissue on the contralateral side. Here we report on the surgical pathology findings and outcome data on PP.

**Design:** Detailed pathological findings were studied from PP patients. Post-operative erectile function & biochemical recurrence (BCR) were studied. Clinical selection criteria for PP included: (1) PSA ≤15 ng/mL (2) clinical stage ≤cT2 (3) a dominant unilateral lesion with grade group (GG) ≤3 (4) no primary Gleason score ≥4 contralaterally.

**Results:** A total of 77 patients were studied, with median age 59 (range 47-75). Median pre-operative PSA was 5.5 (1.4 -23) and median number of positive biopsies was 3 (1-9). A second mapping biopsy was performed in 35/77 (45%). Most (64/77, 83%) had frozen section evaluation of the precision side. Of the PP specimens, median GG was 2 (1-5), median tumor percentage was 6% (1-32%). Almost all (75/77, 97%) had a DN, whereas 2/77 (3%) showed scattered microscopic tumor foci. Median DN size was 20 mm (4-35) & most (60/77, 78%) had secondary nodule(s) (SN). Median number of SN was 2 (1-6) & median size was 8 mm (1-30). Positive resection margin was present in 33/77 (43%) with a median linear extent of 3 mm (0.5 - 48). This was at the DN in 16/33 (49%), SN in 10/33 (30%), & both in 7/33 (21%). The DN was incompletely excised in the PP side in 4 cases (3 of these were midline, whereas the diagnostic biopsy missed

the DN in the 4th). For the remainder, positive margin was present on the radical side, which would render the same results as a radical prostatectomy (RP) approach. Overall 20/77 had positive margin at the PP side (See Table 1). Only one patient (1%) had a positive lymph node. Median follow up was 8 months (1-24). All patients had excellent results with post-op erectile function & 3 had BCR. BCR was not significantly correlated with the status of DN excision (p= 0.8) (Table & Figure1).

| DATA | Cases (%) | | | | |
|---|---|---|---|---|---|
| **Post-operative overall analysis:** | | | | | |
| **Grade Group** | | **Gleason pattern at positive margin** | | **TNM Stage** | |
| 1 | 9/77 (12) | Pattern 3 | 15/33 (45) | pT2 | 56/77 (73) |
| 2 | 54/77 (70) | | | | |
| 3 | 11/77 (14) | | | pT3a | 18/77 (23) |
| 4 | 0/77 (0) | Pattern 4 or 5 | 18/33 (55) | pT3b | 3/77 (4) |
| 5 | 3/77 (4) | | | | |
| **Dominant Nodule Analysis:** | | | | | |
| **Location of dominant nodule in relation to PP side** | | **Dominant nodule excised** | | **Location of incompletely excised dominant nodule** | |
| Contralateral | 61/77 (79) | Yes | 54/77 (70) | Radical side | 19/23 (83) |
| Ipsilateral | 5/77 (6) | | | PP side | 2/23 (8.5) |
| Midline | 9/77 (12) | No | 23/77 (30) | Both (radical and PP sides) | 2/23 (8.5) |
| No dominant nodule | 2/77 (3) | | | | |
| **Gleason pattern at positive margin of incompletely excised dominant nodule (Radical and PP)** | | **Grade Group of the pre-op biopsy of incompletely excised dominant nodule at PP side** | | **Grade Group of incompletely excised dominant nodule at PP side** | |
| Pattern 3 | 9/23 (39) | 2 | 3/4 (75) | 2 | 3/4 (75) |
| Pattern 4 or 5 | 14/23 (61) | 3 | 1/4 (25) | 3 | 1/4 (25) |
| **Gleason pattern at positive margin of incompletely excised dominant nodule at PP side** | | | | | |
| Pattern 3 | | 1/4 (25) | | | |
| Pattern 4 or 5 | | 3/4 (75) | | | |
| **Secondary Nodule(s) Analysis:** | | | | | |
| **Presence of secondary nodule(s)** | | **Location of secondary nodule(s) in relation to PP side** | | **Grade Group of secondary nodule(s)** | |
| Yes | 60/77 (78) | Bilateral | 21/60 (35) | GG1 | 43/60 (72) |
| | | Contralateral | 7/60 (11.5) | | |
| No | 17/77 (22) | Ipsilateral | 31/60 (52) | GG2 to GG5 | 17/60 (28) |
| | | Midline | 1/60 (1.5) | | |
| **Location of clinically significant (GG2-GG5) secondary nodule(s) in relation to PP side** | | **Clinically significant (GG2-GG5) secondary nodule(s) margin** | | **Location of clinically significant (GG2-GG5) secondary nodule(s) with positive margin** | |
| Bilateral | 1/17 (6) | Positive | 6/17 (35) | Radical side | 0/6 (0) |
| Contralateral | 7/17 (41) | | | PP side | 5/6 (83) |
| Ipsilateral | 8/17 (47) | Negative | 11/17 (65) | Both sides | 1/6 (17) |
| Midline | 1/17 (6) | | | | |

Figure 1 - 870

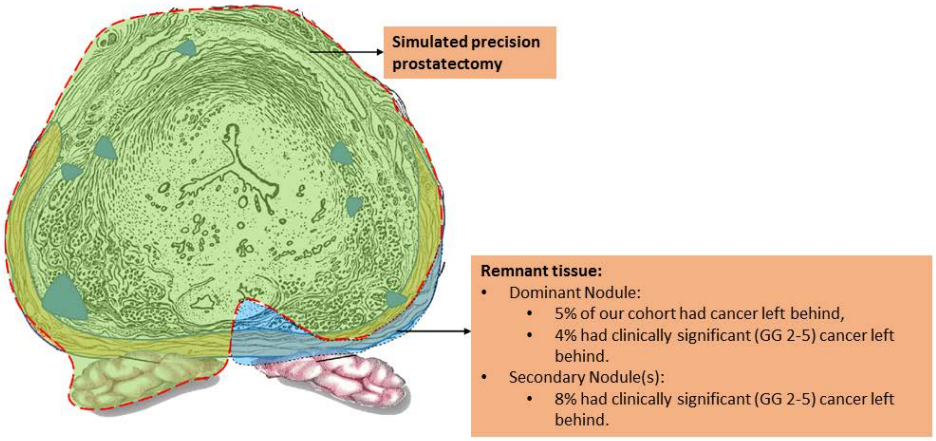


**Conclusions:** PP promises excellent post-op erectile function compared to RP. Pre-op saturation biopsy to map the tumor may aid in optimizing cancer control in these patients. Although initial results are promising, longer follow up is needed to assess long-term outcomes.

## 871 How Close is Too Close? Molecular Heterogeneity in Intraprostatic Collision Tumors

Hussein Alnajar[1], Jacqueline Fontugne[2], Kyung Park[3], Huihui Ye[4], Shaham Beg[1], Javed Siddiqui[5], Arul Chinnaiyan[6], Christopher Barbieri[7], Mark Rubin[8], Juan Miguel Mosquera[1]
*[1]Weill Cornell Medicine, New York, NY, [2]New York, NY, [3]NYU Langone Health, New York, NY, [4]University of California Los Angeles, Los Angeles, CA, [5]University of Michigan, Ann Arbor, MI, [6]Plymouth, MI, [7]Weill Cornell Medical College, New York, NY, [8]University of Bern, Bern, Switzerland*

**Disclosures:** Hussein Alnajar: None; Jacqueline Fontugne: None; Kyung Park: None; Huihui Ye: *Consultant*, Janssen (Johnson &Johnson); Shaham Beg: None; Javed Siddiqui: None; Arul Chinnaiyan: *Employee*, University of Michigan; Christopher Barbieri: None; Mark Rubin: *Grant or Research Support*, NCI; Juan Miguel Mosquera: None

**Background:** Radical prostatectomy (RP) specimens often harbor multiple prostate cancer (PCa) nodules that are spatially separated. These tumor nodules can be molecularly heterogeneous. The current practice is to separate the dominant tumor nodule histologically, usually the one with highest Gleason score and/or largest size, and assign individual Grade Groups. There is no current recommendation to use ancillary studies to further differentiate theses nodules molecularly. Current assays that interrogate biopsies and RP assume that only one tumor is present in the tissue sample. The aim of this study was to establish the frequency of molecularly heterogeneous tumors within one spatially distinct nodule in RP specimens.

**Design:** 269 RP specimens – Grade Groups 1 to 5 – collected prospectively from three participating institutions of the Early Detection Research Network (EDRN) trial were reviewed. Dual ERG/SPINK1 IHC was performed on all tumor foci. The nodule with the highest Grade Group score was defined as dominant. In case of multiple nodules with the same Gleason score, the largest one was considered as the dominant. A “collision tumor” was defined as having two molecular subtypes within one spatially distinct nodule. The presence of cribriform pattern and intraductal carcinoma (IDC-P), both features associated with unfavorable outcome were also recorded.

**Results:** IHC slides from 260 RP cases were available for analysis. 25 collision tumors (9.6%) were identified (Table), of which, 48% included nodules with different grade groups. The most common collision being between the ERG+/SPINK1– and ERG–/SPINK1–(64%) (Fig. 1). The frequency of cribriform morphology and IDC-P when applicable was 15% and 12%, respectively. Finally, we found ERG+ benign-appearing glands in 8% of total cases (Fig. 2), which were present close to ERG+ tumors in only 15% of these cases.

Molecular and grade of collision tumor cases

| Case # | Primary nodule GS | SPINK1/ERG status | Secondary nodule GS | SPINK1/ERG status |
|---|---|---|---|---|
| 1 | 347 | SPINK1- ERG+ | 347 | ERG–/SPINK1– |
| 2 | 437 | ERG–/SPINK1– | 437 | SPINK1+ ERG- |
| 3 | 437 | ERG–/SPINK1– | 437 | SPINK1- ERG+ |
| 4 | 437 | SPINK1- ERG+ | 437 | ERG–/SPINK1– |
| 5 | 347 | SPINK1- ERG+ | 336 | SPINK1+ ERG- |
| 6 | 437 | ERG–/SPINK1– | 437 | SPINK1+ ERG- |
| 7 | 336 | SPINK1- ERG+ | 336 | ERG–/SPINK1– |
| 8 | 347 | SPINK1- ERG+ | 336 | ERG–/SPINK1– |
| 9 | 336 | SPINK1- ERG+ | 336 | ERG–/SPINK1– |
| 10 | 347 | SPINK1- ERG+ | 347 | SPINK1+ ERG- |
| 11 | 347 | SPINK1- ERG+ | 336 | ERG–/SPINK1– |
| 12 | 347 | SPINK1- ERG+ | 336 | ERG–/SPINK1– |
| 13 | 347 | SPINK1+ ERG- | 347 | ERG–/SPINK1– |
| 14 | 347 | SPINK1- ERG+ | 347 | ERG–/SPINK1– |
| 15 | 347 | ERG–/SPINK1– | 336 | SPINK1- ERG+ |
| 16 | 5510 | SPINK1- ERG+ | 459 | ERG–/SPINK1– |
| 17 | 347 | ERG–/SPINK1– | 336 | SPINK1- ERG+ |
| 18 | 336 | SPINK1+ ERG- | 336 | SPINK1- ERG+ |
| 19 | 437 | ERG–/SPINK1– | 336 | SPINK1+ ERG- |
| 20 | 336 | ERG–/SPINK1– | 336 | SPINK1- ERG+ |
| 21 | 347 | ERG–/SPINK1– | 336 | SPINK1- ERG+ |
| 22 | 347 | SPINK1- ERG+ | 347 | ERG–/SPINK1– |
| 23 | 347 | ERG–/SPINK1– | 336 | SPINK1- ERG+ |
| 24 | 437 | SPINK1+ ERG- | 336 | SPINK1- ERG+ |
| 25 | 347 | ERG–/SPINK1– | 336 | SPINK1- ERG+ |

Figure 1 - 871

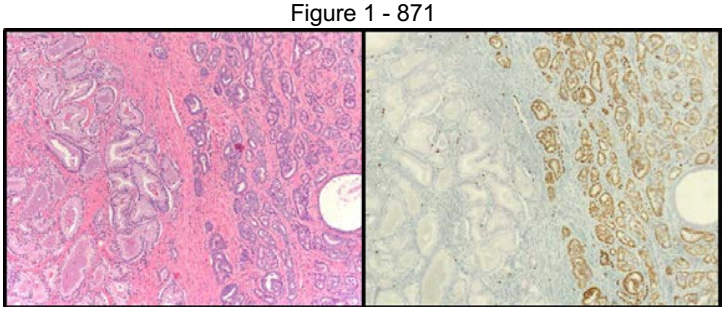

Figure 2 - 871

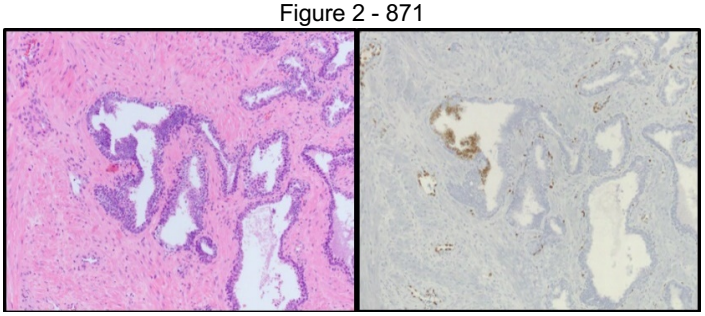

**Conclusions:** Collison tumors of two molecular subclasses of prostate cancer are not uncommon, affecting the final Grade Group in about half of these cases. Ancillary studies – e.g. dual IHC – may be indicated to better characterize different tumor foci in RP specimens. With the increased use of molecular tests on prostatectomies to predict survival and risk of metastasis or on biopsies to predict the presence of adverse pathology, it is clinically relevant to determine intra-prostatic molecular heterogeneity before choosing the appropriate block on which to do these tests.

## 872 Validation of NEAT1 RNAish: A Tissue-Based Biomarker in Prostatic Cancer

Hussein Alnajar[1], Andrea Sboner[1], Kshitij Arora[2], Kyung Park[3], Jacqueline Fontugne[4], Himisha Beltran[5], Mark Rubin[6], Juan Miguel Mosquera[1]

*[1]Weill Cornell Medicine, New York, NY, [2]Jackson Memorial Hospital/University of Miami Hospital, Miami, FL, [3]NYU Langone Health, New York, NY, [4]New York, NY, [5]Dana-Farber Cancer Institute, Harvard T.H. Chan School of Public Health, Boston, MA, [6]University of Bern, Bern, Switzerland*

**Disclosures:** Hussein Alnajar: None; Andrea Sboner: None; Kshitij Arora: None; Kyung Park: None; Jacqueline Fontugne: None; Himisha Beltran: None; Mark Rubin: *Primary Investigator*, US Patent on the field of diagnostics and therapeutics for Neat1 in prosate cancer; Juan Miguel Mosquera: None

**Background:** We previously identified nuclear enriched abundant transcript 1 (NEAT1) – ERα-regulated intergenic long non-coding RNA (lncRNA) – as the most overexpressed lncRNA in prostate cancer (PCa), its oncogenic role, association with cancer progression and potential therapeutic target (*Nat Commun* 2014). The goal of this study was to validate an RNA *in situ* hybridization (ish) assay and assess NEAT1 expression with emphasis in castrate-resistant prostate cancer (CRPC).

**Design:** We evaluated NEAT1 expression 378 cases represented in tissue microarray, including 130 benign prostate (BP), 138 localized PCa, 47 small cell carcinoma (SCC), and 8 CRPC with adenocarcinoma histology (CRPC-Adeno), and 54 with neuroendocrine differentiation (CRPC-NE). NEAT1ish (Affymetrix) was performed and HALO software (Indica Labs) was used to analyze digital images. We calculated the average and standard deviation for each category based on the average signal per cell **(Fig.1)**. Statistical difference of the average probe signal was determined using a two-tailed t-test.

**Results:** The average NEAT1 signal per cell was 3.94 in BP, 6.3 in PCa, 8.89 in SCC, 10.65 in CRPC-NE and 7.0 in CRPC-Adeno **(Fig.2)**. The average signal in BP was significantly lower than prostate cancer in general (p value <0.01). The average signal in advanced PCa – both SCC, CRPC-Adeno and CRPC-NE – was significantly higher than localized PCa (p value <0.01).

Figure 1 - 872

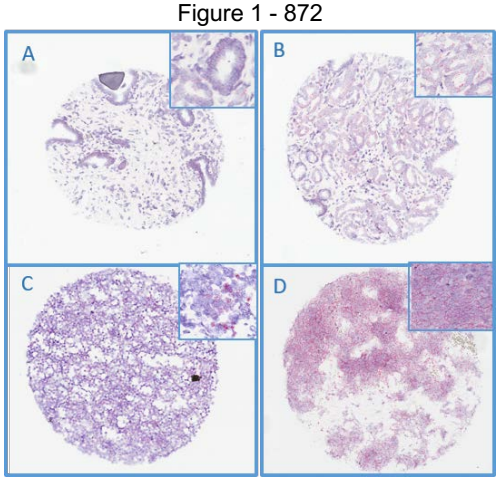


Figure 2 - 872

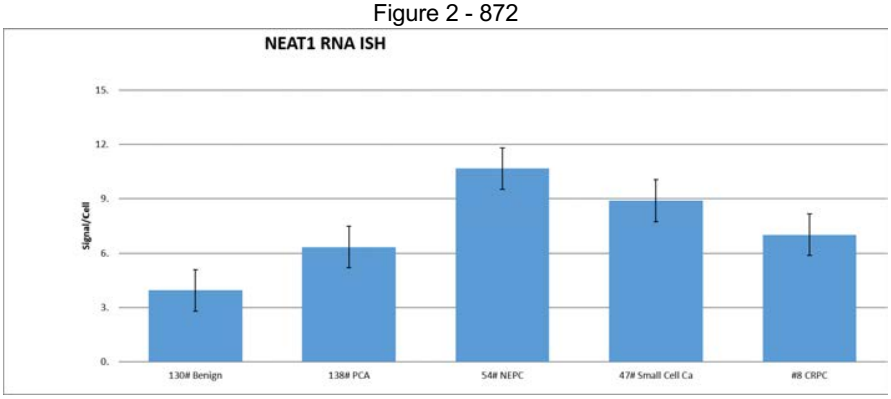


**Conclusions:** This is the first systematic study to use RNAish to evaluate NEAT1 expression in benign and malignant prostate tissues. We demonstrate significant differential expression between localized and advanced tumors. There is significant overexpression of NEAT1 in CRPC – with and without neuroendocrine differentiation. Since NEAT1 can regulate PSMA (prostate-specific membrane antigen), further studies are needed to elucidate NEAT1 expression in CRPC-NE and SCC. Should NEAT1 becomes a target in PCa and other malignancies, this RNAish assay may become a robust companion biomarker.

## 873 Invasive Poorly Differentiated Adenocarcinoma of the Bladder Status-Post Augmentation Surgery: A Multi-Institutional Study

Joshua Anderson[1], Andres Matoso[2], Belkiss Murati Amador[3], Liang Cheng[4], Bradley Stohr[5], Emily Chan[5], Adeboye O. Osunkoya[6]
*[1]Emory, Atlanta, GA, [2]Johns Hopkins Medical Institutions, Baltimore, MD, [3]Johns Hopkins University School of Medicine, Baltimore, MD, [4]Indiana University School of Medicine, Indianapolis, IN, [5]University of California San Francisco, San Francisco, CA, [6]Emory University, Atlanta, GA*

**Disclosures:** Joshua Anderson: None; Andres Matoso: None; Belkiss Murati Amador: None; Liang Cheng: None; Bradley Stohr: None; Emily Chan: None; Adeboye O. Osunkoya: None

**Background:** Augmentation cystoplasty is a surgical procedure used in the management of patients with neurogenic bladder. This procedure involves anastomosis of the bladder with gastrointestinal grafts, including portions of ileum, colon, or stomach. A rare but important complication of augmentation cystoplasty is the development of malignancy. The majority of malignancies arising in this setting have been described in case reports.

**Design:** A search for cases of carcinoma following augmentation cystoplasty was conducted through the Urologic Pathology and expert consultation files of 4 major academic institutions. Cases that had urothelial carcinoma were excluded. Clinicopathologic data was obtained.

**Results:** Ten cases were included in the study (6 cystoprostatectomy/cystectomy, 2 partial cystectomy, and 2 transurethral resection of bladder tumor specimens). The mean age at diagnosis was 47 years (range: 27-87 years). The male:female ratio was 4:6. The type of augmentation cystoplasty varied, including gastrocystoplasty (5 cases), colocystoplasty (3 cases), and ileocystoplasty (2 cases). The tumors tended to present at an advanced stage; 5 cystoprostatectomy/cystectomy cases were categorized as pT3a with one categorized as pT4. Lymph node metastases were present in all cases which had lymph node excision (range: 1-16 positive nodes per case). The majority of cases (9/10) were predominantly characterized by a poorly differentiated adenocarcinoma with diffuse signet ring cell features. Other morphologic features included focal mucinous features (3/10) and plasmacytoid features (2/10). The least common features present in 1/10 cases each included enteric/villous architecture and large cell neuroendocrine differentiation. A desmoplastic stromal response and tumor necrosis were present in 5/10 and 4/10 cases respectively. In the cases in which immunohistochemical stains were performed, the tumor cells were positive for CK20 (3/5), CDX2 (3/4), CK7 (3/4), synaptophysin (2/3), chromogranin (2/3), p63 (1/2), and negative for GATA3 (0/4), and beta-catenin (0/2, non-nuclear).

**Conclusions:** This is the largest study to date on the clinicopathologic features of invasive carcinoma of the bladder status-post augmentation cystoplasty. The tumors are typically poorly differentiated adenocarcinoma, with diffuse signet ring cell features, aggressive, and present at high stage. Further molecular characterization may provide additional insights into the pathogenesis of this entity.

## 874 Impact of Multiparametric (MP) – MRI and its Correlation with Prostate Biopsy Guided by Transrectal Ultrasound. A Prospective Study in 79 Patients from a Closed Hospital Community

Maria Aon Bertolino[1], Sebastián Otto Krause[2], Eliana Cefalo[2], Valeria Jurío[2], Florencia Cora[2], Luis Alposta[2], Gonzalo Goñi Lamela[2], Mónica Carassai[2]
*[1]Federal Police Hospital, Lujan, Buenos Aires, Argentina, [2]Federal Police Hospital, Caba, Buenos Aires, Argentina*

**Disclosures:** Maria Aon Bertolino: None; Sebastián Otto Krause: None; Eliana Cefalo: None; Valeria Jurío: None; Florencia Cora: None; Luis Alposta: None; Gonzalo Goñi Lamela: None; Mónica Carassai: None

**Background:** Prostate cancer is the second most common solid neoplasm in men. In Argentina, annual incidence calculated for our closed hospital community is 52.42 cases/100,000. Prostate-specific antigen (PSA) as a screening method has a limited specificity: unnecessary biopsies, over-diagnosis and treatment of clinically non-significant tumors. The USPTF (U.S. Preventive Services Task Force) recommends PSA-based screening for prostate cancer in men 70 ≥ aged, and emphasizes in new methods to differentiate indolent from aggressive tumors. MRI is a promising method to locate, determine size and aggressiveness of prostate tumors.

**Design:** Multicenter, prospective, longitudinal and observational study from 2013–2015; 103 male patients >50 years with indication of prostate biopsy (PSA> 10 or between 4 - 10 and PSAt/PSAl ratio <18% and/or abnormal rectal examination. Exclusion criteria: claustrophobia (n=5), cardiac pacemaker (n=10) and projectiles in the body (n=9). MP- MRI imaging was considered positive with pathological images in at least two sequences. Randomized transrectal ultrasound guided biopsy later performed. 12 samples were taken in virgin biopsy patients (n=59) and 18 samples in patients with previous negative biopsy (n=20). Routine processing with Hematoxilin and Eosin were made. Data were collected in EXCEL tables. Statistical analysis was made with STATA and McNemar test. Significant prostate cancer was defined according to Epstein criteria: Gleason >6, PSA >10 ng/ml, 3 or more biopsy positive samples or more than 50% commitment.

**Results:** 79 patients mean ages 66.4. The median PSA was 9.2 ng/ml and 28% (n=22) had an abnormal rectal examination. Prostatic filaments (n=1059) with H&E were studied; 25% of patients (n=20) has negative previous biopsy. Cancer was detected in 43 patients (54%)

of whom 15/79 were Gleason 6, (3+3=6; Grade Group 1/5 ISUP); 17/79 Gleason 7 (3+4 =7; Grade Group 2/5 ISUP, n= 16; 4+3=7; Grade Group 3/5 ISUP, n=1); 9/79 Gleason 8 (4 +4=8, Grade Group 4/5 ISUP) and 2/79 Gleason 9 (5+4=9, Grade Group 5/5 ISUP). Clinically significant tumor was detected in 46% (37/79). MRI presented a sensitivity of 89.2% (95% CI = 75 - 96%) and a specificity of 85.7%.

Figure 1 - 874

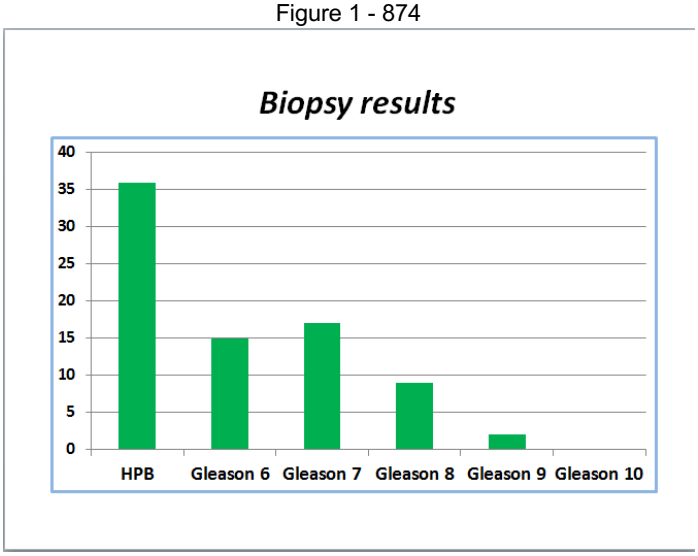


Figure 2 - 874

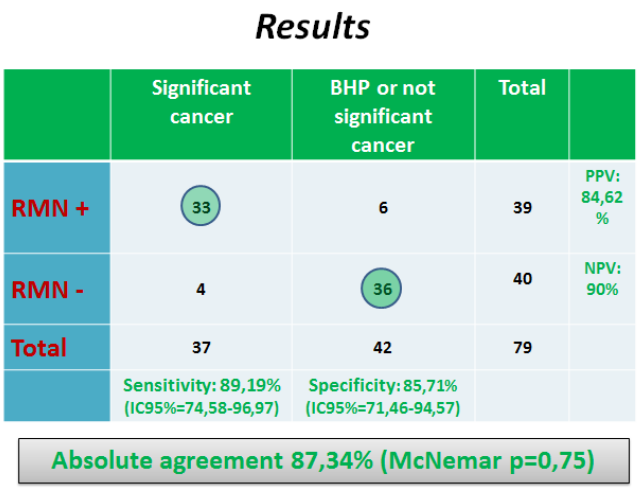


**Conclusions:** MP-MRI had a high correlation between transrectal prostate biopsy for the diagnosis of clinically significant prostate cancer. Despite high initial costs, it allows the prevention of unnecessary radical treatments in non-significant tumors and reduces the chance of detecting aggressive late cancer.

## 875 Neoadjuvant Therapy Does Not Alter Desmoplastic Response at Invasive Tumor Front in Bladder Urothelial Carcinoma

Aileen Grace Arriola[1], Sahar Farahani[2], Francesca Khani[3], Anupma Nayak[4], Lauren Schwartz[5], Abhishek Shah[6], Priti Lal[7], Bruce Malkowicz[4]

*[1]Temple University Hospital, Philadelphia, PA, [2]Renaissance School of Medicine at Stony Brook University, Stony Brook, NY, [3]Weill Cornell Medicine, New York, NY, [4]Perelman School of Medicine at the University of Pennsylvania, Philadelphia, PA, [5]Perelman School of Medicine at the University of Pennsylvania, Bala Cynwyd, PA, [6]Hospital of the University of Pennsylvania, Philadelphia, PA, [7]University of Pennsylvania, Philadelphia, PA*

**Disclosures:** Aileen Grace Arriola: None; Sahar Farahani: None; Francesca Khani: None; Anupma Nayak: None; Lauren Schwartz: None; Abhishek Shah: None; Priti Lal: None; Bruce Malkowicz: None

**Background:** As immunotherapy comes to the forefront of cancer treatment, factors within the tumor microenvironment are coming to light as affecting treatment response such as tumor infiltrating T-cells (TILs) and more recently, tumor stromal cells. A recent study in colon cancer has shown that the quality of desmoplastic reaction (DR) at the tumor front was predictive of survival. In addition, a recent study in urothelial cancer has shown that resistance to PD-1 targeted therapy might be related to genes expressed by the tumor stroma. With this increasing role of tumor stroma, we wanted to examine the relationship of the invasive tumor front TILs, stromal reaction, and PD-L1 expression in a cohort of patients who underwent cystectomies for invasive disease with and without neoadjuvant chemotherapy (NAC).

**Design:** 73 cystectomy cases from 2 institutions were included in the study. A representative slide of the invasive tumor front was assessed for TILs and DR. TILs were graded qualitatively as none, mild, moderate, or severe and DR was graded as mature, intermediate, immature, and no reaction based on the presence of myxoid stroma and/or keloidal collagen. These features were compared to tumoral PD-L1 expression (when available), tumor stage, LN status, CIS, and NAC.

**Results:** 38 cystectomies were performed after NAC and 35 were without NAC. The DR at the invasive front was characterized as no reaction in 28.8% (21/73), immature in 30.1% (22/73), intermediate in 24.7% (18/73), and mature in 16.4% (12/73). No difference between DR type was appreciated in NAC vs. No NAC cases (p-value=0.29). There were 32 PD-L1 positive cases, with H-scores ranging from 1-300, and 18 PD-L1 negative cases. PD-L1 status also did not show any significant differences with respect to DR (p-value=0.36) or history of NAC (p-value=0.88). Furthermore, history of NAC did not show any statistically significant differences when examining other parameters such as TILs response at the invasive tumor front, pathologic stage, lymph node status, or presence/absence CIS (Table 1).

**Table 1.** Pathologic features in cystectomy cases with and without neoadjuvant chemotherapy (NAC).

| | NAC | No NAC | p-value |
|---|---|---|---|
| **Stromal reaction** | | | 0.29 |
| None | 10 | 11 | |
| Immature | 15 | 7 | |
| Intermediate | 7 | 11 | |
| mature | 6 | 6 | |
| **Lymphocytic response** | | | 0.72 |
| None | 10 | 7 | |
| Mild | 17 | 22 | |
| Moderate | 6 | 7 | |
| marked | 2 | 2 | |
| **PD-L1 status** | | | 0.88 |
| Negative | 6 | 12 | |
| Positive | 10 | 22 | |
| **Pathologic stage** | | | 0.31 |
| pT2 | 5 | 4 | |
| pT3 | 14 | 22 | |
| pT4 | 16 | 2 | |
| **Lymph node status** | | | 0.16 |
| pN0 | 4 | - | |
| pN1 | 8 | 11 | |
| pN2 | 15 | 20 | |
| pN3 | 8 | 7 | |
| **CIS** | | | 0.98 |
| present | 18 | 20 | |
| absent | 17 | 18 | |

**Conclusions:** Despite maximum treatment with neoadjuvant chemotherapy, the stroma at the invasive front of UC does not show any difference when compared to those without therapy. This may be one of the multiple reasons why long-term outcomes remains dismal despite the introduction of NAC. Further validation in larger cohorts is warranted.

## 876 Tumor Budding as a High Risk Prognostic Factor in Progression of pT1 Bladder Urothelial Carcinomas

Ana Aula Olivar[1], Luisa Sofía Silva Alcoser[2], Mario Giner Pichel[2], Fernando Lozano[3], Carles Raventos Busquets[2], Ines de Torres[4], Santiago Ramon Y Cajal[2], Maria Eugenia Semidey-Raven[2]

*[1]Vall d'Hebron University Hospital (HUVH), Barcelona, Spain, [2]Vall d'Hebron University Hospital, Barcelona, Spain, [3]University Hospital Vall d' Hebron, Barcelona, Spain, [4]Vall d'Hebron Campus and Autonomous University of Barcelona (UAB), Barcelona, Spain*

**Disclosures:** Ana Aula Olivar: None; Luisa Sofía Silva Alcoser: None; Mario Giner Pichel: None; Fernando Lozano: None; Carles Raventos Busquets: None; Ines de Torres: None; Santiago Ramon Y Cajal: None; Maria Eugenia Semidey-Raven: None

**Background:** Tumor recurrence and progression is commonly observed in non-muscle invasive bladder urothelial carcinomas (NMIC,pT1), with a frequency of 41% in recurrence and 11%-20% progression in 1-5 years of follow up, despite its treatment with BCG and/or mitomycin C. The cohesion of the tumor cells can be lost in the infiltrative border of the tumor which can lead to a more aggressive behaviour. Tumor budding (TB) is defined as the presence of discohesive cells or groups less than 5 cells in the infiltrative front. Our hypothesis is that TB could be an independent high risk prognostic factor in progression of pT1 bladder carcinomas.

**Design:** A cohort of 168 TUR cases of bladder urothelial carcinomas (pT1) were selected from pathology files between 2013-2016 with a minimum of 2 years follow-up. In each case, TB number was determined by counting isolated cells and groups <5 cells in 200X (0.785 $mm^2$) field, on the “hot spot” infiltrating margin. Those cases with abundant inflammatory cells were excluded. Other clinical features such as age, gender, smoke habit, pT substaging (lamina propia infiltration a/b/c) and presence of CIS and squamous metaplasia (SM) were included. Statistical analysis was done with SPSS Data Analysis Program (v.20).

**Results:** A total of 168 cases were evaluated with a median age of 75,3y and male predominance (90,5%). 79,5% of patients had smoke habit. There was CIS associated in 16,7% of cases and SM in 25,6%. Lymph/vascular invasion was seen in 6% of the sample. Regarding the substaging; 54,6% cases were pT1a, 27,6% pT1b and 17,79% pT1c, respectively. There were 80% of initial tumors and 77,4% received BCG induction therapy. There was a median follow up of 34m with a progression rate of 19% (32 cases). TB had a cut-off point (ROC curve) of 6 buds/200X and was seen in 29,2% of cases. In the univariant analysis, there was a statistically significant association between BCG induction (p=0,012), presence of CIS (p=0,004), lymphovascular invasion (p=0,007) and tumor budding (p=0,005) and

progression free survival (PFS). In the multivariate analysis, presence of tumor budding (p=0,035) and CIS (p=0,002) were independent prognostic factors of lower PFS and BCG induction (p=0,022) of better PFS.

**Conclusions:** TB could be considered a new independent high risk prognostic factor of progression in NMIC (pT1) in TUR biopsies that could help stratify patients and determine the best treatment options in patients with progression tumors.

## 877 PD-L1 Expression Patterns in Muscle-Invasive Bladder Carcinoma and Their Association with Immunohistochemical Phenotypes and CD8+ Tumor Infiltrating Lymphocytes

Yanfeng Bai[1], Xiaodong Teng[1]
[1]*The First Affiliated Hospital, College of Medicine, Zhejiang University, Hangzhou, Zhejiang, China*

**Disclosures:** Yanfeng Bai: None

**Background:** The emergency of immune checkpoint inhibitors (ICI) has achieved outstanding duration of disease control. The PD-L1 expression assessed by immunohistochemical (IHC) analysis is a favourable predictive biomarker of ICI efficacy. It was reported there was an relationship between molecular subtypes and clinical prognosis of bladder carcinoma. Besides, IHC phenotypes can represent molecular subtypes. Bladder carcinoma is also known to show an adaptive immune resistance, particularly affecting lymphocytes. We aimed to determine PD-L1 expression status in muscle-invasive bladder carcinoma (MIBC), and to analyze the relationship between their expression and IHC phenotypes. The associations between PD-L1 expression and CD8+ tumor infiltrating lymphocytes were also evaluated.

**Design:** IHC staining for PD-L1,CK5/6,CK20, CD44 and P53 was analysed in 122 patients with MIBC. The antibody used for PD-L1 was SP263. Among these patients, 65 cases with metastatic lesions, preoperative biopsy or electrotomy received multiple PD-L1 detection. CD8+ T lymphocytes were detected in 56 cases.

**Results:** Totally 122 patients received radical cystectomy, the overall PD-L1 positivity was 34.43% (42/122). Tumor cells and immune cells positive for PD-L1 was 26.23% (32/122) and 16.39% (20/122), respectively. If metastatic lesions, preoperative biopsy and electrotomy were detected simultaneously, the positive rate of PD-L1 increased to 40.15 (49/122) , positive patients increased by 7 cases. There was a reverse correlation between overall PD-L1 positive and intravascular tumor thrombus ($P$<0.05). The tumor cells positive for PD-L1 was inversely correlated with intravascular tumor thrombus and positively correlated with tumor size ($P$<0.05). The expression of PD-L1 for overall assessment and tumor cells was different among the four IHC phenotypes ($P$<0.05). Compared with non-basal cell type, the positive rate of PD-L (overall assessment, tumor cells or immune cells) in basal cell type was higher ($P$<0.05). CD8+ T cell infiltration did not correlate with PD-L1expression.

| Feature | Overall PD-L1 expression | | | TC PD-L1 expression | | | IC PD-L1 expression | | |
|---|---|---|---|---|---|---|---|---|---|
| | Positive | Negative | P-value | Positive | Negative | P-value | Positive | Negative | P-value |
| Gender | | | >0.05 | | | >0.05 | | | >0.05 |
| Female | 4 | 12 | | 2 | 14 | | 3 | 13 | |
| Male | 38 | 68 | | 30 | 76 | | 17 | 89 | |
| Age(years) | | | >0.05 | | | >0.05 | | | >0.05 |
| >60 | 35 | 66 | | 28 | 73 | | 14 | 87 | |
| ≤60 | 7 | 14 | | 4 | 17 | | 6 | 15 | |
| T stage | | | >0.05 | | | >0.05 | | | >0.05 |
| T2 | 14 | 19 | | 11 | 22 | | 8 | 25 | |
| T3+T4 | 28 | 61 | | 21 | 68 | | 12 | 77 | |
| Lymph node metastasis | | | >0.05 | | | >0.05 | | | >0.05 |
| Yes | 12 | 15 | | 10 | 19 | | 7 | 22 | |
| No | 30 | 65 | | 22 | 71 | | 13 | 80 | |
| Intravascular tumor thrombus | | | <0.05 | | | <0.05 | | | >0.05 |
| Yes | 11 | 36 | | 5 | 42 | | 6 | 41 | |
| No | 31 | 44 | | 27 | 48 | | 14 | 61 | |
| Nerve infiltration | | | >0.05 | | | >0.05 | | | >0.05 |
| Yes | 9 | 18 | | 7 | 20 | | 2 | 25 | |
| No | 33 | 62 | | 25 | 70 | | 18 | 77 | |
| Tumor size | | | >0.05 | | | <0.05 | | | >0.05 |
| >3cm | 29 | 44 | | 25 | 49 | | 13 | 61 | |
| ≤3cm | 13 | 36 | | 7 | 41 | | 7 | 41 | |
| Tumor number | | | >0.05 | | | >0.05 | | | >0.05 |
| Single | 40 | 70 | | 31 | 79 | | 18 | 92 | |
| Multiple | 2 | 10 | | 1 | 11 | | 2 | 10 | |
| IHC phenotypes | | | <0.05 | | | <0.05 | | | >0.05 |
| Luminal | 10 | 43 | | 6 | 47 | | 5 | 48 | |
| Basal | 22 | 21 | | 16 | 27 | | 11 | 32 | |
| P53 | 10 | 13 | | 10 | 13 | | 4 | 19 | |
| Others | 0 | 3 | | 0 | 3 | | 0 | 3 | |
| IHC phenotypes | | | <0.05 | | | <0.05 | | | <0.05 |
| Basal | 22 | 21 | | 16 | 27 | | 11 | 32 | |
| Non-basal | 20 | 59 | | 16 | 63 | | 9 | 70 | |

**Conclusions:** It is necessary to detect PD-L1expression in multiple tumor lesions for the same patient. The intrinsic and extrinsic of PD-L1 expression patterns are both detected. The positive rate of PD-L1 was inconsistent among different IHC phenotypes.

## 878 Histopathological, Clinical, and Molecular Characteristics of Prostatic Adenocarcinoma Diagnosed in Men Aged up to 45 Years

Nicholas Baniak[1], Michelle Hirsch[1], Anthony D'Amico[1], Andres Acosta[2]
*[1]Brigham and Women's Hospital, Boston, MA, [2]Brigham and Women's Hospital, Harvard Medical School, Boston, MA*

**Disclosures:** Nicholas Baniak: None; Michelle Hirsch: None; Anthony D'Amico: None; Andres Acosta: None

**Background:** Early onset prostate cancer (PC) represents a distinct cohort of patients that has been infrequently studied. In prior series, early-onset PC has been defined as PC diagnosed before 50-60 years of age. Results of these studies suggest that PC presenting in young patients has good overall clinical outcomes. Also, PC in young men may show enrichment for certain genetic alterations, including deleterious germline variants. The clinical and molecular characteristics of PC in 'very' young patients (up to 45 years-old) remains largely unexplored due to the rarity of these cases. In this study, we examined the histopathological features, clinical behavior, and genetic alterations of PC in a series of patients aged up to 45 years.

**Design:** A 15 year (2004-2019) retrospective review was completed. Pathologic review was performed on core biopsies and subsequent radical prostatectomies. Follow-up data were obtained from a prospectively maintained institutional database. FFPE tissue was obtained for nucleic acid extraction and sequencing of "clinically significant" cases (defined by the presence of any amount of cribriform PC and/or Gleason score ≥ 4+3=7).

**Results:** We identified 91 patients with a median age of 43 (range 35-45 years old). The median PSA was 4.4 ng/dL (0.04 - 1419 ng/dL) and the median number of positive cores was 2 (1-11). On biopsy, the most common Gleason score was 3+3 (GrGp1) (64%), followed by 3+4 (GrGp2) (20%), 4+3 (GrGp3) (5%), 4+4 (GrGp4) (3%), and 4+5/5+4/5+5 (GrGp5) (8%). The most common treatment modality was radical prostatectomy (91%); the remaining patients were treated with active surveillance (6%), anti-hormonal therapy (2%), and radiation (1%). Prostatectomy Gleason scores were as follows: 3+3 (GrGp1) (56%), 3+4 (GrGp2) (27%), 4+3 (GrGp3) (12%), 4+4 (GrGp4) (1%), and 4+5/5+4/5+5 (GrGp5) (4%). Follow-up data was available for 90 patients (median follow up time 68 months, range 1-173). Biochemical recurrence (BCR) developed in 6 patients (7%) with a median time to recurrence of 22 months (1-65). Death from disease occurred in 2 (2%) of patients. Overall/global GrGp5 on biopsy and PSA > 10 ng/dL were associated with risk of BCR (figure).

Figure 1 - 878

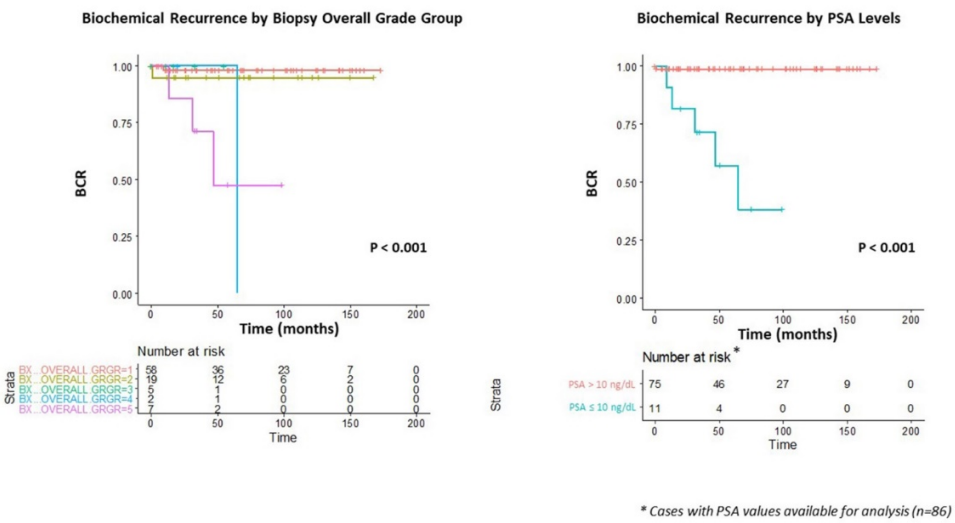


**Conclusions:** Our study adds to the limited data on young patients with PC. Overall, the patients had favorable disease characteristics and remarkably good long-term outcomes. Comparison with a cohort of PC patients aged 60-65 years and molecular characterization of cases with cribriform PC and/or GrGp3 PC or higher are forthcoming.

## 879 Carbonic Anhydrase IX (CA9) Expression in Multiple Renal Epithelial Tumor Subtypes

Nicholas Baniak[1], Michelle Hirsch[1]
*[1]Brigham and Women's Hospital, Boston, MA*

**Disclosures:** Nicholas Baniak: None; Michelle Hirsch: None

**Background:** Renal epithelial neoplasms (RENs) can be difficult to subclassify due to overlapping morphologic features, and in some cases, small sample size (ie, core biopsies). CA9 is a commonly used biomarker to support the diagnosis of clear cell renal cell carcinoma (CCRCC); however, it's overall sensitivity and specificity across a broad range of RENs is less clear. This study investigates the expression of CA9 in a wide variety of RENs, especially those in the differential diagnosis with CCRCC and less common entities, to determine its reliability as a diagnostic biomarker.

**Design:** CA9 immunostaining was performed on 233 RENs; most had diagnoses confirmed by cytogenetic evaluation. The distribution of tumors was as follows: 119 CCRCCs, 44 papillary (P) RCCs, 17 chromophobe (Ch) RCCs, 16 Xp11.2 (Tr) RCCs, 11 oncocytomas, 8 unclassified (UNC) RCCs, 6 mucinous tubular and spindle cell carcinomas, 3 collecting duct carcinomas (CDCA), 3 clear cell tubulopapillary (CCTP) RCCs, 4 FH-deficient RCCs, 2 tubulocystic RCCs, and 1 eosinophilic solid and cystic RCC (ESC). Immunoreactivity was evaluated semi-quantitatively as negative (0%), very focally positive (1+, 1–10% of cells), focally positive (2+, 11–50% of cells) or diffusely positive (3+, >50% of cells).

**Results:** CCRCCs were diffusely (3+) CA9 positive in 93% of cases; an additional 3% showed focal staining and 4% were completely negative. 68% of PRCCs were focally (1+/2+) positive for CA9, whereas 32% were negative. ChRCCs were nearly always negative (88%) for CA9, with 12% showing focal (1+) reactivity. CCTPRCC were consistently 3+ positive, but with a cup-like staining pattern. TrRCCs were negative for CA9 in 55% of cases, however, 9% were diffusely positive and 36% were focally positive. 2 of 4 FH-deficient RCCs were 3+ CA9 positive, 2 of 3 CDCAs showed 2+ CA9 expression, and 5 of 8 UNCRCCs showed focal to diffuse CA9 expression. The tubulocystic RCCs and ESC were CA9 negative.

**Conclusions:** Diffuse CA9 expression was identified in nearly all CCRCCs and all CCTPRCCs (high sensitivity); however, CA9 was not entirely specific. Diagnostic pitfalls include rare CCRCCs that are negative or only focal for CA9, and a subset of TrRCC, CDCAs and UNCRCC that also express significant CA9. Focal CA9 expression can also been in a subset of RCCs (up to 50% of cases) and such findings should be taken into consideration with other morphologic, immunophenotypic, and clinical findings; the latter is especially true with core biopsy or small metastatic specimens.

## 880 SNP Microarray Analysis is a Useful Diagnostic Tool for RCC Subtyping

Nicholas Baniak[1], Paola Dal Cin[1], Azra Ligon[1], Adrian Dubuc[1], Michelle Hirsch[1]
*[1]Brigham and Women's Hospital, Boston, MA*

**Disclosures:** Nicholas Baniak: None; Paola Dal Cin: None; Azra Ligon: None; Adrian Dubuc: None; Michelle Hirsch: None

**Background:** Renal cell carcinomas (RCC) are known to have significant morphologic overlap yet distinct genetic findings. Previously at our institution, prospective conventional G-band karyotype was frequently performed to help classify RCCs; however, not all cases required such genetic evaluation for diagnosis. More recently, following validation with a cohort of RCCs with known chromosomal changes, single nucleotide polymorphism (SNP) microarray analysis has replaced karyotype for difficult to classify RCCs. The goal of this study was to describe our experience with RCC SNP analysis including its utility in resolving difficult to diagnose RCCs.

**Design:** A retrospective review was completed for RCC cases that required SNP microarray analysis over a 28 month period. SNP analysis was performed using the Affymetrix Oncoscan assay. SNP microarray results were evaluated for diagnostic findings and were compared to proposed histological diagnoses during clinical evaluation.

**Results:** SNP microarray was performed on 34 renal tumors, 32 of which successfully yielded chromosomal abnormalities; the remaining 2 demonstrated normal microarray results. The most common indication for SNP microarray was the need to subtype a RCC with unusual morphology (ie, not otherwise specified (NOS)/unclassified) (13 cases, 38%). Other indications included differentiating clear cell (CC) RCC, TCEB1-mutated RCC, and clear cell tubulopapillary RCC (5 cases, 15%), papillary (P) RCC vs mucinous tubular and spindle cell carcinoma (3 cases, 9%), cases with tubulocystic carcinoma architecture (4 cases, 12%), differentiating chromophobe RCC, oncocytoma and other oncocytic neoplasms (4 cases, 12%), ruling out translocation RCC (2 cases, 5%), and question of a collecting duct carcinoma (3 cases, 9%). Definitive diagnostic information was obtained in 18/32 cases (56%), including 10 CCRCCs, 6 PRCCs, 1 oncocytoma, and 1 TCEB1-mutated RCC. Abnormal, but non-specific, results were found in 14/32 cases (44%). Of the 13 NOS/unclassified RCCs prior to SNP analysis, 9 (69%) received diagnostic chromosomal changes with SNP microarray, allowing for definitive RCC subtyping.

**Conclusions:** When used selectively, SNP analysis is a very useful ancillary study for renal tumor subclassification, particularly when RCC NOS/unclassified RCC would otherwise be the final diagnosis. Even when diagnostic results are not obtained by SNP microarray, the exclusion of certain entities, such as TCEB1-mutated RCC, still provides useful diagnostic information.

## 881 The Clinical Significance of Perineural Invasion on Prostate Needle Biopsy: Involvement of Single vs. Multiple Parts of the Specimen

Phoenix Bell[1], Pratik Gurung[1], Numbereye Numbere[2], Yuki Teramoto[1], Zhiming Yang[1], Hiroshi Miyamoto[1]
*[1]University of Rochester Medical Center, Rochester, NY, [2]University of Rochester Medical Center, Pittsford, NY*

**Disclosures:** Phoenix Bell: None; Pratik Gurung: None; Numbereye Numbere: None; Yuki Teramoto: None; Zhiming Yang: None; Hiroshi Miyamoto: None

**Background:** The presence of perineural invasion (PNI) by prostate cancer has been associated with adverse pathologic features, including extraprostatic extension, and resultant poor patient outcomes. However, the impact of PNI quantification on biopsy (Bx) specimens remains poorly understood. In the present study, we compare radical prostatectomy (RP) findings and oncologic outcomes in prostate cancer patients in whom Bx has exhibited PNI in single vs. multiple sites.

**Design:** We assessed consecutive patients who had undergone sextant prostate needle Bx (6 parts, ≥12 cores) followed by RP from 2010-2016. Within our Surgical Pathology database, we identified a total of 539 men who met the inclusion criteria for PNI on Bx. Cases showing PNI on target Bx were excluded.

**Results:** PNI was found in 1 (n=320), 2 (n=131), 3 (n=52), 4 (n=23), 5 (n=7), and 6 (n=6) parts of the Bx specimens. Multiple PNIs were associated with higher Grade Group (GG) on Bx (GG1 vs. GG2-5, $P$=0.003; GG1-2 vs. GG3-5, $P$<0.001; GG1-3 vs. GG4-5, $P$=0.020; GG1-4 vs. GG5, $P$=0.012) or RP (GG1 vs. GG2-5, $P$=0.010; GG1-2 vs. GG3-5, $P$=0.022; GG1-3 vs. GG4-5, $P$=0.030; GG1-4 vs. GG5, $P$=0.010), higher pT (2 vs. 3, $P$<0.001; 2/3a vs. 3b, $P$<0.001), lymph node metastasis (pN0 vs. pN1, $P$=0.001), positive surgical margin (SM) ($P$=0.002), larger estimated tumor volume ($P$<0.001), and higher preoperative prostate-specific antigen (PSA) level ($P$=0.031), compared with a single PNI. When these were compared in subgroups of patients (based on Bx GG), significant ($P$<0.05) differences in pT (GG2, GG1-2, GG3, GG1-3), pN (GG2, GG1-2), SM status (GG3, GG1-3), or tumor volume (GG2, GG1-2, GG3, GG1-3) were observed. Kaplan-Meier analysis coupled with log-rank test revealed a significantly higher risk of biochemical recurrence (BCR) after RP in all ($P$<0.001) or subgroups (Bx GG3: $P$=0.045; Bx GG1-3: $P$<0.001) of patients with multiple PNIs on Bx, compared to those with a single PNI. There were no significant differences in RP findings or BCR in Bx GG1 or Bx GG4-5 cases. Meanwhile, statistically significant differences in GG on Bx or RP, pT or pN stage, SM, tumor volume, PSA, and BCR between 1-2 vs. 3-6 parts of PNI were still seen.

**Conclusions:** Compared with a single site of PNI, multiple parts with PNI on prostate Bx were associated with worse histopathologic features in RP specimens and poorer prognosis. Pathologists may thus need to report PNI, if present, in every part of the prostate Bx specimen, especially those showing GG1-3 cancer.

## 882 Biochemical Recurrence after Radical Prostatectomy in Patients with Organ-Confined Prostate Cancer (pT2), Gleason Score 7, and Negative Surgical Margins: Which Method (Extent vs Percent) Best Evaluates Influence of Gleason Grade 4?

Athanase Billis[1], Leandro Freitas[2], Larissa Costa[1], Icleia Barreto[1], Mariana Deininger[1], Natalia Lima[1], Vitor Assad[1], Luís Magna[1], Wagner Matheus[1], Ubirajara Ferreira[3]
*[1]State University of Campinas (Unicamp), Campinas, SP, Brazil, [2]UNICAMP - Brazil, Valinhos, SP, Brazil, [3]UNICAMP, Campinas, SP, Brazil*

**Disclosures:** Athanase Billis: None; Leandro Freitas: None; Larissa Costa: None; Mariana Deininger: None; Natalia Lima: None; Vitor Assad: None

**Background:** The amount of Gleason pattern 4 in a score 7 case has prognostic value and may be helpful for patient management. There are questions that arise relating to the reporting of Gleason pattern 4: extent or percent?

**Design:** From a total of 530 patients submitted to RP, 88 consecutive patients had organ-confined disease (pT2), negative surgical margins and Gleason score 7. The surgical specimens were totally step-sectioned. Total tumor extent, extent of grade 3, and extent of each grade 4 pattern were evaluated by a semiquantitative point-count method. Briefly, drawn on a sheet of paper, each quadrant of the transverse sections contained 8 equidistant points each one corresponding to 10-15% of the quadrant area. During the microscopic examination of the slides, the tumor area of grade 3 and grade 4 patterns were drawn on the correspondent quadrant seen on the paper using different colors. In each case. Gleason grade 4 was evaluated as tumor extent (total positive points) and as percent of the total tumor area. Biochemical recurrence was defined as PSA $\geq$ 0.2 ng/ml. Kaplan-Meier curves were performed for time to biochemical recurrence (TBCR), and Cox stepwise logistic regression model to identify significant predictors of shorter TBCR.

**Results:** Age, prostate weight, total tumor extent, percent of fused glands, and percent of ill-defined glands were not significantly predictive of shorter TBCR. Gleason grade 4 extent (p=0.027), percent of glomeruloid pattern (0.011), percent of cribriform pattern (p=0.009), preoperative PSA (p=0.003), percent Gleason grade 4 (p=0.001), and PSA density (p=0.001) were significantly predictive of shorter TBCR in univariate analysis, but only PSA density (p=0.004), and percent Gleason grade (p=0.004) were significantly predictive in multivariate

analysis. Stratifying percent Gleason grade 4, the results for shorter TBCR by Kaplan-Meier curves were ≤ 5% vs 6-10% (p=0.421), 6-10% vs 11-20% (p=0.630), 11.20% vs 21.30% (p=0.571), and 21-30% vs >30% (p=0.057).

**Conclusions:** The findings favor that percent is superior to extent in evaluating Gleason grade 4 influence on biochemical recurrence and was the only significant method of evaluation in multivariate analysis. In this cohort of patients >30% Gleason grade 4 was significantly associated with shorter TBCR. Both cribriform and glomeruloid patterns, but not fused and ill-defined glands, were significantly predictive of shorter TBCR in univariate analysis.

## 883 PD-L1 Expression in Metastatic Clear Cell Renal Cell Carcinoma Using Sp142, Sp263 and E1L3N

Matteo Brunelli[1], Anna Calio'[2], Enrico Munari[3], Serena Pedron[2], Elisa Ciocchetta[2], Giuseppe Bogina[4], Giuseppe Zamboni[2], Guido Martignoni[5]
*[1]Verona, Italy, [2]University of Verona, Verona, Italy, [3]Sacro Cuore Hospital, Verona, Italy, [4]Sacro Cuore Hospital, Negrar di Valpolicella, Italy, [5]University of Verona, Ospedale Pederzoli, Peschiera del Garda, Italy*

**Disclosures:** Matteo Brunelli: None; Anna Calio': None; Serena Pedron: None; Elisa Ciocchetta: None; Giuseppe Zamboni: None; Guido Martignoni: None

**Background:** PD-L1 different clones has not been simultaneously tested on metastatic renal cell carcinoma.

**Design:** 101 clear cell metastatic RCCs were collected; TMAs built and immunoreactions performed using PD-L1 clones: Sp142, Sp263 and E1L3N.

**Results:** Both primitive clear cell RCC and lung/liver metastasis were available in 9 cases. The remaining cases were tissue metastases: 21 pulmonary, 3 liver, 24 cerebral localization, 31 pancreatic metastasis and 13 from peripheral sites (5 skin, 1 stomach, 4 bone and 3 thyroid gland). >1% PD-L1 clone sp142 expressed in 20/101(17%), sp263 in 19/101(19%) and E1L3N 17/101(17%) on metastases. >50% cut-off, a single case was observed (1%, with agreement by all clones); no >50% immunoexpression was observed by using sp263 and E1L3N clones. >5%x<49% cut-off , again a single case was observed (1%, with concordance along three antibodies). PD-L1 sp142 showed positivity >1% in 6/25(24%), sp256 in 6/25(24%) and clone E1L3N in 5/25(20%) of cerebral metastasis, 1/25(4%) scored positivity >5% for all three antibodies. Pancreatic metastasis were positive in 2/32(6%) in all three different clones. Lung localizations scored >1% positive for sp142 in 6/27(22%), sp263 in 4/27(15%) and E1L3N 5/27(19%). 1/27(4%) showed positivity >50% to PD-L1 sp142 clone. Liver localizations scored >1% with sp142 clone in 1/4(25%), sp263 and E1L3N clones in 0/4 cases. Metastasis on distant peripheral sites scored >1% positivity in 5/13(38%) with sp142 staining and 5/13(38%) using sp263 and E1L3N clones. Skin metastasis showed positivity >1 for all clones in 1/5(20%), stomach localization positivity >1% in 1/1 for all clones, bone metastasis showed >1% score in 3/4(75%) for all antibodies and thyroid gland localization showed positivity in 0/3 cases for all three evaluations.

**Conclusions:** >1% PD-L1 expression is observed in 17%, 19% and 17% of tissue metastases by using respectively sp142, sp262 and E1L3N clones. Tissue metastases are rarely representative of the primary renal cell carcinoma after matching immunohistochemical values.

## 884 Subcategorization of T1 Bladder Cancer on Biopsy and Transurethral Resection Specimens for Predicting Progression

Anna Budina[1], Sahar Farahani[2], Priti Lal[3], Anupma Nayak[4]
*[1]North Wales, PA, [2]Renaissance School of Medicine at Stony Brook University, Stony Brook, NY, [3]University of Pennsylvania, Philadelphia, PA, [4]Perelman School of Medicine at the University of Pennsylvania, Philadelphia, PA*

**Disclosures:** Anna Budina: None; Sahar Farahani: None; Priti Lal: None; Anupma Nayak: None

**Background:** Patients (pts) with lamina propria-invasive urothelial carcinoma of the bladder (T1) have highly variable prognosis, with a significant subset of pts (up to 50%) progressing to muscle-invasive disease or metastasis despite surveillance and intravesical therapy. The WHO classification system (2016) and the AJCC staging manual (8th edition) recommend more studies to analyze the value of pathologic subcategorization of T1 disease in predicting progression. Herein, we compare previously published and novel methodologies of measuring the extent of lamina propria invasion to predict the likelihood of progression to muscle invasion or metastasis.

**Design:** This study includes a cohort of 73 pts with a diagnosis of pT1 disease on TUR specimens identified from our pathology database (2007–2014). Cases with a prior history of T1 or muscle invasive (T2) disease were excluded. The H&E slides were reviewed by a pathologist subspecializing in GU pathology. Sub-staging was performed using the following measurement criteria for each specimen: 1) muscularis mucosae involvement (above vs into) 2) number of invasive foci 3) focal vs extensive invasion where focal is defined as 2 or less foci each measuring <1 mm 4) micrometric measurement of maximal depth of invasion 5) aggregate length of tumor invasion and 6) the size of largest invasive focus. Clinicopathologic variables, progression (=/>T2/nodal/distant metastasis) and survival data were compared.

**Results:** Univariate analysis indicate that the best predictors of T1 carcinoma progression are depth of invasion (p=0.02), largest invasive focus (p=0.01), aggregate invasion (p=0.009) and number of invasive foci (p=0.008) (Table 1). Our data showed no significant correlation with gender, prior treatment status, grade, presence of CIS between progressors and non-progressors. Survival analysis revealed that depth of invasion (HR=1.5, p=0.01), largest invasive focus (HR= p=0.01) aggregate invasion (HR=1.02, p=0.002) and number of foci (HR=1.16, p=0.002) were associated with reduced progression-free survival. Finally, using ROC analysis we calculated optimal cut-off values for the statistically significant measurement methods (Figure 1).

| **Table 1.** | | | |
|---|---|---|---|
| T1 Measurement Criteria in Predicting Progression Status | | | |
| Criteria | Description | Coefficient | p value |
| Depth of invasion, μm | measured from the basement membrane to the deepest point of invasion | 0.524 | 0.024 |
| Largest invasive focus, μm | measurement of largest contiguous focus of invasion in any direction | 0.281 | 0.011 |
| Aggregate invasion, μm | (measures greatest dimension of each invasive tumor focus in specimen and adds them together) | 0.076 | 0.009 |
| Number of foci | multiple foci defined by the presense of pT1 disease at different location in bladder or separate invasive foci in specimen | 0.257 | 0.008 |
| Above vs. Into muscularis mucosae | uses the muscularis mucosae anotamic landmark to determine depth of invasion | 0.628 | 0.347 |
| Focal or extensive invasion | focal defined as 2 or less foci of invasion of <1mm each; "extensive" is more than focal | 0.693 | 0.323 |

Figure 1 - 884

| Optimal Cut-off Value for Statistically Significant Methods | | | | | | | | |
|---|---|---|---|---|---|---|---|---|
| | Cut-off Value | Correctly Predicted Rate, Progressive Disease | Correctly Predicted Rate, Non-progressive Disease | Correctly Predicted Rate, Total | Hazard Ratio | 95% CI of HR | | P-value |
| Depth of Invasion | >=1.3592 | 73.33% | 65.45% | 67.14% | 4.200384 | 1.335008 | 13.21583 | 0.014 |
| Largest Contiguous Focus | >=3.561 | 50% | 80.70% | 73.97% | 3.115028 | 1.12757 | 8.605588 | 0.028 |
| Aggregate Length of Invasion | >=8.915 | 50% | 87.70% | 80.80% | 4.868033 | 1.757365 | 13.48482 | 0.002 |
| Number of Invasion Foci | >=3 | 68.75% | 70.18% | 69.86% | 4.461473 | 1.5114 | 13.16973 | 0.007 |

**Conclusions:** These quantitative T1 substaging methods might be useful for classifying pts into low-risk and high-risk categories for progression. A larger cohort is needed to increase the power of the analysis and we are continuing to add subjects to this study.

## 885 Stimulator of Interferon Genes (STING) Immunohistochemical Expression in the Spectrum of Perivascular Epithelioid Cell (PEC) Lesions of the Kidney

Anna Calio'[1], Matteo Brunelli[2], Diego Segala[3], Serena Pedron[1], Enrico Munari[4], Stefano Gobbo[5], Guido Martignoni[6]
*[1]University of Verona, Verona, Italy, [2]Verona, Italy, [3]Peschiera del Garda, Italy, [4]Sacro Cuore Hospital, Verona, Italy, [5]Ospedale Pederzoli, Peschiera del Garda, Italy, [6]University of Verona, Ospedale Pederzoli, Peschiera del Garda, Italy*

**Disclosures:** Anna Calio': None; Matteo Brunelli: None; Diego Segala: None; Serena Pedron: None; Enrico Munari: None; Stefano Gobbo: None; Guido Martignoni: None

**Background:** Angiomyolipoma is the prototype of the renal perivascular epithelioid cells (PEC) lesions whose pathogenesis is determined by mutations affecting *TSC* genes, with eventual deregulation of the mTOR pathway. It is well known that mTOR complex protein is

involved in autophagy and recently it has been demonstrated the role of STING in this process. Based on this background, we sought to investigate STING immunohistochemical expression in a series of PEC lesions of the kidney.

**Design:** Fifty common angiomyolipomas, fifteen pure epithelioid PEComas, two angiomyolipomas with epithelial cysts (AMLEC) and two intraglomerular lesions were collected. Immunostaining for STING (anti-TMEM173, clone SP338, dilution 1:150, Abcam) was carried out in all cases and FISH analysis using dual color break-apart TFE3 and TFEB probes was performed in all pure epithelioid PEComas. 150 control cases (50 clear cell renal cell carcinomas, 20 papillary renal cell carcinomas, 20 chromophobe renal cell carcinomas, 20 oncocytomas, 10 clear cell papillary renal cell carcinomas and 30 MiT family renal cell carcinomas) were also immunohistochemically stained with STING.

**Results:** Strong and diffuse expression of STING was observed in 100% of common angiomyolipomas, AMLEC and intraglomerular lesions and in 87% (13/15) of pure epithelioid PEComas. *TFE3* gene rearrangement was demonstrated in two pure epithelioid PEComas, whose one was positive. None of papillary renal cell carcinomas, chromophobe renal cell carcinomas, oncocytomas, clear cell papillary renal cell carcinomas and MiT family renal cell carcinomas expressed STING. Among clear cell renal cell carcinomas, immunolabeling for STING was observed in less than 10% of tumors.

**Conclusions:** We demonstrated the expression of STING in almost all PEC lesions of the kidney. This finding is useful for diagnostic purposes, particularly in distinguishing pure epithelioid PEComa from MiT family renal cell carcinoma. The finding also suggests the hypothesis of the alteration of autophagic process in the PEC lesions of the kidney.

## 886 Pathological Features of Benign and Malignant Epithelial Abnormalities of the Penis in Transgenic Mice. An Experimental Model to Study HPV-Related Penile Carcinogenesis. Evaluation of 87 Cases

Sofía Cañete-Portillo[1], Beatriz Medeiros-Fonseca[2], Verónica Mestre[2], Diogo Estêvão[3], Diego F Sanchez[1], María José Fernandez-Nestosa[4], Fátima Casaca[5], Sandra Silva[5], Haissa Brito[6], Ana Félix[7], Rui Medeiros[8], Bruno Colaço[9], Paula Oliveira[10], Margarida Bastos[11], Peter Nelson[12], Funda Vakar-Lopez[13], Isabel Gaivão[14], Luciane Brito[6], Carlos Lopes[15], Antonio Cubilla[16], Rui Gil da Costa[17]

*[1]Instituto de Patologia e Investigacion, Asuncion, Paraguay, [2]CITAB, Universidade de Trás-os-Montes e Alto Douro, UTAD, Vila Real, Vila Real, Portugal, [3]Grupo de Oncologia Molecular e Patologia Viral, CI-IPOP, IPO-Porto, Porto, Portugal, [4]Facultad Politécnica, Universidad Nacional de Asunción, San Lorenzo, Paraguay, [5]Botelho Moniz Análises Clínicas (BMAC), Porto, Portugal, [6]Biobanco de Tumores e DNA do Maranhão, PPGSAD, Universidade Federal do Maranhão (UFMA), São Luís, MA, Brazil, [7]NMS/IPO, Lisboa, Portugal, [8]Grupo de Oncologia Molecular e Patologia Viral, CI-IPOP, IPO-Porto; Faculdade de Medicina, Universidade do Porto; Serviço de Virologia, IPO- Porto; CEBIMED, Faculdade de Ciências da Saúde, Universidade Fernando Pessoa, Porto, Portugal, [9]CITAB, Universidade de Trás-os-Montes e Alto Douro, UTAD; Departamento de Zootecnia, Universidade de Trás-os-Montes e Alto Douro, UTAD, Vila Real, Vila Real, Portugal, [10]CITAB, Universidade de Trás-os-Montes e Alto Douro, UTAD; Departamento de Ciências Veterinárias, Universidade de Trás-os-Montes e Alto Douro, UTAD, Vila Real, Vila Real, Portugal, [11]LEPABE, Faculdade de Engenharia, Universidade do Porto, Porto, Portugal, [12]Fred Hutchinson Cancer Research Center; University of Washington, Seattle, WA, [13]University of Washington, Seattle, WA, [14]CECAV, Universidade de Trás-os-Montes e Alto Douro, UTAD, Vila Real, Vila Real, Portugal, [15]Departamento de Patologia Molecular, ICBAS, Universidade do Porto, Malta Vila Do Conde, Porto, Portugal, [16]Instituto de Patologia e Investigacion, Asunción, Central, Paraguay, [17]Fred Hutchinson Cancer Research Center, Seattle, WA*

**Disclosures:** Sofía Cañete-Portillo: None; Beatriz Medeiros-Fonseca: None; Verónica Mestre: None; Diogo Estêvão: None; Diego F Sanchez: None; Haissa Brito: None; Ana Félix: None; Bruno Colaço: None; Paula Oliveira: None; Funda Vakar-Lopez: None; Isabel Gaivão: None; Carlos Lopes: None; Antonio Cubilla: None; Rui Gil da Costa: None

**Background:** We are presenting detailed pathological features of lesions identified in a transgenic mouse experimental model for the study of HPV-related penile neoplasia.

**Design:** Transgenic mice with the expression of all HPV16 early genes expressed in squamous epithelia by the cytokeratin 14 (CK14) gene promoter were evaluated. 87 penile specimens stained with H&E and Ki-67 were analyzed. We employed two experimental groups based on exposure to carcinogen dimethylbenz(o)anthracene (DMBA): group 1 (n = 54, HPV+/DMBA-) and group 2 (n = 33, HPV+/DMBA+). The mice were sacrificed four weeks after the last treatment, at 30 weeks-old. Fisher's exact test was used for statistical evaluation.

**Results:** 50 specimens (57%) showed lesions that occurred predominantly in the foreskin, rarely in glans and were uni and multicentric There were 34 lesions found in 26 animals of the non-treated group (1.3 lesions per animal) whereas in the treated group there were 46 lesions in 24 animals (1.9 lesions per animal) (Table). Spontaneous lesions, mostly condylomas (Fig. 1) and PeIN (3 cases) appeared in group 1 in 30 weeks. In group 2, we found non-atypical and atypical condylomas, PeINs and invasive squamous cell carcinomas. Subtypes of PeIN were differentiated (1 case), warty (Fig. 2A) (6 cases), basaloid (4 cases) and warty-basaloid (4 cases). Subtypes of invasive carcinomas were warty (3 cases), warty-basaloid (Fig. 2B) (2 cases), usual, sarcomatoid and undifferentiated (1 case each). The latter tumor was mixed with medullary and lymphoepithelioma-like features. Ki-67 staining showed positivity in basal and parabasal layers in the majority of condylomas, typical or atypical, whereas in PeIN and invasive carcinomas the staining rate was higher.

| Table. Lesions according to experimental design | | | |
|---|---|---|---|
| | **HPV+DMBA-**<br>**No. of cases**<br>**(%)** | **HPV+DMBA+**<br>**No. of cases**<br>**(%)** | ***Total*** |
| **Non-atypical condylomas** | 30<br>(*68*) | 14<br>(*32*) | ***44*** |
| **Atypical condylomas** | 1<br>(*8*) | 12<br>(*92*) | ***13*** |
| **PeIN** | 3<br>(*20*) | 12<br>(*80*) | ***15*** |
| **Invasive carcinoma** | 0 | 8<br>(*100*) | ***8*** |
| ***Total*** | *34*<br>*(43)* | *46*<br>*(57)* | ***80*** |

P value=1.062e-06

Figure 1 - 886

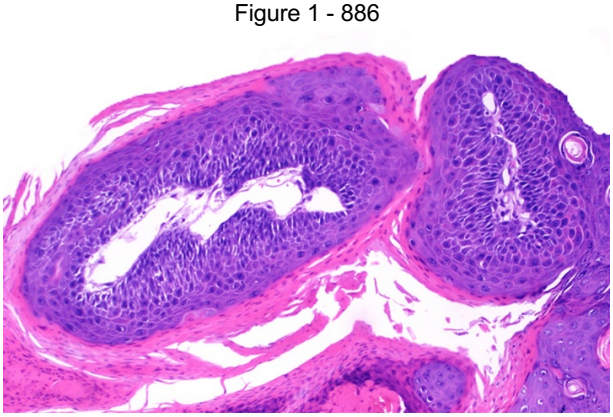

**Condyloma acuminatum (classic condyloma).** Condylomatous papillae with central fibrovascular core. There are hyper and parakeratosis, papillomatosis and isolated koilocytes.

Figure 2 - 886

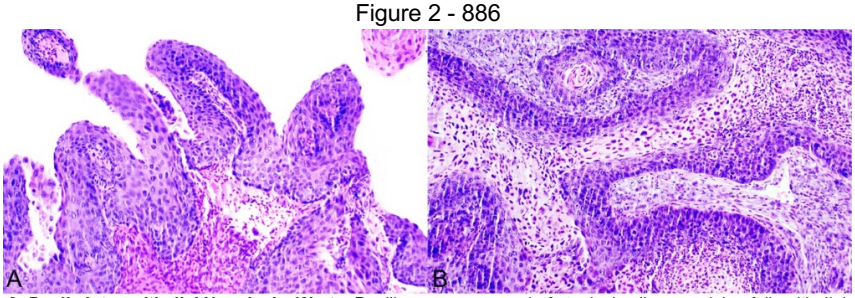


**A. Penile Intraepithelial Neoplasia. Warty.** Papillae are composed of atypical cells comprising full epithelial thickness. There are distinctive fibrovascular cores. **B. Invasive carcinoma. Warty-basaloid.** Confluent neoplastic nests of invasive carcinoma with central warty and peripheral basaloid features.

**Conclusions:** Non-atypical flat and classic condylomas were identified in HPV-induced non-treated cases (88%), whereas atypical condylomas, PeINs and invasive carcinomas significantly predominated in HPV-induced DMBA-treated cases (70%). The pathological features of the lesions encountered in this model were strikingly similar to the morphology of HPV-related human penile neoplasia, providing experimental evidence for the causal role of HPV16 in penile squamous cell carcinomas. This novel model recapitulates key steps of HPV-related penile carcinogenesis reproducing morphological and molecular features of penile cancer. It provides a unique in vivo tool for studying its biology and advancing translational research.

## 887 The Value and Limitations of P16 and Ki67 Immunostains in the Diagnosis and Subtyping of Differentiated Penile Intraepithelial Neoplasia (DPeIN)

Sofía Cañete-Portillo[1], Diego F Sanchez[1], Maria Cabanas[2], Ingrid RodrÃguez[3], Enrique Ayala[4], María José Fernandez-Nestosa[5], Carmelo Caballero[6], Antonio Cubilla[7]
*[1]Instituto de Patologia e Investigacion, Asuncion, Paraguay, [2]Instituto Nacional del Cancer, Lambare, Paraguay, [3]Universidad Nacional de Asuncion, Asunción, Paraguay, [4]Instituto Nacional del Cancer, Mexico, [5]Facultad Politécnica, Universidad Nacional de Asunción, San Lorenzo, Paraguay, [6]GenPat, Asuncion, Central, Paraguay, [7]Instituto de Patologia e Investigacion, Asunción, Central, Paraguay*

**Disclosures:** Sofía Cañete-Portillo: None; Diego F Sanchez: None; Antonio Cubilla: None

**Background:** Penile Intraepithelial Neoplasia is separated in HPV- (warty and basaloid) and non-HPV-related (differentiated). Differentiated PeINs are characterized by prominent squamous maturation. Histologically, they are heterogeneous and squamous hyperplasia (SH) need to be ruled out. The purpose of this study was to evaluate the role of Ki67 and p16 immunostaining in the separation of HPV- from non-HPV-related PeINs and in the differential diagnosis of hyperplasia and subtypes of Differentiated PeIN.

**Design:** Studied cases were 16 patients with 26 lesions classified as follow: Squamous hyperplasia (8 lesions), Differentiated PeIN (18 lesions), subclassified in 1. Hyperplasia-like (HLDPeIN) (mild atypia at basal layer), 2. Classic (atypia in basal and parabasal layers) and 3. Pleomorphic (atypia in more than one third of the epithelial thickness). Most cases were associated with invasive squamous cell carcinomas except three. Lichen sclerosus was present in half of the cases. In addition to H&E, Ki67 and p16 immunostains were performed. Statistical evaluation was done using Fisher's exact test.

**Results:** P16 was negative in all lesions. The pattern of Ki67 nuclear staining according to subtypes of DPeIN is shown in the Table.

| Ki67 pattern in SH and DPeINs | | | | | |
|---|---|---|---|---|---|
| **Ki67** | **SH** | **HLDPeIN** | **Classic DPeIN** | **Pleomorphic DPeIN** | **Total** |
| **Negative** | 2 (25) | 0 (0) | 1 (11) | 0 (0) | 3 (11) |
| **Basal spotty** | 6 (75) | 1 (17) | 4 (45) | 1 (33) | 12 (46) |
| **Basal/parabasal continuous** | 0 (0) | 4 (66) | 3 (33) | 0 (0) | 7 (27) |
| **Basal/suprabasal** | 0 (0) | 1 (17) | 1 (11) | 0 (0) | 2 (8) |
| **At least third** | 0 (0) | 0 (0) | 0 (0) | 2 (67) | 2 (8) |
| **Total** | 8 (100) | 6 (100) | 9 (100) | 3 (100) | 26 (100) |

Fisher's exact test p-value = 0.01157

**Conclusions:** Squamous hyperplasia and DPeINs were all negative for p16. The Ki67 profile of negative to spotty basal layer staining was typical of SH. Continuous basal to parabasal staining was noted in HL and classic DPeINs. Pleomorphic DPeIN was p16 negative and Ki67 was positive in at least a third of the epithelial thickness. The negativity of p16 in hyperplasia and DPeIN would separate these epithelial abnormalities as non-HPV-related. Ki67 was useful to separate SH from all subtypes of DPeIN. There was a limited value of Ki67 in the differential diagnosis of subtypes of DPeIN.

## 888 Papillary Renal Cell Carcinomas Demonstrating Micropapillary Features: An Investigation into the Diagnostic and Prognostic Implications

Beatriz Caraballo Bordon[1], Maha Abdulla[2], Guang-Qian Xiao[3], Pamela Unger[2]
*[1]Northwell Health Lenox Hill Hospital, New York, NY, [2]Lenox Hill Hospital, New York, NY, [3]Keck Medical Center of USC, Los Angeles, CA*

**Disclosures:** Beatriz Caraballo Bordon: None; Maha Abdulla: None; Guang-Qian Xiao: None; Guang-Qian Xiao: None; Pamela Unger: None

**Background:** Micropapillary carcinoma (MC) is associated with early lymph node metastasis and poor prognosis and has been reported in carcinoma of various origins. MC arising in any renal cell carcinoma is described in rare case reports and not previously in papillary renal cell carcinoma (PRCC). The aim of this study is to examine the incidence and pathology of PRCC containing micropapillary elements.

**Design:** A database search of all nephrectomy specimens made at the University of Southern California and Lenox Hill Hospital (NY) June 2016-June 2019, retrieved a total of 847 RCC cases (690 from USC and 157 from LHH). 70 cases were PRCC (54 from USC, 16 from

LHH). Of these 70 cases, 10 had a micropapillary component. The diagnosis of MC was made using routine histology and based on the presence of small clusters of cells without a vascular core and with or without being surrounded by lacunar spaces. Various pathologic parameters were evaluated.

**Results:** Nine of the 10 cases with a micropapillary component were from radical nephrectomies, and one from a partial nephrectomy. Grossly, cases were equally divided into well circumscribed and infiltrative (5 each) and average tumor size was 9.7 cm (range 2-16 cm). The percentage of micropapillary elements ranged from 5% to 80% (average 33.2 %). See Fig. 1. Eight cases were PRCC type 2 and two were type 1. Nuclear features revealed seven (7/10) grade 3, two (2/10) grade 2. One case had sarcomatoid features and was nuclear grade 4 (1/10). Eight tumors presented with extra-renal extension and two were confined to the kidney. Six (6/7) cases containing lymph nodes revealed metastatic tumors and three had no lymph nodes submitted. See Fig. 2.

Figure 1 - 888

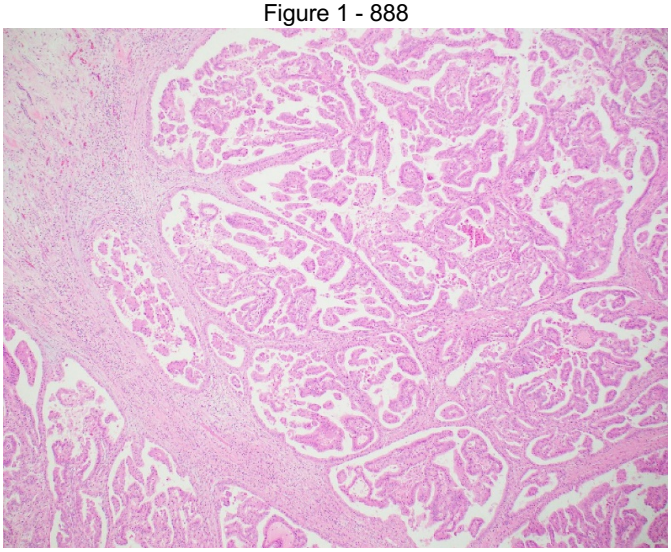

Figure 2 - 888

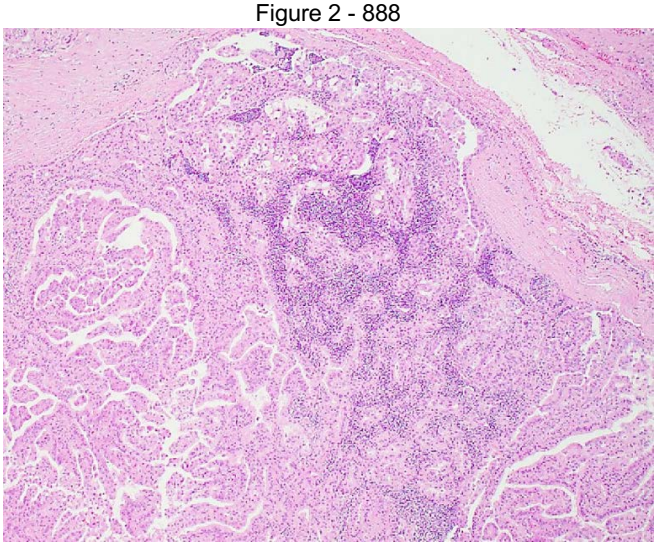

**Conclusions:** The presence of a micropapillary component in PRCC was found to be 14.2% in this series. It was mostly associated with high pathologic stage and early lymph node metastases, and the clinical course of these tumors seems similar to those in other organ systems. Though the sample size was limited and further study with a large cohort is required, given their significant association with adverse pathology, we advocate reporting such patterns when identified.

## 889 Association of Cribriform Architecture on Transrectal Ultrasound-Guided Prostate Biopsy with Adverse Histologic Features at Radical Prostatectomy among Filipino Males with Gleason Score 7 Prostatic Adenocarcinoma

Faye Victoria Casimero[1], Jeffrey So[2]
*[1]St. Luke's Medical Center - Quezon City, Quezon City, Metro Manila, Philippines, [2]St. Luke's Medical Center, Quezon City, Metro Manila, Philippines*

**Disclosures:** Faye Victoria Casimero: None; Jeffrey So: None

**Background:** The outcome of patients with Gleason score (GS) 7 prostate cancer (PCa) on transrectal ultrasound-guided (TRUS) biopsy varies, possibly due to the broad definition of Gleason pattern (GP) 4, which includes cribriform & non-cribriform patterns (poorly formed, fused, and glomeruloid pattern). Selected patients may be candidates for active surveillance; but some may harbor more aggressive disease. Several studies showed the presence of cribriform pattern is associated with biochemical recurrence, metastasis, and mortality. This study aimed to determine the association of cribriform pattern on biopsy with adverse histologic features (AHF) at RP. This is the first study done on Southeast Asian data.

**Design:** A review of patients with GS 7 PCa on TRUS biopsy & RP from January 2013 to June 2019 identified 40 patients out of 285 RPs. A blinded uropathologist assessed the biopsies for GP 4 architectural types. Data on AHF- lymphovascular invasion (LVI), perineural invasion (PNI), extraprostatic extension (EPE), seminal vesicle invasion (SVI), vasa deferentia invasion (VDI), positive surgical margins (PSM), regional lymph node metastasis (RLNM), and GS upgrading (GSU), were retrieved from RP reports. Prevalence was computed using AHF frequency. To test for the association of cribriform pattern with AHF, a Chi-square test was done with statistical significance of $\alpha=0.05$ and power of $(1-\beta)=0.80$. Odds ratio (OR) was used to compare the likelihood of AHF between the 2 groups.

**Results:** Of the 40 cases included in the study, 27 were classified as grade group (GG) 2 (GS 3+4=7) and 13 as GG3 (GS 4+3=7). In GG2 category, 16 had cribriform pattern at TRUS. Except for VDI, the prevalence of all AHFs at RP was higher in cribriform cases. The likelihood of LVI, PNI, EPE, SVI and PSM at RP was higher (OR>1) among cribriform cases; however, this was not statistically significant (P>0.05). In the GG3 category, 9 had cribriform pattern; and had a higher prevalence and likelihood (OR>1) of LVI, EPE and SVI. Interestingly, these cases are less likely (OR<1) to have PNI, PSM and GSU. Among the AHF, the association was significant only for EPE (P0.03).

| Adverse Histologic Feature at RP | Grade Group 2 (Gleason Score 3+4=7) | | | | Grade Group 3 (Gleason Score 4+3=7) | | | |
|---|---|---|---|---|---|---|---|---|
| | Cribriform | Non-cribriform | Odds Ratio | P-value (Chi-square) | Cribriform | Non-cribriform | Odds Ratio | P-value (Chi-square) |
| Total number | 16 | 11 | | | 9 | 4 | | |
| Lymphovascular invasion* | 31% | 18% | 2.0 | 0.45 | 22% | 0% | 2.3 | 0.31 |
| Perineural invasion | 38% | 9% | 6.0 | 0.10 | 22% | 25% | 0.9 | 0.91 |
| Extraprostatic extension | 50% | 36% | 1.8 | 0.48 | 67% | 0% | 16.0 | 0.03 |
| Seminal vesicle invasion | 25% | 0% | 7.3 | 0.07 | 33% | 25% | 1.5 | 0.76 |
| Vasa deferentia invasion* | 0% | 0% | 0.7 | 0.85 | 0% | 0% | 0.4 | 0.69 |
| Positive surgical margins | 63% | 55% | 1.4 | 0.68 | 33% | 50% | 0.5 | 0.57 |
| Total number | 12 | 5 | | | 8 | 3 | | |
| Regional lymph node metastasis* | 8% | 0% | 0.9 | 0.96 | 0% | 0% | 0.4 | 0.63 |
| *For both OR and Chi-square test, a Haldane-Anscombe correction was done. | | | | | | | | |

Figure 1 - 889

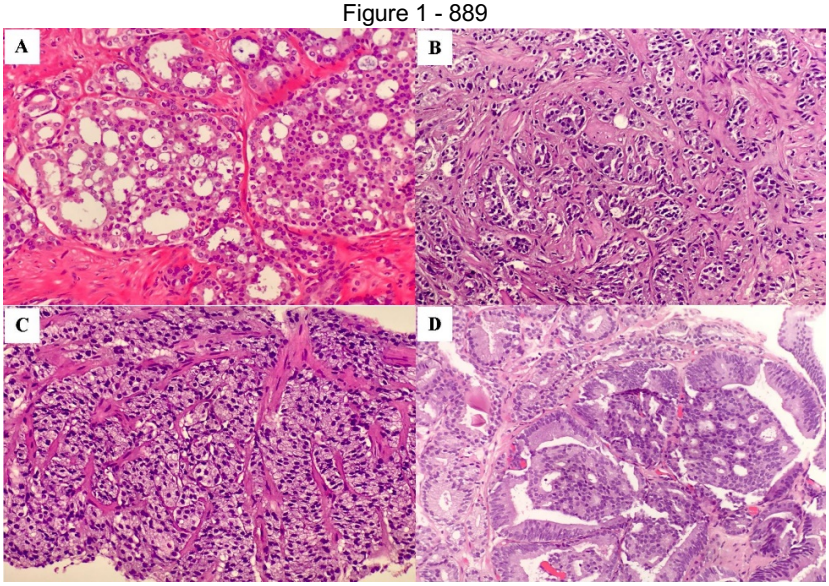


**Conclusions:** Filipinos with GG3 PCa with cribriform pattern on TRUS biopsy are more likely to have EPE at RP. The other AHFs show a difference between the cribriform & non-cribriform groups, however further studies are needed to fully establish these differences. Our study has provided a good start for our region in identifying the value of reporting cribriform pattern.

## 890 Loss ATRX Expression and TERT promoter mutation (TERTp) in Urothelial Carcinoma

Marcelo Cassini[1], Haiyan Li[2], Rugved Pattarkine[2], Minghao Zhong[2]
*[1]Westchester Medical Center, Fairfield, NY, [2]Westchester Medical Center, Valhalla, NY*

**Disclosures:** Marcelo Cassini: None; Haiyan Li: None; Rugved Pattarkine: None; Minghao Zhong: None

**Background:** Unlimited replication is a hallmark of cancer. This limitless replicative potential employs different molecular mechanisms, such as: *TERT* promoter mutations (*TERTp*), Alternative Lengthening of Telomeres (ALT). ALT is a homologous recombination-mediated, telomerase- independent mechanism of telomere elongation and is associated with ATRX mutations/loss expression. Interestingly, *TERTp* mutation and loss of ATRX are mutually exclusive and are standard tests (for prognosis purpose) in glioma. It is well established that ~70% of urothelial carcinoma (UC) carry *TERTp* mutation. In this study, we want to evaluate ATRX loss expression and its relationship with *TERTp* mutation in UC.

**Design:** One hundred and ten (110) urothelial carcinoma (UC) cases were collected from our institute for this study. The tissue microarrays (TMA) were constructed and TMA slides were subjected for ATRX IHC staining. The genomic DNA was extracted from each case from FFPE tissue. *TERTp* mutations were identified by PCR and Sanger sequencing as previously described. We also analyzed ~400 UC cases in TCGA data base for *ATRX* mutations and deletion.

**Results:** 1. We detected *TERTp* mutation in 84 (76%) out of 110 UC cases. 2. Twenty one cases (19%) had intact expression of ATRX, 44(40%) and 45(41%) cases had reduced expression and completely loss expression, respectively. 3. In more than 400 TCGA UC cases, only <5% cases had *ATRX* mutations; <1% cases with *ATRX* deletion.

Figure 1 - 890

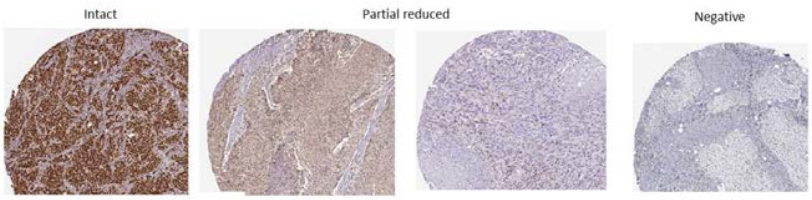


**Figure 1.** Showing different intensities of ATRX immunostaining on tissue microarrays (TAM).

Figure 2 - 890

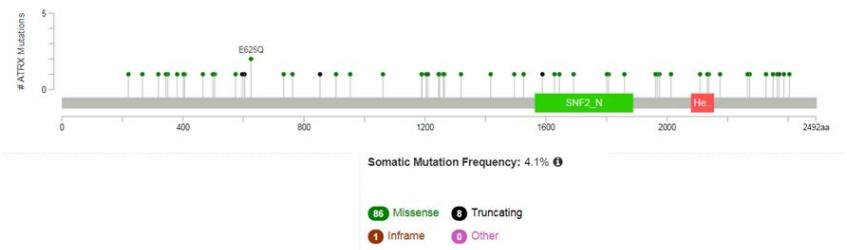


**Figure 2.** From TCGA data base, showing the frequency of ATRX mutation in Urothelial Carcinoma (UC).

**Conclusions:** Our study demonstrates that loss/reduce expression of ATRX are in majority of UC and are not excluded from *TERTp* mutation. This suggests that UC may use more than one molecular mechanism to maintain limitless replicative potential. Interestingly, only <6% UC cases showed *ATRX* mutations or deletion. Other molecular mechanisms, such as: epigenetic or post-translational regulation, may contribute to the loss expression ATRX in UC.

## 891 Computerized Quantification of Invasive Cribriform Adenocarcinoma on Radical Prostatectomy Specimens is Prognostic of Biochemical Recurrence

Sacheth Chandramouli[1], Patrick Leo[2], Andrew Janowczyk[1], Robin Elliott[3], Xavier Farré[4], Lauri Eklund[5], Natalie NC Shih[6], Michael

Feldman[7], Jesse McKenney[8], Anant Madabhushi[1]
*[1]Case Western Reserve University, Cleveland, OH, [2]Pittsburgh, PA, [3]University Hospitals Cleveland Medical Center, Case Western Reserve University, Cleveland, OH, [4]Public Health Agency of Catalonia, Lleida, Spain, [5]University of Turku, Turku, Southwest Finland, Finland, [6]University of Pennsylvania, Philadelphia, PA, [7]University of Pennsylvania, Wilmington, DE, [8]Cleveland Clinic, Cleveland, OH*

**Disclosures:** Sacheth Chandramouli: None; Patrick Leo: None; Andrew Janowczyk: None; Robin Elliott: None; Xavier Farré: None; Natalie NC Shih: None; Jesse McKenney: None; Anant Madabhushi: *Consultant*, Inspirata Inc; *Stock Ownership*, Inspirata Inc

**Background:** Invasive cribriform adenocarcinoma (ICC) in radical prostatectomy (RP) specimens has been correlated with biochemical recurrence (BCR) and metastasis of prostate cancer (CaP). However, manual identification of cribriform on H&E slides is laborious. To quantify extent of ICC across many patients, an automated method is needed. In this study, we trained a deep learning (DL) model to segment ICC on diagnostic H&E-stained RP slides and assessed cribriform-to-tumor area ratio (CAR) as a predictor of BCR.

**Design:** A single H&E-stained diagnostic slide was collected from each of N=261 RP patients from a single institution. All slides were annotated for a representative tumor region. The training dataset, D1, was composed of N=69 patients. The remaining N=192 patients composed the validation set D2. Two pathologists reviewed D1 and sparsely annotated ICC regions on 30 patients using standard criteria for cribriform carcinoma. A 1000x1000-pixel region at 10X magnification was extracted from 325 ICC lesions. To increase diversity in the negative class of non-ICC tissue presentation, 21 1000x1000 pixel regions were manually selected from 6 additional patients. These patches included common confounding cribriform patterns such as Grade 5 (excluding Comedonecrosis) and pseudo-cribriform areas along with lymphocytic regions and benign glands. The 36 patients were randomly divided into training (33 patients) and testing (3 patients) sets. Training set patches were augmented prior to use in a UNet DL model. After training for 500 epochs the model associated with the lowest test set loss was selected. This model was then applied to the representative tumor region on each slide. Model output was post-processed to remove areas smaller than the smallest ICC area in the training set, .024 $mm^2$. CAR was calculated for every patient. D1 was used to identify a threshold of CAR best separating outcomes and then subsequently applied to patients in D2.

**Results:** The ICC segmentation model achieved a per pixel sensitivity and specificity of 95% and 80% respectively in the test set (Figure 1). A CAR threshold of .039 was best shown to separate out BCR and non-BCR patients. CAR (p-value < .0046, HR=2.06, 95% CI: 1.09-3.88) was prognostic of BCR in D2 (Figure 2).

Figure 1 - 891

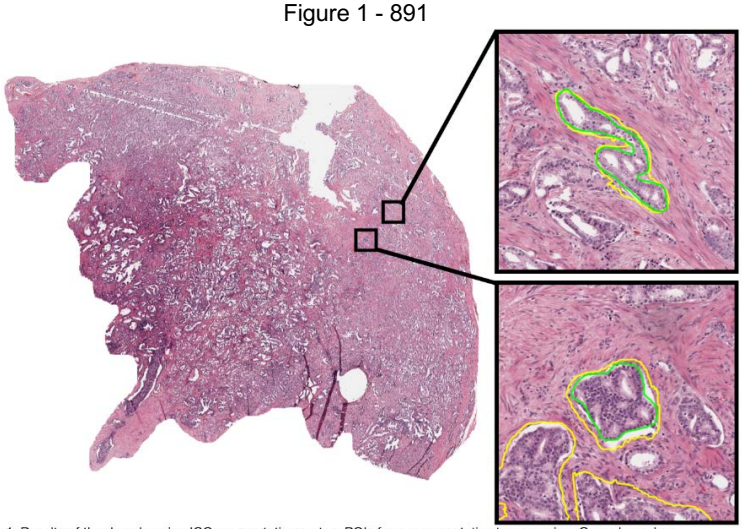

Figure 1: Results of the deep learning ICC segmentation on two ROIs from representative tumor region. Green boundary corresponds to sparsely annotated ICC regions by two pathologists. Yellow boundary corresponds to predicted ICC areas.

Figure 2 - 891

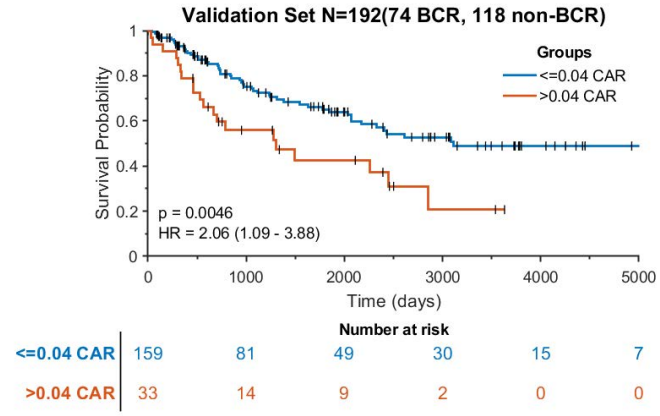


Figure 2: Kaplan-Meier BCR survival curve of patients using CAR with a threshold of . 0392 on patients within D2 (N=192). The curve is truncated at 5000 days.

**Conclusions:** We have demonstrated that an automatically derived CAR from H&E post-RP slides is prognostic of BCR. Limitations to this work include that IHC was not performed to differentiate and study both ICC and intraductal carcinoma of the prostate (IDC-P).

## 892 Methylation Profiling of Clear Cell Papillary Renal Cell Carcinoma

Fei Chen[1], Fangming Deng[2], Jonathan Serrano[3], Paolo Cotzia[4], Matija Snuderl[3], Kyung Park[1]
*[1]NYU Langone Health, New York, NY, [2]New York University Medical Center, New York, NY, [3]New York University, New York, NY, [4]New York University Langone Medical Center, New York, NY*

**Disclosures:** Fei Chen: None; Fangming Deng: None; Jonathan Serrano: None; Paolo Cotzia: None; Matija Snuderl: None; Kyung Park: None

**Background:** Clear cell papillary renal cell carcinoma (ccpRCC) is a relatively new entity and it has been described as an indolent renal neoplasm. ccpRCC shares features of clear cell RCC (ccRCC) and papillary RCC (pRCC) morphologically and immunohistochemically, even though it carries a very different prognostic potential. Epigenetic alterations play a significant role in the development and progression of human tumors. A large scale sequencing efforts demonstrated that hypermethylation in RCC tumors is associated with poor prognosis and may dictate treatment options. However, ccpRCC has not been included and further molecular elucidation is to be done. In this study, we attempt to investigate the methylation patterns in ccpRCC and test if differential patterns can be correlated with histologic subtypes and known biological behaviors.

**Design:** Nephrectomy specimens from our institution were reviewed and 8 cases from 2017-2019 were selected and confirmed as ccpRCC by three pathologists. Tumors were microdissected and DNA from FFPE was extracted and profiled using the Illumina MethylationEPIC array. Methylation data were analyzed with the R Bioconductor package minfi, including quality control, data normalization and differentially methylated CpG site analysis. Subsequent filtering was performed using a p-value cutoff = 0.01 and a minimum mean difference of the Beta-value of 0.1. Clustering was performed using tSNE analysis. Copy numbers were analyzed using conumee package. The methylation data were compared to ccRCC and pRCC from publicly available TCGA dataset.

**Results:** All 8 cases passed QC metrics on bisulfite conversion, hybridization and signal intensity confirming that the DNA quality was optimal for methylation study. ccpRCC clustered very tightly together illustrating that they represented a homogeneous group of tumors. When this cluster was compared to the TCGA dataset, ccpRCC was found to be located in between ccRCC and pRCC which might explain the characteristic features of this tumor subtype (figure 1).

Figure 1 - 892

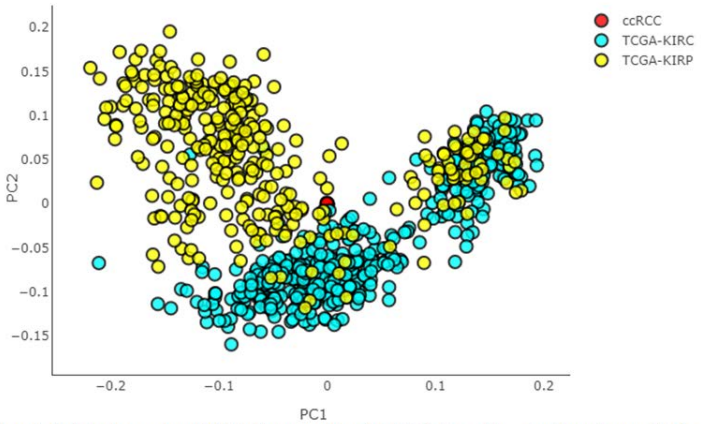


Figure1: Tightly clustered ccpRCC (red) compared to the TCGA clear cell renal cell carcinoma (blue) and papillary renal cell carcinoma (yellow) based on methylation.

**Conclusion:** 1. DNA methylation is a useful molecular hallmark of many cancers including renal cancers and is increasingly utilized in diagnosis, prognostication, and clinical trials (epigenetic therapy). 2. Morphologically and immunohistochemically confirmed ccpRCC forms a tight cluster validating the use of methylation assay for future studies. 3. Promotor and pathway specific methylation patterns will be further studied which can distinguish the indolent clinical behavior.

## 893 Intratumoral Benign Glandular Atrophy is Associated with Unfavorable Grade Group of Prostatic Carcinoma

Zhengshan Chen[1], Kyle Hurth[2], Guang-Qian Xiao[3]
*[1]LAC + USC Medical Center, Los Angeles, CA, [2]Keck School of Medicine of University of Southern California, Los Angeles, CA, [3]Keck Medical Center of USC, Los Angeles, CA*

**Disclosures:** Zhengshan Chen: None; Kyle Hurth: None; Guang-Qian Xiao: None

**Background:** In the prostate of an individual without endocrine disorder, atrophic glands are usually related to inflammatory or post-inflammatory process. Prostatic adenocarcinoma (PC) often presents with infiltrative pattern and benign glands are frequently entrapped inside the tumor. To date, the relation between morphology of intratumoral glandular atrophy and tumor Gleason grade has not been explored. Our aim is to investigate the association between the morphology of intratumoral benign glands and grade group of the associated PC.

**Design:** 100 radical prostatectomies accessioned in the past year were reviewed. Intratumoral atrophic glands were defined as benign acini/ducts with complete or near complete (>90%) loss of luminal cells and are surrounded by PC. Correlation between the PC Gleason scores and the atrophic status of intratumoral glands was performed. IHC was performed with BCL2 (38 cases), EGFR (28 cases) and CD44 (27 cases) to assess the intratumoral benign glands. The difference of immunoreactivity in atrophic and non-atrophic glands was statistically analyzed.

**Results:** Of the 100 cases of PC, 38 were group 1, 15 group 2, 19 group 3, 22 group 4 and 6 group 5. The percentage of intratumoral benign atrophic glands was 3% in group 1, 53% in group 2, 95% in group 3, 91% in group 4 and 100% in group 5 (Table 1; Fig 1, A: non-atrophy in low grade PC; B: atrophy in high grade PC). There were significantly more intratumoral atrophic glands in high grade groups (3, 4 and 5) compared to low grade groups (1 and 2) of PC ($p<0.0001$). IHC showed that intratumoral atrophic glands expressed higher level of BCL2 ($p<0.0001$), EGFR ($p=0.007$) and lower level of CD44 ($p=0.002$) in the high grade groups compared to the non-atrophic glands in low grade groups.

**Table 1.** The association of atrophic status of intratumoral benign glands with the grade group of their associated PC.

| | Group 1 (GS 3+3) (n=38) | Group 2 (GS 3+4) (n=15) | Group 3 (GS 4+3) (n=19) | Group 4 (GS 4+4) (n=22) | Group 5 (GS 4+5) (n=6) |
|---|---|---|---|---|---|
| # and % cases with intratumoral benign atrophic glands | 1 (2.63%) | 8 (53.33%) | 18 (94.74%) | 20 (90.91%) | 6 (100.00%) |
| # and % cases with intratumoral benign non-atrophic glands | 37 (97.37%) | 7 (46.67%) | 1 (5.26%) | 2 (9.09%) | 0 (0.00%) |

Figure 1 - 893

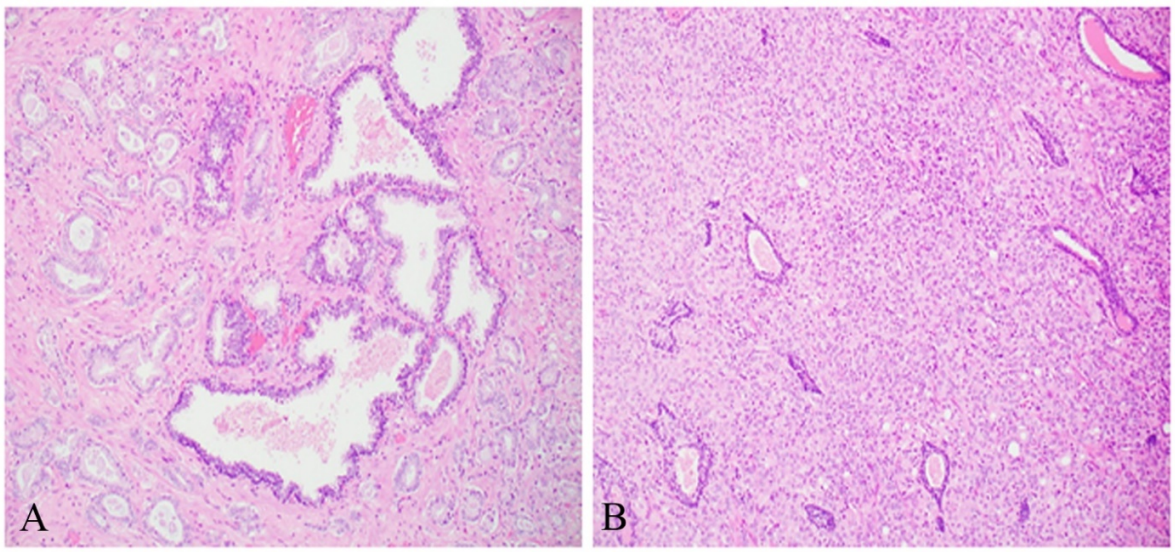


**Conclusions:** This study demonstrated that intratumoral benign glandular atrophy was strongly associated with unfavorable grade group of PC. Such glandular atrophy might signify a rapid growth of the associated PC and may be potentially used as an indicator of tumor aggression. The mechanism for such association is yet unknown. It might be related to alterations of the paracrine microenvironment, such as the disadvantage of benign glands in competing for androgen or growth factors or inhibitory factors secreted by tumor cells. The basal cells of the atrophic glands expressed higher levels of BCL2, EGFR and lower levels of CD44, which may reflect a survival mechanism that benign basal cells developed in an effort to counter the hostile microenvironment.

## 894 Lymphovascular Invasion and Lymph Node Metastasis is Highly Associated with Small Cribriform Pattern of Invasive Prostatic Carcinoma

Zhengshan Chen[1], Catherine Suen[2], Pamela Unger[3], Guang-Qian Xiao[4]
*[1]LAC + USC Medical Center, Los Angeles, CA, [2]Fullerton, CA, [3]Lenox Hill Hospital, New York, NY, [4]Keck Medical Center of USC, Los Angeles, CA*

**Disclosures:** Zhengshan Chen: None; Catherine Suen: None; Catherine Suen: None; Pamela Unger: None; Guang-Qian Xiao: None

**Background:** Prostate cancer (PC) is common in the elderly male population. Majority of PC cases follow an indolent course. Lymphovascular invasion (LVI) and lymph node metastasis (LN-M) are uncommon and often associated with high grade (Gleason 4 or 5) PC. The cribriform pattern of PC is graded as Gleason 4. Based on size, the cribriform pattern can be divided into small and large types. It has been recently demonstrated that cribriform pattern is more aggressive than noncribriform Gleason 4 PC. Some studies have also shown that large cribriform PC is associated with high tumor stage. The association of small cribriform PC with aggressive pathologic parameters has not been investigated. In this study, we aim to correlate the presence of small cribriform PC with LVI and LN-M.

**Design:** A total of 48 radical prostatectomies with LVI/LN-M were retrospectively reviewed to assess the presence of small cribriform PC. Small cribriform was defined as cribriform glands smaller in size than adjacent normal prostate glands. The volume of small cribriform PC was recorded as the number of low power fields (4x) with small cribriform pattern. The associations between small cribriform PC and LVI/LN-M were analyzed.

**Results:** Among the 48 cases, 9 had only LVI, 10 had only LN-M and 29 had both LVI and LN-M. 45/48 (93.7%) cases had small cribriform growth pattern ranging from 1 to 6 low power fields and 10% to 60% of the tumor volume. The remaining 3 cases had fused, ill-defined glands and no small cribriform pattern. All of the 38 cases with LVI had small cribriform growth pattern. 7/10 cases with LN-M only had small cribriform growth pattern (Table 1). The grade group of the associated PC ranged from group 2 (Gleason 3+4) to group 5 (Gleason 4+5). Vast majority of the cases presented with tumor stage pT3.

**Table 1.** Association of small cribriform pattern of prostatic carcinoma with LVI and LN-M, grade group and tumor stage

| | LVI only | LVI and LN-M | LN-M only |
|---|---|---|---|
| # of cases with small cribriform PC | 9 (100%) | 29 (100%) | 7 (70%) |
| # of cases without small cribriform PC | 0 (0%) | 0 (0%) | 3 (30%) |
| Grade group and # of cases | 0 (0%) (group 2)<br>4 (44%) (group 3)<br>4 (44%) (group 4)<br>1 (11%) (group 5) | 1 (3%) (group 2)<br>6 (21%) (group 3)<br>7 (24%) (group 4)<br>15 (52%) (group 5) | 3 (30%) (group 2)<br>4 (40%) (group 3)<br>1 (10%) (group 4)<br>2 (20%) (group 5) |
| Tumor stage and # of cases | 2 (22%) (pT2N0)<br>2 (22%) (pT3aN0)<br>5 (56%) (pT3bN0)<br>0 (0%) (pT4N0) | 2 (7%) (pT2N1)<br>4 (14%) (pT3aN1)<br>22 (76%) (pT3bN1)<br>1 (3%) (pT4N1) | 0 (0%) (pT2N1)<br>4 (40%) (pT3aN1)<br>5 (50%) (pT3bN1)<br>1 (10%) (pT4N1) |

**Conclusions:** We demonstrated that LVI/LN-M is closely associated with small cribriform pattern of PC. PC in LVI is often seen in the form of small clusters/small cribriform pattern. Recently, some researchers have found that the formation of cell groups is essential for tumor cells to survive in blood or the lymphatic as well as to establish tumor colonies at metastatic sites. Our study further supports the propensity of cribriform PC for LVI and LN-M and is, at least in part, an explanation of their aggressive nature. Therefore, in practice, in addition to reporting the cribriform type (glomeruloid vs nonglomeruloid), it may also be worthwhile to include the size of the cribriform pattern in the report.

## 895 Grading of Intraductal Carcinoma of the Prostate: Impact on Overall Grade Group Assignment at Diagnostic Biopsy

Daphne Chen-Maxwell[1], Susan Prendeville[2]
*[1]Cork University Hospital, Ballincollig, Cork, Ireland, [2]Cork University Hospital, Cork, Ireland*

**Disclosures:** Daphne Chen-Maxwell: None; Susan Prendeville: None

**Background:** Intraductal carcinoma of the prostate (IDCP) is established as a poor prognostic parameter in prostate cancer (PCa) and is typically associated with high grade invasive carcinoma. Based on current WHO guidelines, the IDCP component is not graded and does not factor into the Gleason score (GS)/Grade Group (GG). This study evaluated the impact of grading IDCP at diagnostic biopsy (PBx) on overall GG assignment, which may have implications for subsequent clinical management in individual patients.

**Design:** The study included cases with IDCP diagnosed at PBx with associated invasive carcinoma component ≤GG3 (cases with invasive carcinoma GG4/5 were excluded). The original GG was based on the grade of the invasive component only. All cases were retrospectively re-graded incorporating both invasive and IDCP components. Parameters at diagnostic biopsy and follow-up pathology were recorded.

**Results:** 83 cases were identified, all of which contained both IDCP and invasive PCa. The original GG at biopsy (excluding IDCP) was GG1 in 3 cases (4%), GG2 in 37 cases (45%) and GG3 in 43 cases (52%). The median number of sites involved by IDCP was 2 (1-6) and the median number of cores involved by IDCP was 3 (1-12).The type of IDC morphology was: dense cribriform/solid (n=76, 92%), flat/loose cribriform with marked cytological atypia (n=5, 6%) or a combination of both patterns (n=2, 2%).

Inclusion of IDCP in grading changed the global GG in 22 cases (27%) (Table 1). Upgrading was due to presence of comedo necrosis (n=10), solid growth (n=1) or increased proportion of Gleason pattern 4 (n=10). In 12 of 22 cases, the GG increased by two grades. Among cases with original GG1 or GG2 (n = 40), 15 (38%) were upgraded.

16 of 83 patients underwent subsequent radical prostatectomy, including 4 of 22 upgraded patients (table 1).

| TABLE 1 | | | | |
|---|---|---|---|---|
| **Original GG/GS (excluding IDCP)** | **GG/GS incorporating both invasive carcinoma and IDCP (*upgraded cases)** | | | |
| | **2 (3+4)** | **3 (4+3)** | **4 (3+5 or 4+4)** | **5 (4+5)** |
| **1 (3+3)** | 2 * | 1* | | |
| **2 (3+4)** | 25 | 6 * | 5 * | 1 * |
| **3 (4+3)** | - | 36 | 2 * | 5* |
| | **Pathologic parameters in all cases with subsequent RP (n=16)** | | | |
| **pT Stage** | **N %** | | | |
| **pT2** | 3 (18%) | | | |
| **pT3a** | 7 (44%) | | | |
| **pT3b** | 6 (38%) | | | |
| **pN+** | 2 (13%) | | | |
| | **Pathologic parameters in upgraded cases with subsequent RP (n=4)** | | | |
| **Change in GG** | **pT stage** | **pN+** | | |
| **GG2 to GG3** | pT3b | Yes | | |
| **GG2 to GG5** | pT3b | No | | |
| **GG3 to GG5** | pT3a | No | | |
| **GG3 to GG5** | pT3b | No | | |

**Conclusions:** While the GG was unchanged in the majority of cases, grading of IDCP altered the overall GG in a substantial minority and sometimes by two grades. In addition to determining eligibility for active surveillance, GG at PBx may influence further investigations and type of therapeutic intervention. Consensus on grading of IDCP and optimal incorporation of IDCP into clinical nomograms is needed to guide appropriate clinical management.

## 896 MDM2 and CDK4 Molecular Alterations in Leydig Cell Tumor. Proposal of Leydig Scaling Score (LeSS) for Predicting Metastatic Disease

Maurizio Colecchia[1], Biagio Paolini[2], Alessia Bertolotti[1], Gian Paolo Dagrada[1], Andrea Necchi[1], Anna Maria Paganoni[3]
*[1]Fondazione IRCCS Istituto Nazionale Tumori Milano, Milan, Italy, [2]Fondazione IRCCS Istituto Nazionale Tumori Milano, Milan, Lombardia, Italy, [3]MOX - Modeling and Scientific Computing Dipartimento di Matematica, Milan, Italy*

**Disclosures:** Maurizio Colecchia: None; Biagio Paolini: None; Alessia Bertolotti: None; Gian Paolo Dagrada: None; Anna Maria Paganoni: None

**Background:** Leydig cell tumors (LCTs) occurs at any age and currently there are no validated methods for identification of cases that may metastasize.

**Design:** Morphological and molecular features of 3 benign LCTs and 14 malignant cases have been investigated; 6 morphological parameters for a predictive model of the metastatic risk in primary testis LCTs (Leydig Scaled Score= LeSS) have been evaluated. In 10 malignant tumors from 9 patients we assessed *MDM2* (12q15) and *CDK4* copy number status by FISH analysis and high resolution oligoarray comparative genomic hybridization. MDM2 and CDK4 immunostains were performed in all the 51 cases.

**Results:** There was a significant difference between tumoral diameters of benign LCTs (mean cm. 1.33) and malignant cases (mean cm. 4.4) (Wilcoxon text p value <0.001). The other five predictive parameters investigated, infiltrating margins, necrosis, vascular invasion, mitotic count and nuclear atypia, showed significant differences (Wilcoxon text p value <0.001). Eight metastatic tumors and one benign LCTs had infiltrating margins. Nuclear atypia was graded with three scores: 29 out of 37 benign LCTs had grade 0 atypia and 8 grade 1 atypia. Among 14 metastatic cases 7 LCTs had grade 1 atypia and 7 grade 2 atypia. Extensive foci of coagulative necrosis occurred as feature of malignancy (10/14), while two benign LCTs showed microscopic foci of necrosis. Vascular invasion was identified in 9/14 metastatic cases and in 0/37 benign LCTs. Mitotic activity ≥ 1/10 HPFs was observed in 20 out of 37 (54%) benign LCTs), none showed more than 2 mitoses. Mitotic count ranging from 3 to 50 mitoses in 10 HPFs was a feature of malignant LCTs. These parameters and the diameter were selected by an inferential analysis based on univariate logistic regression models to develop a Leydig scaled score (LeSS). A LeSS of < 4 accurately identified all histologically and clinically benign LCTs. A LeSS score of ≥ 4 correctly identified all LCTs that had a metastatic course. FISH showed high level of *MDM2* and *CDK4* amplifications in 3 out of 10 malignant LCTs. All benign LCTs were negative, while 3/11 metastatic LCTs (27%) showed strong immunopositivity for MDM2 and CDK4 in all tumoral cells. The results of CGH analysis are under evaluation.

**Conclusions:** 27% LCTs with metastatic behavior in the present series have *MDM2* and *CDK4* amplifications. A scaling score system (LeSS) is proposed to identify high and low risk for metastatic behavior in testis LCTs.

## 897 A Subset of TCEB1-Like Renal Cell Carcinomas are Aggressive Tumors with Early Metastasis

Brian Cone[1], Sung-Hae Kang[2], Brian Shuch[2], Dipti Sajed[2], Huihui Ye[2]
*[1]David Geffen School of Medicine at UCLA, Los Angeles, CA, [2]University of California Los Angeles, Los Angeles, CA*

**Disclosures:** Brian Cone: None; Sung-Hae Kang: None; Brian Shuch: None; Dipti Sajed: None; Huihui Ye: None

**Background:** TCEB1-mutated renal cell carcinoma is a recently described (Hakimi, *et al*) subtype of RCC characterized by its distinct morphology and genotype. The characteristic morphologic features include thick fibromuscular bands, pure clear cell cytology, and acinar and tubulopapillary architectural patterns. These tumors demonstrate a loss of chromosome 8 and have hotspot driver mutations in the *TCEB1* gene, located on 8q. A definitive diagnosis of TCEB1-RCC requires molecular studies not typically available in clinical practice. Current literature suggests that these are indolent tumors. We aim to identify and characterize a group of RCCs demonstrating a distinct karyotype suggestive of TCEB1-mutated RCC (named here as TCEB1-ike RCCs).

**Design:** We identified 16 consecutive patients (1997-2019) whose tumor karyotype demonstrated monosomy 8 and no loss of 3p. Histopathological features (including morphology, nuclear grade, size, pathologic stage) were centrally reviewed by 3 pathologists and an IHC panel consisting of carbonic anhydrase IX (CA9), cytokeratin 7 (CK7), Racemase, CD10, and cytokeratin 903 was evaluated. Clinical chart review was performed to obtain patient demographics and outcomes.

**Results:** Of the 16 RCCs with monosomy 8 and intact 3p/VHL, all but two showed thick fibromuscular bands transecting the tumor with a multinodular appearance. Pure clear cell cytology with voluminous cytoplasm, and acinar and tubulopapillary architectural patterns were seen in a majority of cases. Importantly, 4 of the patients (25%) presented with distant metastases, including one fatality. All 4 with metastases presented with low stage tumors (pT1), and 2 of the 4 had low-grade histology. The immunoprofile of these tumors wer similar to that described by Hakimi (CA9+, CK7+, CD10+, CK903-) with some notable differences in CA9 (more patchy cases in this cohort), CK7 (more negative cases), and CK903 (more positive cases). The majority of tumors showed Racemase positivity. See Table 1.

| Clinicopathologic Features | M0 Disease (n=12) | M1 Disease (n=4) |
|---|---|---|
| Age, years | | |
| median (range) | 60 (28-75) | 60.5 (42-66) |
| Sex, no. (%) | | |
| male | 9 | 3 |
| female | 3 | 1 |
| Morphologic Features | | |
| Tumor size (cm) | | |
| median (range) | 2.9 (9.6) | 4.05 (5) |
| Thick fibromuscular bands transecting the tumor | 11/12 (91.7%) | 3/4 (75%) |
| Pure clear cell cytology & voluminous cytoplasm | 12/12 (100%) | 3/4 (75%) |
| Tubular or papillary architecture | 5/12 (41.7%) | 1/4 (25%) |
| Acinar or solid acinar architecture | 12/12 (100%) | 4/4 (100%) |
| High nuclear grade (3-4) | 2/12 (16.6%) | 2/4 (50%) |
| High pathologic TNM stage (pT3a or above) | 1/12 (8.3%) | 0/4 (0%) |
| Immunohistochemistry | | |
| CA9 | | |
| Diffusely Positive | 7/12 (58.3%) | 3/4 (75%) |
| Patchy Positive, Extensively Distributed | 3/12 (25%) | 1/4 (25%) |
| Focal Positive | 2/12 (16.6%) | 0/4 (0%) |
| Neg | 0/12 (0%) | 0/4 (0%) |
| CK7 | | |
| Diffusely Positive | 1/12 (8.3%) | 0/4 (0%) |
| Patchy Positive, Extensively Distributed | 3/12 (25%) | 0/4 (0%) |
| Focal Positive | 4/12 (33.3%) | 1/4 (25%) |
| Neg | 4/12 (33.3%) | 3/4 (75%) |
| Racemase | | |
| Diffusely Positive | 9/12 (75%) | 3/4 (75%) |
| Patchy Positive | 2/12 (16.6%) | 1/4 (25%) |
| Negative | 1/12 (8.3%) | 0/4 (0%) |
| CD10 | | |
| Diffusely Positive | 4/12 (33.3%) | 1/4 (25%) |
| Patchy Positive | 6/12 (50%) | 3/4 (75%) |
| Negative | 2/12 (16.6%) | 0/4 (0%) |
| CK903 | | |
| Diffusely Positive | 0/12 (0%) | 0/4 (0%) |
| Patchy Positive | 3/12 (25%) | 0/4 (0%) |
| Negative | 9/12 (75%) | 4/4 (100%) |

**Conclusions:** Using karyotype, we have identified a cohort of RCCs with the morphology and karyotypes resembling the recently described TCEB1-muated RCCs. Although these tumors have not yet been sequenced, they demonstrate monosomy 8/intact 3p,

suggesting that they might belong to the TCEB1-mutated RCC group. As such, given that a subset of our cases (25%) are clinically aggressive, careful consideration should be made in suggesting a diagnosis of TCEB1-mutated RCC which has thus far been described as indolent.

## 898 BK (Polyoma) Virus-Associated Urothelial Carcinoma in Post-Transplant Patients: Clinicopathologic Correlation with Tumor Cell Origin and Survival Outcomes

Kristine Cornejo[1], Shulin Wu[1], Yun Miao[2], Robert Colvin[1], Chin-Lee Wu[3]
*[1]Massachusetts General Hospital, Boston, MA, [2]Nanfang Hospital, Guangzhou, China, [3]Massachusetts General Hospital, Newton Center, MA*

**Disclosures:** Kristine Cornejo: None; Shulin Wu: None; Yun Miao: None; Robert Colvin: None; Chin-Lee Wu: None

**Background:** BK polyomavirus (BKPyV) has been identified as a causative agent for urothelial carcinoma (UC). The aim of the study is to review the clinicopathologic features of BK (Polyoma) virus-associated urothelial carcinoma (BK-UC) in post-transplant patients with an emphasis on identifying tumor cell origin and survival outcomes.

**Design:** We identified 5 cases of BK-UC and determined the duration of immunosuppression, morphologic features, stage and clinical outcomes. Immunohistochemistry for SV-40 and molecular analysis (e.g. DNA sequencing) was performed to determine whether the tumor originated from the donor or recipient. A meta-analysis of our data combined with previous reports from the literature was also performed.

**Results:** All 5 patients underwent renal transplantation of which 3 BK-UCs originated in the bladder (BK-UC-B) and 2 in the graft kidney (BK-UC-GK) with a mean interval from transplant to BK-UC diagnosis of 183 months. All tumors were SV-40+, high grade (HG) and most of high stage (≥T2, n=4). Of the 4 cases tested, both patients with BK-UC-GK were of donor origin and 2 patients with BK-UC-B were of recipient origin. Both patients with donor origin BK-UC-GK had significant metastatic disease and underwent graft nephrectomy, 1 additionally treated with radiation and atezolizumab. Both patients are alive with stable disease with resolution of most metastasis at 8 and 23 months, respectively. 1 patient with recipient origin BK-UC-B, underwent cystectomy who later died of disease (DOD) at 8 months. The remaining patient with recipient origin BK-UC-B underwent resection with reduction of immunosuppression. 1 patient with BK-UC-B is undergoing tumor cell origin testing but is alive at 2 months after resection and chemotherapy.

Literature review identified an additional 37 cases of BK-UC-GK (n=8) and BK-UC-B (n=29), all of which were HG and most of high stage (≥T2, n=28). All 8 BK-UC-GK patients underwent graft nephrectomy and all 7 with follow-up are alive without disease (mean 28 months) of which 3 identified donor tumor cell origin. Of the 20 BK-UC-B with follow-up, 8 DOD (mean 9.5 months). The Kaplan-Meier survival curve demonstrated the CSS is significantly better in patients with BK-UC-GK than those with BK-UC-B (P=0.0454).

**Conclusions:** BK-UC are typically HG and of high stage, but those with BK-UC-GK, often of donor origin, are associated with a better prognosis. Therefore, determining the tumor cell origin may be predictive of patient outcomes and aid with treatment decisions.

## 899 GPNMB is a Sensitive but not Specific Marker for the Diagnosis of MiT Family Translocation Renal Cell Carcinoma

Daniela Correia Salles[1], Kaushal Asrani[1], Thiago Vidotto[2], Igor Damasceno Vidal[3], George J. Netto[4], Pedram Argani[5], Tamara Lotan[6]
*[1]Johns Hopkins Medical Institutions, Baltimore, MD, [2]Department of Pathology, The Johns Hopkins Medical Institutions, Baltimore, MD, [3]Johns Hopkins University, Baltimore, MD, [4]The University of Alabama at Birmingham, Birmingham, AL, [5]Johns Hopkins Hospital, Ellicott City, MD, [6]Johns Hopkins School of Medicine, Baltimore, MD*

**Disclosures:** Daniela Correia Salles: None; Kaushal Asrani: None; Thiago Vidotto: None; Igor Damasceno Vidal: None; George J. Netto: None; Pedram Argani: None; Tamara Lotan: *Grant or Research Support*, Ventana/Roche

**Background:** GPNMB (Glycoprotein nonmetastatic B) is a melanocytic marker and TFE3 transcriptional target that has been proposed as a potential marker for *TFE3* translocation renal cell carcinomas (tRCC) and Birt-Hogg-Dube-associated RCC. In addition, previous studies have shown that GPNMB is upregulated in tuberous sclerosis-associated tumors, such as angiomyolipomas. We examined GPNMB expression at the RNA and protein levels in a series of RCCs and PEComas to evaluate sensitivity and specificity of this marker.

**Design:** We examined Level 3 PanCan-normalized RNAseq data from 10,952 tumors representing 33 histologies from The Cancer Genome Atlas cohort. Median GPNMB expression was determined for each tumor type, including renal chromophobe RCC (ChRCC), clear cell RCC (CCRCC), papillary RCC (PRCC) and tRCC. We scored GPNMB immunohistochemistry (IHC) expression in tissue microarrays (TMA) containing *TFE3* or *TFEB* tRCC, CCRCC, PRCC, ChRCC, eosinophilic solid and cystic renal cell carcinoma (ESC), as well as angiomyolipomas (AML) and PEComas, scoring its membranous and/or cytoplasmic expression as dichotomously negative or positive and using a simple intensity scoring system (1-3+).

**Results:** By RNAseq, we found that kidney tumors are among the most highly GPNMB-expressing cancers. Among RCC cases, CCRCC had the lowest GPNMB RNA expression level compared with PRCC and ChRCC (P<0.001). Conversely, tRCC cases from the PRCC and CCRCC cohorts had the highest RNA levels of GPNMB (p<0.01). By IHC staining, the rate of positivity for GPNMB was 100% (18/18) for *TFEB* tRCC, 97% (30/31) for *TFE3* tRCC, compared to 79% (26/33) for ChRCC, 34% (21/61) for PRCC, and 8% (8/96) for CCRCC. Among tuberous sclerosis-associated lesions, GPNMB was expressed in 100% (8/8) of PEComas, 100% (32/32) of AMLs and 100% (4/4) of ESC RCC.

**Conclusions:** GPNMB is consistently and strongly expressed in renal cell carcinomas driven by genes in the MiT family and those driven by *TSC1/2* mutations. Nevertheless, it is not specific for these tumors and is also highly expressed in subsets of ChRCC and PRCC. Compared to previous studies of Cathepsin K, GPNMB is potentially a more sensitive marker for the diagnosis of tRCC or *TSC1/2*-associated tumors, however, Cathepsin K is more specific.

## 900 Association of PTEN Status with Response to Salvage Radiation Therapy with or without Anti-Androgen Therapy: A Study of RTOG 96-01

Daniela Correia Salles[1], Bruce Trock[2], William Shipley[3], Phuoc Tho[4], Angelo De Marzo[5], Felix Feng[6], Jeffry Simko[7], Allan Pollack[8], Jean-Paul Bahary[9], Himanshu Lukka[10], Michael Straza[11], Sean Cleary[12], Judith Hopkins[13], Mark Macher[14], Alan Hartford[15], Anand Desai[16], Viroon Donavanik[17], Daniel Spratt[18], Kosj Yamoah[19], James Dignam[20], Tamara Lotan[21]
*[1]Johns Hopkins Medical Institutions, Baltimore, MD, [2]The Johns Hopkins Medical Institutions, Baltimore, MD, [3]Massachusetts General Hospital, Boston, MA, [4]Johns Hopkins University/Sidney Kimmel Cancer Center, Baltimore, MD, [5]Johns Hopkins University, Baltimore, MD, [6]University of California San Francisco Medical Center, San Francisco, CA, [7]University of California San Francisco, San Francisco, CA, [8]University of Miami Miller School of Medicine, Miami, FL, [9]Centre Hospitalier de l`Université de Montréal, Montreal, QC, [10]McMaster Univ, Juravinski Can Ctr, Hamilton Health Sciences, Hamilton, ON, [11]Froedtert and the Medical College of Wisconsin, Milwaukee, WI, [12]Mayo Clinic, Rochester, MN, [13]Novant Health Oncology Specialists, Kernersville, NC, [14]John F. Kennedy Medical Center accruals under Thomas Jefferson University Hospital, Philadelphia, PA, [15]Dartmouth-Hitchcock Medical Center and Geisel School of Medicine at Dartmouth, Lebanon, NH, [16]Summa Akron City Hospital, Akron, OH, [17]Christiana Care Health Services, Inc. CCOP, New Castle, DE, [18]University of Michigan, Ann Arbor, MI, [19]Moffitt Cancer Center, Tampa, FL, [20]NRG Oncology Statistics and Data Management Center, Pittsburgh, PA, [21]Johns Hopkins School of Medicine, Baltimore, MD*

**Disclosures:** Daniela Correia Salles: None; Bruce Trock: None; Phuoc Tho: *Consultant*, RefleXion Medical; *Grant or Research Support*, Astellas Pharm; *Grant or Research Support*, Bayer Healthcare; *Grant or Research Support*, RefleXion Medical; Angelo De Marzo: None; Jeffry Simko: None; Jean-Paul Bahary: None; Himanshu Lukka: *Advisory Board Member*, Bayer; *Advisory Board Member*, Astellas, Sanofi; *Advisory Board Member*, Jansen; *Advisory Board Member*, Abbvie; *Advisory Board Member*, Tersera; Michael Straza: None; Judith Hopkins: None; Anand Desai: None; Daniel Spratt: None; Kosj Yamoah: None; Tamara Lotan: *Grant or Research Support*, Ventana/Roche

**Background:** Limited human data and pre-clinical mouse models have shown that prostate tumors with PTEN loss have lower AR levels and AR signaling output compared to those with intact PTEN. We tested if PTEN status modifies the benefit associated with treatment in RTOG 96-01, a phase III trial that demonstrated a benefit for anti-androgen therapy (AAT) with bicalutamide at the time of radiation therapy (RT) for non-metastatic PSA recurrence after radical prostatectomy.

**Design:** Using a genetically validated assay, we performed PTEN immunohistochemistry on primary prostate cancer (PCa) from 146 patients treated with RT/AAT vs. 160 patients treated with RT alone; these were subsets with tissue available on tissue microarray (TMA) from the total 760 enrolled. The analysis used Cox proportional hazards regression to evaluate metastasis-free survival (MFS), accounting for competing risk due to death from causes other than PCa.

**Results:** In this subset of RTOG96-01, PTEN was lost in 32% of cases and the distribution of clinical-pathologic variables and PTEN status was not significantly different for RT/AAT vs. RT patients. The hazard ratio (HR) for metastasis for RT/AAT vs. RT was 0.63 (95% CI: 0.38-1.04, p=0.073), similar to the HR in analysis of the entire trial. The only clinical-pathologic variable that was statistically significantly associated with MFS was Gleason Grade Group (GG) 5 vs. GG1-GG4 (HR =5.05; 95% CI: 2.62-9.71, p<0.0001); PTEN loss was non-significantly associated with MFS (HR=1.20; 95% CI: 0.72-1.98). When included in a model with treatment arm and GG5, PTEN loss remained non-significant (HR=1.07; 95% CI: 0.63-1.82). However, there was a strong suggestion of an interaction between treatment group and PTEN status while controlling for GG. Among patients with PTEN intact, the HR for metastasis for RT/AAT vs. RT was 0.52 (95% CI: 0.27-1.00) compared to 1.04 (95% CI: 0.45-2.39) for patients with PTEN loss. The interaction was not statistically significant (p=0.206), however, analysis of 200 additional cases is ongoing.

Figure 1 - 900

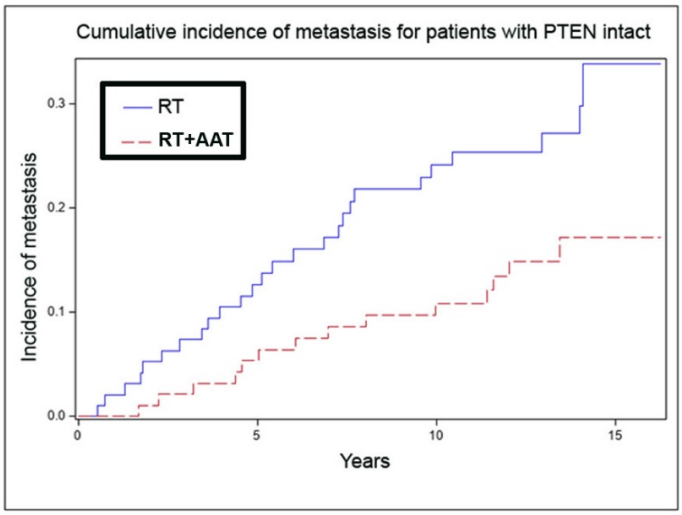


Figure 2 - 900

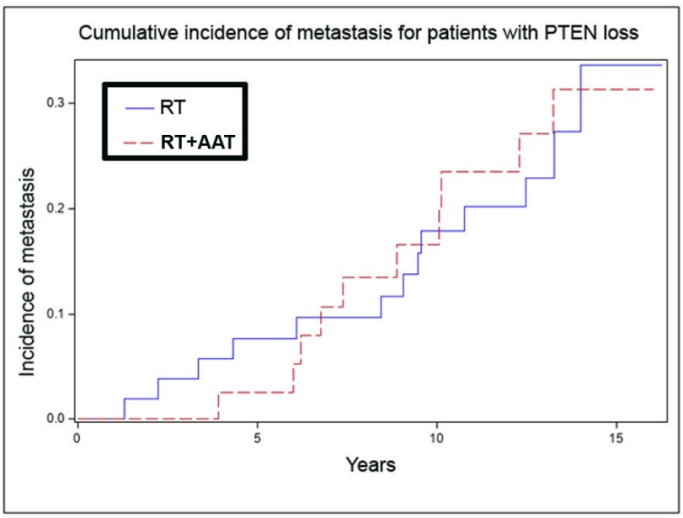


**Conclusions:** In this subset of the RTOG96-01 trial population, PTEN was not significantly associated with cumulative incidence of metastasis. However, among patients with intact PTEN, the risk of metastasis was nearly 50% lower among patients with RT/AAT compared to RT alone, while in patients with PTEN loss, metastasis was similar in both treatment groups. These data suggest that PTEN may be useful to select patients who can benefit from combined RT/AAT after PSA recurrence.

## 901 Genomic Characterization of Small Cell Bladder Cancer

Bogdan Czerniak[1], Guoliang Yang[1], Jolanta Bondaruk[1], Ziqiao Wang[1], Peng Wei[1], David Cogdell[1], Hui Yao[1], Charles Guo[1]
*[1]The University of Texas MD Anderson Cancer Center, Houston, TX*

**Disclosures:** Bogdan Czerniak: None; Guoliang Yang: None; Jolanta Bondaruk: None; Ziqiao Wang: None; Peng Wei: None; David Cogdell: None; Hui Yao: None; Charles Guo: None

**Background:** Small cell carcinoma (SCC) is an aggressive variant of bladder cancer. We performed comprehensive genomic characterization of SCC, which identified unique molecular features associated with its aggressive nature that may be relevant for the early detection and treatment of this highly lethal disease.

**Design:** Genome-wide analyses, including micro-RNA expressions, genomic mRNA expressions, and whole-exome mutational profiles, were performed on 34 cases of SCC and 84 cases of conventional muscle-invasive urothelial carcinoma (UC). The Cancer Genome Atlas (TCGA) cohort of 408 muscle-invasive bladder cancers served as the control group.

**Results:** SCCs showed a distinct mutational landscape with enrichment of *TP53* and *RB1* mutations. They were related to the so-called double-negative molecular subtype of conventional UC and evolved with the dominance of Sanger mutational signature three consistent with BRCA1/2 insufficiency. Expression analysis showed that SCC were driven by the dysregulation of EMT regulatory network combined with urothelial to neural phenotypic switch. SCCs were characterized by the depletion of immune infiltration and showed upregulation of a unique immune checkpoint inhibitor ADORA2A.

**Conclusions:** We conclude that SCCs are driven by profound dysregulation of the EMT network combined with the loss of urothelial and activation of neural phenotype. Immune depletion with overexpression of a novel immune checkpoint inhibitor, ADORA2A, may represent a novel yet unexplored therapeutic target.

## 902 Reporting Trends, Practices, and Resource Utilization in Neuroendocrine Tumors of the Prostate Gland: A Survey of Genitourinary (GU) Pathologists

Jasreman Dhillon[1], Sean Williamson[2], Sangeeta Desai[3], Santosh Menon[4], Rajal Shah[5], Deepika Sirohi[6], Bonnie Balzer[7], Murali Varma[8], Daniel Luthringer[9], Lovelesh Nigam[10], Paromita Roy[11], Seema Kaushal[12], Divya Midha[11], Manju Aron[13], Kavita Jain[14], Subhasini Naik[15], Manas Baisakh[16], Lata Kini[17], Shivani Sharma[17], Mukund Sable[18], Ekta Jain[17], Spinderjeet Samra[19], Jae Ro[20], Adeboye O. Osunkoya[21], Mahesha Vankalakunti[22], Anil Parwani[23], Anuradha Gopalan[24], Cristina Magi-Galluzzi[25], Sambit Mohanty[26]

*[1]Moffitt Cancer Center, Tampa, FL, [2]Henry Ford Health System, Detroit, MI, [3]Tata Memorial Centre, Mumbai, India, [4]Tata Memorial Hospital, Mumbai, India, [5]University of Texas Southwestern Medical Center, Plano, TX, [6]University of Utah, Salt Lake City, UT, [7]Cedars-Sinai Medical Center, Los Angeles, CA, [8]University Hospital of Wales, Cardiff, Wales, United Kingdom, [9]Cedars-Sinai Medical Center, West Hollywood, CA, [10]IKDRC-ITS, Ahmedabad, Gujarat, India, [11]Tata Medical Center, Kolkata, West Bengal, India, [12]All India Institute of Medical Sciences, New Delhi, Delhi, India, [13]Keck School of Medicine of University of Southern California, Los Angeles, CA, [14]Max Super Specialty Hospital, Shalimar Bagh, Delhi, New Delhi, India, [15]Prolife Diagnostics and Apollo Hospitals, Bhubaneswar, India, [16]Apollo Hospitals, Bhubaneswar, India, [17]Core Diagnostics, Gurgaon, Haryana, India, [18]All India Institute of Medical Sciences, Bhubaneswar, Odisha, India, [19]Westmead Hospital, Westmead, NSW, Australia, [20]Houston Methodist Hospital, Houston, TX, [21]Emory University, Atlanta, GA, [22]Manipal Hospital, Bangalore, Karnataka, India, [23]The Ohio State University, Columbus, OH, [24]Memorial Sloan Kettering Cancer Center, New York, NY, [25]The University of Alabama at Birmingham, Birmingham, AL, [26]AMRI Hospital, Bhubaneswar, India*

**Disclosures:** Jasreman Dhillon: None; Sean Williamson: None; Sangeeta Desai: None; Santosh Menon: None; Rajal Shah: None; Deepika Sirohi: None; Bonnie Balzer: None; Murali Varma: None; Daniel Luthringer: None; Lovelesh Nigam: None; Paromita Roy: None; Seema Kaushal: None; Divya Midha: None; Manju Aron: None; Kavita Jain: None; Subhasini Naik: None; Manas Baisakh: None; Lata Kini: None; Shivani Sharma: None; Mukund Sable: None; Ekta Jain: None; Spinderjeet Samra: None; Jae Ro: None; Adeboye O. Osunkoya: None; Mahesha Vankalakunti: None; Anil Parwani: None; Anuradha Gopalan: None; Cristina Magi-Galluzzi: None; Sambit Mohanty: None

**Background:** Neuroendocrine tumors of the prostate gland were recently classified in the WHO. Despite increasing experience in this area, the specifics and the new clinical and molecular emerging data from prostate cancers treated by contemporary androgen deprivation therapies, as well as primary lesions, need refinement of the diagnostic terminology to encompass the full spectrum of neuroendocrine differentiation. Use of immunohistochemistry (IHC) as a diagnostic, prognostic, and/or predictive tool remains unclear. This study aims at questionnaire- and scenario-based survey among the GU pathologists. Although some of the questions may appear superfluous, this topic based on discussions at multiple levels has evoked surprisingly passionate responses from some who have adopted a “more objective approach” using IHC, citing that recommendations imply that IHC is necessary to be certain.

**Design:** An online survey containing 35 questions was undertaken by 39 GU pathologists (with 5 to 10 years, >10 years and >20 years experience) from four continents, focusing on ascertaining practice patterns in this area. Specific questions included whether, when, and how the respondents classify neuroendocrine differentiation/mixed carcinomas/Paneth cell change/neuroendocrine carcinoma (small, SCC/large cell, LCNEC) of the prostate gland. Additionally questions were posed regarding frequency and indications of IHC with respect to these issues. Some therapy and biomarker-related questions were added as well. De-identified respondent data was tabulated and analyzed by routine statistics. The responses were scored in percentage for each question.

**Results:** 70% and 63% of the responders correctly diagnosed a SCC and mixed acinar adenocarcinoma-SCC, respectively. 37% pathologists felt the need of IHC in a SCC, even if the morphology is classical. A majority (87%) of the responders have the correct idea about the immunopanel and therapeutic options for a SCC. Most importantly, pathologists (85%) correctly mentioned that there is no role of TTF1 indifferentiating pulmonary from prostatic SCC, and determination of site of origin of a high-grade neuroendocrine carcinoma has no importance, as these are treated similarly. In the mixed carcinoma cases, exact quantitation of both the elements, grading of the acinar component as the therapy includes both androgen deprivation and platinum-based chemotherapy, and importance of androgen receptor immunoreactivity have been voted by 85% responders. 49% failed to diagnose Paneth cell-like differentiation, nor were they clear about its prognostic implications.

**Conclusions:** 1. Awareness on morphological features and management of SCC across the pathologists was consistent and IHC work up was necessary for a subset of pathologists for confirmation. 2. Majority failed to recognize Paneth cell-like differentiation, nor were they clear about its prognostic implications, while a small subset failed to identify small cell-like PIN. 3. There still lies some confusion in recognizing Gleason 10 acinar adenocarcinoma and large cell neuroendocrine carcinoma. 4. In the mixed carcinoma cases, there seems to have a legitimate call for appropriate IHC work up, including prostatic and neuroendocrine markers and exact quantitation and grading of the acinar component as the therapy includes both androgen deprivation and platinum-based chemotherapy. 5. Based on the responses, practising trends are different between North America and Asia. Further study and consensus on best practice guidelines based on NCCN parameters are needed to provide guidance with regards to the appropriate indications for IHC use in the various scenarios and patterns of neuroendocrine features in the prostate gland.

## 903 The Cystic Variant of HLRCC Renal Cell Carcinoma. A Tumor with Indolent Appearance and Aggressive Behavior

Esra Dikoglu[1], Mark Ball[2], Rafael Parra-Medina[3], W Linehan[4], Maria Merino[5]

*[1]National Cancer Institute, National Institutes of Health, Bethesda, MD, [2]Johns Hopkins University, Baltimore, MD, [3]National*

*Institutes of Health/National Cancer Institute, Bethesda, MD, [4]National Institutes of Health, Bethesda, MD, [5]National Cancer Institute, Bethesda, MD*

**Disclosures:** Esra Dikoglu: None; W Linehan: None; Maria Merino: None

**Background:** Hereditary leiomyomatosis and renal cell carcinoma (HLRCC) is an autosomal dominant familial syndrome characterized by the development of cutaneous, uterine leiomyomas and aggressive renal tumors. Common morphological patterns of the RCC are papillary, tubulo-papillary, tubular and mixed. Here we describe a cystic type of HLRCC with indolent appearance that can be the predominant or only pattern identified that has propensity to metastasize as cysts some with a sarcomatoid component.

**Design:** Eleven patients with kidney tumors with cystic pattern who were diagnosed as HLRCC Syndrome included in this study. Clinical data and pathology materials were collected from the Urologic Oncology branch, Laboratory of Pathology, NCI. Histopathological features of the tumor were analyzed. Immunohistochemical studies and molecular testing were performed.

**Results:** Patients ranged in age from 16 to 71 years (mean 50). The male-female ratio was 5:6. Family history was positive for nine patients. Tumor was detected either in a single kidney or both kidneys. Partial resection of the lesions was performed as an initial treatment for eight patients and seven of these relapsed in a range of 1 to 5 years. The cystic tumors were ranged in size from 1 to 4 cm and all had either simple or complex cystic pattern. Cysts extended into or presented in adipose tissue and recurred with cystic and sarcomatoid component in two patients and only cystic component in one patient. Six patients had multiple metastasis. Four patients died in a range of 3 to 12 years. *FH* gene mutations and loss of FH expression were detected in all patients and 2SC overexpression was observed in 83% (5/6).

**Conclusions:** Kidney tumors in HLRCC Syndrome may present with different morphological patterns. Recognition of cystic pattern is very important to evaluate because benign appearance of these cysts doesn't imply good prognosis in HLRCC kidney tumors and requires close follow up. Involvement of adipose tissue is common with frequent recurrence. Surgery should be considered to excise additional surrounding fibroadipose tissue of the kidney. Adipose tissue should be evaluated very carefully for cysts since these cysts have tendency to recur in the fat as well as in the kidney and tumor invade local structures, lymph nodes and distant organs. Accurate diagnosis of cysts in HLRCC kidney tumors allows early detection of the disease, personalized management strategies and appropriate genetic counseling.

## 904 Morphological Criteria Predict Early Biochemical Recurrence in Men with Intraductal Carcinoma of the Prostate

Mame Kany Diop[1], Roula Albadine[2], Fred Saad[3], Dominique Trudel[4]
*[1]CRCHUM, Montreal, QC, [2]Montreal, QC, [3]Centre Hospitalier de l`Université de Montréal, Montreal, QC, [4]Centre Hospitalier de l`Université de Montréal, Montréal, QC*

**Disclosures:** Mame Kany Diop: None; Dominique Trudel: None

**Background:** Intraductal carcinoma of the prostate (IDC-P) is an aggressive subtype of prostate cancer identified in approximately 20% of men with prostate cancer. Despite its strong association with recurrence and death, roughly 40% of men with IDC-P are still free of biochemical recurrence (BCR) after 5 years of follow-up, therefore not necessarily needing the "aggressive" label. The objective of this study was to identify if histologic criteria could be used to identify men with IDC-P and early recurrence.

**Design:** Forty-eight patients with IDC-P from our institutional biorepository were included in this study (2013-2018). The most representative block from each specimen containing IDC-P was selected and analysed to visually define characteristic features of the lesion before comparison with survival and clinical data. Time to BCR was defined as time from diagnosis to first PSA level ≥0.2 ng/ml; patients were grouped into early (before 18 months) and late (after 18 months) recurrence. Patients with <18 months of follow-up were removed from the study (n = 6).

**Results:** Out of 16 patients with BCR, 50% experienced BCR before 18 months of follow-up (8/16). Deleterious criteria were identified, including a high mitotic score (>1.59 mitoses/mm$^2$) ($p = 0.012$, Fisher's exact test) and larger duct size (>570 µm in diameter) ($p = 0.020$, Fisher's exact test), according to the third quartile of the distribution. Overall, the number of adverse criteria per patient was lower in men without early BCR compared to men with early BCR (0.7 versus 2.9, respectively, $p = 0.002$, Mann-Whitney U test). There was no significant difference in tumor stage and grade between the 2 groups ($p = 0.173$ and $p = 0.126$, respectively, Mann-Whitney U test), although both tended to be lower in men with late recurrence.

**Conclusions:** We found criteria significantly associated with early BCR in men with IDC-P, including high mitotic score in IDC-P and larger duct sizes. As these are simple measures, we expect clinical application will follow shortly after validation in larger cohorts.

## 905 Cribriform Architecture Prostatic Adenocarcinoma in Needle Biopsies is a Strong Independent Predictor for Lymph Node Metastases in Radical Prostatectomy

Michelle Downes[1], Bin Xu[2], Theodorus Van Der Kwast[3]
*[1]Sunnybrook Health Sciences Centre, Toronto, ON, [2]Memorial Sloan Kettering Cancer Center, New York, NY, [3]University Health Network, Toronto, ON*

**Disclosures:** Michelle Downes: None; Bin Xu: None; Theodorus Van Der Kwast: None

**Background:** The presence of lymph node metastases (LN) at radical prostatectomy is infrequent but a critical prognostic factor. The decision to perform a pelvic lymph node dissection (PLND) is determined by nomograms such as the National Comprehensive Cancer Network or D'Amico risk stratification scheme which assess parameters such as biopsy Gleason score, serum PSA and clinical stage. Cribriform architecture carcinoma (cribriform pattern 4 and intraductal carcinoma- CC/IDC) are associated with high volume, high Gleason score, high stage carcinomas but their impact on LN has yet to be explored.

**Design:** 474 radical prostatectomy cases were reviewed for ISUP grade (G), presence of CC/IDC, T stage and N stage. 249 cases had matched pre-operative biopsies which were reviewed for G, CC/IDC, serum PSA and patient age at diagnosis. The association of CC/IDC with LN in both the prostatectomy and biopsy setting was assessed using Fisher's exact test, Student's t test, univariable and multivariable logistic regression analysis.

**Results:** 286/474 (60%) prostatectomy patients had a PLND of which 27 (9.4%) were N1. G (p=0.004), stage (p <0.001) and CC/IDC (p <0.001) were all significantly associated with LN. On univariate logistic regression, both G (p=0.003) and CC/IDC (p=0.003, odds ratio [OR] 8.940) were associated with LN. On multivariate logistic regression neither were significant, however CC/IDC was the only factor that demonstrated a nonsignificant trend (p=0.052, OR 4.398, 95% confidence interval 0.985-19.643). 179/249 matched biopsy/prostatectomy group had PLND. 18/179 (10%) were N1. On univariate logistic regression, serum PSA (p=0.007), biopsy G (p=0.000) and biopsy CC/IDC (p=0.009) correlated with LN. Multivariate logistic regression showed all three parameters to retain significance: G (p=0.000, OR 2.193), PSA (p=0.034, OR 1.070) and CC/IDC (p=0.004, OR 6.922).

**Conclusions:** The presence of CC/IDC in prostatectomy material is strongly associated with LN. In this cohort, CC/IDC in needle biopsies outperformed the usual nomogram parameters of biopsy G and serum PSA in predicting LN. These findings further support the adverse prognostic nature of cribriform architecture prostate carcinomas which could be of use in pre-operative planning.

## 906 Mismatch Repair Gene Mutations on Low to Intermediate Risk and Metastatic Prostate Cancer

Marie-Lisa Eich[1], Maria Del Carmen Rodriguez Pena[2], Carlos Prieto-Granada[2], Cristina Magi-Galluzzi[2], Shuko Harada[2], George J. Netto[2]
*[1]University Hospital Cologne, Cologne, NRW, Germany, [2]The University of Alabama at Birmingham, Birmingham, AL*

**Disclosures:** Marie-Lisa Eich: None; Maria Del Carmen Rodriguez Pena: None; Carlos Prieto-Granada: None; Cristina Magi-Galluzzi: None; Shuko Harada: None; George J. Netto: None

**Background:** High risk prostate cancer (PCa) has been shown to be associated with somatic mismatch repair pathway defect (dMMR) and rarely with Lynch syndrome. The majority of these tumors show loss of MHS2. African-American (AA) patients with prostate cancer are known to have a worse outcome. Herein, we set out to compare the presence of dMMR in patients of African-American (AA) and Caucasian descent.

**Design:** The study was performed on a tissue micro-array (TMA) constructed from radical prostatectomies performed at our institution between 2013 and 2018. Each specimen was spotted 3 times for tumor and 2 for corresponding benign tissue. In addition, the pathology database was searched between 2017 and August 2019 for metastatic PCa with prior dMMR immunohistochemical (IHC) analysis. Clinical, histopathological and follow-up data was obtained on all cases. IHC staining was performed using a Leica Bond autostainer for MLH1 (Leica PA0610), MSH2 (Biocare FE11), MSH2 (Cell Marque PA0804), PMS2 (Cell Marque MRQ28). Retained expression was defined as nuclear staining. Loss of expression was defined as absence of nuclear staining within tumor cells with retained expression in internal controls. Benign prostatic tissue, stromal cells and infiltrating lymphocytes were used as internal controls.

**Results:** The TMA consisted of 380 spots from 76 radical prostatectomies obtained from 35 AA (46%) and 41 (54%) Caucasian patients (age 40 – 74; median 60 years). PSA average was 8.5 ng/mL (range 1.1 – 37). Forty-eight cases were grade group (GG) 2 and 28 were GG 3. Average follow-up length was 3 months (range: 4 – 62). Five of 74 (7%) patients with available follow-up showed biochemical recurrence; 4 of the 5 patients were AA. None of the 76 cases showed lack of expression for dMMR.

Our cohort also included 3 metastatic PCa cases (2 Caucasian, 1 AA). Whole slides from a supraclavicular node, liver and brain metastases were analyzed by IHC. Two of the 3 tumors showed concomitant loss of MSH2 and MSH6. One patient was Caucasian, one African-American.

**Conclusions:** Our cohort of low and intermediate risk tumors (GG 2 and 3) lacked evidence of dMMR. In contrast, 2 of 3 metastatic PCa cases demonstrated dMMR. In our study, no difference in rate of dMMR was demonstrated between AA and Caucasian patients. The current cohort will be expanded to include additional high risk primary and metastatic tumors from patients of AA descent.

## 907 Ejaculatory Ducts and Utricle Anatomy in Verumontanum: A Histomorphologic Study from Adult Prostates

Ziad El-Zaatari[1], Jae Ro[1], Ngoentra Tantranont[2], Ahmed Shehabeldin[1], Steven Shen[3]
*[1]Houston Methodist Hospital, Houston, TX, [2]The Houston Methodist Hospital, Houston, TX, [3]Houston Methodist; Weill Cornell Medical College of Cornell University, Houston, TX*

**Disclosures:** Ziad El-Zaatari: None; Jae Ro: None; Ahmed Shehabeldin: None; Steven Shen: None

**Background:** The ejaculatory ducts (EDs) open into the prostatic urethra at the level of the verumontanum. The prostatic utricle (PU), an invagination of the prostatic urethra, is also found in this anatomic region. Conventionally, it is known that the openings of the EDs are posterior and lateral to and separate from the opening of the prostatic utricle (PU). In addition, EDs epithelium has conventionally been characterized by features shared by the contiguous seminal vesicles, namely enlarged “monster” cells and yellow lipofuscin pigment. However, by examining a number of whole mount prostates, we have found variations in these histomorphologic patterns.

**Design:** Of 750 screened cases of radical prostatectomy specimens from prostate cancer patients, we identified 46 informative cases for evaluation of ED and utricle histomorphology. Selection of the 46 cases was based on sections showing tips of EDs, PU and prostatic urethra within the same 100x microscopic field. The microscopic topography and histologic appearance were evaluated for these 46 cases.

**Results:** 11 of 46 cases (24%) had two ED openings laterally to the utricle into the urethra (Fig. 1c). In 1 case (2%), a direct opening of the EDs into the utricle was observed (Fig. 1a). 34 cases (74%) did not show a definitive final opening but were suggestive of opening of the EDs into the utricle (Fig 1b). Of all 46 cases, 10 cases (22%) versus 36 cases (78%) respectively showed transition of the ED lining from seminal vesicle-type epithelium to prostatic gland-type epithelium versus no transition. Complex, branching invaginations versus simple straight lumens of the distal EDs were respectively observed in 10 cases (22%) versus 36 cases (78%).

Figure 1 - 907

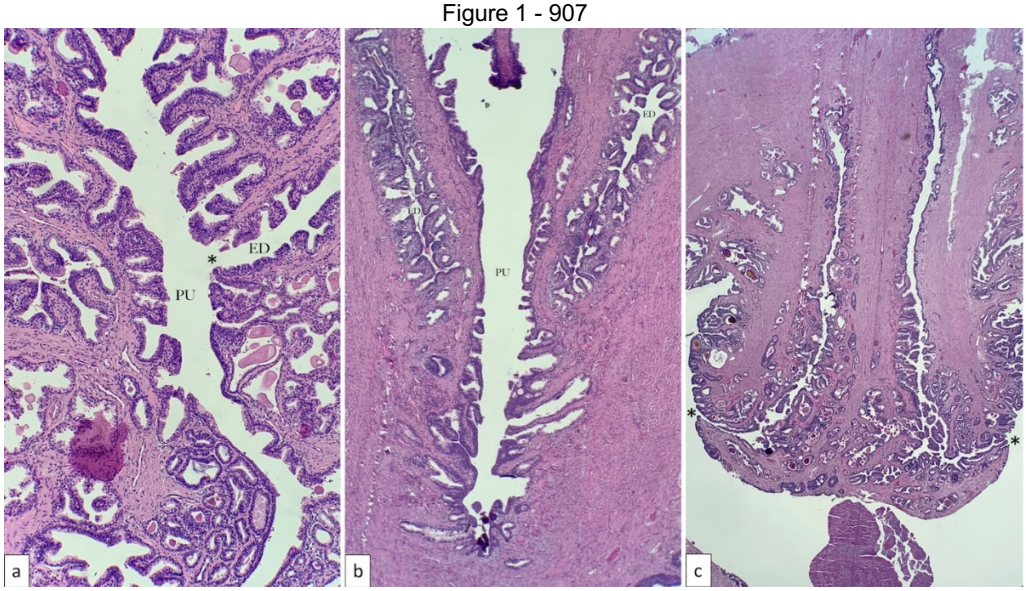


**Conclusions:** Our study provides detailed descriptions of EDs and utricle histomorphologic anatomy in a specific anatomic region of the adult prostate. Previously undescribed features of these structures were found, namely ED directly opening into the utricle and transition to prostatic-type epithelium near ED openings. A thorough understanding of anatomy and histomorphology of this region may have important implications for seminal vesiculoscopy, an emerging procedure used to treat disorders of the prostatic utricle-ED system, such as dilation or cyst, stones, and blood clots. Our findings may also enhance our understanding of pathologic processes of this area of the prostate including seminal vesicle spread of prostatic carcinoma and ductal endometrioid carcinoma, which often arises in this region.

## 908 Limited, Extended and Super-Extended Lymph Node Dissection at Radical Cystectomy/Cystoprostatectomy Preceded by Neoadjuvant Chemotherapy: Anatomic Extent of Dissection Correlates with Overall "N" Stage but not Survival

Carla Ellis[1], Emily Alvey[1]
*[1]Emory University, Atlanta, GA*

**Disclosures:** Carla Ellis: None; Emily Alvey: None

**Background:** Radical cystectomy/cystoprostatectomy (RC) + lymph node dissection (LND) is the gold standard for treatment of high risk, non-muscle invasive bladder cancer (NMIBC) that is unresponsive to intravesicle therapy or, for muscle invasive bladder (MIBC). Conflicting reports exist regarding the optimal anatomical extent of LND and the associated therapeutic outcomes. Super-extended LNDs are associated with increased intraoperative times and blood loss, and higher laboratory costs/labor. Our retrospective study seeks to examine this correlation in a unique cohort: a single pathology laboratory system with a standard LN grossing protocol in a cohort of patients treated with neoadjuvant chemotherapy (NAC).

**Design:** A search of our pathology data system was performed. All RC specimens in patients who received NAC for urothelial cancer (UCa) between 2009 and 2016 were analyzed in terms of the total number of lymph nodes obtained (and # positive) and the defined anatomical extent (limited [lLND] – internal iliac, external iliac, and obturator; extended [eLND] – limited + common iliac and/or presacral; and super-extended [sLND] – extended + inferior mesenteric artery, paracaval, and/or para-aortic. Overall N stage and outcome (alive, alive with disease, dead) were analyzed.

**Results:** A total of 207 cases yielding an overall total of 4,747 LNs were reviewed. 276 (5.8%) were positive for metastatic disease. All patients had at least 3 cycles of NAC (range: 3-6 cycles), most commonly with gemcitabine and cisplatin. The average number of follow up months was 31.5. The majority of patients (142/207, 68.5%) had a pre-surgical pathologic stage of pT2. Of the total 4,747 LNs, 5.1%, 6.0% and 6.3% of were positive in the each of the l, e and sLND categories, respectively (see table). Of the 276 positive lymph nodes, 75%, 17% and 8% were in l, e and sLND anatomic regions, respectively.

| | N (% +) | N0 | N1 | N2 | N3 | A | AWD | D |
|---|---|---|---|---|---|---|---|---|
| lLND | 5.1 | 73 (75%) | 9 (9%) | 15 (15%) | N/A | 63 (65%) | 24 (25%) | 10 (10%) |
| eLND | 6.0 | 51 (76%) | 3 (4%) | 7 (10%) | 6 (9%) | 35 (52%) | 20 (30%) | 12 (18%) |
| sLND | 6.3 | 25 (68%) | 3 (8%) | 2 (5%) | 7 (19%) | 24 (65%) | 11 (30%) | 2 (5%) |

**Conclusions:** In all LND categories, there was a higher percentage of living patients than dead at last follow up (see table); however, there was no statistically significant correlation between mortality and LND category in this post-NAC cohort. The overall N stage at time of RC correlated to LND category (p=0.009). Our results indicate that varying types of LND correspond to accurate N stage at RC; however, overall mortality (particularly in the setting of increased peri-operative complications and laboratory labor) is not affected. Additional studies are necessary to support this novel finding.

## 909 Routine Clinical RNA-Sequencing in Castration-Resistant Prostate Cancer

Mark Evans[1], Max Jan[2], Harrison Tsai[3], Alexander Farahani[2], Valentina Nardi[2], Long Le[2], John Iafrate[2], Dora Dias-Santagata[2], Jochen Lennerz[4]
*[1]University of California Irvine, Orange, CA, [2]Massachusetts General Hospital, Boston, MA, [3]Brigham and Women's Hospital, Boston, MA, [4]Massachusetts General Hospital, Harvard Medical School, Boston, MA*

**Disclosures:** Mark Evans: None; Max Jan: None; Harrison Tsai: None; Alexander Farahani: None; Valentina Nardi: None; Long Le: *Advisory Board Member*, ArcherDx; *Stock Ownership*, ArcherDx; John Iafrate: *Stock Ownership*, ArcherDx; Dora Dias-Santagata: None; Jochen Lennerz: None

**Background:** Abiraterone and enzalutamide are approved for the treatment of castration-resistant metastatic prostate cancer. Certain splice-variants of the androgen receptor (AR-v7) and the presence of certain intergenic fusions (e.g. involving the oncogenic transcription factor ERG) have been reported as associated with reduced response to enzalutamide, abiraterone, and/or taxane-based chemotherapies. As a result, there is a demand for a reliable and highly sensitive method for detecting these alterations when selecting appropriate treatment. We report routine clinical RNA-sequencing as a reliable strategy to identify inter- and intragenic aberrations in prostate cancer.

**Design:** Cases of castration-resistant prostate carcinoma were identified from the medical record that had been submitted for routine next-generation sequencing from 2010 to 2019. We included all histological subtypes and results of the RNA-sequencing were reviewed retrospectively to determine the presence of intergenic fusions, gene mutations, and specifically expression of AR-v7.

**Results:** We examined 49 samples from castration-resistant prostate cancer patients (median age: 69 years; range, 49-89). The histotypes were n=48 cases of acinar and/or intraductal carcinoma, with one exception of small cell morphology. Among the 49 patients,

we successfully identified n=28 intergenic fusions (57%; n=24 ERG-TMPRSS2 fusions). Each of the patients had been treated with androgen deprivation therapy (ADT) in combination with several additional treatment modalities, including abiraterone and enzalutamide, and we identified n=20 cases with AR-v7 transcripts.

**Conclusions:** In a specific castration-resistant cohort of prostate cancers, our review demonstrates that routine RNA-sequencing is able to reliably detect ERG-TMPRSS2 fusions and AR-v7 expression. RNA-sequencing has clinical utility in detecting both intragenic and intergenic alterations in prostate cancer.

## 910 High-Grade Oncocytic Tumor (HOT) of Kidney is Characterized by Frequent TSC1, TSC2 and mTOR Mutations – a Further Characterization of an Emerging Entity

Mihaela Farcas[1], Zoran Gatalica[2], Jeffrey Swensen[2], Farshid Siadat[3], Yuan Gao[4], Kiril Trpkov[3], Ondrej Hes[5]
*[1]Colentina Hospital, Bucharest, Romania, [2]Caris Life Sciences, Phoenix, AZ, [3]University of Calgary, Calgary, AB, [4]Eastern Health/Memorial University, St. John's, NL, [5]Biopticka laborator s.r.o., Plzen, Plzensky kraj, Czech Republic*

**Disclosures:** Mihaela Farcas: None; Zoran Gatalica: *Employee*, CARIS life sciences; Jeffrey Swensen: *Employee*, Caris Life Sciences; Farshid Siadat: None; Yuan Gao: None; Kiril Trpkov: None; Ondrej Hes: None

**Background:** Within the spectrum of hybrid oncocytic tumors, a subtype of high-grade oncocytic tumor (HOT) has emerged, characterized by eosinophilic cells with large cytoplasmic vacuoles, high-grade nuclei, and invariable Cathepsin K reactivity (He H et al. Virchows Arch. 2018;473:725-38). Such tumor has also been found in a Tuberous Sclerosis Complex (TSC) patient (Trpkov K, et al. Histopathology. 2019;75:440-2). A recent study found somatic mutations of *TSC2* or *mTOR* as characteristic features in a distinct subset of tumors labelled "sporadic renal cell carcinoma with eosinophilic and vacuolated cytoplasm", which in our view, represent the same entity as HOT (Chen Y-B et al, Am J Surg Pathol. 2019;43:121-31).

**Design:** We identified 14 cases with hybrid oncocytic morphology, compatible with HOT and we evaluated them by immunohistochemistry and next generation sequencing (NGS). NGS of microdissected tumor DNA was performed using a 592-gene panel. None of the patients were known to have a TSC.

**Results:** Patients were 7 males and 7 females, with mean age of 49.8 y (median 52; range 25-78 y). Average tumor size was 3.1 cm (median 3.1; range 1.5 to 7 cm). All tumors were positive for PAX8, AE1-AE3, CK18, MIA, SDHB, CD117, and Cathepsin-K; CK7 was only focally positive. Negative stains included HMB45, Melan-A, and TFE3. Ten of 14 cases showed mTOR pathway mutations with exclusive *TSC1* (4), or *TSC2* (3), or *MTOR* (3) mutations. In 2 other patients only *FLCN* mutations were found; on additional investigations, a clinical Birt-Hogg-Dubé (BHD) phenotype was found in one patient. The last 2 patients showed no clinically significant mutations.

**Conclusions:** HOT is an emerging renal entity that shows characteristic morphology, Cathepsin-K expression, and frequent, non-overlapping mutations in either *TSC1*, or *TSC2*, or *mTOR* genes. Within the group of hybrid oncocytic tumors, there is a morphologic overlap between HOT and cases with *FLCN* mutation (or unrecognized BHD), which can be conclusively distinguished by molecular analysis.

## 911 Comparative Analysis of Renal Sarcomas: A Cohort Study of the SEER Database

Giovanna A Giannico[1], Justin Cates[1], Jennifer Gordetsky[1]
*[1]Vanderbilt University Medical Center, Nashville, TN*

**Disclosures:** Giovanna A Giannico: None; Justin Cates: None; Jennifer Gordetsky: None

**Background:** Primary renal sarcomas are uncommon, and there is a paucity of information on the clinicopathologic and natural history of the disease. In this study we performed a comparative analysis of adult sarcomas arising in the kidney (RS) and retroperitoneum (RPS) using the National Cancer Institute's SEER database (Surveillance, Epidemiology. and End Results).

**Design:** The SEER database was queried for RSs and RPSs (leiomyosarcoma, undifferentiated pleomorphic sarcoma, and sarcoma, NOS) from 1973 to 2013. Cox multivariate regression was performed to identify prognostic factors. Kaplan-Meier curves were used to assess disease-specific survival (DSS). Given the lack of an AJCC 8$^{th}$ edition stage grouping for sarcomas of visceral organs, other staging algorithms (those of the extremities and trunk [AJCC] and the Vanderbilt staging system, [VS]) were applied. Patients <19 years of age and those without confirmatory surgery were excluded.

**Results:** A total of 280 RSs and 2045 RPSs were available for analysis. Clinical and pathologic variables are summarized in Table 1. Median follow up of censored patients was 47 months (range 0.5-474). Half of all patients died of sarcoma a median of 21 months after surgical resection (range 0.5-301). For RS, male gender (HR 1.61, p=0.003), year of diagnosis (HR 0.98, p=0.007) , UPS diagnosis (HR 1.43, p=0.03), tumor size (HR1.26, p=0.002), metastasis (HR 2.31, p<0.0001) and stage (IV, HR 3.07, p=0.003) were statistically significant prognostic factors by univariate analysis. Renal origin was a significant predictor of DSS (HR 1.28, CI 1.03-1.58, $P = 0.024$) after adjusting

for patient age (HR 1.12, p<0.0001), year of diagnosis (HR 0.99, p=0.03), UPS diagnosis (HR 1.16, p=0.0054), and AJCC stage (IV, HR 6.56, p=0.0012). Comparison of Kaplan-Meier plots by AJCC stage showed poor separation for Stages IB, II, IIIA, and IIIB (Figure 1). In contrast, the VS showed much better discrimination of risk between tumor stages (Figure 2). Receiver-operating characteristic curves confirmed significantly higher accuracy of the VS (72%) compared to the AJCC (66%, *P*=0.03) in predicting 5-year DSS.

**Table 1.** Clinicopathologic characteristics of the SEER cohort

| Factor | Retroperitoneal Sarcomas | Renal Sarcomas | p-value |
|---|---|---|---|
| N | 2045 | 280 | |
| Age at diagnosis, median (IQR) | 62.00 (52.00, 72.00) (n=2045) | 60.50 (51.00, 70.00) (n=280) | 0.30 |
| Sex M/F, (Ratio) | 766/1279 (0.6) | 122/158 (0.77) | 0.049 |
| Histologic diagnosis, N (%) | | | 0.008 |
| LMS/Sarcoma, NOS | 1317 (64.4) | 157 (56.1) | |
| UPS | 728 (35.6) | 123 (43.9) | |
| Tumor size (cm), median (IQR) | 12.50 (8.50, 18.00) (n=1458) | 10.50 (6.50, 15.00) (n=218) | <0.001 |
| Histologic grade, N (%) | | | 0.003 |
| 1 | 135 (6.6) | 12 (4.3) | |
| 2 | 408 (20.0) | 32 (11.4) | |
| 3 | 843 (41.2) | 126 (45.0) | |
| Missing data | 659 (32.2) | 110 (39.3) | |
| AJCC stage, 8th ed., N (%) | | | <0.001 |
| Stage IA | 15 (0.7) | 1 (0.4) | |
| Stage IB | 108 (5.3) | 8 (2.9) | |
| Stage II | 65 (3.2) | 22 (7.9) | |
| Stage IIIA | 255 (12.5) | 39 (13.9) | |
| Stage IIIB | 779 (38.1) | 63 (22.5) | |
| Stage IV | 238 (11.6) | 54 (19.3) | |
| Missing data | 585 (28.6) | 93 (33.2) | |
| Vanderbilt Stage, N (%) | | | 0.007 |
| Stage IB | 54 (2.6) | 5 (1.8) | |
| Stage II | 287 (14.0) | 28 (10.0) | |
| Stage IIIA | 357 (17.5) | 49 (17.5) | |
| Stage IIIB | 491 (24.0) | 44 (15.7) | |
| Stage IV | 197 (9.6) | 39 (13.9) | |
| Missing data | 659 (32.2) | 115 (41.1) | |
| Radiation/Surgery Sequence, N (%) | | | <0.001 |
| No RT | 1427 (69.8) | 231 (82.5) | |
| Neoadjuvant RT | 92 (4.5) | 2 (0.7) | |
| Adjuvant RT | 478 (23.4) | 42 (15.0) | |
| Sequence unknown | 3 (0.1) | 1 (0.4) | |
| Missing data | 45 (2.2) | 4 (1.4) | |

Figure 1 - 911

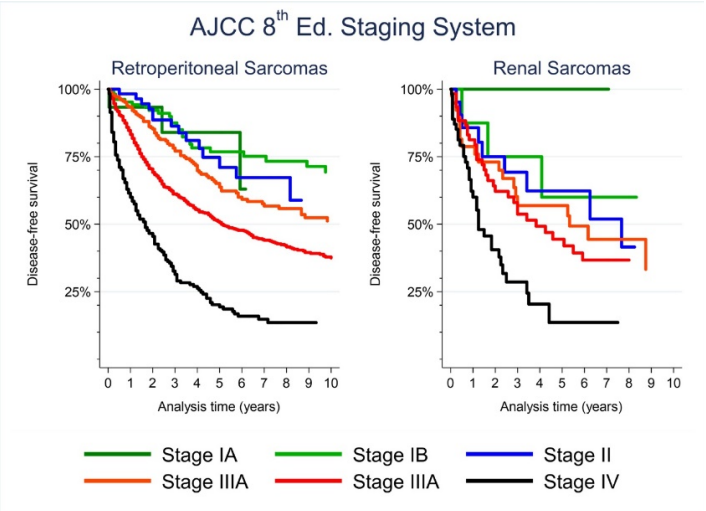


Figure 2 - 911

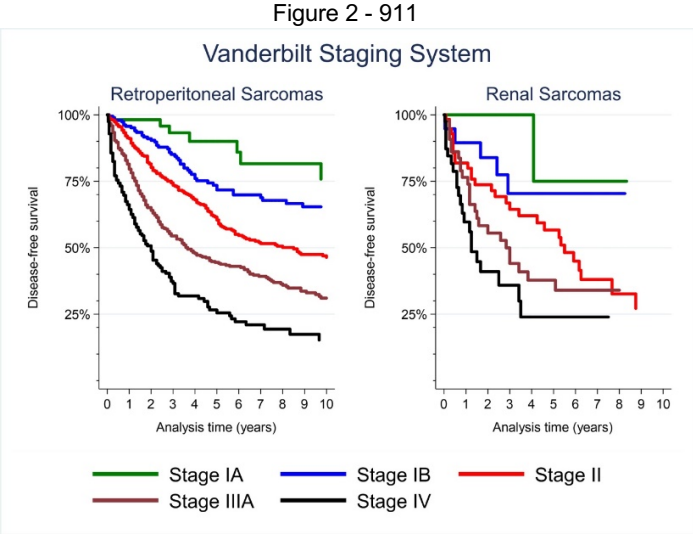


**Conclusions:** Compared to RPSs, RSs are more often high grade and present at advanced stage. Even after adjusting for these factors, patient with RS show a greater risk of sarcoma-related death than those with RPS. Finally, the VS shows greater accuracy in predicting DSS than the AJCC system for RPS.

## 912 Prostate Cancer with Germline DNA Damage Repair Gene Alterations: A Clinical and Pathologic Assessment

Anuradha Gopalan[1], Samson Fine[1], Ying-Bei Chen[1], Hikmat Al-Ahmadie[1], Judy Sarungbam[1], Wassim Abida[1], Howard Scher[1], Satish Tickoo[1], Victor Reuter[1]
[1]*Memorial Sloan Kettering Cancer Center, New York, NY*

**Disclosures:** Anuradha Gopalan: None; Samson Fine: None; Ying-Bei Chen: None; Hikmat Al-Ahmadie: None; Judy Sarungbam: None; Wassim Abida: None; Howard Scher: None; Satish Tickoo: None; Victor Reuter: None

**Background:** Pathogenic alterations in DNA damage repair (DDR) genes have been reported in approximately 27% of prostate cancer (PC), of which over two thirds are in the germline. The presence of these mutations (MUT) predicts for sensitivity to specific classes of drug and has implications for genetic counseling. Recent studies have reported associations between histologic patterns of prostate adenocarcinoma and DDR MUT.

**Design:** We evaluated 99 cases of prostatic adenocarcinoma – primary (PRIM) and metastatic (MET) with clinically significant germline MUT in DDR genes (*BRCA* 1 and 2, *ATM*, *CHEK*2, *PALB*2, *NBN* and *BRIP*1) identified by an FDA approved next generation sequencing assay, for clinical and pathologic associations. 93 cases had slides available for assessment. Four cases with morphologic effects of androgen deprivation therapy were excluded from morphologic evaluation.

**Results:** Overall, *BRCA*2 MUT was the most frequent (42/99; 41%). Slides were available in 56 PRIM and 33 MET PC for evaluation. 10 cases had matched PRIM/MET samples or more than one MET sample. Of 39 available *BRCA*2 MUT cases, 26 (67%) were Grade group 4-5, 12 (31%) were grade group 3 and 1 was grade group 2. Intraductal histology was present in 33/56 (59%) PRIM PC. Ductal phenotype was present in 7/56 (12%). Three of these had *BRCA*2, 2 had *CHEK*2 and 1 each had *BRCA*1 and *PALB*2 MUT. 26/56 (46%) had at least focal cribriform architecture. 25/56 (45%) had predominant non-intraductal/ductal/cribriform histology. Concordance in morphologic features between the PRIM and MET was present in 5 of 6 evaluable cases. Five cases had high tumor mutation burden. Two had *BRCA*2 MUT, of which one was also mismatch repair deficient (MMR-D). One each had *ATM*, *CHEK*2 and *PALB*2 MUT, the latter two with MMR-D.

**Conclusions:** *1. BRCA*2 is the most common germline DDR gene alteration in prostatic adenocarcinoma. 2. More than half of prostatic adenocarcinoma with germline DDR gene alterations show intraductal/ductal/cribriform histology; however, a significant number have conventional acinar morphologic features.

## 913 Molecular Diagnostic-Associated Changes in Prostate Cancer Biopsy NCCN Category are Linked to Histopathologic Features

Nancy Greenland[1], Janet Cowan[1], Emily Chan[1], Peter Carroll[1], Bradley Stohr[1], Jeffry Simko[1]
[1]*University of California San Francisco, San Francisco, CA*

**Disclosures:** Nancy Greenland: None; Janet Cowan: None; Emily Chan: None; Peter Carroll: None; Bradley Stohr: None; Bradley Stohr: None; Jeffry Simko: None

**Background:** The GPS (Genomic Prostate Score, OncotypeDx) assay is designed for prostate biopsies with Gleason score 3+3=6 or 3+4=7 that predicts more severe pathology at prostatectomy. The GPS test is most useful when it changes a patient's NCCN category, as that could result in a change in patient management. We hypothesized that histopathologic features would be associated with the direction of NCCN category change attributed to the GPS test.

**Design:** We included patients who had the GPS test performed on their prostate biopsy from September 2013 to March 2019. The GPS and pre- and post-test NCCN categories were noted. For patients in whom the NCCN category changed with the test, the biopsy cores that had received a GPS were re-reviewed by three pathologists in a blinded manner for percentage and type of Gleason pattern 4 tumor, degree of stromal reaction, severity of inflammation, and nuclear polarization of the Gleason pattern 3 tumor.

**Results:** Of 521 patients, there were 131 patients (25%) for whom the NCCN category changed with the test. Slides from 130 of the biopsies were available for re-review, with 8 (6%) increasing from intermediate to high, 15 (11%) increasing from low to intermediate, 33 (25%) decreasing from intermediate to low, and 74 (57%) decreasing from low to very low. Patients moved at most one level in NCCN category. Biopsies in which the NCCN category increased were associated with stromal reaction ($P<0.01$) and inflammation ($P<0.01$), whereas biopsies in which the NCCN category decreased were not associated with those features ($P<0.01$). In the subset of Gleason 3+3=6 cases, increase in NCCN category was associated with a lack of nuclear polarization, whereas NCCN category decreases were associated with nuclear polarization ($P<0.01$).

**Conclusions:** Stromal reaction, inflammation, and lack of nuclear polarization were associated with NCCN category increase and vice versa. Our results suggest that more detailed histopathologic analysis of prostate biopsies could substitute for some of the information gleaned from the GPS test.

## 914 Molecular Profiling of Penile Intraepithelial Neoplasia (PeIN) Highlights Subtype-Specific Recurrent and Unique Oncogenic Driving Alterations

Laurie Griesinger[1], Chia-Jen Liu[1], Rohit Mehra[1], Scott Tomlins[1], Aaron Udager[2]
[1]*University of Michigan, Ann Arbor, MI,* [2]*University of Michigan Medical School, Ann Arbor, MI*

**Disclosures:** Laurie Griesinger: None; Chia-Jen Liu: None; Rohit Mehra: None; Scott Tomlins: *Employee*, Strata Oncology; *Stock Ownership*, Strata Oncology; Aaron Udager: None

**Background:** Penile squamous cell carcinoma (PeSCC) arises via distinct human papillomavirus (HPV)-dependent and HPV-independent pathways, and its precursor lesion (PeIN) shows characteristic clinical, morphologic, and immunohistochemical features depending on HPV status. Previously, our group utilized targeted next-generation sequencing (NGS) to establish the molecular landscape of invasive and metastatic PeSCC. In the current study, we employed a similar approach to explore the genomic underpinnings of PeIN.

**Design:** PeIN cases were retrospectively identified from a single large academic institution and reviewed by an experienced genitourinary pathologist. Each case was subtyped as HPV-independent [differentiated (dPeIN)] or HPV-dependent (hPeIN) by histology and available ancillary material. Targeted NGS was performed on an Ion Torrent S5 sequencer using a custom pan-cancer AmpliSeq panel and formalin-fixed paraffin-embedded (FFPE)-extracted DNA from representative tumor areas. NGS data was processed using in-house bioinformatics pipelines, and filtered variants were manually curated.

**Results:** 27 PeIN cases from unique patients were analyzed, including 15 dPeIN and 12 hPeIN. A total of 44 prioritized variants were identified (median = 1; range = 0-5), including recurrent mutations in *TP53* ($n$ = 15), *CDKN2A* ($n$ = 7), *FBXW7* ($n$ = 4), *PIK3CA* ($n$ = 4), *BRCA2* ($n$ = 2), and *NFE2L2* ($n$ = 2). Compared to hPeIN, dPeIN harbored more total recurrent prioritized mutations (odds ratio = 2.768; Mann-Whitney U test, $P < 0.05$) and was significantly associated with *TP53* or *CDKN2A* mutations (Fisher's exact test, $P < 0.05$; see Figure). Logistic regression demonstrated that total recurrent prioritized mutations and *TP53* mutation status were significant predictors of the dPeIN subtype in univariate analyses; however, only *TP53* mutation status (odds ratio = 7.325) was independently predictive in a multivariate model with total recurrent prioritized mutations. Finally, unique potential oncogenic driving alterations ($n$ = 1) included *PTPN14* in dPeIN and *RB1*, *PTEN* or *FGFR3* in hPeIN.

Figure 1 - 914

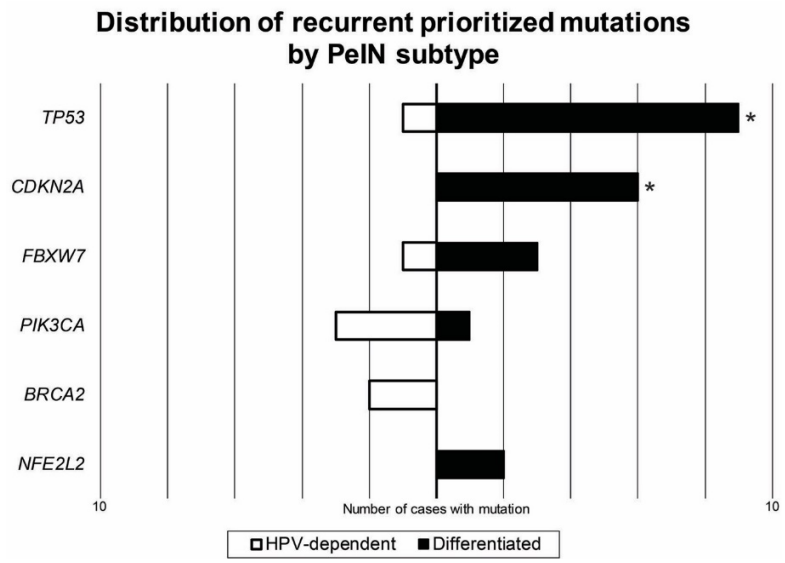


**Conclusions:** Our data highlight the unique molecular spectrum of HPV-dependent and HPV-independent PeIN subtypes. dPeIN is associated with higher total recurrent prioritized mutations, including frequent *TP53* and *CDKN2A* mutations and potential unique *PTPN14* mutations. In contrast, hPeIN shows recurrent prioritized mutations in the PI3K/AKT pathway (*PIK3CA* and *PTEN*), as well as potential unique *BRCA2*, *RB1*, and/or *FGFR3* mutations.

## 915 Clear Cell Adenocarcinoma of the Genitourinary Tract in Men: A Series of 14 Cases

Daniel Grosser[1], Jonathan Epstein[1]
[1]*Johns Hopkins Medical Institutions, Baltimore, MD*

**Disclosures:** Daniel Grosser: None; Jonathan Epstein: None

**Background:** Clear cell adenocarcinoma (CCA) is a rare tumor in the bladder usually in women with less than 20 reported cases in men.

**Design:** We searched for cases of CCA reviewed at our institution in men in any genitourinary site from 2007-2018.

**Results:** We identified 14 cases of CCA in men. There were 5 in the bladder, 5 in prostate or prostatic urethra, 2 in membranous urethra, 1 near the right anterolateral region of the prostate likely in a Mullerian remnant, and 1 between bladder and rectum likely in a prostatic utricle cyst. Although endometriosis can rarely be found in men, no cases showed endometriosis. 11 patients underwent surgical resection, including 3 TURs and 1 urethrectomy. 1 patient experienced recurrence following TUR. Mean tumor size in resected cases (excluding TUR and urethrectomy) was 4.5 cm (range 0.7-9.3). 4 cases showed direct extension to other organs (1 bladder and rectum, 1 bladder alone, 1 prostate, 1 seminal vesicle). 4 cases showed metastases to lymph nodes with 3 of these showing other metastases (1 to right flank, 1 to lung and adrenal gland, 1 to bladder). PAX8 immunohistochemistry was positive in 11/11 cases; other cases had classic CCA morphology. Mean age at time of initial pathology was 61 years (range 29-89), excluding the case of a 17-year-old patient with tumor located in the unusual site of prostatic utricle. 7 patients underwent additional treatment [1 chemotherapy & radiation (RT), hormonal therapy (HT) & immunotherapy; 1 chemotherapy, RT & targeted therapy; 1 RT & HT; 1 chemotherapy; 2 RT; 1 HT]. Mean follow-up was 37 months (range 1-138 months). At last follow-up, 7 patients showed no evident disease, 2 patients were alive with disease, and 4 patients were deceased with cause of death not known. Mean time to death was 16 months (range 6-39). Of patients who died, all had tumors localized to the prostate or prostatic urethra. No follow-up was available on 1 patient.

**Conclusions:** CCA in men is exceedingly rare and the above cases reflect the results of an expert consultation practice enriched in unusual cases. Nonetheless, they demonstrate that CCA should be included in the differential diagnosis in men. CCA in men can arise not only in the bladder and urethra similar to females, but also in unusual adjacent sites. The mortality rate varied with tumor site, with death the outcome in 4 of 5 tumors in the prostate or prostatic urethra, and no tumors in bladder, membranous urethra, Mullerian remnant, or prostatic utricle.

## 916 Presence and Type of Cribriform Pattern (CP) 4 in Prostate Biopsies (Bx) with Gleason Score (GS) 7 Prostate Cancer (PCa) is Significantly Associated with High-Risk Clinical Features (HRF)

Chhavi Gupta[1], Atsuko Iwata[2], Mahul Amin[3], Akash Sali[4], Suzanne Palmer[4], Shakir Aliasger[2], Andre Abreu[4], Manju Aron[4]
*[1]Tata Memorial Hospital, Mumbai, Maharashtra, India, [2]Keck Medical Center of USC, Los Angeles, CA, [3]Methodist University Hospital, Memphis, TN, [4]Keck School of Medicine of University of Southern California, Los Angeles, CA*

**Disclosures:** Chhavi Gupta: None; Atsuko Iwata: None; Mahul Amin: *Consultant*, Urogen; *Consultant*, Advanced Clinical; *Advisory Board Member*, Cell Max; *Advisory Board Member*, Precipio Diagnostics; Akash Sali: None; Suzanne Palmer: None; Shakir Aliasger: None; Andre Abreu: None; Manju Aron: None

**Background:** The significance of reporting CP on bx with GS 7 PCa is debated and is currently not a mandated data element in PCa reports. There is accumulating data documenting increased association of CP with adverse features on radical prostatectomy (RP), prompting the advocacy of excluding these patients from active surveillance (AS). However, a systematic analysis of CP (including its subtypes) on extended bx protocols and its association with HRF has not been widely reported.

**Design:** 108 patients with GS 7 PCa were diagnosed between 2017-19, with a total of 1582 bx of which 687 were positive for PCa. Positive bx were re-reviewed to document the presence and percentage of various Gleason patterns (GP) 4 including CP (Table 1). CP was further subdivided into small and large (> 2x normal glands or glands with ≥ 12 lumina). Cribriform glands with comedonecrosis and as part of intraductal carcinoma were excluded. Multiparametric MRI (mpMRIs) were reviewed and scored (PIRADS v2 scoring system). Clinical features including HRF (PSA ≥ 20, stage ≥ cT3, and non-organ confined PCa) were documented. Adverse pathology on RP, where available was noted ( ≥ pT3, Grade Group (GG) ≥ 3, positive margins or pN1). Presence, type and percentage of CP on bx were compared for association with HRF and adverse pathology on RP.

**Results:** 37(34%) patients had CP and 66% of CP lesions were detected on mpMRI. Patients with CP were younger (median: 65(60-69) vs 68(63-72), p=0.034) with more GG 3 at bx (65% vs 25%, p<0.0001). Any CP (26 vs 11, p<0.0001) and presence of mixed GP 4 patterns with CP (p=0.012) were significantly associated with HRF. Large CP was significantly more associated with HRF than small CP (p=0.030), while percentage CP was not. On multivariate analysis of factors associated with HRF in GS 7 PCa, PSA density (357(8.40-15163), p=0.0001) and presence of any CP (8.39(2.84-24.85), p=0.0003) were significant. Only 24 patients with CP on bx underwent RP. Majority (15; 63%) of these patients had adverse features on RP, including 13 pT3a, 2 pN1, and 4 with positive surgical margins.

**Table 1.** Comparison of pathological findings for Gleason Score 7 prostate carcinoma with and without High-Risk Clinical Features

| | All | High-Risk Clinical Features | | |
|---|---|---|---|---|
| | | No | Yes | p |
| N | 108 | 60 | 48 | |
| Morphological types of Gleason pattern 4 | 37 | 11 | 26 | **<0.0001** |
| Cribriform | 104 | 57 | 47 | 0.63 |
| Fused | 46 | 21 | 25 | 0.074 |
| Poorly formed | 11 | 4 | 7 | 0.21 |
| Glomeruloid | | | | |
| Gleason pattern 4 type | 35 | 20 | 15 | **0.012** |
| Mixture except cribriform | 36* | 10 | 26 | |
| Mixture including cribriform | | | | |
| Cribriform percent (%)** | 70(30-88) | 50(30-80) | 70(29-90) | 0.52 |
| Cribriform subtype** | 16 | 8 | 8 | **0.030** |
| Small | 21 | 3 | 18 | |
| Large | | | | |

High-risk clinical features: PSA ≥ 20 or Clinical Stage ≥ cT3 on DRE or GG ≥ 3 or non-organ confined PCa on MRI (EPE, SVI, LNI). Significant p value: <0.05
*One patient had pure cribriform pattern
**Only for patients with Cribriform on biopsy

**Conclusions:** GP 4 patterns in GS 7 bx are usually mixed with CP seen in 30%. Majority of CP lesions are detected on mpMRI. CP on biopsy is likely to have adverse features at RP. Along with PSA density, presence of CP is independently associated with HRF for GS 7 tumors. Our study highlights the importance of including CP as a data element in reporting GS 7 tumors on bx and supports its presence as an exclusion criteria for AS.

## 917 Urothelial Carcinoma with Sarcomatoid Transformation: An Analysis of PD-L1 Expression Status

Sounak Gupta[1], Nooshin K. Dashti[2], Prabin Thapa[1], Loren Herrera Hernandez[1], Aditya Raghunathan[1], William Sukov[1], Rafael Jimenez[1], Stephen Boorjian[1], Igor Frank[1], John Cheville[1]
*[1]Mayo Clinic, Rochester, MN, [2]Vanderbilt University Medical Center, Nashville, TN*

**Disclosures:** Sounak Gupta: None; Nooshin K. Dashti: None; Prabin Thapa: None; Loren Herrera Hernandez: None; Aditya Raghunathan: None; William Sukov: None; Rafael Jimenez: None; Stephen Boorjian: None; Igor Frank: None; John Cheville: None

**Background:** Urothelial carcinoma with sarcomatoid transformation (sUC) is a pattern of dedifferentiation with poor clinical outcomes. Due to its rarity there are few contemporary studies of large series of histopathologically reviewed cases. Given the changing paradigm in the management of bladder cancer involving the use of immune checkpoint inhibitors (ICIs), PD-L1 expression status was evaluated in a subset of sUC.

**Design:** Histopathologic review of cases in the institutional cystectomy registry led to the identification of 55 cases of sUC. These patients were matched for age, sex and pathologic stage to 55 patients with pure urothelial carcinoma (pUC) and outcomes were evaluated using the Kaplan-Meier method. Immunohistochemistry for tumor-specific PD-L1 expression was performed on whole slide sections and calculated using H-scores (product of intensity of staining, graded from 0 to 3, and the percentage of positive cells; H-score range, 0 to 300). This was done using antibody clones 22C3 (n=33), SP263 (n=34), and SP142 (n=35), that are used to predict response to ICIs.

**Results:** For patients with sUC the mean age at presentation was 70.1 years (range, 46.3 to 90); 64% were in males and the mean duration of follow up was 5 months (range, 0.1 to 26.3). Six patients (10.9%) received prior neoadjuvant chemotherapy. Most patients with sUC had locally advanced disease (=>pT2, 90.9%; =>pT3, 63.6%), while lymph node involvement was documented for 20% of cases. No statistically significant differences were identified for overall survival (OS) (p=0.44) or cancer-specific survival (CSS) (p=0.19) when sUC were matched to pUC for age, sex and pathologic stage.

Mean PD-L1 H-scores were: 22C3, 132.6 (IQ range, 20-250); SP142, 139.6 (IQ range, 70-220); SP263, 168.1 (IQ range, 70-260). High and likely constitutive PD-L1 expression (H-score=>240 of 300) was seen in at least 5 cases using all 3 antibody clones (Figure 1). Cox modeling suggested an association of SP263 expression with improved cancer-specific survival on univariate analysis (HR 0.994, p=0.01) and composite analysis using all 3 clones (HR 0.98, p=0.02).

Figure 1 - 917

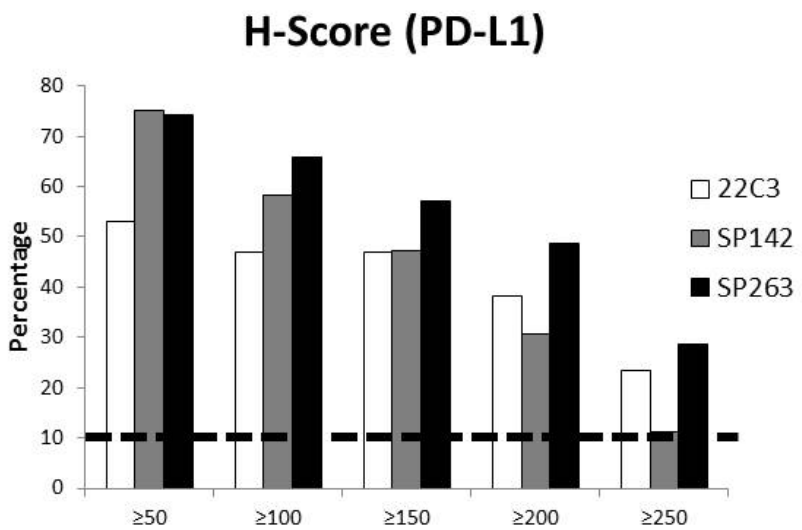


**Conclusions:** sUC tends to present with locally advanced disease at radical cystectomy (=>pT2, 90.9%), however, an adverse impact on OS or CSS was not identified when stage-matched to cases of pUC. High PD-L1 expression in sUC (mean H-score, 132.6 to 168.1) independent of the clone, and likely constitutive expression in a subset suggests that patients with sUC may show favorable response to ICIs.

## 918 Association of Current Molecular Subtypes in Urothelial Carcinoma with Patterns of Muscularis Propria Invasion

Koorosh Haghayeghi[1], Ali Amin[2], Shaolei Lu[3], Andres Matoso[4]
*[1]Brown University Lifespan Academic Medical Center, Providence, RI, [2]Lifespan, Providence, RI, [3]Alpert Medical School of Brown University, Providence, RI, [4]Johns Hopkins Medical Institutions, Baltimore, MD*

**Disclosures:** Koorosh Haghayeghi: None; Ali Amin: None; Shaolei Lu: None; Andres Matoso: None

**Background:** Urothelial Carcinoma (UC) is subdivided into luminal (L), basal (B) and p53 wild-type (WT) subtypes. The basal and p53 WT groups are believed to show aggressive course and poor treatment response, respectively. The literature includes a mixture of different stages of UC. Herein, we investigate the immunophenotypes of a pure cohort of muscle invasive UC (pT2) followed by comparison of the clinical behavior of two distinct patterns of muscularis propria (MP) invasion and B/L profile.

**Design:** 43 cystectomy specimens harboring stage pT2 were retrospectively identified over span of 15 years. MP invasion was subclassified into patterns 1 (tumor encasing intact detrusor muscle bundles) and 2 (tumor dissecting/replacing detrusor muscle). Using IHC, B/L phenotypes (indeterminate when IHC was inconclusive), p53 and Ki67 were assessed; and survival data was collected. The follow-up ranged between 4-202 months (median: 60.7mo). The statistical analysis was performed using JMP Pro 14.1.

**Results:** Pattern 1 invasion was noted in 16 (37%) and pattern 2 in 27 (63%), both more common in male and mean age of pattern 1 was 10 years younger than pattern 2. (Table 1). B/L phenotypes were successfully determined in 36 UC (83.7%) (Figure 1). 48.8% and 34.8% revealed L and B phenotypes, respectively (indeterminate phenotype in 16.4%). Pattern 1 was predominantly associated with L phenotype: GATA3 and Her2 were significantly enriched in pattern 1 (p=0.02 & p=0.04, respectively). Higher rate of margin positivity was noted in B phenotype but the differences between the latter and invasion pattern were not significant. Higher proliferation index was noted in pattern 2 (Ki67≥5/10HPF) and B phenotype revealed Ki67≥5/10HPF (p=0.03). B phenotype showed association with p53 WT (higher p53 WT in CK14 expression) (p=0.007). 63.6% of pattern 1 cases were alive without disease (mean follow-up: 78.5mo) compared to 32% of pattern 2 cases (73mo), although the difference was not significant.

| Feature | Total | Basal | Luminal | Indeterminate | Pattern 1 | Pattern 2 |
|---|---|---|---|---|---|---|
| *Age (years)* | | | | | | |
| Median (IQR) | 68.3 (64.0, 78.0) | 70 (59.0, 75.0) | 72 (62.5, 77.0) | 73 (60.0, 83.0) | 63.5 (55.5, 73.5) | 73 (64.0, 78.75) |
| *Follow-up (months)* | | | | | | |
| Median (IQR) | 40 (16.0, 80.0) | 60 (25.0, 161.0) | 37 (18.5, 92.5) | 35 (7.0, 67.0) | 30.5 (12.5, 66.7) | 58 (25.0, 105.0) |
| *Sex, N %* | | | | | | |
| Female | 11 (25.5) | 6 (46.1) | 3 (14.2) | 2 (28.5) | 3 (18.8) | 8 (29.6) |
| Male | 32 (74.6) | 7 (53.9) | 18 (85.8) | 5 (71.4) | 13 (81.2) | 19 (70.3) |
| *Vital Status, N %* | | | | | | |
| Alive | 19 (44.2) | 7 (53.9) | 8 (38.1) | 2 (28.5) | 12 (75.0) | 9 (33.3) |
| Dead | 24 (55.8) | 6 (46.1) | 13 (61.9) | 5 (55.6) | 4 (25.0) | 18 (66.7) |

Figure 1 - 918

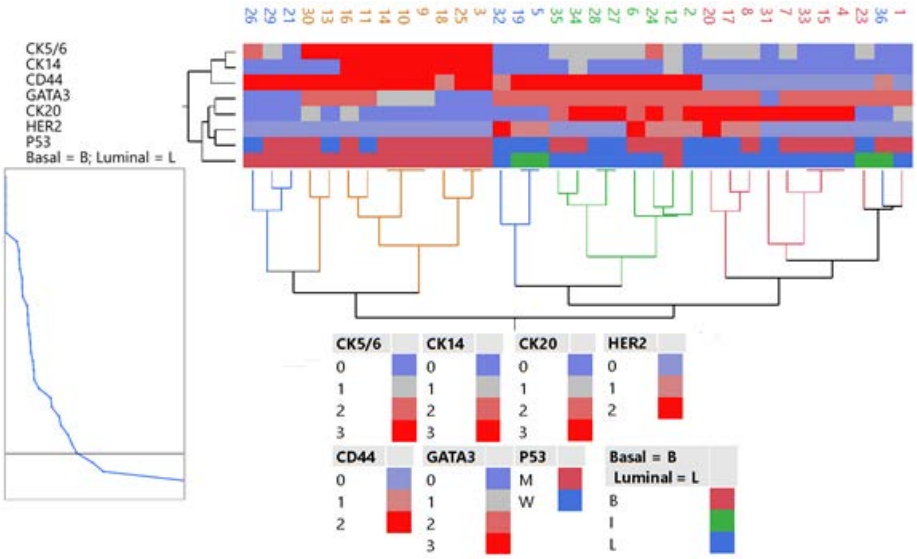


**Conclusions:** Morphological features like pattern of MP invasion correlates with B/L phenotypes in UC. Tumors with L phenotype commonly show pattern 1 invasion, with presumed longer survival compared to B phenotype. The clinical course of UT can be predicted using pattern of MP invasion.

## 919 Secondary Tumors of the Bladder: A Report of 84 cases

Ameer Hamza[1], Michael Hwang[1], Bogdan Czerniak[1], Charles Guo[1]
[1]*The University of Texas MD Anderson Cancer Center, Houston, TX*

**Disclosures:** Ameer Hamza: None; Michael Hwang: None; Bogdan Czerniak: None; Charles Guo: None

**Background:** The urinary bladder may be involved by a variety of secondary tumors that originate from other organs. Bladder secondary tumors are rare and may be mistaken as bladder primary tumors because of their overlapping morphologic features. To avoid the diagnostic pitfalls, we analyzed the clinicopathologic features of bladder secondary tumors in a large cohort of patients from a single institute.

**Design:** We identified 84 patients with secondary tumors of the bladder from our pathology database. Pathologic features were evaluated on the specimens, including transurethral biopsy (n=51) and radical cystectomy (n=33). Clinical data and outcome were collected from medical records.

**Results:** Our patient cohort consisted of 45 females and 39 males with a mean age of 59 years (range 10-87 years). The tumors involved the bladder via direct extension from adjacent organs (n=42) or distant metastasis (n=41). In females, the majority of secondary tumors originated from the gynecologic tract (n=25), and other common origins included the colon/rectum (n=5) and breast (n=4). In males, the most common origin was the prostate (n=18), followed by the colon/rectum (n=4) and kidney (n=3) (Table 1). 75% of the secondary tumors were adenocarcinoma (n=63), and other common tumor types included sarcoma (n=6), melanoma (n=4), squamous cell carcinoma (n=5), and neuroendocrine carcinoma (n=3). 67% of patients (n=56) died of the disease with a median overall survival of 23 months from the time of secondary involvement of the bladder. Patients with secondary tumors via direct extension had a median survival time of 20 months, which was not significantly different from that for patients with secondary tumors via distant metastasis (24 months) (p=0.97). The median survival times did not have any significant difference between female (25 months) and male (20 months) patients (p=0.14).

| Primary Site | Males | Females | Total |
|---|---|---|---|
| Prostate | 18 | -- | 18 |
| Ovary | -- | 12 | 12 |
| Colon and rectum | 4 | 5 | 9 |
| Uterus | -- | 7 | 7 |
| Cervix | -- | 6 | 6 |
| Esophagus and stomach | 2 | 3 | 5 |
| Bone and soft tissue | 3 | 1 | 4 |
| Kidney | 3 | 1 | 4 |
| Skin | 3 | 1 | 4 |
| Breast | 0 | 4 | 4 |
| Appendix | 1 | 2 | 3 |
| Small bowel | 1 | 1 | 2 |
| Lung and pleura | 1 | 1 | 2 |
| Thyroid | 1 | 0 | 1 |
| Gall bladder | 0 | 1 | 1 |
| Anal canal | 1 | 0 | 1 |
| CLL/SLL | 1 | 0 | 1 |
| Total | 39 | 45 | 84 |

**Conclusions:** Secondary tumors of the bladder show a female predominance in spite of a male predominance in primary tumors of the bladder. The majority of secondary tumors are composed of adenocarcinoma, which highlights the importance of differentiating primary from secondary involvement in bladder adenocarcinoma. Regardless of the origin, bladder secondary tumors are associated with a poor prognosis.

## 920 Comprehensive Analysis of Genetic Aberrations of 641 Chinese Prostate Cancer Patients - An 11-Year Retrospective Study from One Single Center

Bo Han, Jinan, Shandong, China

**Disclosures:** Bo Han: None

**Background:** The incidence of prostate cancer (PCa) increase rapidly in China in recent years, which cannot be entirely explained by increased PSA screening. Clinically, a significant number of patients present with metastatic disease, a phenomenon rarely seen in the US. Here we propose a 11-year retrospective study from one single center, summarizing the clinico-pathological characteristics and investigating the unique genomic aberrations of PCa patients in China.

**Design:** We retrospectively selected a total of 641 PCa patients at Qilu Hospital from 2006 to 2017, among which 410 cases with needle biopsy and 231 patients with radical prostatectomy. The clinico- pathological and molecular characteristics of patients were systematically analyzed using immunohistochemistry, fluorescent in situ hybridization and exon sequencing, etc. A total of 52 PCa cases with matched tumors and adjacent benign prostatic tissue were also sequenced using' targeted depth sequencing encompassing 450 tumor-related genes.

**Results:** Our study revealed high percentage of patients with high Gleason score (GS>7, 71.8%), relatively late clinical stage and high rate of metastasis (17.1%) for the newly diagnosed PCa patients in China. Overall, young PCa patients (< 55-year-old) had a high percentage of high GS score and Ki67 index than those of other two group patients. The presence of intraductal carcinoma of the prostate (IDC-P) is an independent unfavorable factor for PCa patients. Exon sequencing of 5 cases suggested that IDC-P and adjacent invasive cancer may share the same clone origin. In addition, several novel molecular markers such as BTF3 were identified for Chinese PCa patients. Our cohort further confirmed that the percentage of TMMPRSS2-ETS fusion is much lower in cancers from Chinese patients (15.7%). Of the 52 PCa patients sequenced, 8 (15.4%) had germline mutation involving BRCA2 and SPINK1. Interestingly, one case with both RAD51D and TSC2 germline mutations was identified. TMPRSS2 was arranged in 6 out of 52 (11.5%) cases, among which 4 with TMPRSS2-ERG gene fusion, and 1 case with TMPRSS2-MIR99A fusion.

**Table 1.** Association of Ki67 P53 HER2 status with clinicopathological parameters in radical specimen

| | Ki67 negative n=136 | Ki67 positive n=14 | | P53 negative n=145 | P53 positive n=5 | | HER2 negative n=145 | HER2 positive n=5 | |
|---|---|---|---|---|---|---|---|---|---|
| ***Categorical variable*** | n (%) | n (%) | p-value | n (%) | n (%) | p-value | n (%) | n (%) | p-value |
| **Age** | | | | | | | | | |
| **<65** | 41(30.8) | 8(61.5) | 0.0252 | 48(33.8) | 1(25) | 1.0000 | 46(32.4) | 3(75) | 0.1101 |
| ≥65 | 92(69.2) | 5(38.5) | | 94(66.2) | 3(75) | | 96(67.6) | 1(25) | |
| **Diagnostic PSA Value (ng/mL)** | | | | | | | | | |
| <4 | 11(8.8) | 1(8.3) | 0.3766 | 11(8.3) | 1(25) | 0.2305 | 11(8.3) | 1(25) | 0.2305 |
| 4-10 | 32(25.6) | 1(8.3) | | 33(24.8) | 0(0) | | 33(24.8) | 0(0) | |
| >10 | 82(65.6) | 10(83.3) | | 89(66.9) | 3(75) | | 89(66.9) | 3(75) | |
| **Pathological Gleason Score** | | | | | | | | | |
| ≤6 | 4(2.9) | 0(0) | 0.0019 | 4(2.8) | 0(0) | 0.6240 | 4(2.8) | 0(0) | 0.2872 |
| 3+4 | 45(33.1) | 0(0) | | 44(30.3) | 1(20) | | 45(31) | 0(0) | |
| 4+3 | 23(16.9) | 0(0) | | 23(15.9) | 0() | | 23(15.9) | 0(0) | |
| ≥8 | 64(47.1) | 14(100) | | 74(51) | 4(80) | | 73(50.3) | 5(100) | |
| **Pathological Tumor stage** | | | | | | | | | |
| pT2 | 113(83.1) | 12(85.7) | 1.0000 | 121(83.4) | 3(60) | 0.2071 | 122(84.1) | 2(40) | 0.0368 |
| pT3,pT4 | 23(16.9) | 2(14.3) | | 24(16.6) | 2(40) | | 23(15.9) | 3(60) | |
| **Lymph node status** | | | | | | | | | |
| negative | 135(99.3) | 13(92.9) | 0.1785 | 143(98.6) | 5(100) | 1.0000 | 143(98.6) | 5(100) | 1.0000 |
| postitive | 1(0.7) | 1(7.1) | | 2(1.4) | 0(0) | | 2(1.4) | 0(0) | |
| **Distant metastases** | | | | | | | | | |
| M0 | 132(97.1) | 13(92.9) | 0.3916 | 140(96.6) | 5(100) | 1.0000 | 140(96.6) | 5(100) | 1.0000 |
| M1 | 4(2.9) | 1(7.1) | | 5(3.4) | 0(0) | | 5(3.4) | 0() | |

Figure 1 - 920

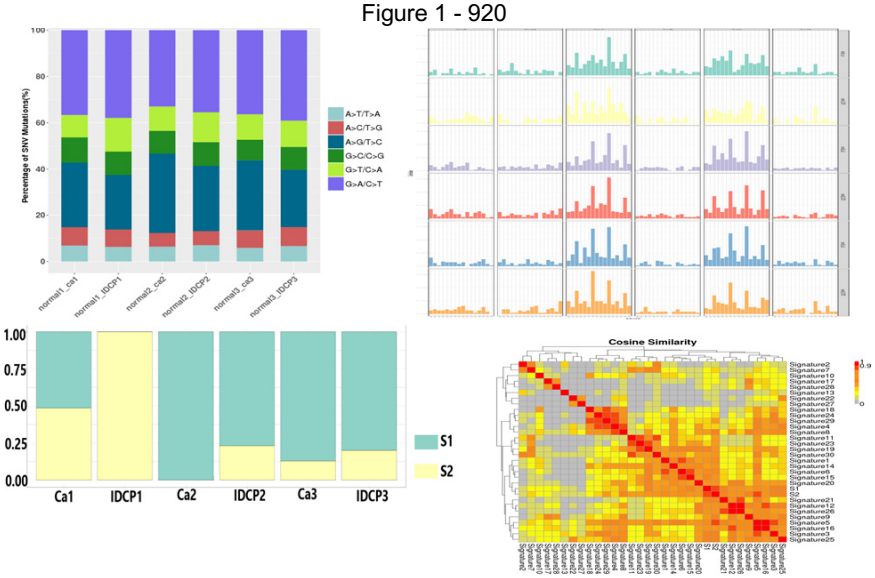

Figure 2 - 920

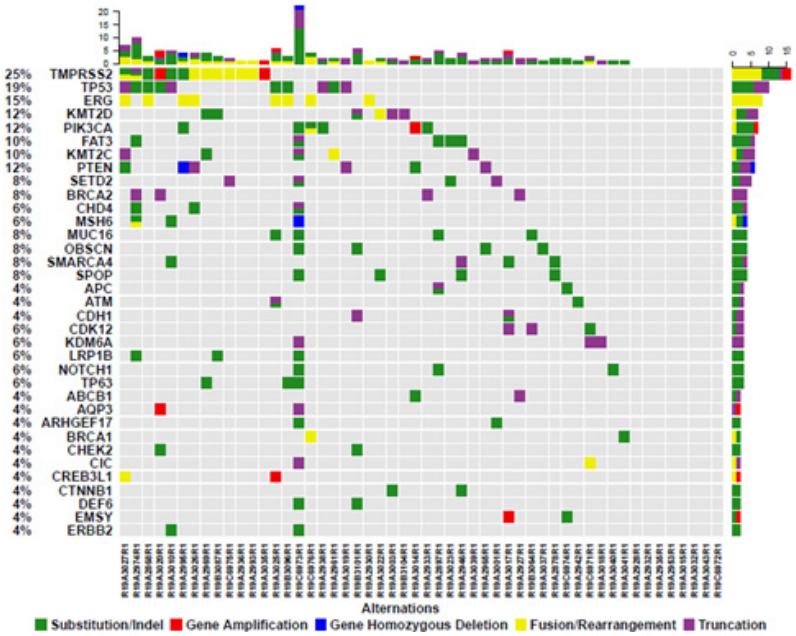


**Conclusions:** Prostate cancer patients in China may have unique clinical pathology and genetic characteristics, which merits further investigation. Our study will stimulate more discussion and research in the area of comparative studies of PCa in relation to racial and ethnic differences.

## 921 Telomere Lengths Differ Significantly Between Small Cell Carcinoma and Adenocarcinoma of the Prostate

Christopher Heaphy[1], Michael Haffner[2], Harrison Tsai[3], Jonathan Epstein[4], Angelo De Marzo[5], Alan Meeker[1], Tamara Lotan[6]
*[1]Johns Hopkins University School of Medicine, Baltimore, MD, [2]Fred Hutchinson Cancer Research Center, Seattle, WA, [3]Brigham and Women's Hospital, Boston, MA, [4]Johns Hopkins Medical Institutions, Baltimore, MD, [5]Johns Hopkins University, Baltimore, MD, [6]Johns Hopkins School of Medicine, Baltimore, MD*

**Disclosures:** Christopher Heaphy: None; Michael Haffner: None; Harrison Tsai: None; Jonathan Epstein: None; Angelo De Marzo: None; Alan Meeker: None; Tamara Lotan: *Grant or Research Support*, Ventana/Roche

**Background:** Small cell neuroendocrine carcinoma (SCC) of the prostate is an aggressive subtype with frequent *TP53* mutation and *RB1* inactivation. However, the molecular phenotype remains an area of active investigation. Here, we compared telomere lengths in prostatic SCC and usual-type prostatic adenocarcinoma (AdCa).

**Design:** We studied 32 cases of prostatic SCC (including 11 cases with concurrent AdCa) and 347 cases of usual-type AdCa on tissue microarrays (TMA). Telomere lengths in tumor cells were qualitatively compared to those in adjacent benign cells using a telomere-specific fluorescence *in situ* hybridization (FISH) assay. *ERG*, *PTEN* and *TP53* status were assessed in a proportion of cases using genetically validated immunohistochemistry protocols. Clinical-pathologic and molecular characteristics of cases with normal or long telomeres were compared to those with short telomeres using the chi-square test.

**Results:** A significantly higher proportion of prostatic SCC cases (50%, 16/32) displayed normal/long telomere lengths compared to AdCa cases (11%, 39/347; p<0.0001). In 82% (9/11) of cases with concurrent SCC and AdCa, the components were concordant for telomere length status. Among AdCa cases, the proportion of cases with normal/long telomeres significantly increased with increasing tumor Grade Group (p=0.01) and pathologic stage (p=0.02). Cases with normal/long telomeres were more likely to be ERG positive (p=0.04) and to have a *TP53* missense mutation (p=0.01) compared to cases with short telomeres. Although, among a small cohort of 54 surgically-treated very high grade (Gleason 9 and 10) AdCa cases, there were no significant associations between cancer cell telomere length category and biochemical recurrence- or metastasis-free survival.

**Conclusions:** Normal or long telomere lengths are significantly more common in prostatic SCC compared to AdCa and are similar between concurrent SCC and AdCa tumors supporting a common origin. Among AdCa cases, longer telomere lengths are significantly associated with high risk pathologic and molecular features, although in a small high grade AdCa cohort, there were not significant associations with oncologic outcomes.

## 922 SPOP and CHD1 Alterations in Prostate Cancer. Relationship with PTEN Loss and Grade Group Classification

Silvia Hernández-Llodrà[1], Laura Segales Tana[1], Nuria Juanpere-Rodero[2], Marta Lorenzo[2], Lluís Fumadó[2], Lluís Cecchini[2], Belen Lloveras[3], Josep Lloreta-Trull[4]
*[1]Universitat Pompeu Fabra, Barcelona, Spain, [2]Hospital del Mar-Parc de Salut Mar-IMIM, Barcelona, Spain, [3]Hospital del Mar, Barcelona, Spain, [4]Hospital del Mar, Parc de Salut Mar, Universitat Pompeu Fabra, Barcelona, Spain*

**Disclosures:** Silvia Hernández-Llodrà: None; Laura Segales Tana: None; Nuria Juanpere-Rodero: None; Marta Lorenzo: None; Lluís Fumadó: None; Lluís Cechinni: None; Belen Lloveras: None; Josep Lloreta-Trull: None

**Background:** Prostate cancers (PrCa) belong to two main pathways, one related to the *ETS* fusions, and the other related to somatic mutations. *ERG* fusion is the most prevalent oncogenic driver subclass, and *PTEN* loss is a concomitant event that cooperates in progression. In the non-*ETS* fusion PrCa pathway, *SPOP* mutations represent another oncogenic driver subclass. Different studies reported that *SPOP* mutations are mutually exclusive with *ERG* fusions and represent an alternative pathogenic event associated with an increase in ERG protein levels. *SPOP* mutations are associated with *CHD1* loss, and reflect a common molecular PrCa subclass with increased AR activity.

**Design:** The aim of this study has been to analyze the role of SPOP and CHD1 alterations in PrCa. Cases were selected retrospectively from the files of the Parc de Salut MAR Biobank (MARBiobanc, Barcelona, Spain). SPOP, PTEN and ERG protein expression were analyzed by immunohistochemistry (IHC) in 198 PrCa from FFPE TMA sections. Presence of *SPOP* mutations was assessed by PCR and Sanger sequencing in 86, and *CHD1* loss by TaqMan® Copy Number Assay in 66 PrCa. Relationship with clinical and pathological variables was also assessed.

**Results:** Loss of SPOP and PTEN protein expression was detected in 85 (42.9%) and 73 (36.4%) PrCa, respectively, and ERG overexpression in 96 (48.5%). SPOP loss was strongly associated with PTEN loss ($p<0.001$), but not with ERG overexpression ($p= 0.95$). SPOP protein loss was detected in 22.2% of GG1, 41.7% of GG2, 50% of GG3, 43% of GG4 and 60% of GG5 tumors ($p= 0.02$). *SPOP* mutations were detected in 5 of 86 (5.8%) PrCa, 4 of them (80%) showed SPOP protein loss ($p= 0.36$), but any *SPOP* mutated case showed ERG overexpression. *CHD1* loss was present in 18 of 66 (27.3%) cases, and was associated with *SPOP* mutations ($p= 0.001$), but not with SPOP protein expression ($p= 0.68$). *CHD1* loss was detected in 0% of GG1, 26.5% of GG2-3, 33.3% of GG4 and 50% of GG5 PrCa ($p= 0.04$).

**Conclusions:** SPOP protein loss is present in a high percentage of PrCa, being statistically less frequent in the lowest grade tumors. SPOP loss was associated with PTEN loss but not with ERG overexpression. *CHD1* copy number loss was associated with *SPOP* mutations, and with the highest grade tumors. *SPOP* mutations do not appear to be related with an increase in ERG protein. SPOP and CHD1 alterations could be markers of PrCa aggressiveness (Support Grants: FIS/Carlos III/FEDER/ PI15/00452, Spanish Ministry of Health).

## 923 Novel Four-Antibody Classifier for Urothelial Carcinoma and its Correlation with p53 Expression and Divergent Differentiation

Anjelica Hodgson[1], Danny Vesprini[2], Stanley Liu[3], Bin Xu[4], Michelle Downes[3]
*[1]University of Toronto, Toronto, ON, [2]Sunnybrook Health Sciences Centre, University of Toronto, Toronto, ON, [3]Sunnybrook Health Sciences Centre, Toronto, ON, [4]Memorial Sloan Kettering Cancer Center, New York, NY*

**Disclosures:** Anjelica Hodgson: None; Danny Vesprini: None; Stanley Liu: None; Bin Xu: None; Michelle Downes: None

**Background:** Previous work from the Lund group has successfully utilized immunohistochemistry (IHC) to identify five categories of muscle invasive bladder cancer (MIBC) with prognostic and predictive utility. This schema has been incorporated into the new consensus molecular classification of MIBC. This IHC approach requires 8 separate antibodies to define the three most common categories: genomically unstable (GU), urothelial-like (Uro) and basal squamous (bas/sq) groups. We aimed to (1) assess the utility of a 4 antibody panel in assigning these subtypes, (2) compare tumour histology with molecular subtype, and (3) correlate p53 expression as a surrogate of TP53 status with the assigned subtype.

**Design:** A triplicate core tissue microarray was created from a MIBC cystectomy cohort in which all tumours with variant histology comprised <50% of tumour. Sequential sections were stained with GATA3, CK5/6, p16, RB and p53. Tumours with >20% expression of GATA3 or CK5/6 were assigned to a luminal or bas/sq categories, respectively. The luminal subgroup was divided into GU (p16+/RB-) or Uro (p16-/RB+) groups. p53 was assessed as abnormal (0%, >50%) or wild type (1-49%). Statistical analysis with Fisher's exact test was used for group comparisons.

**Results:** 158/206 cases (77%) were successfully classified using the 4 antibody approach as follows: bas/sq n=35, GU n=40 and Uro n=83. p16/RB expression was mutually exclusive in 84% of cases ($p<0.001$). Variant histology was present in 50/206 cases (24%). The tumour histology/molecular subtype comparison is shown in Fig 1. Tumours with squamous differentiation showed the most molecular

heterogeneity with 67% (20/30) classified as either GU or Uro type. The bas/sq molecular group showed abnormal p53 expression in 54%. A significant difference in luminal p53 expression was noted: GU group - 73% and the Uro group - 36% (p<0.001).

Figure 1 - 923

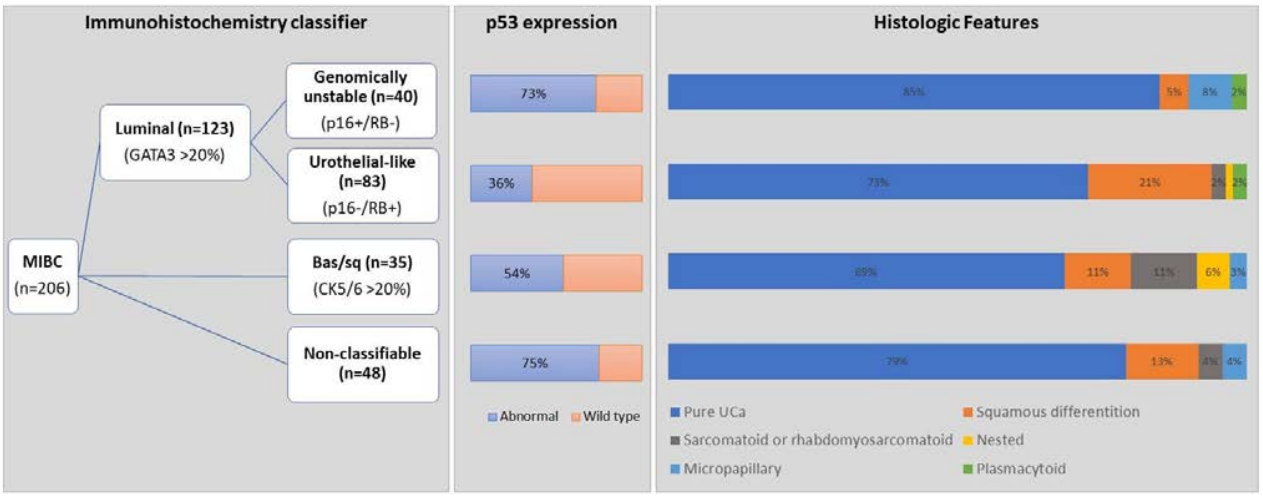


**Conclusions:** A 4 antibody IHC approach is a reasonable alternative to the 8 antibodies used in the Lund schema for assigning molecular subtype in MIBC. We identified Uro subtype as the most frequent in high grade urothelial carcinoma in keeping with the literature. The molecular-tumour histology discordance was most notable in the bas/sq group. We found the rate of TP53 mutation in each subtype to be comparable to published data further supporting the utility of this 4 antibody IHC approach for molecular classification.

## 924 Clinical Outcomes of Penile Intraepithelial Neoplasia Variants

Melissa Hogan[1], Giovanna A Giannico[1], Jonathan Epstein[2], Antonio Cubilla[3], Jennifer Gordetsky[1], Lan Gellert[1], Michael Orejudos[4]
*[1]Vanderbilt University Medical Center, Nashville, TN, [2]Johns Hopkins Medical Institutions, Baltimore, MD, [3]Instituto de Patologia e Investigacion, Asunción, Central, Paraguay, [4]Johns Hopkins Hospital, Timonium, MD*

**Disclosures:** Melissa Hogan: None; Giovanna A Giannico: None; Jonathan Epstein: None; Antonio Cubilla: None; Jennifer Gordetsky: None; Lan Gellert: None; Michael Orejudos: None

**Background:** Penile intraepithelial neoplasia (PeIN) is the histologic precursor of penile squamous cell carcinoma (SCC). PeIN can be morphologically and pathogenetically classified into non–HPV-related (differentiated) and HPV-related (warty, basaloid and warty-basaloid). HPV 16 has been, more frequently, identified in basaloid PeIN compared to warty PeIN (70% vs 20%). However, the prognostic significance of the different morphologic subtypes of PeIN is unknown. This study aims to 1) Determine the prognostic relevance of the morphologic subtypes of PeIN by correlating with progression to SCC; 2) Assess the correlation of PeIN morphologic subtype with HPV status.

**Design:** A retrospective review was performed for cases of PeIN from the collaborating institutions (2002-2019). Forty-three patients/lesions were pathologically evaluated and p16 immunostain was performed in 42 cases (Enzo Life Sciences, ENZ-ABS377-0100; 1:100 dilution).

**Results:** The patient cohort's average age was 58 and consisted of 63% Caucasian, 14% African American, 5% Asian and 18% unknown. PeIN subtyping included differentiated 1/43 (2%), basaloid 26/43 (61%), warty 1/43 (2%), and warty-basaloid 14/43 (33 %) subtypes; 1 case was unclassifiable. P16 was positive in 20/26 (77%) basaloid, 1/1 (100%) warty and 11/14 (79%) warty-basaloid types. At initial diagnosis, 25/43 (58%) received a biopsy, 15/43 (35%) an excision and 3/43 (7%) a partial penectomy. Five patients were lost to follow-up, the remaining 38 showed an average follow-up of 34 months. Further treatment in patients included observation in 17/38 (45%), laser ablation (LA) in 6/38 (16%), LA and fluorouracil (FU) in 2/38 (5%), FU in 4/38 (11%), imiquimod (IM) in 3/38 (8%), local re-excision in 2/38 (5%), 1/38 in FU and IM, photoradiation, cryoablation and Moh's respectively. Progression to invasive squamous cell carcinoma occurred in 2/38 (5%, p16 positive basaloid in immunocompetent patients). The first was treated with 5FU + LA and multiple re-excisions before presenting with invasion at a follow-up of 55 months. The second was treated initially with observation and presented with invasion and metastasis at follow-up at 36 months.

**Conclusions:** In this study, progression of PeIN to invasive SCC is limited after different treatment modalities and occurred within the 2 p16 positive basaloid subtypes . Study limitations are the sample size and the short follow up time. Our future goal is to expand this cohort as well as perform HPV subtyping.

## 925 Anatomical Complexity of Renal Masses by PADUA and R.E.N.A.L. Nephrometry Scores and Diagnostic Adequacy by Core Needle Biopsy and Fine Needle Aspiration

Melissa Hogan[1], Giovanna A Giannico[1], Justin Cates[1], Peter Clark[2], Jennifer Gordetsky[1], Ricardo Fonseca[1]
*[1]Vanderbilt University Medical Center, Nashville, TN, [2]Atrium Health, Charlotte, NC*

**Disclosures:** Melissa Hogan: None; Giovanna A Giannico: None; Justin Cates: None; Peter Clark: None; Jennifer Gordetsky: None; Ricardo Fonseca: None

**Background:** Fine needle aspiration (FNA) and core needle biopsy (CNB) are commonly used for diagnosis and management of renal masses. Nephrometry scoring systems are useful tools to assess the anatomical complexity of renal masses and suitability to different surgical modalities. Our goal is to determine the association between the anatomical tumor complexity determined by R.E.N.A.L. and PADUA nephrometry scores and the diagnostic adequacy accuracy of FNA, CNB and concurrent FNA with CNB (FNA+CNB) in the pathologic diagnosis of renal masses.

**Design:** Computed tomography or magnetic resonance images of 490 consecutive renal masses from 435 patients who underwent FNA, CNB and FNA+CNB (2003-2017) were retrospectively reviewed by a radiologist (RBF) to evaluate R.E.N.A.L. and PADUA nephrometry scores. Multivariable logistic regression was used to evaluate the effect of these scores on FNA and CNB adequacy.

**Results:** The patient cohort's average age was 64 (62%, males; 38% female) and 87% were Caucasian, 10% African American, <1% Asian, <1% Hispanic, < 1% Not Reported, 1<% Other. FNA was performed in 93/490 (19%) patients (Group 1), CNB in 303/490 (19%) (Group 2) and FNA + CNB in 94/490 (19%) (Group 3). Adequacy is reported in Table 1. Patients were treated with ablation (168, 34%), partial nephrectomy (86, 17%), nephrectomy (63, 13%), observation (146, 30%), systemic therapy, (28, 6%), percutaneous resection (1, 0.2%). Radiologically, 416/490 (85%) masses were solid, 17/490 (4%) cystic/necrotic and 57/490 (12%) solid-cystic/solid necrotic. The average nephrometry scores were 8.4 (range 5-13) for PADUA and 7.3 (range 3-11) for R.E.N.A.L. Average follow up time was 33 months. Fifty (11.5%) patients progressed to metastasis (average 11 months), and 11(3%) died of disease (average of 14 months). After adjusting for solid or cystic features of the masses, PADUA and R.E.N.A.L. scores were not significant predictors of adequacy for CNB (P = 0.76), FNA (P = 0.61) and FNA+CNB (P = 0.79).

**Table 1**: Adequacy based on procedure type

| Procedure | N. Adequate (%) | N. Inadequate (%) | N. Total | P |
|---|---|---|---|---|
| **Fine needle aspiration (FNA, Group 1)** | 67 (72) | 26 (28) | 93 | < 0.0001 |
| **Core needle biopsy (CNB, Group 2)** | 273 (90) | 30 (10) | 303 | |
| **FNA+CNB (Group 3)** | **5 (5)** | 89 (5) | 94 | |
| **FNA+CNB (Group 3)** | **N (%)** | | | < 0.0001 |
| **FNA adequate + CNB inadequate** | 11 (12) | | 94 | |
| **FNA inadequate + CNB adequate** | 20 (21) | | 94 | |
| **FNA + CNB adequate** | 58 (62) | | 94 | |
| **FNA + CNB inadequate** | 5 (5) | | 94 | |

**Conclusions:** Diagnostic adequacy of CNB is superior to FNA, while CNB+FNA is superior to FNA and CNB (P<0.0001). Anatomical tumor complexity determined by R.E.N.A.L and PADUA nephrometry scores is not a significant predictor of adequacy for CNB, FNA and CNB. These data suggest that concurrent FNA+ CNB as opposed to CNB alone or FNA alone can increase diagnostic adequacy, which may allow for a decrease in repeat biopsies in this population

## 926 Using Artificial Intelligence (AI) to Reduce Inter-Observer Variability in Gleason Scoring of Prostate Cancer

Wei Huang[1], Parag Jain[2], Ramandeep Randhawa[3]
[1]*University of Wisconsin, Madison, WI,* [2]*PathomIQ, Inc, Sunnyvale, CA,* [3]*PathomIQ, Hermosa Beach, CA*

**Disclosures:** Wei Huang: *Grant or Research Support*, Dhristi, Inc (PathomIQ); *Stock Ownership*, Dhristi, Inc; Parag Jain: *Stock Ownership*, PathomIQ, Inc.; Ramandeep Randhawa: *Stock Ownership*, PathomIQ Inc

**Background:** Gleason scoring is the gold standard for assessing aggressiveness of prostate cancer. It is well known that Gleason grading suffers from high inter- and intra-observer variability with over 40% discordance between general and sub-specialty pathologists. A universal and standardized Gleason Grading platform trained by GU pathologists is needed for better patient care and clinical research.

**Design:** PathomIQ Inc's AI-based Gleason grading software was used for this study. This software has been trained using annotations from GU pathologists to identify various morphologies, including cancer of all Gleason patterns (GP3, GP4 and GP5), HGPIN, perineural invasion (PNI), vessels and lymphocytes, etc. The algorithm is deep learning based and comprises multiple Deep Convolutional Neural Networks that are a combination of classification and segmentation networks. This architecture was fine-tuned to be sensitive to very small amounts of high-grade cancer. The software automatically annotates entire whole slide images (WSI) into the various cancer and benign pattern groups, and further provides summary statistics of Gleason score, quantification of cancer area, and the percentage of each cancer pattern. The software also allows pathologists to modify the annotations upon review.

For this study, two additional GU specialist pathologists were recruited. 165 prostate biopsy cases encompassing all Gleason Grade Group (GGG) cancers were selected from the pathology archive at the University of Wisconsin-Madison, and were scanned with Aperio CS2 (Leica) at 40x to create WSI.

The two pathologists scored each WSI twice: first, manually, and then, using the software (in which they could make changes). The grading disagreement between the two pathologists was settled by the third pathologist (WH). A consensus grading for each WSI slide was achieved for both manual and AI approaches. The ground truth of grading for each WSI was defined as the consensus grading by all three pathologists using our software.

**Results:** Comparing the manual consensus grading to the ground truth, we found that the concordance was 69.6% (k = 0.59) and majority of the discordance arises from under-grading using manual approach (Figure 1).

We also found that the concordance between the AI-assisted grading done by the two pathologists and the ground truth increased

Figure 1 - 926

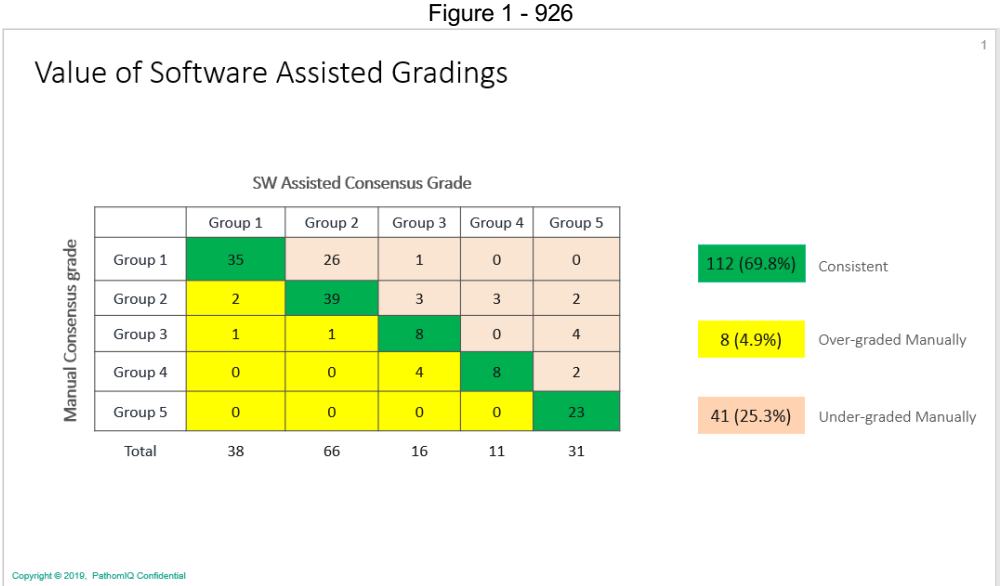


**Conclusions:** Deep learning enabled cancer grading software has tremendous potential in improving inter-observer agreement, and especially in identification of high grade cancer.

## 927 Somatic-Type Malignancy in Testicular Germ Cell Tumor - A Clinicopathologic Analysis of 53 Cases

Michael Hwang[1], Ameer Hamza[1], Bogdan Czerniak[1], Charles Guo[1]
[1]*The University of Texas MD Anderson Cancer Center, Houston, TX*

**Disclosures:** Michael Hwang: None; Ameer Hamza: None; Bogdan Czerniak: None; Charles Guo: None

**Background:** Testicular germ cell tumor (GCT) may develop a distinct secondary component that resembles a somatic-type malignancy (STM) in other organs. There have been limited studies on this phenomenon because of its rarity. We aimed to study a large series of patients who developed STM in association with testicular GCT from a single institute.

**Design:** We searched our pathology database and identified 53 patients with testicular GCT who developed STM in the primary tumors or metastases. The histopathologic features of the primary and metastatic tumors were evaluated. Clinical data were collected, and patient outcomes were analyzed.

**Results:** Our cohort consisted of 53 patients with a mean age of 37 years (range 17-67 years) at the time of STM diagnosis (Table 1). 16 patients developed STM in the primary testicular tumors, and 37 patients showed STM in the metastases. The median time interval from the initial presentation of testicular GCT to the development of metastatic STM was 79 months (range 0-384 months). The STM was composed of carcinoma (n=18), sarcoma (n=17), PNET (10), or others (n=8). Sarcoma was the most common STM in the primary testicular tumors, while carcinoma was the most common in the metastases. Patients with STM in the metastases showed a 5-year survival rate of 37%, which was lower than that for patients with STM in the testis (82%) (Figure 1). Furthermore, patients with carcinomatous STM demonstrated a 5-year survival rate of 19%, which was significantly worse than those for PNET (69%) or sarcomatous (80%) STM (Figure 2).

| | | STM in the testis (n=16) | STM in the metastasis (n=37) | All (n=53) |
|---|---|---|---|---|
| Age (mean, range; years) | | 31 (17-55) | 42 (23-67) | 37 (17-67) |
| STM (n,%) | Sarcoma | 8 (50%) | 9 (24%) | 17 (32%) |
| | Carcinoma | 1 (6%) | 17 (46%) | 18 (34%) |
| | PNET | 5 (31%) | 5 (14%) | 10 (19%) |
| | Other | 2 (13%) | 6 (16%) | 8 (15%) |
| Coexistent GCTs (n) | | 16 | 12 | 28 |
| Coexistent GCT type (n) | Mixed GCT | 13 | 5 | 2 |
| | Teratoma | 3 | 5 | 8 |
| | YST | 0 | 2 | 18 |
| 5-year survival rate | | 82% | 37% | 50% |

Figure 1 – 927

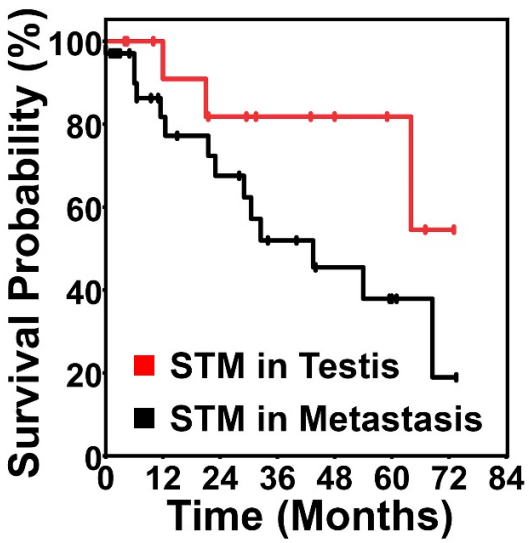


Figure 2 – 927

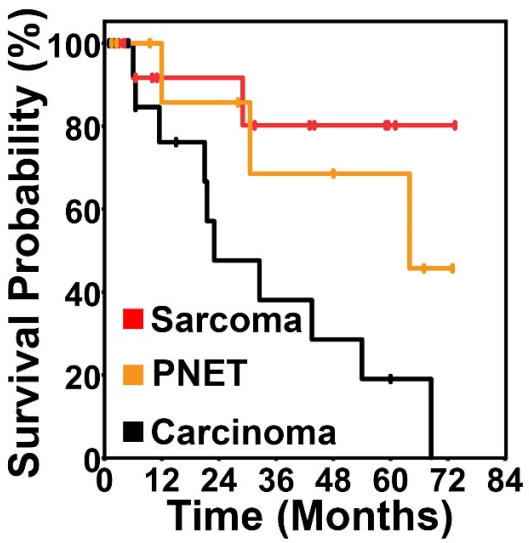

**Conclusions:** STM is more common in metastases than in the primary testicular GCTs. Sarcoma is the most common STM in the testis, while carcinoma is the most common STM in metastases. STM in metastases is associated with a poorer prognosis than those in the testis. Carcinomatous STM carries a significantly worse prognosis than sarcomatous STM.

## 928 Sarcomatoid Renal Cell Carcinoma Demonstrates an Immunosuppressive Tumor Microenvironment – Implication for Therapeutic Benefit in the Immunotherapy Era

Michael Hwang[1], BJ Kerns[2], Yong Lee[3], Debrah Thompson[2], Jose Karam[1], Priya Rao[1], Pheroze Tamboli[1], Krishna Bhat[1], Kanishka Sircar[1]
*[1]The University of Texas MD Anderson Cancer Center, Houston, TX, [2]HTG Molecular Diagnostics, Inc., Tucson, AZ, [3]HTG Molecular Diagnostics, Tucson, AZ*

**Disclosures:** Michael Hwang: None; BJ Kerns: *Employee*, HTG Molecular; Yong Lee: *Employee*, HTG Molecular; Debrah Thompson: *Employee*, HTG Molecular Diagnostics; *Stock Ownership*, HTG Molecular Diagnostics; Jose Karam: None; Priya Rao: None; Pheroze Tamboli: None; Krishna Bhat: None; Kanishka Sircar: None

**Background:** Renal cell carcinoma (RCC) with sarcomatoid features (sRCC) is an aggressive form of RCC with poor response to conventional therapies. Immune checkpoint inhibitors have shown promising therapeutic effect for sRCC in recent small series and sRCC has demonstrated higher PD-L1 expression and PD-1 positive tumor-infiltrating lymphocytes compared to high-grade clear cell RCC (ccRCC). Our aim was to use multiplexed gene expression assays to gain a broader view of the underlying tumor microenvironment in sRCC.

**Design:** Our cohort consisted of 48 patients with the clinical and histopathologic findings summarized in Table 1. The sarcomatous (S-) and epithelioid (E-) components from sRCC as well as the RCC tumor cells were macrodissected prior to interrogation by the Precision Immuno-Oncology Panel (HTG EdgeSeq) which assays the RNA expression of 1392 immune related genes.

**Results:** Sarcomatoid RCC demonstrated increased expression of T-cell inhibitory genes, including for *CD274* (PD-L1) (p=1.8E-4), *CD86* (p=1.8E-2), and *ITGB3* (p=6.6E-4) and the T-cell regulatory gene *IL2RA* (p= 2.6E-02) as compared with non-sarcomatoid RCC. When genes related to T-cell stimulation were compared, sRCC showed decreased gene expression, including for *CD40LG* (p=1.9E-03), *ICOSLG* (p=2.6E-04), and *TNFRSF9* (p=2.8E-04). Moreover, sRCC showed lower expression of myeloid derived suppressor cell genes including *ARG1* (p= 7.3E-03) and *FUT4* (p=4.2E-02). The S- and E- foci within sRCC did not show consistent, significant differences in gene expression related to T-cell stimulation or inhibition.

| | sRCC<br><br>n=24 | RCC<br><br>n=24 |
|---|---|---|
| Age, median (range), year | 57.5 (38-79) | 57 (38-73) |
| Diagnosis, n | | |
| Clear cell RCC | 17 (71%) | 24 (100%) |
| Papillary type 2 RCC | 5 (21%) | 0 (0%) |
| Chromophobe RCC | 1 (4%) | 0 (0%) |
| RCC, unclassified | 1 (4%) | 0 (0%) |
| Size, median (range), cm | 11.2 (1.1-18) | 10 (4.5-17) |
| Tumor grade (WHO/ISUP) | | |
| 3 | 0 (0%) | 11 (46%) |
| 4 | 24 (100%) | 13 (54%) |
| Stage, n | | |
| I | 2 (8.5%) | 0 (0%) |
| II | 1 (4%) | 4 (17%) |
| III | 13 (54%) | 19 (79%) |
| IV | 8 (33.5%) | 1 (4%) |

**Conclusions:** Our results suggest that sRCC harbors a different immunological milieu compared to non-sarcomatoid RCC with minimal intratumoral differences between the E- and S- components. Notably, sRCC demonstrates an immune resistant tumor microenvironment that may facilitate tumor progression through immunological evasion. Our findings strengthen the biological rationale for using immune checkpoint blockade therapy in sRCC.

## 929 Effect of Gleason Pattern 4 Percentage on Adverse Radical Prostatectomy Outcomes

Oleksii Iakymenko[1], Isabella Lugo[2], Ivan Nemov[3], Merce Jorda[3], Oleksandr Kryvenko[3]
*[1]Jackson Memorial Hospital, Miami, FL, [2]University of Miami, Davie, FL, [3]University of Miami Miller School of Medicine, Miami, FL*

**Disclosures:** Oleksii Iakymenko: None; Isabella Lugo: None; Ivan Nemov: None; Merce Jorda: None; Oleksandr Kryvenko: None

**Background:** Increasing percentage of Gleason pattern 4 (GP4) at biopsy is associated with higher likelihood of upstaging on radical prostatectomy (RP) and its percentage on RP correlates with likelihood of biochemical recurrence. However, there are no detailed RP studies assessing the effect of GP4% on likelihood of extraprostatic extension (EPE), seminal vesicle invasion (SV+), and positive surgical margin (SM+). We conducted such a study where the effect of GP4% was controlled by Grade Group (GG), tumor volume (TV), prostate weight (PW), and PSA density (PSAD).

**Design:** 1,306 consecutive entirely submitted RPs were re-reviewed. Each tumor nodule (TN) was assessed for TV, GG, presence of focal vs. non-focal EPE (fEPE vs. nfEPE), SV+, and SM+. We recorded GP4% for all GG2 and GG3 TNs utilizing a scale of 0, <5, 5, 10, 20, 30% etc. We conducted a univariate analysis (UVA) on discrete TNs to assess significance of GP4%, TV, GG, patient age, PW, and PSAD for the likelihood of adverse RP outcomes. Significant variables were then included in a multivariate analysis (MVA) for risk of EPE, SV+, and SM+. We then tested the effect of GP4% on fEPE vs. nFEPE by multinomial regression

**Results:** 1,273 patients remained with treatment naïve prostate cancer after excluding 1 small cell carcinoma, 1 carcinoid, 5 vanishing prostate cancers, 1 peripheral gland adenosis, and 25 hormonally treated cancers. There were 2,973 discrete GG1-GG4 TNs leaving apart 25 3+5=8, 1 5+3=8, 228 4+5=9, 57 5+4=9, and 9 5+5=10 TNs. There were 42 GG2 and 48 GG3 TNs with minor high-grade pattern. In UVA, GP4%, GG, TV, PW, and PSAD demonstrated statistically significant association with EPE, SV+, and SM+ (all $p<0.001$). Although patients with EPE were older (63 vs 61 yrs.; $p<0.001$), it was not the case for SV+ and SM+ ($p>0.05$). In MVA, GP4% was significant for risk of EPE ($p<0.001$) and SV+ ($p=0.05$) when it was controlled by GG, TV, PW, and PSAD. Although GP4% lost its relevance for SM+ ($p>0.62$), TV retained its significance ($p=0.001$). In GG2&3 TNs, GP4% (OR 1.03) and TV (OR 4.58) predicted nfEPE ($p<0.001$). While GP4% did not predict fEPE ($p=0.3$), TV did (OR 1.7, $p=0.001$).

**Conclusions:** GP4% controlled by GG, TV, PW, and PSAD is a risk factor for EPE (particularly nfEPE) and SV+ on RP. Such findings in correlation with assessed TV may be useful for proper preoperative planning or in the settings when active surveillance is considered in biopsy proven GG2 cancer.

## 930 Geographic Differences in Prostate Cancer Grading Practice Between USA and Non-USA Urologic Pathologists

Kenneth Iczkowski[1], Christopher Hartley[1], Glen Kristiansen[2], Murali Varma[3], Jesse McKenney[4], Andrew Evans[5], Geert van Leenders[6]
*[1]Medical College of Wisconsin, Milwaukee, WI, [2]University of Bonn, Bonn, Germany, [3]University Hospital of Wales, Cardiff, Wales, United Kingdom, [4]Cleveland Clinic, Cleveland, OH, [5]Toronto General Hospital, Toronto, ON, [6]Erasmus Medical Centre, Rotterdam, Zuid-Holland, Netherlands*

**Disclosures:** Kenneth Iczkowski: None; Christopher Hartley: None; Murali Varma: None; Jesse McKenney: None; Geert van Leenders: None

**Background:** The Association of Directors of Anatomic and Surgical Pathology (PMID: 17707261), comprising mostly USA pathologists, has long endorsed reporting Gleason scores on individual prostatic biopsy cores; the International Collaboration on Cancer Reporting (PMID: 30477882) favors adding a global Gleason score for the entire biopsy set. The presence of cribriform/large gland pattern within Gleason 4 is a newly recognized, major adverse prognosticator (PMID: 28820750). These factors might drive practice differences.

**Design:** The International Society of Urological Pathology surveyed members with 31 questions about grading practices, to which 278 members responded. Groups with >5% representation were USA (66 members), Europe (65), South America (22), and Canada (13).

**Results:** 7 questions showed significant geographic differences. When Gleason 4 cancer is present in specimens, 49% of USA pathologists would not mention pattern types in biopsies (Bx) and 59% would not in prostatectomy (Px); Europeans usually mentioned at least the presence of cribriform pattern. European pathologists were more likely to use multiple criteria to distinguish cribriform from fused glands.

66-69% of USA pathologists gave Gleason scores per core only for systematic or targeted biopsies, despite different grade or size of cancer; Europeans more often global Gleason scores (but less often when biopsies were targeted). Practices did not differ on how to report 2 spatially separate tumors with different grades in Px ($p=0.2$), use of global Gleason for Px ($p=0.6$), or grading of individual cores in a vial ($p=0.6$). Academic (n=143) pathologists did not differ from non-academic (n=71) pathologists for any of the survey questions.

| | Biopsy | | Prostatectomy | | | |
|---|---|---|---|---|---|---|
| When Gleason 4 is present, I mention: | USA | Europe | USA | Europe | | |
| all patterns present | 9% | 14% | 9% | 13% | | |
| cribriform presence/absence | 12% | 16% | 9% | 13% | | |
| cribriform presence only | 28% | 38% | 22% | 32% | | |
| do not mention patterns | 49% | 30% | 59% | 43% | | |
| other | 2% | 2% | 1% | 0% | | |
| P (chi-square based on numbers, not %) | 0.0004 | | 0.003 | | | |
| **Situation:** | **8 mm of 3+3 cancer & 2 mm of 4+3** | | **8 mm of 3+3 cancer & 0.6 mm of 4+5** | | **8 mm systematic 3+3 cancer & 2 mm targeted 4+3** | |
| In biopsies, I designate: | USA | Europe | USA | Europe | USA | Europe |
| score per biopsy only | 66% | 46% | 66% | 48% | 69% | 52% |
| global Gleason only | 3% | 7% | 1% | 3% | 2% | 3% |
| global Gleason & score per biopsy | 20% | 33% | 22% | 36% | 19% | 30% |
| other | 10% | 13% | 10% | 11% | 11% | 15% |
| P (Fisher Exact based on numbers, not %) | 0.00002 | | 0.0002 | | 0.0008 | |

**Conclusions:** Certain regions of the world, following disparate sets of recommendations, vary in specifying of patterns of Gleason 4 cancer (particularly large-gland), and on whether to issue a global Gleason score or let clinicians default to using the highest score. These practices drive therapy decisions, and will require consensus recommendations and raising of clinician awareness.

## 931 Comparative Study of Prostate Cancer Subtypes and Cribriform Gleason Pattern 4 in Men of African and European Descent

Brittney Imblum[1], Sahar Farahani[2], Abhishek Shah[1], Lake Jonathan[1], Kosj Yamoah[3], Timothy Rebbeck[4], Priti Lal[5]
*[1]Hospital of the University of Pennsylvania, Philadelphia, PA, [2]Renaissance School of Medicine at Stony Brook University, Stony Brook, NY, [3]Moffitt Cancer Center, Tampa, FL, [4]Dana-Farber/Harvard Cancer Center, Boston, MA, [5]University of Pennsylvania, Philadelphia, PA*

**Disclosures:** Brittney Imblum: None; Sahar Farahani: None; Abhishek Shah: None; Lake Jonathan: None; Kosj Yamoah: None; Timothy Rebbeck: None; Priti Lal: None

**Background:** Amongst geographically diverse populations with similar access to care, African descent men (AFM) have higher prostate cancer (PC) incidence rates and poorer prognosis when compared to European American men (EAM). Additionally, Gleason pattern 4 (GP4), intra-ductal (IDC-P) and ductal carcinoma (DC) subtypes confer poorer prognosis. Within patients with Gleason score (GS) 7 PC, cribriform pattern (CP) is associated with decreased biochemical recurrence (BCR) free survival, metastases, and shorter median time to disease specific death. Ethnic differences in the prevalence of the architectural patterns of GP4, IDC-P and DC are currently unknown. In this retrospective study, we sought to evaluate these differences.

**Design:** In this study, 102 entirely submitted prostate cancer cases with detailed clinical data and status of biochemical failure were reviewed. GS and Grade Group (GG) assignment were performed according to 2014 WHO/ISUP recommendations. Cases that were re-assigned GG1, GG4 and GG5 were omitted. The distribution of GG2 and GG3 is summarized in Table 1. Each case was assigned total percentage of GP4 and percentage of small & large cribriform (SC & LC). Additionally, presence/absence and % of IDC-P and DC were recorded. Correlation of these patterns and subtypes with PSA before prostatectomy and BCR were performed using Stata/SE 13.1 software.

**Results:** A multivariate analysis adjusted for stage, ethnicity and pretreatment PSA revealed an increase number of patients with BCR in the presence of GP4-LC {OR=4.3 (1.59-11.61), p-value=0.01}. The odds ratio was attenuated when % GP4-LC was analyzed {OR=1.12 (1.01-1.23), p-value=0.03}. Presence of any cribriform (SC or LC) was associated with higher stage {GP4-SC OR=2.91 (1.23-6.84), p-value=0.02; GP4-LC OR=2.61 (1.03-6.60), p-value=0.04}. Two-Sided Fisher's Exact test revealed a significant increase (p=0.015) in the number of patients with BCR in the AFM population in the presence of GP4 CP. This significance was lost when tertiary Gleason pattern 5 (GP5) was discounted in both populations. EAM population revealed increased IDC-P with OR=2.93 (1.10-7.77) (p-value: 0.03).

| Total number of cases (n=93) | EAM | AFM |
|---|---|---|
| | 44 | 49 |
| **Total number with cribriform pattern 4** | 31 | 37 |
| **stage T2** | 13 | 11 |
| **Stage T3** | 12 | 16 |
| **BCR** | 14 | 24 |
| **Total number with prostatic ductal carcinoma** | 5 | 5 |
| **stage T2** | 4 | 1 |
| **stage T3** | 1 | 4 |
| **BCR** | 1 | 2 |
| **Total number with prostatic intraductal carcinoma** | 16 | 8 |
| **stage T2** | 9 | 2 |
| **stage T3** | 7 | 6 |
| **BCR** | 5 | 4 |

Table 1: Distribution of Grade Group 2 (GG2) and Grade Group 3 (GG3).

**Conclusions:** Consistent with the current literature, presence of GP4 CP was associated with poorer prognosis. The AFM patients had increased BCR in the presence of GP4 CP. The reason for losing this statistical difference by eliminating tertiary GP5 is not understood. Larger studies may be helpful in further understanding these differences.

## 932 Quantitative Assessment of PTEN Loss (qPTEN) is Strongly Associated with Biochemical Recurrence and May Improve Treatment Decisions after Surgery

Tamara Jamaspishvili[1], Palak Patel[2], Yi Niu[3], Thiago Vidotto[4], Véronique Ouellet[5], Anne-Marie Mes-Masson[6], Tamara Lotan[7], Jeremy Squire[8], Yingwei Peng[1], D. Siemens[1], David Berman[1]

*[1]Queen's University, Kingston, ON, [2]Queen's University, Brantford, ON, [3]Dalian University of Technology, Dalian, Liaoning, China, [4]Department of Pathology, The Johns Hopkins Medical Institutions, Baltimore, MD, [5]Centre de recherche du CHUM/Institut du cancer de Montreal, Montréal, QC, [6]Centre de recherche du CHUM, Montreal, QC, [7]Johns Hopkins School of Medicine, Baltimore, MD, [8]Faculty of Medicine University of Sao Paulo, São Paulo, Ribeirao Preto, Brazil*

**Disclosures:** Tamara Jamaspishvili: None; Palak Patel: None; Yi Niu: None; Thiago Vidotto: None; Véronique Ouellet: None; Anne-Marie Mes-Masson: None; Tamara Lotan: *Grant or Research Support*, Ventana/Roche; Jeremy Squire: None; Yingwei Peng: None; D. Siemens: None; David Berman: None

**Background:** Men with positive surgical margins and/or extra-prostatic extension have diverse outcomes after radical prostatectomy (RP). Expectant management or immediate adjuvant therapy are currently in equipoise. Quantitative cut-offs for prognostically significant PTEN loss (qPTEN) have not yet been established and might provide guidance for management.

**Design:** PTEN protein levels were measured in RP samples from training (n=410) and validation(n=272) cohorts. PTEN loss was quantified per cancer cell and per cancer. Cut-offs for PTEN loss were determined for the training cohort by log-rank statistics and Kaplan-Meier survival estimates and independently validated.

**Results:** For each case, PTEN loss in >65% of cancer cells or >50% of TMA cancer cores was defined as qPTEN loss. In an independent validation cohort, qPTEN loss was associated with significantly reduced biochemical recurrence free survival (BRFS) (% cells, HR=4.22, p<0.001 and % cores, HR=2.75, p=0.002). In Kaplan-Meier analysis Median BRFS was 10.2 yrs for any PTEN loss (p<0.001) vs 5.4 yrs for >65% cells with PTEN loss (p<0.001). In men with positive surgical margins and/or extra-prostatic extension, PTEN loss was independently associated with increased risk of biochemical recurrence (HR=2.04, p=0.01).

**Conclusions:** In men with low and intermediate risk prostate cancer, low level PTEN loss is not strongly associated with adverse outcomes after RP. In contrast, qPTEN protein loss above cut-off levels is strongly associated with disease progression. Compared to previously reported qualitative approaches, qPTEN improves risk stratification of post-RP patients and may be considered as a complementary tool to guide management after surgery.

## 933 Image-Guided Targeted Prostate Biopsies: Impact on Summary Synoptic Reporting

Tyler Jankowski[1], Sarah Bowman[1], Jeffry Simko[1], Bradley Stohr[1], Emily Chan[1]
[1]*University of California San Francisco, San Francisco, CA*

**Disclosures:** Tyler Jankowski: None; Sarah Bowman: None; Jeffry Simko: *Stock Ownership*, 3D Biopsy Incorporated; Bradley Stohr: None; Emily Chan: None

**Background:** Transrectal (TR) ultrasound (US) and magnetic resonance imaging (MRI) are now two commonly used techniques in the initial evaluation for prostate cancer (PCa). Studies have shown that TRUS-MRI fusion targeted biopsies (MRI TB) may reduce sampling error and improve risk stratification in the initial evaluation for prostate cancer. At our institution, both MRI TB and more traditional US targeted biopsies (US TB) are routinely performed in addition to systematic biopsies (SB). The reporting of image guided biopsy findings in a pathology report and how to incorporate the findings into routinely used nomograms remains uncertain. In this study, frequencies of cancer detection for these various modalities were evaluated.

**Design:** We performed retrospective review of 200 consecutive cases from 2017 in which SB and at least one image guided TB (US or MRI) was performed. Parameters typically reported in a summary synoptic for prostate cancer were collected from the pathology reports in our pathology archives and frequency of cancer detection determined.

**Results:** Of the 200 cases, 140 cases included US TB and 167 cases included MRI TB, (113 cases had both a US TB and MRI TB). The sensitivity for both US and MRI TB for detecting cancer in the case is significantly less when compared to SB (US: 75% versus 98%, $p<0.01$; MRI: 71% versus 95%, $p<0.01$). When compared to SB alone, the addition of US TB upgraded the highest grade part Gleason score in 10/140 (7%) cases and the highest grade part in the TB was less than the SB alone in 53/140 (38%) cases; and the addition of a MRI TB upgraded the highest grade part Gleason score in 24/167 (14%) cases and the highest grade part in the TB was less than the SB alone in 66/167 (40%) cases. For both US and TRUS-MRI TB, when tumor was present in both the TB and SB, the change in the percent overall tissue involved by tumor increased by 3% when incorporating the TB compared to SB alone.

**Conclusions:** In our cohort, SB outperforms both US and MRI TB in the detection of PCa as well as detection of highest Gleason score in a single part. On average, the change in percent overall tissue involved by tumor was minimal. However, given the small subset of patients in which PCa is detected only on TB alone or a higher grade lesion is detected on TB, TB may continue to provide additional management and prognostic information for some patients.

## 934 Immunohistochemistry of BXDC2 and GULP1 in Bladder Cancer as Predictors of Chemosensitivity

Guiyang Jiang[1], Yuki Teramoto[2], Hiroshi Miyamoto[2]
[1]*China Medical University, Shenyang, Liaoning, China,* [2]*University of Rochester Medical Center, Rochester, NY*

**Disclosures:** Guiyang Jiang: None; Yuki Teramoto: None; Hiroshi Miyamoto: None

**Background:** Cisplatin-based systemic chemotherapy remains the mainstream treatment for advanced bladder cancer. However, its efficacy is often limited due to the development of resistance for which underlying mechanisms are poorly understood. Our DNA microarray analysis in control versus cisplatin-resistant bladder cancer sublines identified molecules whose expression was down-regulated in the latter, including BXDC2 and GULP1. The present study aims to determine the expression status of BXDC2 and GULP1 in bladder cancer and its prognostic significance.

**Design:** We immunohistochemically stained for BXDC2 and GULP1 in 129 bladder tumor and paired non-neoplastic bladder tissue specimens as well as in a separate set of tissue microarray consisting of muscle-invasive bladder cancer specimens from patients who received at least 3 cycles of cisplatin + gemcitabine neoadjuvant chemotherapy.

**Results:** BXDC2 / GULP1 was positive in 77% (47% 1+, 22% 2+, 7% 3+) / 74% (49% 1+, 23% 2+, 2% 3+) of tumors, which was significantly ($P$=0.022 / $P$=0.005) lower than in non-neoplastic urothelial tissues [90% (46% 1+, 29% 2+, 15% 3+) / 90% (46% 1+, 37% 2+, 7% 3+)], respectively. The positive rates of BXDC2 / GULP1 expression were also lower in high-grade carcinomas (71%, $P$=0.056 / 68%, $P$=0.062) than in lower grade tumors (86% / 84%) as well as in muscle-invasive carcinomas (69%, $P$=0.091 / 61%, $P$=0.007) than in non-muscle-invasive tumors (82% / 83%). Lymph node metastasis was significantly more often seen in those with BXDC2-negative tumor (pN0: 81% positive vs. pN1-3: 46% positive; $P$=0.031), but not GULP1-negative tumor (pN0: 64% positive vs. pN1-3: 46% positive; $P$=0.331). Kaplan-Meier analysis coupled with the log-rank test revealed that patients with BXDC2-positive non-muscle-invasive tumor tended to have a higher risk of disease recurrence ($P$=0.074). However, there were no significant associations between BXDC2 expression and prognosis of muscle-invasive tumors or between GULP1 expression and that of non-muscle-invasive or muscle-invasive tumors. In a separate set of tissue specimens, BXDC2 ($P$=0.083) / GULP1 ($P$=0.044) was positive in 26 (60%) / 32 (74%) of 43 cases with chemotherapy, including 76% / 53% of responders vs. 50% / 23% of non-responders.

**Conclusions:** BXDC2 and GULP1 expression is down-regulated in bladder cancer, which is further associated with lower tumor grade and stage. Moreover, our results suggest that BXDC2 or GULP1 loss may serve as a predictor of chemoresistance in patients with muscle-invasive tumor.

## 935 Clinicopathologic Findings in Patients Who Have Undergone Radical Cystectomy/ Cystoprostatectomy with Extended Versus Standard Lymph Node Dissection for Urothelial Carcinoma of the Bladder

Joshua Kagan[1], Mehrdad Alemozaffar[2], Bradley Carthon[2], Adeboye O. Osunkoya[2]
*[1]Emory University, Decatur, GA, [2]Emory University, Atlanta, GA*

**Disclosures:** Joshua Kagan: None; Mehrdad Alemozaffar: None; Bradley Carthon: None; Adeboye O. Osunkoya: None

**Background:** Cystectomy/cytoprostatectomy with pelvic lymph node dissection (with or without neoadjuvant chemotherapy) is the gold standard in the management of patients with urothelial carcinoma (UCa) with muscularis propria (Detrusor muscle) invasion. However, it remains somewhat controversial how extensive the lymph node dissection should be. Herein we analyzed the clinicopathologic findings in patients who had radical cystectomy/ cystoprostatectomy with extended versus standard lymph node dissection.

**Design:** A search was made through our Urologic Pathology files for cystectomy/cystoprostatectomy cases with extended and standard lymph node dissection for UCa. Standard lymph node dissection was defined as removal of the regional lymph nodes (obturator, perivesical, sacral, internal and external iliac) and extended involved removal of common iliac nodes and beyond. Clinicopathological data was obtained.

**Results:** A total of 264 cases were included in the study (218 cystoprostatectomy and 46 cystectomy specimens). There were 203 cases with extended lymph node dissection and 61 cases with limited lymph node dissection. Mean patients age was 68 years (range: 32-92 years), with a male predominance 6:1. There were 52 cases with only UCa in situ and 25 cases with no residual UCa present at the time of surgery. The mean case yield was 33 lymph nodes with 56 (21%) cases having at least one positive lymph node metastasis. Upon comparison of extended versus standard lymph node dissection 23% and 16% of the cases showed lymph node metastasis, respectively. Patients in all stage categories had more extended lymph node dissection performed compared to limited lymph node dissection: pT0 (20 vs 7), pTis (40 vs 12), pTa (8 vs 4), pT1(27 vs 5), pT2 (39 vs 8), pT3 (51 vs 17), and pT4 (18 vs 8). Women were found to have lymph node metastasis in 27% of cases while men had a 20% positivity rate. In cases with neoadjuvant therapy there was a 19% lymph node positivity rate compared to a 24% positivity rate in those with no presurgical therapy. The only cases categorized as pT2 and below with positive lymph node metastasis where those that had extended lymph node dissection performed.

**Conclusions:** Positive lymph nodes were more frequently detected in cases that had extended lymph node dissection. Over 35% of the positive lymph nodes were in the non-regional distribution. Extended lymph node dissection should be considered in patients with UCa even in the low stage or post-neoadjuvant chemotherapy setting.

## 936 Differentially Expressed Genes Associated with Unfavorable Prognosis in Prostate Cancer Based on The Cancer Genome Atlas Data

Dmitry Kalinin[1], Elena Pudova[2], George Krasnov[2], Anastasiya Kobelyatskaya[2], Maria Fedorova[2], Vladislav Pavlov[2], Anastasiya Snezhkina[2], Anna Kudryavtseva[2]
*[1]A.V. Vishnevsky National Medical Research Center of Surgery of the Russian Ministry of Healthcare, Moscow, MOS, Russian Federation, [2]Engelhardt Institute of Molecular Biology, RAS, Moscow, Russian Federation*

**Disclosures:** Dmitry Kalinin: None; Elena Pudova: None; George Krasnov: None; Anastasiya Kobelyatskaya: None; Maria Fedorova: None; Vladislav Pavlov: None; Anastasiya Snezhkina: None; Anna Kudryavtseva: None

**Background:** Prostate cancer is one of the most common cancers in men all over the world. Locally advanced prostate cancer (LAPC) is characterized by the invasion of the prostatic capsule without evidence of nodular or distant metastatic spread. Patients within this clinical category have different risks of recurrence. Our research is aimed at identifying novel prognostic biomarkers for LAPC, which will lead to optimization of treatment and development of appropriate clinical recommendations.

**Design:** We performed bioinformatics analysis of The Cancer Genome Atlas (TCGA) project RNA-Seq data. Eighty three LAPC samples derived from Caucasian patients only with certain criteria (no neoadjuvant therapy, primary tumor categories of pT3a-3b, negative resection margins, no lymphatic dissemination) were divided into two groups, favorable and unfavorable prognosis, depending on the presence of biochemical reoccurrence (increase in postoperative PSA level > 0.2 ng/mL). To perform differential expression analyses, we used edgeR package. Trimmed mean of M-values (TMM) normalization method and quasi-likelihood F-test (QLF test) were used. Additionally, we evaluated statistical significance of the gene expression differences between groups with non-parametric Mann-Whitney (MW) test. Finally, we selected only genes that have both at least 1.5-fold expression level change between two groups and $p < 0.05$ according to MW and QLF tests.

**Results:** In result of the analysis, we identified differentially expressed genes involved in various cellular processes associated with the tumor development and progression, which can be considered as potential markers of unfavorable prognosis in LAPC. Among upregulated genes, TWIST1 and PLCB3 are of interest; these genes have a previously established association with progression in various malignant

diseases, including prostate cancer. Among the downregulated genes, we selected the following ones as associated with LAPC unfavorable prognosis: *PARM1, TUSC3, B2M, MFHAS1, ARMCX2, GNE, FKBP4, HSP90B1, KIAA1324,* and *KLF12*.

**Conclusions:** Thus, we identified a number of genes as potential markers associated with unfavorable prognosis of LAPC without lymphatic dissemination. These genes can further be validated by qPCR and used as a basis for the development of a test system for improving the prognosis, treatment strategy, and management of prostate cancer patients.

This work was funded by the Russian Science Foundation, grant 18-75-10127.

## 937 Leiomyosarcoma of the Bladder: A Comparison to Soft Tissue Leiomyosarcoma

Sonia Kamanda[1], Giovanna A Giannico[1], Justin Cates[1], Jennifer Gordetsky[1]
[1]*Vanderbilt University Medical Center, Nashville, TN*

**Disclosures:** Sonia Kamanda: None; Giovanna A Giannico: None; Justin Cates: None; Jennifer Gordetsky: None

**Background:** Primary leiomyosarcoma (LMS) of the bladder is a rare tumor, with little information on predictors of clinical outcome. The National Cancer Institute's SEER (Surveillance, Epidemiology, and End Results) database contains abundant information on the natural history of soft tissue sarcomas. Therefore, we investigated the clinical outcomes of primary LMS of the bladder utilizing the SEER database.

**Design:** The SEER database was queried for LMS entered between 1973 and 2013. LMS of the bladder was compared to LMS arising in soft tissues of the extremities and trunk. Multivariable Cox regression was used to identify prognostic factors. Kaplan-Meier curves were plotted to assess cancer-specific survival (CSS). Given the lack of an AJCC 8th edition stage grouping for sarcomas of visceral organs, a new staging algorithm based primarily on histologic grade was applied.

**Results:** A total of 182 bladder LMS and 2830 soft tissue LMS were available for analysis. Bladder LMS tended to be larger than those in the soft tissues (5.5 cm vs. 4.2 cm; $P<0.001$) and of higher histologic grade (65% compared to 53% of soft tissue LMS), $P=0.06$. Median follow up for all cases was 70 months (range <1-488). The overall mortality for patients with LMS of the bladder was 30%, with a median CSS of 12.5 months (range <1-160) after surgical resection. Most patients (90%) did not receive neoadjuvant or adjuvant chemotherapy or radiation therapy. Unadjusted 10-yr survival rates were greater for patients with soft tissue LMS compared to those with bladder LMS (74% vs. 62%). On univariate analysis, significant predictors of worse CSS for bladder LMS included older age ($p<0.0001$), female sex ($p=0.003$), tumor size ($p=0.006$), and presence of metastatic disease ($p<0.0001$). On multivariate analysis, age, sex, and tumor size remained statistically significant predictors of CSS. Bladder LMS were associated with higher risk of death than soft tissue LMS (HR 1.82; 95% CI 1.25-2.65; $P=0.0016$). The new staging system eliminating size cutoffs for low-grade tumors, and using 5 cm for higher grade LMS of the bladder (Table 1) showed better discrimination between tumor stages than the AJCC 8$^{th}$ edition soft tissue staging system for sarcomas of the extremities and trunk (Figure 1).

**Table 1.** Proposed staging system for LMS of the urinary bladder

| Stage | Grade | T category | N category | M category |
|---|---|---|---|---|
| I | 1 | Any | N0 | M0 |
| II | 2-3 | T1 (≤5 cm) | N0 | M0 |
| III | 2-3 | T2 (>5 cm) | N0 | M0 |
| IV | Any | Any | N1 | M0 |
| | Any | Any | Any | M1 |

Figure 1 - 937

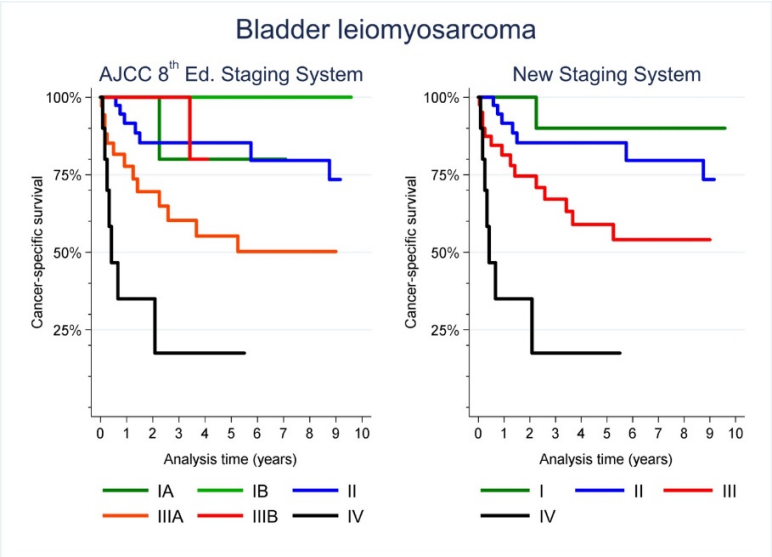


**Conclusions:** LMS of the bladder shows worse clinical outcomes compared to soft tissue LMS, with increasing age, female sex, and increasing tumor size being adverse prognostic factors for CSS. A revised staging system also shows utility in predicting CSS.

## 938 Squamous Cell Carcinoma of the Bladder: Relationship to HPV?

Sonia Kamanda[1], Giovanna A Giannico[1], Soroush Rais-Bahrami[2], Maria Del Carmen Rodriguez Pena[2], Carlos Prieto-Granada[2], Eva Compérat[3], Michelle Hirsch[4], Kenneth Iczkowski[5], Lauren Schwartz[6], John Cheville[7], Brittney Imblum[8], Andrew Spieker[1], Jennifer Gordetsky[1]

*[1]Vanderbilt University Medical Center, Nashville, TN, [2]The University of Alabama at Birmingham, Birmingham, AL, [3]Tenon Hospital, Paris, France, [4]Brigham and Women's Hospital, Boston, MA, [5]Medical College of Wisconsin, Milwaukee, WI, [6]Perelman School of Medicine at the University of Pennsylvania, Bala Cynwyd, PA, [7]Mayo Clinic, Rochester, MN, [8]Hospital of the University of Pennsylvania, Philadelphia, PA*

**Disclosures:** Sonia Kamanda: None; Giovanna A Giannico: None; Soroush Rais-Bahrami: None; Maria Del Carmen Rodriguez Pena: None; Carlos Prieto-Granada: None; Eva Compérat: None; Michelle Hirsch: None; Kenneth Iczkowski: None; Lauren Schwartz: None; John Cheville: None; Brittney Imblum: None; Andrew Spieker: None; Jennifer Gordetsky: None

**Background:** Squamous cell carcinoma (SCC) is the most common variant of urothelial carcinoma that arises in the bladder. This tumor has been associated with chronic inflammatory conditions as well as conditions that cause chronic irritation, such as stones, catheterization, and recurrent urinary tract infections. Human papilloma virus (HPV) is a known cause of SCC of the external genitalia and distal urethra. The literature is inconsistent regarding the association of HPV with squamous cell carcinoma of the bladder.

**Design:** A multi-institutional study was performed to identify cases of SCC of the bladder. Pure squamous histology and the absence of a urothelial carcinoma in situ lesion was required for inclusion. Clinical and pathologic features were collected, and tissue evaluated for high-risk HPV via *in-situ* hybridization and p16 immunohistochemistry. Only diffuse p16 staining was considered positive.

**Results:** We identified 194 cases of bladder SCC. Mean age was 66±14 years and 170/194 (88%) patients were Caucasian. SCC was more common in men (56%) than women (44%). Most patients underwent radical cystectomy (92%) with the remainder undergoing partial cystectomy. A history of smoking was found in 129/194 (66%) patients and conditions causing chronic irritation to the bladder was found in 81/194 (42%) patients. SCC of the bladder tended to present at a high stage with 74% of patients having pT3 or pT4 tumors. Mean tumor size was 5.5±2.9 cm. An average of 14.7 lymph nodes per patient were taken during surgery and 33/194 (17%) patients had N+ disease. Of those, the mean lymph node density was 0.18±0.1. Perineural invasion was present in 13% of cases and lymphovascular invasion was present in 23%. Positive margins were found in 10% of cases. Only 17% of patients underwent neoadjuvant chemotherapy. 73/194 (38%) patients had disease recurrence, with a mean of 1.0±5.1 months to recurrence. Death from SCC of the bladder occurred in 82/194 (42%) patients. On multivariate analysis, predictors of cancer-specific death included tumor size (p=0.0015), perineural invasion (p=0.046), total lymph nodes (p=0.0026), and positive lymph nodes (p=0.0010). Tissue was present for IHC and *in-situ* studies in 152 patients. Although p16 was positive in 48/152 (32%) cases, high-risk HPV was not identified in any cases.

**Conclusions:** Squamous cell carcinoma of the bladder is associated with smoking and chronic inflammatory conditions. Although squamous cell carcinoma can express p16, it is not associated with high risk HPV.

## 939 Neuroendocrine Differentiation in Usual-Type Prostatic Adenocarcinoma: Molecular Characterization and Clinical Significance

Harsimar Kaur[1], Iryna Samarska[2], Jiayun Lu[3], Farzana Faisal[4], Benjamin Maughan[5], Sanjana Murali[4], Jonathan Epstein[6], Corinne Joshu[3], Juan Miguel Mosquera[7], Emmanuel Antonarakis[4], Tamara Lotan[8]
*[1]Johns Hopkins University, Baltimore, MD, [2]Maastricht University Medical Centre+, Maastricht, Limburg, Netherlands, [3]Johns Hopkins Bloomberg School of Public Health, Baltimore, MD, [4]Johns Hopkins University School of Medicine, Baltimore, MD, [5]Salt Lake City, UT, [6]Johns Hopkins Medical Institutions, Baltimore, MD, [7]Weill Cornell Medicine, New York, NY, [8]Johns Hopkins School of Medicine, Baltimore, MD*

**Disclosures:** Harsimar Kaur: None; Iryna Samarska: None; Jiayun Lu: None; Farzana Faisal: None; Benjamin Maughan: None; Sanjana Murali: None; Jonathan Epstein: None; Corinne Joshu: None; Juan Miguel Mosquera: None; Emmanuel Antonarakis: None; Tamara Lotan: *Grant or Research Support*, Ventana/Roche

**Background:** Small cell neuroendocrine (NE) carcinomas of the prostate classically lose androgen receptor (AR) expression, harbor loss of the *RB1*, *TP53* and *PTEN* tumor suppressor genes and are associated with a poor prognosis. However usual-type adenocarcinomas may also contain areas of NE differentiation and in this context, the molecular features and biological significance are less certain.

**Design:** We examined the molecular phenotype and oncologic outcomes of primary prostate adenocarcinomas with >5% NE differentiation using 3 independent study sets, including a set of tumors with Paneth cell-like NE differentiation (n=30), a retrospective case-cohort of intermediate- and high-risk patients enriched for adverse outcomes (n = 267), and primary tumors from a retrospective series of men with castration resistant metastatic prostate cancer (CRPC) treated with abiraterone or enzalutamide (n=55). Chromogranin and INSM1 labeling identified NE cells and androgen receptor (AR) and ERG expression were quantified by immunofluorescence. The rate of *PTEN*, *TP53* and *RB1* tumor suppressor loss was assessed by genetically validated immunohistochemistry assays.

**Results:** AR expression was significantly lower in chromogranin-labelled benign NE cells (0.34 vs 1; p<0.001), the INSM1-labelled Paneth-like carcinoma cells (0.36 vs 1; p<0.001) and the chromogranin-labeled adenocarcinoma cells (0.34 vs 1; p<0.001) compared to unlabeled cells. ERG expression was seen in only a minority of tumors with Paneth-like cells (23% or 5/22), and quantified nuclear ERG expression was significantly lower in chromogranin-labeled adenocarcinoma cells compared to unlabeled cells (0.43 vs 1; p<0.001). Despite evidence of lower AR signaling in NE cells, adenocarcinomas with NE differentiation did not differ in rates of *TP53* missense mutation, *PTEN* loss or *RB1* loss compared to those without NE differentiation. Finally, NE differentiation was not associated with time to metastasis in intermediate- and high-risk patients (p=0.6 on multivariate analysis), nor with overall survival or progression-free survival in CRPC patients treated with abiraterone or enzalutamide (p=0.7 and 0.9).

**Conclusions:** NE differentiation in usual-type primary prostate adenocarcinoma is molecularly and clinically distinct form of lineage plasticity from that occurring in small cell NE carcinoma.

## 940 Genomic and Clinical-Pathologic Characterization of Primary Prostate Cancers with ATM Loss

Harsimar Kaur[1], Jessica Hicks[2], Colin Pritchard[3], Angelo De Marzo[1], William Isaacs[2], Jerry Lanchbury[4], Kirsten Timms[4], Emmanuel Antonarakis[2], Tamara Lotan[5]
*[1]Johns Hopkins University, Baltimore, MD, [2]Johns Hopkins University School of Medicine, Baltimore, MD, [3]University of Washington, Seattle, WA, [4]Myriad Genetics, Inc., Salt Lake City, UT, [5]Johns Hopkins School of Medicine, Baltimore, MD*

**Disclosures:** Harsimar Kaur: None; Jessica Hicks: None; Angelo De Marzo: None; William Isaacs: None; Kirsten Timms: *Employee*, Myriad Genetics, Inc.; *Employee*, Myriad Genetics, Inc.; Emmanuel Antonarakis: None; Tamara Lotan: *Grant or Research Support*, Ventana/Roche

**Background:** ATM, a protein kinase involved in double-strand DNA break repair, is mutated in a significant fraction of prostate cancers, and targeted therapies such as ATR inhibitors appear promising for ATM-deficient tumors. However, few ATM-deficient primary prostate cancers have been clinically and genomically characterized.

**Design:** We validated an automated dichotomously-scored clinical-grade IHC assay to detect ATM protein loss using prostate cancer cell lines and 52 high-grade prostate tumors with known *ATM* genomic status. We then examined the frequency of ATM protein loss among 23 tumors with known pathogenic germline *ATM* mutations and somatic *ATM* sequencing, as well as more than 800 additional primary prostate carcinomas using tissue microarrays (TMA). Targeted somatic genomic sequencing using HRD Plus (Myriad Genetics) was conducted in a subset of immunostained tumors.

**Results:** ATM loss by IHC was found in 13% (7/52) of high-grade tumors with somatic genomic sequencing data. Of 7 cases with ATM protein loss, 4 had a deleterious *ATM* mutation (including 2 inferred as germline) and 3 had single copy *ATM* genomic loss. Of the remaining 45 cases without ATM protein loss, none had ATM genomic alterations. In the cohort of men with pathogenic germline *ATM* mutations, 74% (17/23) had ATM protein loss. Of these, 76% (13/17) had homogeneous protein loss in all tumor cells sampled. On TMA analysis, ATM loss was present in 3% (25/824) of evaluable tumors, and was significantly more common in tumors from Grade Group 5 (12/130; 9.2%) compared to all other Grade Groups (13/694; 1.9%) (P<0.0001). Of tumors found by TMA screening with

available sequencing, 80% (4/5) with homogeneous ATM protein loss and 58% (7/12) with heterogeneous ATM protein loss had genomic *ATM* alterations detected. Of these, 82% (9/11) were inferred to have somatic *ATM* variants (with one tumor having likely somatic and germline alterations) while the remaining two cases were indeterminate based on variant allele fraction.

**Conclusions:** Validated ATM IHC is a sensitive assay for detecting underlying genomic *ATM* alterations, however not all tumors with ATM protein loss have detectable genomic alterations. ATM protein loss is likely an early event in tumors with germline mutations and is significantly enriched in high-grade prostate cancers.

## 941 PIN-Like Ductal Carcinoma of the Prostate has Frequent Activating MAPK Mutations

Harsimar Kaur[1], Daniela Correia Salles[2], Adina Paulk[3], Jonathan Epstein[2], James Eshleman[4], Tamara Lotan[5]
*[1]Johns Hopkins University, Baltimore, MD, [2]Johns Hopkins Medical Institutions, Baltimore, MD, [3]Joint Pathology Center, Silver Spring, MD, [4]Johns Hopkins University School of Medicine, Baltimore, MD, [5]Johns Hopkins School of Medicine, Baltimore, MD*

**Disclosures:** Harsimar Kaur: None; Daniela Correia Salles: None; Adina Paulk: None; Jonathan Epstein: None; James Eshleman: None; Tamara Lotan: *Grant or Research Support*, Ventana/Roche

**Background:** Prostatic intraepithelial neoplasia like (PIN-like ductal) carcinoma are rare tumors characterized by cystically dilated glands architecturally resembling high-grade prostatic intraepithelial neoplasia (HGPIN) and lined by pseudostratified columnar epithelium. These tumors are usually accompanied by Gleason score 6 (Grade Group 1) acinar cancer and behave relatively indolently. Another variant of prostate cancer with similar histologic features - ductal adenocarcinoma - is an aggressive variant and considered comparable to Gleason score 8 (Grade Group 4) acinar cancer. Here, we molecularly profile PIN-like ductal carcinoma to differentiate this entity from HGPIN and conventional ductal adenocarcinoma.

**Design:** Five PIN-like ductal carcinoma samples at radical prostatectomy with sufficient tumor tissue available were analyzed for genomic alterations by targeted next generation sequencing using the JHU solid tumor panel. DNA was captured using SureSelect for ~400 genes and sequenced on the Illumina HiSeq platform.

**Results:** Targeted sequencing revealed that three of five (60%) of the PIN-like ductal carcinomas showed activating MAPK mutations which are extraordinarily rare in conventional primary prostate carcinoma (<2% of cases). Case #4 had an activating hotspot *BRAF* mutation (p.K601E), which has been shown to confer sensitivity to MEK inhibitors. Case #5 showed an activating hotspot mutation in *HRAS* (p.Q61K) and a co-occurring in-frame deletion of *BRAF* (p.G32_A33del) of uncertain significance which has been reported in the germline of a single patient with a Rasopathy. Case #1 showed an in-frame deletion in *BRAF* (p.T488_Q493delinsK) which has been reported to shorten and lock the β3/αC-helix loop into a conformation that favors dimer formation and BRAF activation. Two of the cases harboring *BRAF* mutations also showed co-occurring *ASXL1* nonsense mutations (p.K586X and p.K580X), which have previously been reported in castration-resistant metastatic prostate cancers only. Cases #2 and #3 lacked *BRAF* or *HRAS* mutations but showed in-frame insertions in *MAP2K4* and *MAP3K6,* respectively, of uncertain significance.

**Conclusions:** PIN-like ductal carcinoma represents a molecularly unique tumor, enriched with potentially targetable oncogenic driver mutations in MAPK genes. This is in contrast to conventional ductal adenocarcinoma of the prostate, which are enriched with mutations in mismatch repair (MMR) and homologous recombination (HR) DNA repair pathways.

## 942 Type 1 Papillary Renal Cell Carcinomas with High Grade Features – Morphologic and Molecular Analysis

John Kennedy[1], Renzo DiNatale[1], Hikmat Al-Ahmadie[1], Samson Fine[1], Anuradha Gopalan[1], Judy Sarungbam[1], S. Joseph Sirintrapun[1], Satish Tickoo[1], Victor Reuter[1], Ying-Bei Chen[1]
*[1]Memorial Sloan Kettering Cancer Center, New York, NY*

**Disclosures:** John Kennedy: None; Renzo DiNatale: None; Hikmat Al-Ahmadie: None; Samson Fine: None; Anuradha Gopalan: None; Judy Sarungbam: None; S. Joseph Sirintrapun: None; Satish Tickoo: None; Victor Reuter: None; Ying-Bei Chen: None

**Background:** Type 1 papillary renal cell carcinomas (T1-PRCC) are traditionally thought to behave in an indolent manner. However, a small subset of T1-PRCC cases exhibit high-grade features and metastasize. Recent genomic studies show that nearly all T1-PRCCs have gains of chromosome 7 and 17 while about 15% harbor *MET* mutations. We aim to better define the morphologic and molecular features of high-grade T1-PRCC in a cohort enriched with patients with recurrence/metastasis to improve their distinction from other subtypes of RCC with papillary architecture.

**Design:** The study cohort included 62 PRCC cases (65 samples; 48 primary, 17 metastases) sequenced by a CLIA-approved targeted next-generation sequencing (NGS) platform. Mutational and copy number alteration (CNA) data, and clinicopathologic features were analyzed. Primary resections in patients with NGS results from metastases were also reviewed.

**Results:** The median age of patients (N=62) was 65 years (41-83), with a M:F female ratio of 14.5. Of primary resections, median tumor size was 4.6 cm (range 1.5-16). 36 (58%), 13 (21%) and 13 (21%) were staged as T1, T2, and T3, respectively, and 5 (8%), 7 (11%) and 50 (81%) were staged as N1, N0, and NX, respectively. Three patients (5%) were staged as M1. With a median follow-up of 51 months, 37 (60%) patients had metastases and 13 (21%) died of disease. Table 1 summarizes the three molecular groups identified in the cohort and their corresponding survival status. 33 (51%) had classic CNA characteristic of T1-PRCC (gains in chromosomes 7, 17, 12, 16 and 20). *MET* mutation (N=9) or amplification (N=7) (one case had both), mostly accompanied by the classic CNA pattern, were seen in 15 (23%) cases and associated with higher rates of metastases and death. Cases with ambiguous or non-T1 CNA (26%, N=17) were also associated with metastases and death, but to a lesser degree than T1 tumors with *MET* alterations. The distribution of mutations showed differences across the 3 molecular subgroups, most notably a higher frequency of TERT mutations in the *MET*-altered group. PRCCs with adverse outcome in Group 1 and 2 exhibited high nuclear grade and some morphologic features not fitting into either type 1 or type 2.

**Table 1. PRCC copy number alterations and mutations (N=65 samples, 62 patients)**

| | N (%) | Other mutations (frequency) | Metastases | Dead of disease | Alive with disease |
|---|---|---|---|---|---|
| Group 1- Type 1 CNA | 33 (51) | TERT (22%)<br>KDM6A (9%) | 36.7% (N=11) | 6.7% (N=2) | 50.0% (N=15) |
| Group 2<br>- *MET* mutation/amplification | 15 (23) | TERT (60%)<br>ARID1A (20%) | 86.7% (N=13) | 40.0% (N = 6) | 46.7% (N=7) |
| Group 3 - Ambiguous/Non-Type 1 CNA | 17 (26) | TERT (12%)<br>NF2 (12%) | 76.5% (N=13) | 29.4% (N=5) | 47.1% (N=8) |

Figure 1 - 942

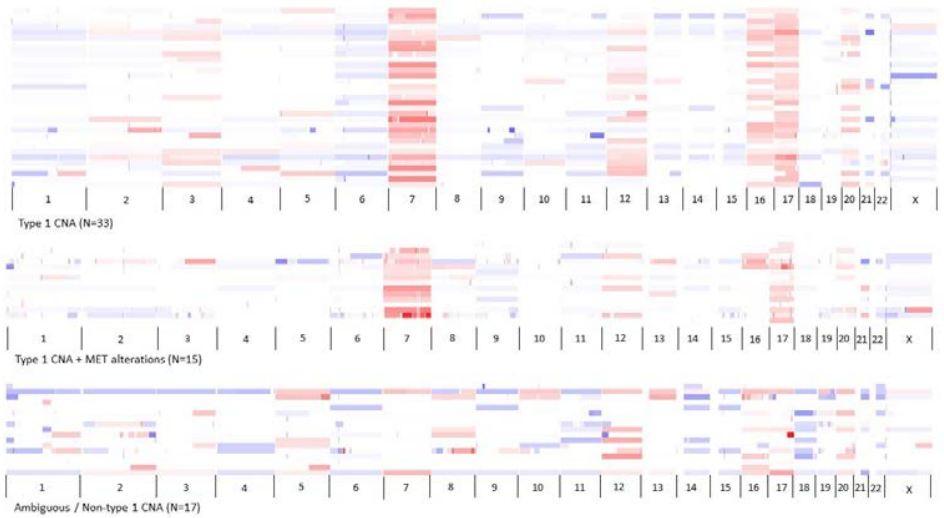


Figure 1. Chromosomal copy number alternations of papillary renal cell carcinoma cohort

**Conclusions:** In a PRCC cohort highly enriched with advanced disease, we demonstrate the presence of cases with high-grade histologic features and molecular features of T1-PRCC. High-grade T1-PRCC with *MET* alterations have higher rates of metastases and death compared to those without *MET* alterations.

## 943 Genomic Landscape of Non-invasive Urothelial Carcinoma of the Bladder

John Kennedy[1], Timothy Clinton[1], Nima Almassi[1], Eugene Pietzak[1], Bernard Bochner[1], Samson Fine[1], Anuradha Gopalan[1], Ying-Bei Chen[1], Judy Sarungbam[1], S. Joseph Sirintrapun[1], Maria Arcila[1], David Solit[1], Satish Tickoo[1], Victor Reuter[1], Hikmat Al-Ahmadie[1]
[1]*Memorial Sloan Kettering Cancer Center, New York, NY*

**Disclosures:** John Kennedy: None; Timothy Clinton: None; Nima Almassi: None; Eugene Pietzak: *Advisory Board Member*, Merck; *Consultant*, Chugai Pharmaceutical; Bernard Bochner: None; Samson Fine: None; Anuradha Gopalan: None; Ying-Bei Chen: None; Judy Sarungbam: None; S. Joseph Sirintrapun: None; Maria Arcila: *Speaker*, Biocartis; *Speaker*, Invivoscribe; David Solit: *Consultant*, Pfizer; *Consultant*, Loxo Oncology; *Consultant*, Lilly Oncology; *Consultant*, Vivideon Oncology; *Consultant*, Illumina; Satish Tickoo: None; Victor Reuter: None; Hikmat Al-Ahmadie: None

**Background:** Non-invasive urothelial carcinoma (NIUC) represents a heterogeneous group of tumors divided into papillary (low or high grade) and flat based on their growth pattern. Few studies reported on the genomic landscape of NIUC primarily within the larger clinical entity of non-muscle invasive bladder cancer, which additionally includes tumors that invaded the lamina propria. The aim of this study is to describe the genomic landscape of NIUC and correlate it with morphologic diagnosis and grade.

**Design:** From a prospectively sequenced UC cohort by a CLIA-certified next generation sequencing assay, we selected NIUC tumors with the diagnosis of low or high grade papillary, or flat/in situ urothelial carcinoma (HGPUC, LGPUC, UCIS). We also examined cases of HGPUC with associated low-grade component or with flat growth pattern on the same tissue that was sequenced. We also compared papillary tumors with inverted versus exophytic growth pattern.

**Results:** We identified 160 tumors from 150 patients (107 males and 43 females; median age 66 years, range 25-92 years). 31 (19%), 110 (69%), and 19 (12%) tumors were LGPUC, HGPUC, and UCIS, respectively. The results are summarized in table 1.
More *FGFR3* and *KRAS* mutations were identified in LGPUC than in HGPUC and UCIS. Conversely, more *TP53*, *RB1*, *ERBB2* and *TSC1* mutations, *CDKN2A* deletions, and *CCND1* amplifications were identified in HGPUC and UCIS than LGPUC. A subset of HGPUC have *FGFR3* mutations, the majority of which also contained a component of low-grade morphology. In a subset of HGPUC with a predominant low-grade morphology, the genetic alterations mostly resembled those of LGPUC except for more frequent *CDKN2A* deletions (50%) than seen in pure LGPUC (16%). *TERT* promoter and chromatin modifying gene mutations (e.g. *KDM6A*, *KMT2D*, *ARID1A*) were prevalent among all three groups. There was no significant difference between HGPUC with or without concurrent flat growth. Similar alterations were identified in tumors with inverted and exophytic growth pattern after controlling for histologic grade.

**Table 1. Frequency of somatic alternations in non-invasive bladder cancer**

| | HG-PUC (%) | HG-CIS (%) | LG-PUC (%) | p-value |
|---|---|---|---|---|
| ***FGFR3*** | 65 (59) | 1 (5) | 24 (77) | **<0.001** |
| ***KRAS*** | 7 (6) | 0 (0) | 8 (26) | **0.002** |
| ***ERBB2*** | 12 (11) | 9 (47) | 1 (3) | **<0.001** |
| ***PIK3CA*** | 33 (30) | 2 (11) | 11 (36) | 0.15 |
| ***TSC1*** | 10 (9) | 4 (21) | 0 (0) | 0.04 |
| ***TP53*** | 14 (13) | 8 (42) | 1 (3) | **<0.001** |
| ***MDM2*** | 5 (5) | 1 (5) | 1 (3) | 0.93 |
| ***RB1*** | 10 (9) | 3 (16) | 0 (0) | 0.11 |
| ***CDKN2A*** | 31 (28) | 1 (5) | 5 (16) | 0.05 |
| ***CDKN1A*** | 24 (22) | 2 (11) | 1 (3) | **0.04** |
| ***CCND1*** | 13 (12) | 1 (5) | 0 (0) | 0.10 |
| ***KDM6A*** | 50 (46) | 8 (42) | 21 (68) | 0.07 |
| ***KMT2D*** | 27 (25) | 4 (21) | 8 (26) | 0.93 |
| ***ARID1A*** | 30 (27) | 5 (26) | 8 (26) | 0.99 |
| ***KMT2A*** | 6 (6) | 1 (5) | 2 (7) | 0.98 |
| ***KMT2C*** | 20 (18) | 1 (5) | 5 (16) | 0.37 |
| ***TERT*** | 86 (78) | 10 (53) | 20 (65) | **0.04** |
| **Total Cases** | N=110 (69) | N=19 (12) | N=31 (19) | **---** |

**Conclusions:** Many genetic alterations were identified in NIUC, most of which have been reported in invasive and advanced disease. Non-invasive low and high-grade papillary tumors harbor distinct molecular alteration patterns. LGPUC is enriched for *FGFR3* mutations whereas HGPUC is enriched for alterations in cell cycle regulators (*TP53*, *RB1*, *CCND1*, *CDKN2A*, *CDKN1A*) and *ERBB2*. More studies are needed to determine the prognostic and predictive role of such alterations.

## 944 Expression of PD-L1/IDO1 and Tumor Infiltrating Lymphocytes Status in Renal Cell Carcinoma with Sarcomatoid Changes and Rhabdoid Features

Daisuke Kiyozawa[1], Dai Takamatsu[2], Kenichi Kohashi[2], Yoshinao Oda[2]
*[1]Fukuoka, Japan, [2]Kyushu University, Fukuoka, Japan*

**Disclosures:** Daisuke Kiyozawa: None; Dai Takamatsu: None; Yoshinao Oda: None

**Background:** Renal cell carcinoma (RCC) with sarcomatoid changes and/or rhabdoid features is the most aggressive variant of RCC. Over the resent several years, some immune checkpoint inhibitors including PD-1/PD-L1 inhibitor were approved for the treatment of RCC. Moreover, PD-L1 expression in RCC associates with poor prognosis, so analyzing PD-L1 expression play in important role in the treatment of RCC. IDO1 catalyzes l-tryptophan metabolism to kynurenine and causes T-cell regulation. Combination therapy of PD-L1 inhibitor and IDO1 inhibitor is paid a lot of attention in the treatment of various malignancies. However, little is known about IDO1 expression and therapeutic effects of IDO1 inhibitor in RCC. In consideration of immune-checkpoint inhibitors efficiency, evaluation of tumor infiltrating lymphocyte (TIL) status is also important. Some studies reported CD8+ TIL status affect worse prognosis in RCC. In this study, we analyzed the expression of PD-L1/IDO1 and examined its relationship with TIL status. We also investigated the effect of PD-L1 and IDO1 expression on clinicopathological factors including prognostic value.

**Design:** PD-L1, IDO1, CD3, CD4 and CD8 immunoexpression status in 60 formalin-fixed paraffin-embedded sarcomatoid/rhabdoid RCC was examined. The determination results of PD-L1 and IDO1 were defined by tumor proportion score (TPS), and we considered TPS≧1% as positive. For evaluation of CD3+, CD4+ and CD8+ TIL density, we counted the number of lymphocytes locating in the tumor and averaged over five high-power fields for each case.

**Results:** PD-L1 expression was observed in 19 cases (31.7%), and IDO1 expression was observed in 26 cases (43.3%). Among them, 13 cases (21.7% in total cases) showed co-expression of PD-L1 and IDO1. PD-L1 expression and co-expression correlated high density of CD3+, CD4+ and CD8+ T cells. There was no significant difference of overall survival among the PD-L1 and/or IDO1 expression. While PD-L1 expression and co-expression related to worse progression free survival (P=0.0015 and P=0.0066).

**Conclusions:** *Both PD-L1 and IDO1 positive 13 cases correlated high density TILs and worse progression free survival. This study also suggests that combination therapy of PD-L1 inhibitor and IDO1 inhibitor may be effective in treatment with sarcomatoid/rhabdoid RCC.*

## 945 Optimal Method for Reporting Gleason Score and Tumor Volume in MRI-Targeted Prostate Biopsies

Qingnuan Kong[1], Suneetha Chintalapati[2], Qi Cai[1], Ming Zhou[3]
*[1]University of Texas Southwestern Medical Center, Dallas, TX, [2]University of Texas Southwestern Medical Center, Irving, TX, [3]Tufts Medical Center, Boston, MA*

**Disclosures:** Qingnuan Kong: None; Suneetha Chintalapati: None; Qi Cai: None; Ming Zhou: None

**Background:** Magnetic resonance imaging targeted biopsies (MRI-TBx) have been increasingly used in prostate cancer (PCa) diagnosis. Multiple cores are taken from MRI suspicious regions and may have different Gleason score (GS) and tumor volume (TV). It is empirically recommended to report “global” GS and TV by averaging GS and TV of all positive cores to best estimate the PCa pathology (GS and TV) within the prostate gland. Evidences to support such recommendations are, however, lacking.

**Design:** 104 patients underwent MRI-TBx followed by radical prostatectomy (RP). Pathological parameters collected included (1) global GS of all positive cores (gGS. Cumulative length of each Gleason pattern in all positive cores was calculated to determine the primary and secondary patterns) and highest GS in any positive core (hGS), highest linear length of tumor in any core (hL), and global linear length of tumor (gL, determined by cumulative length of all tumor foci/number of positive cores); (2) GS and tumor size of the dominant tumor nodule in RP. These different GS and TV measurement methods in biopsies were correlated to the corresponding parameters in RP.

**Results:** Of 104 MRI-TBx, 35 (33.7%) had different GS among positive cores. Of these 35 cases, gGS and hGS of the biopsies matched the RP GS in 28 (80.0%) and 20 (57.1%) (p=0.072). However, in 31 cases with biopsy cores≥3 per case, gGS and hGS of the biopsies matched the RP GS in 25 (80.6%) and 16 (51.6%) (p=0.016). PIRADS scores of the MRI suspicious lesions were 3, 4 and 5 in 3, 54 and 47 cases. The biopsy GS (either hGS or gGS) and RP GS were concordant in 2 (67%), 33 (61%) and 31 (66%) (p=0.63). When correlating TV measurements between biopsies and RP in 104 cases, hL of the biopsies correlated slightly better with RP TV (Pearson correlation coefficient r=0.265, p=0.012) than gL (r=0.195, p=0.066). When biopsy cores were ≤2, neither hL nor gL in biopsy significantly correlated with the RP TV.

**Conclusions:** In MRI-TBx, gGS is significantly better than hGS predicting RP GS, confirming the current recommendation that a global GS should be reported. PIRADA scores do not affect the biopsy and RP GS concordance. Highest tumor length in any biopsy core is a slightly better predictor of tumor size in RP and should be reported. When biopsies have ≤2 cores, none of the Gleason grading and tumor volume

measurement methods significantly correlated with the parameters in RP, suggesting that MRI-targeted biopsy should take at least 3 cores from MRI suspicious regions.

## 946 Molecular Signature of Malignant Cribriborm and Other Similar Lesions of the Prostate: Diagnostic Implications

Qingnuan Kong[1], Qi Cai[1], Ming Zhou[2]
*[1]University of Texas Southwestern Medical Center, Dallas, TX, [2]Tufts Medical Center, Boston, MA*

**Disclosures:** Qingnuan Kong: None; Qi Cai: None; Ming Zhou: None

**Background:** Cribriform prostatic adenocarcinoma (PCa) and intraductal carcinoma (IDC) are recently considered adverse pathological features of PCa as both are similarly associated with poor clinical outcomes. Atypical intraductal proliferation (AIP) refers to lesions that are suspicious for but not diagnostic of IDC. There is controversy whether AIP and IDC should be considered the same morphological spectrum or separate entities. High grade prostatic intraepithelial neoplasia (HGPIN) is considered a precursor lesion to PCa. *ERG* gene fusion is specific for and identified in 40-50% of PCa, while PTEN is a tumor suppressor gene whose expression is lost in 50-80% of PCa. We studied the expression of ERG and PTEN in these lesions to explore the utility of ERG and PTEN in the classification and diagnosis of these prostate lesions.

**Design:** Tissue microarray (TMA) was constructed from 32 radical prostatectomies to include 360 cancer cores (338 non-cribriform cancer and 22 cribriform cancer), 30 IDC, 39 AIP , 67 HGPIN and 156 normal tissue. Non-cribriform cancer comprised of 144 GS≥4+3 PCa and 194 GS≤3+4. ERG and PTEN expression was studied immunohistochemically on TMA slides.

**Results:** Expression of PTEN and ERG in non-cribriform PCa, cribriform PCa, IDC, AIP and HGPIN were summarized in the Table. Compared with non-cribriform PCa, loss of PTEN expression was more common in cribriform PCa (p=0.02), but ERG expression was similar (p=0.92). Cribriform PCa and IDC had similar PTEN expression loss and ERG expression (p=0.23 and 0.71). Compared with IDC, AIP had similar PTEN expression loss (p=0.43), but higher ERG expression (p=0.03). Compared with AIP, HGPIN had significantly less PTEN loss and ERG expression (p<0.001).

**Table:** PTEN and ERG expression in prostate lesions

| | Non-cribriform PCa | Cribriform PCa | IDC | AIP | HGPIN |
|---|---|---|---|---|---|
| PTEN loss #/total (%) | 249/338 (73.6) | 21/22 (95.5%) | 25/30 (83.3%) | 35/39 (89.7) | 27/67 (40.3) |
| ERG expression #/total (%) | 111/338 (32.8%) | 7/22 (31.8%) | 13/30 (43.3%) | 27/39 (69.2) | 1/67 (1.5%) |

**Conclusions:** Cribriform PCa and IDC had similar PTEN and ERG expression patterns, supporting the recent proposal to classify both lesions as the adverse pathology of PCa with similar clinical outcomes. Cribriform PCa had significantly higher PTEN loss than non-cribriform PCa. Compared with IDC, AIP had similar PTEN loss but higher ERG expression, suggesting that AIP and IDC are molecularly similar and should be considered as one entity. AIP and HGPIN had distinct PTEN and ERG expression patterns, suggesting that these two markers can be used to reliably distinguish AIP and HGPIN.

## 947 MRI-Targeted Prostate Biopsies Improve the Detection of Prostate Cancer with Adverse Pathology

Qingnuan Kong[1], Suneetha Chintalapati[2], Qi Cai[1], Ming Zhou[3]
*[1]University of Texas Southwestern Medical Center, Dallas, TX, [2]University of Texas Southwestern Medical Center, Irving, TX, [3]Tufts Medical Center, Boston, MA*

**Disclosures:** Qingnuan Kong: None; Suneetha Chintalapati: None; Qi Cai: None; Ming Zhou: None

**Background:** Cribriform cancer glands (Crib-PCa) and intraductal carcinoma (IDC) have recently emerged as significant adverse pathological features of prostate cancer (PCa) and provide prognostic significance independent of conventional factors such as Gleason score (GS) and tumor volume (TV). Emerging data suggest that MRI-targeted prostate biopsies (MRI-TBx) may improve the detection of PCa with such adverse pathology. However, the data in the literature is scant and conflicting. In this study, we evaluated and compared the MRI-TBx and transrectal ultrasound standard sextant biopsy (SBx) for detecting PCa with adverse pathology.

**Design:** 184 consecutive cases with grade group (GG)≥2 PCa detected in MRI-TBx, including 105 MRI-US fusion-targeted biopsy [FTBx) cases and 79 in-bore targeted biopsy [IBTBx] cases, were included. PIRADS v.2 scores 3-5 were rendered for all MRI suspicious lesions. 105 patients receiving FTBx also underwent concurrent SBx. Adverse pathology (AP) including crib-PCa, IDC and GG≥3 PCa were recorded in addition to other standard PCa parameters including Gleason score and tumor volume.

**Results:** Crib-PCa was detected in 44/184 (23.9%) biopsies by MRI-TBx and in 14/105 (13.3%) by SB (p=0.03). IDC was detected in 23/184 (12.5%) by MRI-TBx and in 7/105 (6.7%) by SB (p=0.12). GG≥3 PCa was detected in 91/184 (49.6%) by MRI-TBx and in 30/105 (28.6%) by SB (p=0.03). The detection rate of these features by FTBx and IBTBx was not significantly different (p=0.31, 0.40 and 0.71). In these 184 cases, MRI detected 272 PCa lesions whose PIRADS scores were 3 in 23 lesions, 4 in 147 and 5 in 102. Crib-PCa was detected in 21/170 (12.4%) PIRADS 3/4 lesions *vs* 23/102 (22.5%) PIRADS 5 lesions (p=0.027). IDC was detected in 9/170 (5.3%) PIRADS 3/4 lesions *vs* 11/102 (10.8%) PIRADS 5 lesions (p=0.093). GG≥3PCa was detected in 48/170 (28.2%) PIRADS 3/4 lesions *vs* 52/102 (51.0%) PIRADS 5 lesions (p<0.001).

**Conclusions:** MRI-TBx improves the detection of PCa with adverse pathology by detecting significantly more crib-PCa and GG≥3 PCa than SBx. PCa lesions with PIRADS score 5 are more likely to harbor crib-PCa and GG≥3 PCa. IDC detection is, however, not improved by MRI-TBx.

## 948 Quantification of Pattern 4 in Patients with Highest Needle Biopsy Gleason Score 4+4=8/Grade Group 4 is Associated with Radical Prostatectomy Downgrading

Pavel Kopach[1], Hikmat Al-Ahmadie[1], Ying-Bei Chen[1], Anuradha Gopalan[1], Judy Sarungbam[1], Satish Tickoo[1], Victor Reuter[1], Samson Fine[1]
*[1]Memorial Sloan Kettering Cancer Center, New York, NY*

**Disclosures:** Pavel Kopach: None; Hikmat Al-Ahmadie: None; Ying-Bei Chen: None; Anuradha Gopalan: None; Judy Sarungbam: None; Satish Tickoo: None; Victor Reuter: None; Samson Fine: None

**Background:** Gleason score (GS) on prostate needle biopsy (NB) may under- or overestimate GS in subsequent radical prostatectomy (RP). Currently, maximum GS in any NB core is typically used for clinical decisions. For patients opting surgery, clinical outcomes are more dependent on RP features, including grade, stage, and margin status, such that the rate of downgrading from NB could portend a different prognosis. Assigning % pattern 4 has become standard for patients with highest GS 7/Grade groups 2-3 on NB. Although downgrading in patients with highest NB GS 4+4=8/Grade group 4 has been reported in up to 50% of cases at RP, it remains unclear whether one should assign % pattern 4 for cores with lower grades (Grade groups 2-3) in such cases. In this pilot project, we studied a cohort of matched NB and RP specimens with maximum NB GS 4+4=8 to determine association of more detailed biopsy features with RP downgrading.

**Design:** We evaluated the association of various pattern 4 tumor quantification parameters (number of NB cores with highest GS, overall % pattern 4 per case [total mm of pattern 4 / total mm of cancer], total length [mm] of pattern 4 per case) with RP GS/Grade group downgrading in 65 patients with maximum NB GS 4+4=8 (Grade group 4).

**Results:** Six of 65 (9%) cases had only Grade group 4 on NB; 38 (58%), 29 (45%), and 33 (51%) cases had at least one core of Grade groups 3, 2, or 1 carcinoma, respectively. On RP, 35 (54%) cases were downgraded to GS≤7 (RP Grade group 2 [n=8], Grade group 3 [27]), while 30 (46%) had GS ≥8 (RP Grade group 4 [n=19], Grade group 5 [n=11]).

31 of 46 (67%) cases with ≤ 2 cores with GS 8/Grade group 4 were downgraded vs. 4/19 (21%) cases with > 2 cores. 28 of 39 (72%) cases with overall % pattern 4 ≤75% were downgraded vs. 7/26 (27%) cases with >75% pattern 4. 22 of 29 (76%) cases with ≤10 mm of pattern 4 were downgraded vs. 13/36 (36%) cases with >10 mm pattern 4.

**Conclusions:** Half of patients in this cohort with highest needle biopsy GS 8/Grade group 4 were downgraded to GS ≤7 at prostatectomy. Various quantitative measures of pattern 4 are associated with downgrading, including overall % and total mm of pattern 4, for which assigning % pattern 4 in NB cores with lower grades (Grade groups 2-3) is necessary. An expanded cohort, including matched NB/RP patients with highest NB GS 4+3=7/Grade group 3, is currently under investigation.

## 949 High-Grade Unclassified Renal Cell Carcinoma with NF2-loss – Morphologic and Molecular Analysis

Pavel Kopach[1], Renzo DiNatale[1], Hikmat Al-Ahmadie[1], Samson Fine[1], Anuradha Gopalan[1], Judy Sarungbam[1], A. Hakimi[1], Satish Tickoo[1], Victor Reuter[1], Ying-Bei Chen[1]
*[1]Memorial Sloan Kettering Cancer Center, New York, NY*

**Disclosures:** Pavel Kopach: None; Renzo DiNatale: None; Hikmat Al-Ahmadie: None; Samson Fine: None; Anuradha Gopalan: None; Anuradha Gopalan: None; Judy Sarungbam: None; A. Hakimi: None; Satish Tickoo: None; Victor Reuter: None; Ying-Bei Chen: None

**Background:** Unclassified renal cell carcinoma (uRCC) with high-grade histologic features is a heterogeneous group of tumors that often show aggressive clinical behavior and lack available standard therapy. We have previously identified a molecular subset of NF2-loss uRCCs with dysregulated Hippo-YAP pathway and particularly poor outcome. In this study, we aimed to delineate the morphologic and molecular features of this subset of tumors to facilitate their stratification from other high-grade RCC.

**Design:** The study cohort included 23 cases of nephrectomy in patients with high-grade uRCC harboring NF2 alterations that were identified by a targeted next generation sequencing platform. The possibility of specific subtypes of RCC (FH-deficient, translocation, etc) was excluded by immunohistochemical or molecular analysis. We conducted clinicopathologic, mutational, and copy number analysis.

**Results:** Patients were predominantly men (78%) with a median age of 61.3 years (range 28-81). At nephrectomy, 14 (61%) patients were pT3/4 and 14 (61%) had metastatic disease; 6 of the remaining 9 (66%) developed metastases with a median time of 33 months. Overall, 15 (65%) patients died of disease (median time to death - 19 months).

Cases were divided into 4 morphologic groups based on the dominant architectural pattern (Table): papillary (n=7, 31%), solid (n=6, 26%), tubular (n=6, 26%), and sarcomatoid (n=4, 17%). Among all groups 13 cases (57%) showed ISUP Grade 3 (14%) or 4 (43%). On molecular level, aside from *NF2* inactivating mutations, recurrent somatic mutations most frequently involved chromatin regulator genes, including *SETD2* (39%), *BAP1* (26%), *PBRM1* (13%), *ARID2*/*ARID5B* (13%), and *KDM5A*/*KDM6A* (13%). A higher mean number of CNA was seen in the groups with sarcomatoid and tubular architecture (21.5 and 20.5%), compared to the groups with papillary and solid morphology (12.2 and 13.4%). Most common CNAs were 22q loss (67-100%), 1p loss (67-100%), 3p loss (29-75%), 7/17 gain (17-50%), many tumors with more than 1 shared CNAs.

**Table 1.** Comparison of molecular features and clinical outcome between different morphologic groups of NF2-mutant uRCC

| Dominant Morphologic Pattern | Frequent Copy Number Loss | Copy Number Gain of 7/17 | Recurrent Mutations | Outcome |
|---|---|---|---|---|
| Papillary (n=7, 31%) | 1p (71%), 3p (29%), 22q (71%) | 7 (0%) 17q (29%) | *SETD2* (14%), *BAP1* (29%), *ARID2/ARID5B* (14%), *KDM5A/KDM6A* (29%) | AWD 29% NED 14% DOD 57% |
| Solid (n=6, 26%) | 1p (83%), 3p (50%), 22q (100%) | 7 (50%) 17 (50%) | *SETD2* (50%), *BAP1* (33%), *PBRM1* (17%), *KDM5A*/*KDM6A* (17%) | AWD 17% NED 17% DOD 66% |
| Tubular (n=6, 26%) | 1p (67%), 3p (50%), 22q (67%) | 7 (17%) 17 (17%) | *SETD2* (50%), *BAP1* (17%), *PBRM1* (17%) | NED 17% DOD 83% |
| Sarcomatoid (n=4, 17%) | 1p (100%), 3p (75%), 22q (100%) | 7 (50%) 17 (0%) | *SETD2* (50%), *BAP1* (25%), *PBRM1* (25%), *ARID2*/*ARID5B* (50%) | AWD 50% DOD 50% |

**Conclusions:** NF2-loss high-grade uRCC is a subset of aggressive tumors with a wide range of morphologic appearances but harboring similar molecular features that are distinct from established subtypes of RCC. Identification of these tumors and targeting of NF2/Hippo-YAP pathway may have clinical utility in this group of rare kidney cancer patients.

## 950 Low-Grade Oncocytic Tumor of Kidney (CK7-Positive, CD117-Negative): A Single Institutional Experience with Incidence and Clinicopathological Characteristics

Oleksandr Kravtsov[1], Sounak Gupta[1], John Cheville[1], Loren Herrera Hernandez[1], Rafael Jimenez[1]
[1]*Mayo Clinic, Rochester, MN*

**Disclosures:** Oleksandr Kravtsov: None; Sounak Gupta: None; John Cheville: None; John Cheville: None; Loren Herrera Hernandez: None; Rafael Jimenez: None

**Background:** Low-grade oncocytic tumor (LOT) of the kidney is a recently described renal eosinophilic neoplasm that resembles but does not meet established diagnostic criteria of oncocytoma (ONC) or chromophobe renal cell carcinoma (ChRCC). While morphologically similar to ONC, LOT is characterized by a CK7-positive (pos) and CD117-negative (neg) immunophenotype. Limited data are available on its incidence and clinical behavior. We describe a series of 7 cases identified retrospectively at a single institution.

**Design:** 290 consecutive cases diagnosed as ONC between 1970 and 2002 were used to construct a TMA, using 4 cores from each tumor. IHC for CK7, CD117, SDHB, FH was performed and evaluated for staining extent and intensity. 1+ (focal and weak) staining for CD117 was considered neg. For 10 cases that were CK7pos/CD117neg on TMA, CK7, CD117, AMACR, SDHB, CK20 were performed on whole slides. Three cases were CD117 strongly pos on whole sections and were excluded from further analysis. Follow-up (F/U) and demographic characteristics were obtained from medical record and our institutional nephrectomy registry.

**Results:** Seven CK7pos/CD117neg tumors were identified, including one tumor with 1+ CD117 staining. CK7 positivity was uniformly diffuse and strong. Patient's age ranged from 56 to 80-year (median 65) with nearly equal gender distribution (4F, 3M). Median tumor size

was 3 cm (range 2.4-4). All tumors were single tumors with no syndromic setting, and showed solid areas of tightly packed nests of cells with eosinophilic cytoplasm and small round nuclei (Figure 1), areas of stromal edema with loose cellularity (Figure 2), and bland cytology. Distinct nucleoli were seen at 200x in 4 cases. Perinuclear halos were present in 4 cases. CK20 and p63, were neg, while SDHB and FH were retained. AMACR was weakly pos in 3 cases. Given that 4986 nephrectomies were performed for renal epithelial tumors at our institution in the study timeframe, the incidence of LOT was 2.4% of historically diagnosed ONC (7/290) and 0.1% of all renal epithelial tumors (7/4986). No local recurrences or metastases were noted in any of the 7 patients (median F/U, 5 years, range 1-28).

Figure 1 - 950

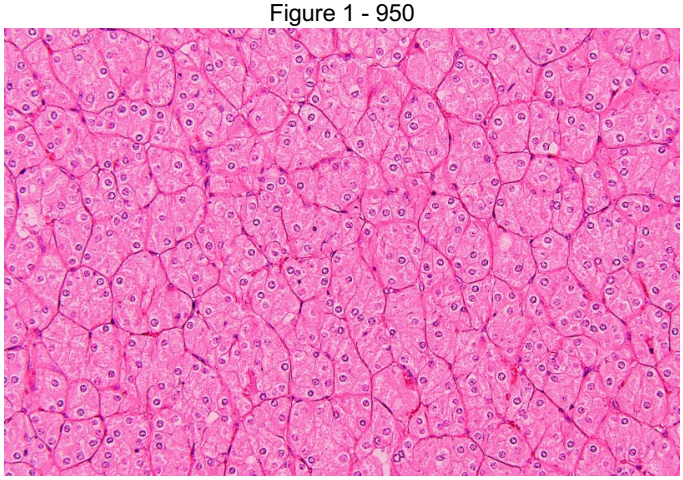

Figure 2 - 950

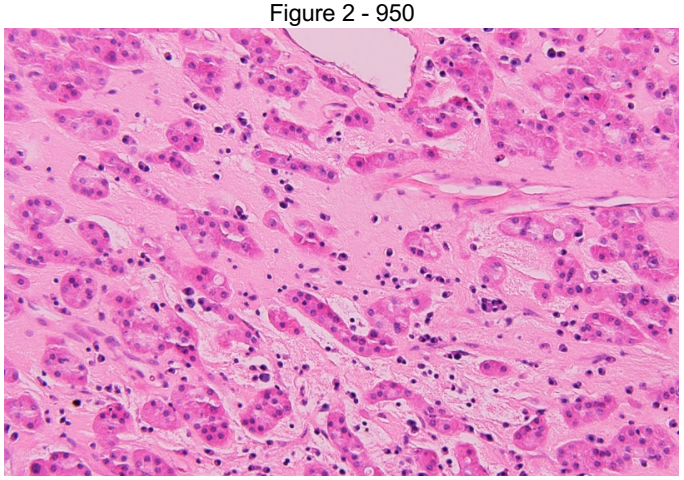

**Conclusions:** LOT is an uncommon but distinct eosinophilic renal tumor, that constitutes 2.4% of tumors historically diagnosed as ONC, and is associated with indolent behavior. Awareness of LOT morphology and immunophenotype may reduce overdiagnosis of ChRCC based on CK7 positivity.

## 951 Melanin and Lipofuscin in Unexpected Renal Contexts

Caroline Kurek[1], Fiona Maclean[2]
[1]Douglass Hanly Moir Pathology, Sydney, NSW, Australia, [2]Douglass Hanly Moir Pathology, Macquaire Park, NSW, Australia

**Disclosures:** Caroline Kurek: None; Fiona Maclean: *Speaker*, Mundipharma; *Consultant*, AstraZeneca

**Background:** Melanin and lipofuscin are pigments found in select cells within the human body. Melanin is produced within melanosomes, in a reaction catalyzed by tyrosinase during the conversion of tyrosine into dopa. Lipofuscin is created in the lysosomes of aging cells and is understood to be a by-product of failed intracellular catabolism. There are isolated entities in which these biochromes have been documented within the kidney. We recently noted the presence of non-siderotic pigment deposition in a more extended setting, including novel examples of both neoplastic and non-neoplastic renal tissue and thus aimed to investigate and document the context of this phenomenon.

**Design:** We conducted a retrospective search of pigment documented in reports within our database over a 10 year period, encompassing 6225 renal specimens, the majority of which represented neoplastic conditions. Cases where the pigment consisted solely of haemosiderin were excluded.

**Results:** We identified 129 cases in patients aged 21 to 83 years. The pigment was identified as melanin in 17 cases (associated with tumour in 14 cases and native kidney in 3 cases) and as lipofuscin in 14 cases (associated with tumour in 9 cases and native kidney in 5 cases). Tumours containing melanin included 3 cases of chromophobe renal cell carcinoma (RCC), 3 cases of melanotic Xp11 translocation RCC, 2 cases of type 2 papillary RCC, and 1 case per entity of oncocytoma, clear cell RCC, PEComa, renal angioadenomatous tumour, RCC unclassified and metastatic melanoma. Tumours containing lipofuscin included 6 cases of pigmented microcystic variant of chromophobe RCC and 1 case of eosinophilic variant of chromophobe, 1 case of type 2 papillary RCC and 1 case of oncocytoma. Melanin and lipofuscin in native kidney was identified in the renal tubular epithelium of all 3 and 5 cases, respectively.

**Conclusions:** Pigmentation of the renal parenchyma occurs in native kidney as well as in a range of benign and malignant tumours. A number of recently described tumours are characterised by their production of pigment and as such, recognising and correctly interpreting the presence of pigmentation may prompt consideration of these entities. This is particularly true of unusual entities such as pigmented microcystic variant of chromophobe RCC and melanotic Xp11 translocation RCC.

## 952 Clinical-Pathologic Survey of Neuroendocrine Differentiation in High-Grade Treatment-Naïve Prostate Cancer

Marietya Lauw[1], Bradley Stohr[1], Jeffry Simko[1], Emily Chan[1]
[1]*University of California San Francisco, San Francisco, CA*

**Disclosures:** Marietya Lauw: None; Bradley Stohr: None; Jeffry Simko: None; Emily Chan: None

**Background:** Neuroendocrine (NE) differentiation in prostatic adenocarcinoma (PCa) is well recognized. Studies have shown that increased NE expression correlates with disease progression and also implicates NE differentiation as a mechanism of resistance in castration-resistant prostate cancer (CRPC). However, NE immunohistochemistry (IHC) has not routinely been used in the evaluation of PCa, particularly in the biopsy setting, due to uncertain clinical significance. Given the propensity for high-grade tumors to develop CRPC, we sought to evaluate NE expression in this population.

**Design:** We retrospectively reviewed all diagnostic biopsies from 2001-2014 containing high-grade (Grade Group 5) prostatic adenocarcinomas in which slides from our department archives were available for review. IHC for two NE markers (synaptophysin and chromogranin) was performed. NE marker staining was scored as follows: no staining: 0, staining in <25% of cells: 1, 25-50%: 2, and >50% of cells: 3. A positive staining pattern was defined as score 1 or higher. The staining patterns for the NE markers were correlated with development of CRPC and development of new metastases, which was obtained from the medical record.

**Results:** Of the 73 cases available for review, 73% and 40% showed positive staining for synaptophysin and chromogranin, respectively. Synaptophysin staining ranged: 0 (27%), 1 (60%), 2 (10%), and 3 (3%); and chromogranin staining ranged: 0 (60%), 1 (38%), 2 (1%), and 3 (0%). There was significantly increased CRPC seen in the double positive cases (17/28, 61%) relative to the double negative cases (5/19, 26%), p=0.03, but not with single positive staining alone (9/26, 35%), p=0.52. Double positive cases showed a higher proportion of development of new metastasis compared to negative cases though this was not statistically significant (14/28, 50% versus 6/19, 32%; p=0.24). In two cases, there was subsequent development of small cell NE carcinoma, one of these cases, the original biopsy showed positive synaptophysin staining (score 2) only, and the second case showed positive staining for both NE markers (score 1 for both markers).

**Conclusions:** High-grade PCa shows a range of NE marker staining. Double positive staining for synaptophysin and chromogranin may be associated with increased risk of developing CRPC. These patients may benefit from further study and potentially more aggressive or alternate therapies.

## 953 Computer-Extracted Features from Radical Prostatectomy Specimens Prognostic of Biochemical Recurrence are Associated with Decipher Risk Groups

Patrick Leo[1], Robin Elliott[2], Andrew Janowczyk[3], Nafiseh Janaki[4], Rakesh Shiradkar[3], Kaustav Bera[3], Cristina Magi-Galluzzi[5], Andrei Purysko[6], Eric Klein[6], Sanjay Gupta[7], Hari Thulasidass[8], Ash Tewari[9], Ayah El-Fahmawi[10], Jessica Kim[10], Mohammed Shahait[10], Natalie NC Shih[10], Abhishek Shah[11], Michael Feldman[12], Priti Lal[10], David Lee[10], Anant Madabhushi[3]
[1]*Pittsburgh, PA,* [2]*University Hospitals Cleveland Medical Center, Case Western Reserve University, Cleveland, OH,* [3]*Case Western Reserve University, Cleveland, OH,* [4]*Brigham and Women's Hospital, Harvard Medical School, Boston, MA,* [5]*The University of Alabama at Birmingham, Birmingham, AL,* [6]*Cleveland Clinic, Cleveland, OH,* [7]*Case Western Reserve University/University Hospitals Cleveland Medical Center, Cleveland, OH,* [8]*Mount Sinai, New York, NY,* [9]*Icahn School of Medicine at Mount Sinai, New York, NY,* [10]*University of Pennsylvania, Philadelphia, PA,* [11]*Hospital of the University of Pennsylvania, Philadelphia, PA,* [12]*University of Pennsylvania, Wilmington, DE*

**Disclosures:** Patrick Leo: None; Robin Elliott: None; Andrew Janowczyk: None; Nafiseh Janaki: None; Rakesh Shiradkar: None; Kaustav Bera: None; Cristina Magi-Galluzzi: None; Andrei Purysko: *Grant or Research Support*, GenomdDx Biosciences; *Grant or Research Support*, profound medical; Eric Klein: None; Ayah El-Fahmawi: None; Mohammed Shahait: None; Natalie NC Shih: None; Abhishek Shah: None; Priti Lal: None; David Lee: None; Anant Madabhushi: *Consultant*, Inspirata Inc.; *Stock Ownership*, Inspirata Inc

**Background:** The Decipher test consists of 22 RNA-expression-based genomic markers that are involved in prostate cancer pathogenesis and is used to estimate the risk of metastasis within 5 years of radical prostatectomy (RP) by stratifying patients into low, intermediate, or high risk Decipher groups (DG). Computer-extracted features of gland morphology from RP specimens have previously been used for prognosis of biochemical recurrence (BCR) post-RP. BCR carries an increased risk for metastasis. In this work we assessed the correlation between risk assessments of a machine learning model for BCR prognosis and DG.

**Design:** A single diagnostic slide per patient was collected from N=525 patients across four institutions. All slides were annotated for a single representative cancer region, from which 26 texture features were extracted. A deep learning model for gland lumen segmentation was subsequently trained on 41 patients and applied to all cancerous regions. From the lumen segmentations, 216 features of lumen arrangement, shape, and disorder were extracted. 406 patients from two institutions with post-RP follow-up for BCR (mean time-to-BCR = 2.0 years, mean time-to-last-follow-up = 5.2 years) were used to fit an elastic-net penalized Cox regression model with these 242 features. The Cox model output a risk score for each patient. The risk score threshold giving the best separation in BCR-free survival was selected to divide patients into low- and high-risk categories. This process was termed “Histotyping”. The Histotype risk groups were then tested for

concordance with DG in the validation set, which contained the remaining 119 patients from three institutions. Patients of one institution were split between the training and validation sets based on availability of BCR outcome and DG.

**Results:** Histotyping identified 1 gland density feature, 10 lumen shape features, and 3 texture features. Histotype high-risk patients had a wider range of lumen shapes, more convoluted lumen boundaries, and less uniform texture. In the training set, Histotype risk groups were prognostic of BCR ($p<0.01$, hazard ratio: 3.16, 95% CI: 2.07-4.82). In the validation set, 76% of DG low-risk patients were Histotyping low-risk, compared to 61% of DG intermediate-risk and 34% of DG high-risk.

| Feature | Hazard ratio |
|---|---|
| Architecture: Disorder of number of neighbors in 240 micron radius | 1.18 |
| Shape: Standard deviation of invariant moment 1 | 0.93 |
| Shape: Median distance ratio | 0.95 |
| Shape: Median of Fourier descriptor 4 | 1.01 |
| Shape: 5$^{th}$ percentile / 95$^{th}$ percentile of shape irregularity | 0.94 |
| Shape: 5$^{th}$ percentile / 95$^{th}$ percentile of smoothness | 1.15 |
| Shape: 5$^{th}$ percentile / 95$^{th}$ percentile of invariant moment 1 | 1.14 |
| Shape: 5$^{th}$ percentile / 95$^{th}$ percentile of fractal dimension | 1.03 |
| Shape: 5$^{th}$ percentile / 95$^{th}$ percentile of Fourier descriptor 1 | 1.02 |
| Shape: 5$^{th}$ percentile / 95$^{th}$ percentile of Fourier descriptor 4 | 1.04 |
| Shape: 5$^{th}$ percentile / 95$^{th}$ percentile of Fourier descriptor 6 | 0.93 |
| Haralick texture: Standard deviation of average contrast | 0.99 |
| Haralick texture: Mean intensity | 1.00 |
| Haralick texture: Standard deviation of correlation | 0.96 |

Figure 1 - 953

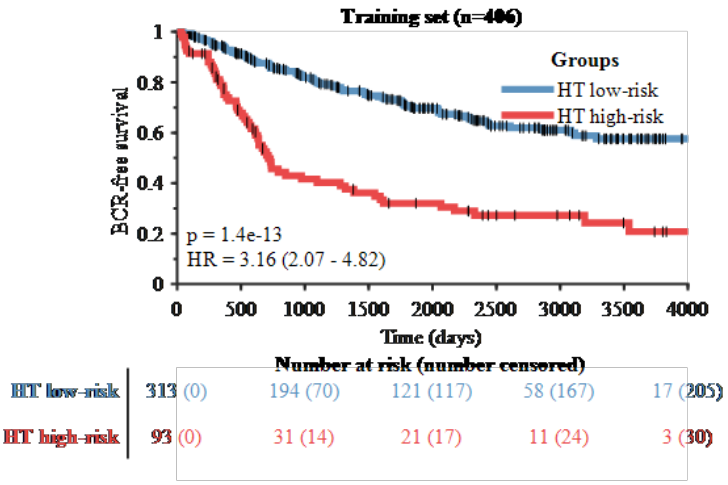


Figure 2 - 953

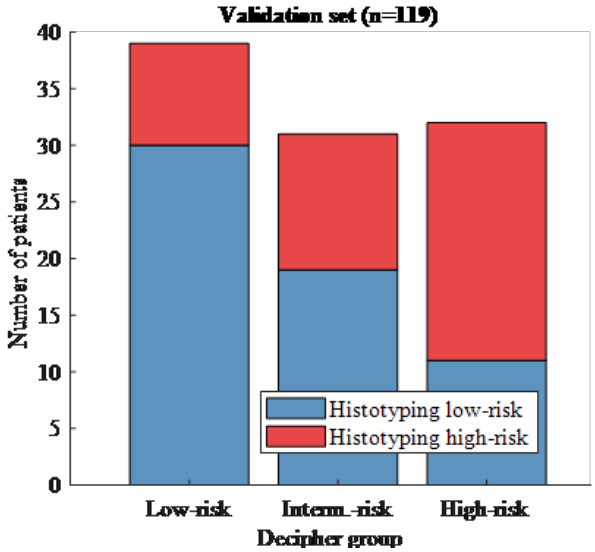


**Conclusions:** A model for BCR prognosis using quantitative features from RP specimens was found to also be correlated with DG. Further work will compare the performance of Histotyping and Decipher in metastasis prognosis.

## 954 A Pilot Study to Determine Expression of SATB2 in Prostatic Adenocarcinoma

Haiyan Li[1], Rugved Pattarkine[1], Kemin Xu[1], Alexandra Budhai[2], Minghao Zhong[1]
*[1]Westchester Medical Center, Valhalla, NY, [2]New York Blood Center, New York, NY*

**Disclosures:** Haiyan Li: None; Rugved Pattarkine: None; Kemin Xu: None; Alexandra Budhai: None; Minghao Zhong: None

**Background:** Special AT-rich sequence-binding protein 2 (SATB2) is a relatively new immunohistochemical (IHC) marker. It is more sensitive and specific than CDX2 for colorectal adenocarcinoma. Previous study shows that CDX2 can be expressed in prostate adenocarcinoma and benign prostate tissue. However, whether SATB2 is expressed in prostate adenocarcinoma remains unknown. In this pilot study our major goal is to address this knowledge gap and determine expression of SATB2 in prostatic adenocarcinoma.

**Design:** One hundred and thirteen (113) prostatectomy specimen with prostatic adenocarcinoma (>10 % by volume) from our institution (2010-2011) were collected to construct tissue microarray (TMA). The TMA slides were subject for IHC staining with antibodies against SATB2 (Cellmarque, EP281) and CDX2 (Cellmarque, EPR2764Y). The SATB2 positive cases on TMA were further subjected to the full section IHC staining for confirmation.

**Results:** Our result shows that in 3 out of 113 (2.7%) cases, tumor cells (two cases with Gleason score 7=3+4, one case with Gleason score 7= 4+3) are positive for SATB2 staining. The staining pattern is nuclear, weak and focal. In contrast, CDX2 staining (tumor cells) is positive in 7 out of 113 (6.2%) cases. SATB2 and CDX2 co-expression is identified only in one case (tumor cells). SATB2 expression is not detected in the benign prostate tissue while CDX2 is positive in the benign prostate tissue for one case (1/113).

Figure 1 - 954

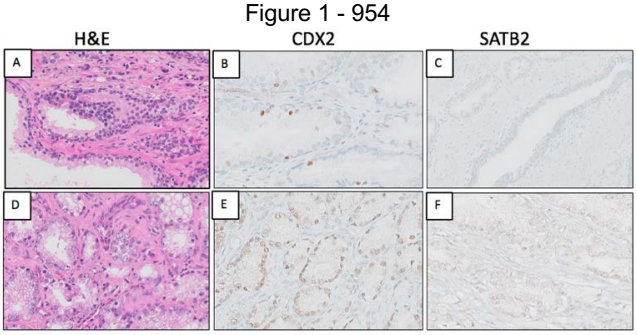


**Figure1. SATB2 and CDX2 expression in prostatic adenocarcinoma**
(A-C) Benign prostatic tissue, focally positive for CDX2 but negative for SATB2. (D-F) Prostatic adenocarcinoma, diffusely positive for CDX2 but negative for SATB2.

Figure 2 - 954

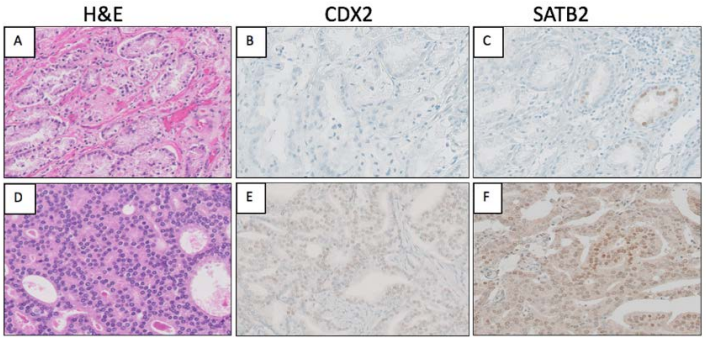


**Figure2. SATB2 and CDX2 expression in prostatic adenocarcinoma (continue)**
(A-C) Prostatic adenocarcinoma, negative for CDX2 but focally weak positive for SATB2. (D-F) Prostatic adenocarcinoma, positive for both CDX2 and SATB2.

**Conclusions:** SATB2 is expressed in a smaller number of prostate adenocarcinoma samples than CDX2, and it is not present in the benign prostate tissue. Moreover, the staining pattern of SATB2 is relatively weak and focal in prostatic adenocarcinoma. Our data support that a subpopulation of prostate adenocarcinoma do exhibit SATB2 staining. Our study indicates that pathologists should be aware of that in rare cases, the prostate cancer can be positive for SATB2.

## 955 Immune Profiles of Invasive Urothelial Carcinoma post Neoadjuvant Therapy and in Positive Lymph Nodes: Parts of the PDL1 Elephant?

Huili Li[1], Qingzhao Zhang[2], Lauren Shuman[1], Matthew Kaag[3], Jay Raman[4], Suzanne Merrill[3], David DeGraff[4], Joshua Warrick[5], Guoli Chen[6]
*[1]Penn State Health Milton S. Hershey Medical Center, Hershey, PA, [2]Penn State Health, Hershey, PA, [3]Penn State College of Medicine, Hershey, PA, [4]Penn State Health Hershey Medical Center, Hershey, PA, [5]Hummelstown, PA, [6]Geisinger Medical Center, Danville, PA*

**Disclosures:** Huili Li: None; Qingzhao Zhang: None; Lauren Shuman: None; Matthew Kaag: None; Jay Raman: None; Suzanne Merrill: None; David DeGraff: None; Joshua Warrick: None; Guoli Chen: None

**Background:** Cisplatin-based neoadjuvant chemotherapy followed by cystectomy is the current standard of care for muscle invasive urothelial carcinoma (MIUC) of the bladder. Unfortunately, even with this treatment, approximately 50% of the patients recur or progress and succumb to metastatic disease. Cisplatin-ineligible and refractory patients carry a higher risk of death. Immune check point inhibitors (ICIs), e.g. anti-PD-L1, offer a new treatment strategy for these patients. Currently, prediction for anti-PD-L1 therapy largely relies on companion diagnostic PD-L1 testing. Thus, assessing expression of PD-L1 and other immune markers in primary lesions following neoadjuvant chemotherapy (NAC) and in metastases in lymph nodes (mLN) are important, which will improve the understanding of PD-L1 landscape for treating cisplatin resistant patients and for selecting patients with metastasis.

**Design:** To simplify study model, we evaluated muscle invasive UC in two separate clinical cohorts via tissue microarray with histologic variants: One set of cases included primary tumors post NAC, and another set of cases was metastatic disease (mLN). The expression levels of PD-L1 (SP142, Ventana) and T lymphocyte markers (CD3, and CD8) were evaluated by immunohistochemistry in a 0-3 scoring system. Overall lymphocytic infiltration was assessed on H&E.

**Results:** We found that CD8 score (but not PD-L1 or CD3) is significantly higher in NAC group compared to untreated ($p$=0.038, Wilcoxon). As to squamous cell variant (SCC) and conventional UC, NAC group appears to be more immune reactive than untreated with increased CD3, CD8 and PD-L1 scores, but with no statistical significance (e.g. $p$=0.07 Wilcoxon in SCC for CD3), probably due to small sample size (e.g. SCC/n=10). In mLN, a similar trend of increased PD-L1 expression is observed in SCC and conventional UC as

compared to metastatic other histologic variants. Interestingly, 18 of 24 mLN with high PD-L1 score show consistently high PD-L1 score in both primary variants and metastasis, while only 3 of 21 mLN with low PD-L1 score show consistency with the primary.

**Conclusions:** In summary, NAC is associated with increased CD8 in UC, which supports immune enhancement effect of chemotherapy. Our finding that SCC and conventional UC with high PD-L1 score appear to preserve their high PD-L1 in mLN provides a new insight to the complicated PDL1 landscape. The variable PD-L1 levels in mLN suggests possible selection of a subset metastatic UC patients who might benefit from ICIs.

## 956 PTEN/ERG/Ki67 Provide Comparable Results as Other Genomic Tests in Risk Stratification of Prostate Cancer

Kirk Lin, Arizona Urology Specialists, Phoenix, AZ

**Disclosures:** Kirk Lin: None

**Background:** PTEN and ERG gene alterations are proven to be associated with poor prognostic outcomes in prostate cancer. Ki67 is a phenotypic expression of tumor cell growth and is associated with progression, metastasis and prognosis in many malignancies. We combined PTEN/ERG gene alterations and Ki67 mitotic index to stratify prostate cancer risk.

**Design:** Prostate cancer diagnosed with biopsies with Gleason Score 6 and 7 were tested for PTEN and ERG using fluorescence in-situ hybridization technique and Ki67 using an immunohistochemical stain. Validations of hemizygous or homozygous deletion in PTEN and ERG gene fusion by delete, split, fusion or amplification were established at P4 Diagnostix. The mitotic rate was expressed at 5% increment and 15-20% was considered significant as validated at our Laboratory. The risk profiles were classified as very low/low, moderate, high/very high. The urologists at our services have options to order other genomic tests such as Prolaris performed at Myriad Genetics and Oncotype DX performed at Genomic Health.

**Results:** From July 2017 to September 2019, a total of 841 cases of prostate cancer had been tested. The age of the patients ranged from 45 to 86 with PSA ranging from 0.9 to 26.7ng/ml. Five hundreds and eighty-five patients had PTEN/ERG/Ki67 tests, 127 patients had Prolaris, and 129 patients had Oncotype DX. Fifteen patients had both PTEN/ERG/Ki67 and Oncotype (or Prolaris) tests for direct comparison. The number of risk profile with very low/low, moderate, high/very high were comparable among these groups as shown in the table. The test failure rate and cost per test were much lower in PTEN/ERG/Ki67.

| Tests | Cases tested /success | Very Low or Low | Moderate | High or Very High | Failure rate | Cost |
|---|---|---|---|---|---|---|
| PTEN/ERG/Ki67 | 585/564 | 335 (59.4%) | 185 (32.8%) | 44 (7.8%) | 19 (32.%) | $800 |
| Prolaris | 127/106 | 60 (56.6%) | 32 (30.2%) | 14 (13.2%) | 21 (16.5%) | $4000 |
| Oncotype DX | 129/111 | 57 (51.4%) | 22 (19.8%) | 32 (28.8%) | 18 (14.0%) | $4000 |

**Conclusions:** Detection of PTEN and ERG gene alterations and Ki67 mitotic index in prostate cancer could not only provide comparable results in cancer risk stratification, but also significantly reduced the cost per test as compared to other genomic tests.

## 957 Molecular Prognostic Testing on Gleason 3+4 Prostate Cancer

Kirk Lin, Arizona Urology Specialists, Phoenix, AZ

**Disclosures:** Kirk Lin: None

**Background:** Selection of patients with Gleason 3+4 cancer for active surveillance is critical in clinical management. Percent Gleason Pattern 4 may provide some useful information. However, the interobserver and intraobserver variability makes it less reliable. Molecular testing is recommended in National Comprehensive Cancer Network (NCCN) guidelines to gauze the risk of prostate cancer. We report our experience of three molecular tests, PTEN/ERG/Ki67, Prolaris and Oncotype DX on Gleason 3+4 cancer.

**Design:** Prostate cancer diagnosed with biopsies with Gleason grades 3+4=7 were tested for at least one of the following tests 1) PTEN/ERG/Ki67, performed at P4 Diagnostix; 2) Prolaris, performed at Myriad Genetics; and 3) Oncotype DX, performed at Genomic Health. The risk profiles were classified as very low/low, moderate, high/very high.

**Results:** From July 2017 to September 2019, a total of 219 cases of Gleason 3+4 prostate cancer had been tested. The age of the patients ranged from 47 to 86 with PSA ranging from 2.5 to 26.7ng/ml. The number of risk profile with very low/low, moderate, high/very high were 67 cases (30.6%), 92 cases (42.0%), and 60 cases (27.4%). The corresponding number of positive cores and longest percent tumor involvement of each risk group are shown in the table.

| Risk Group | Very low or Low | Moderate | High or Very high |
|---|---|---|---|
| # Cases (%) | 30.6% | 42.0% | 27.4% |
| # Positive cores | up to 8 | up to 12 | up to 12 |
| Longest tumor involvement | up to 100% | up to 100% | up to 100% |

**Conclusions:** There is no single best way to select patients for active surveillance. Molecular testing on biopsy tissue provides very useful information. Our results show 30.6% of the patients with Gleason 3+4 cancer are at low risk. If combined with other clinic-pathologic findings, most of these low risk patients can be safely placed in active surveillance program.

## 958 Renal Collision Tumor Composed of Oncocytoma and Mucinous Tubular and Spindle Cell Carcinoma: Characterization of a Perhaps Not-So-Rare Phenomenon

Michelle Lin[1], Elizabeth Jacobi[1], Seema Mullick[2], Jessica Thomas[1], Randall Olsen[3], Jae Ro[1]
*[1]Houston Methodist Hospital, Houston, TX, [2]Methodist Hospital, Sugar Land, TX, [3]Houston, TX*

**Disclosures:** Michelle Lin: None; Elizabeth Jacobi: None; Randall Olsen: None; Jae Ro: None

**Background:** Collision tumors, characterized by two histogenetically distinct neoplasms which develop at the same site, are rare occurrences. Our institution published the first case of a renal collision tumor composed of oncocytoma and mucinous tubular and spindle cell carcinoma (MTSCC) wherein the MTSCC component arose from the centrally scarred portion of the oncocytoma. Here, we describe six additional cases and expand on the clinicopathologic characteristics of this entity.

**Design:** Cases of oncocytomas with grossly identified central scars were selected from our institutional archives for retrospective histologic review. For cases harboring an MTSCC component, immunohistochemical staining was performed with CK7, AMACR, CD117, EMA, and vimentin; and clinical data were obtained from electronic medical records. Next-generation sequencing analysis was performed using the Ion AmpliSeq Cancer Hotspot Panel v2 (ThermoFisher Scientific, Waltham, MA).

**Results:** Seven partial nephrectomy cases, including the index case, were reviewed. The mean age was 66 years, with five male and two female patients. Grossly, the tumors were well-circumscribed tan-brown masses with central fibrotic areas. Microscopically, the tumors displayed nests of oncocytic cells, with the centrally scarred areas showing a variably prominent proliferation of spindle cells and tubules containing mucinous material. The MTSCC components were positive for EMA, vimentin, CK7, and AMACR and were negative for CD117; the oncocytoma components were positive for CD117, variably positive for EMA, and negative for vimentin, CK7, and AMACR. Next-generation sequencing did not detect somatic mutations in either component. All patients are alive and well with no evidence of recurrence or metastasis (mean follow-up 7 months).

Figure 1 - 958

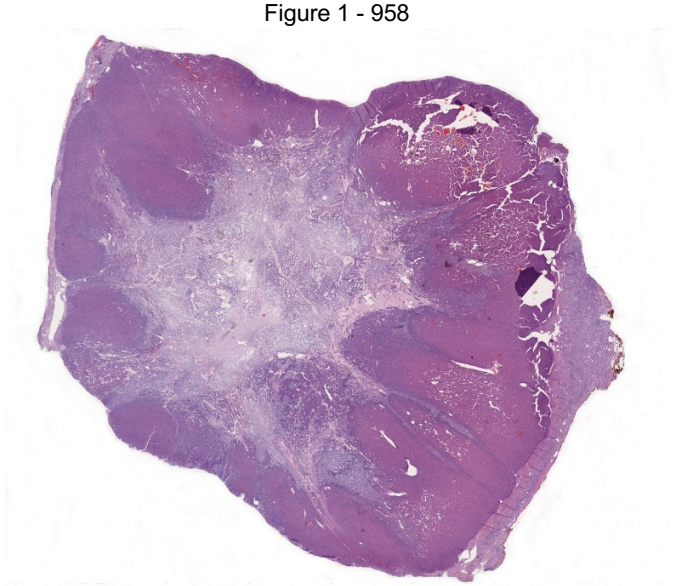

Figure 2 - 958

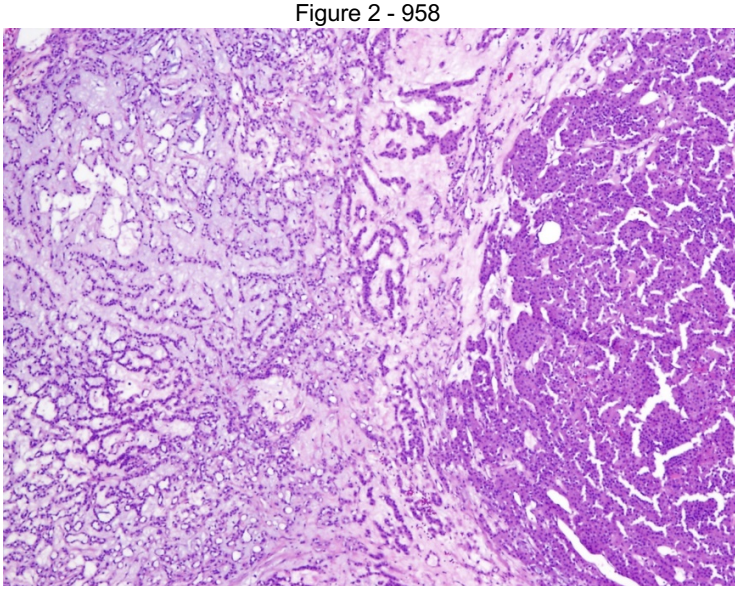

**Conclusions:** Our study provides evidence that renal collision tumors composed of oncocytoma and MTSCC may not be as rare as previously thought. As the MTSCC component was often histologically subtle and overlooked on initial diagnosis, our findings emphasize the need to carefully sample and evaluate the scarred portion of oncocytomas for this component. Our molecular studies did not detect differences in the oncogenic pathways of the two components, suggesting possible derivation from a common progenitor; however, further investigation is required to evaluate this association. While no patients developed recurrence or metastasis, we recommend close follow-up until more cases are accumulated with long-term follow-up.

## 959 The Clinical Prognosis and Mechanistic Study of DDX3X in Renal Cell Carcinoma Progression

Tsung Chieh Lin[1], Yuan Ming Yeh[2], Wen Lang Fan[3]
*[1]Chang Gung Memorial Hospital, Linkou, Taoyuan City, Taiwan, [2]Chang Gung Memorial Hospital, Linkou, Taoyuan, Taiwan, [3]Chang Gung Memorial Hospital, Taoyuan, Taiwan*

**Disclosures:** Tsung Chieh Lin: None; Yuan Ming Yeh: None; Wen Lang Fan: None

**Background:** (Asp-Glu-Ala-Asp) Box Polypeptide 3, X-Linked (DDX3X) is a member of the DEAD-box family of RNA helicases. The function of DDX3X has been uncovered to involve in pre-mRNA splicing, RNA export, transcription, and translation. In cancer, both tumor promoting and suppressing effects of DDX3X have been reported. We previously identified the prognostic significance of DDX3X in colon cancer patients through large cohort survival analysis and further investigated its effects on alleviating cancer progression. However, DDX3X's impacts on renal cell carcinoma (RCC) progression remains obscure.

**Design:** IHC staining was performed to explore the relative DDX3X expression levels in RCC specimens and adjacent normal tissues. Transcriptomics data was retrieved from public database (TCGA and CCLE) to further confirm DDX3X's clinical significances conducted via analysis of medical informatics. Migration and invasion ability of cancer cells were evaluated by transwell assay.

**Results:** In this study, the results reveal that DDX3X level is significantly lower in RCC as compared with adjacent normal tissues. In a large RCC cohort survival analysis, the data indicates DDX3X as a good prognostic biomarker ($P$=0.02), and a multivariate Cox regression analysis further shows DDX3X's statistical independence in predicting patient's survival (Table, $P$=0.029). In addition, cancer patients with low DDX3X expression correlate with frequent distant metastasis status. Our results further show that ectopic overexpression of DDX3X reduces the migration and invasion phenotype in RCC cell line 786-0, 769-P and ACHN. Furthermore, a transcriptome-based analysis of RCC cohort via Ingenuity Pathway Analysis (IPA) suggests the critical inactivation of SPINK1-Metallothionein signaling pathway by DDX3X. High expressions of SPINK1 and Metallothionein isoforms associate with poor survival, and those expression levels are reversely correlated with DDX3X both in RCC cohort (ρ=-0.264, $P$<0.001) and in cancer cell line panel (ρ=-0.534, $P$=0.021, CCLE dataset GSE36133).

| | | Univariate | | Multivariate | |
|---|---|---|---|---|---|
| Variable | Comparison | HR (95% CI) | *P* value | HR (95% CI) | *P* value |
| Gender | F : M | 0.951 (0.694-1.303) | 0.752 | 0.889 (0.564-1.4) | 0.612 |
| Stage | 1-2 : 3-4 | 4.287 (3.089-5.949) | <0.001 | 3.574 (1.672-7.639) | 0.001 |
| T | T1-2 : T3-4 | 2.992 (2.136-4.191) | <0.001 | 0.701 (0.334-1.47) | 0.347 |
| N | N0 : N1 | 2.794 (1.486-5.255) | 0.001 | 1.236 (0.638-2.392) | 0.53 |
| M | M0 : M1 | 4.544 (3.303-6.251) | <0.001 | 2.263 (1.38-3.711) | 0.01 |
| DDX3X | Low : High | 0.589 (0.42-0.826) | 0.002 | 0.583 (0.359-0.946) | 0.029 |

**Conclusions:** In this study, we unravel DDX3X's clinical significance and biological function, suggesting its potentially pivotal role in regulating RCC progression.

## 960 Immune Gene Expression Analysis of Bladder Carcinoma in-situ and Correlation with CK20 Immunohistochemical Staining and Response to BCG Treatment

Kara Lombardo[1], Belkiss Murati Amador[2], Vamsi Parimi (Parini)[3], Bridget McGuire[4], Andres Matoso[1]
*[1]Johns Hopkins Medical Institutions, Baltimore, MD, [2]Johns Hopkins University School of Medicine, Baltimore, MD, [3]Johns Hopkins University School of Medicine, Elkridge, MD, [4]Greenberg Bladder Cancer Institute, Johns Hopkins University School of Medicine, Baltimore, MD*

**Disclosures:** Kara Lombardo: None; Belkiss Murati Amador: None; Vamsi Parimi (Parini): None; Bridget McGuire: None; Andres Matoso: None

**Background:** Carcinoma in-situ (CIS) bears a high risk of progression and standard treatment is intravesical BCG which induces an immune response against tumor cells. Understanding the immune microenvironment could provide clues to specific immunotherapies that could synergize with BCG to improve the response rate.

**Design:** We retrospectively selected 50 cases of bladder CIS. H&E slides were marked, macrodissected in the areas of CIS, and RNA was extracted. Gene expression analysis of 1,409 genes was performed using the HTG EdgeSeq system coupled with NGS. Immunohistochemistry for CK20 was performed in all cases and interpreted positive if there was full thickness staining. Clinical data about treatment and response was obtained through review of medical records.

**Results:** Gene expression data was obtained in 44 cases of CIS, including 28 CK20(+) and 16 CK20(-). The 5 genes most highly expressed in all CIS samples included *CD27*, *COL3A1* and *PRG2*, *NOX1* and *CLCA2*. Comparing CK20(+) versus CK20(-) cases, genes that were most differentially expressed (2 folds difference) included overexpression of *CLCA2*, *CCL19* and *MMP9* and underexpression of *CCL26/27, SIGLEC5*, *CCR10*, *B3GAT1, SERPINE1,* and *HPN.* Thirty-three patients had CIS without concomitant papillary carcinoma, including 20 CK20(+) cases and 13 CK20(-) cases. Within CK20(+) CIS cases, 1 (5%) died of disease, 8 (40%) were alive with disease and 11 (55%) had no evidence of disease at 12 months. Within CK20(-) CIS cases, 1 (8%) died of disease, 3 (23%) were alive with disease, and 9 (69%) had no evidence of disease at 12 months. There were 6 (18%) patients with pure CIS [4 CK20(+), and 2 CK20(-)] who responded to BCG while the rest either progressed or relapsed during follow-up. The genes most expressed in BCG responders included *RPS6, HLA-B, RPL38, RPS19,* and *COL1A2*.

**Conclusions:** Both CK20(+) and CK20(-) CIS cases have similar rates of progression, relapse and response to BCG. We identified a subset of genes that are differentially expressed in these 2 groups which suggest some differences in the immune microenvironment. We identified genes that are most upregulated in patients who responded favorably to BCG which could potentially help to better understand and predict response to therapy.

## 961 Long-Term Oncological Impact of Positive Anterior Surgical Margin after Radical Prostatectomy

Min Lu[1], Shulin Wu[2], Chin-Lee Wu[3]
*[1]Beijing, China, [2]Massachusetts General Hospital, Boston, MA, [3]Massachusetts General Hospital, Newton Center, MA*

**Disclosures:** Min Lu: None; Shulin Wu: None; Chin-Lee Wu: None

**Background:** Positive surgical margin (PSM) has been associated with biochemical recurrence (BCR) after radical prostatectomy (RP) for prostate cancer (PCa). The clinical significance of anterior-predominant PCa (APC) comparing to posterior-predominant PCa (PPC) still remains debatable. The aim of this study is to evaluate the impact of anterior PSM (A-PSM) and posterior PSM (P-PSM) on long-term outcomes after RP including biochemical recurrence (BCR), metastasis and overall mortality.

**Design:** We identified 391 PSM cases after excluding cases with multiple location or cases without information regarding anterior or posterior status from 1993 to 2007 in our hospital. Survival was estimated using the Kaplan-Meier method. Cox proportional hazards regression models were used to analyze the impact of PSM location status on oncological survival.

**Results:** There were 115 cases (29.4%) with Apex-PSM, 257 cases (65.7%) with peripheral PSM and 19 case (4.9%) with bladder neck (BN) PSM. Among the 257 peripheral PSM cases, 58 cases (22.6%) were with A-PSM, 174 cases (67.7%) were with P-PSM, and 25 cases (9.7%) were with both anterior and posterior (AP) PSM. Patients with A-PSM, especially those with low to immediate Gleason score (GS≤7), showed a BCR prognosis similar to those with Apex-PSM. In contrast, patients with P-PSM showed significantly higher BCR risk on both univariate and multivariate analysis when compared to those with Apex-PSM. No impact on metastasis-free survival, or overall survival was observed.

**Conclusions:** Patients with A-PSM had a similar BCR prognosis to those with Apex-PSM which is significantly different from patients with P-PSM. Our findings may help physicians to consider different treatment options including further adjuvant treatment for patients with P-PSM from those with A-PSM.

## 962 Histologic Features Associated with Multiperimetric MRI-Detected Negative Prostatic Targets of Different PI-RADS Scores

Xunda Luo[1], Guangyuan Li[2], Jenny Ross[1], Ximing Yang[3]
*[1]Northwestern University Feinberg School of Medicine, Chicago, IL, [2]Community Healthcare System, Munster, In 46321, Munster, IN, [3]Northwestern University, Chicago, IL*

**Disclosures:** Xunda Luo: None; Guangyuan Li: None; Jenny Ross: None; Ximing Yang: None

**Background:** The use of multiperimetric MRI (mpMRI) in prostatic cancer detection and targeted biopsy has improved diagnostic accuracy of the disease. However, the false positivity introduced by mpMRI has been recognized, which often leads to additional unnecessary biopsies. In this study, we aimed to further characterize the histologic features associated with mpMRI-detected lesions by PI-RADS scores.

**Design:** This prospective study was conducted on patients undergoing mpMRI of the prostate and subsequent systematic (S) and targeted prostate biopsies for PI-RADS3 or higher lesions from December 2018 to August 2019 at the current institution. Correlations between histologic parameters and PI-RADS scores were analyzed with analysis of variance and $X^2$ test.

**Results:** One hundred sixty-nine negative targets (100 PI-RADS3, 62 PI-RADS4, 7 PI-RADS5) and 41 true-positive (TP) targets (9 PI-RADS3, 25 PI-RADS4, 7 PI-RADS5) from 137 patients were included. There was a statistically significant association between PI-RADS scores and tumor volume in TP cores ($F$=7.056, $p$=.002), from 18.9% for PI-RADS3 to 58.6% for PI-RADS5, which indicated that the amount of glandular component played a role in mpMRI target detection of TP targets. Higher grade group lesions were more likely to be found in S cores when TP targets were of low PI-RADS score, with an S-to-target ratio of 6:1 for PI-RADS3 and 7:3 for PI-RADS4. Analyses on negative target cores showed that inflammation, increased stromal and glandular components were top histologic findings in these cores. Inflammation and increased glandular component were more likely associated with PI-RADS3 or 4 (30-35%) than PI-RADS5 (0-14.3%) targets, whereas increased stromal component was more frequently seen in PI-RADS5 lesions (71.4%) than in PI-RADS3 or 4 (37.0-40.3%). Only 1 of 7 negative PI-RADS5 lesions (14.3%) presented with mild acute inflammation, whereas inflammation in PI-RADS3 and 4 lesions were mostly mild-to-moderately chronic/mixed. (Table)

| Parameters | | PI-RADS v2 Category | | | Statistics | |
|---|---|---|---|---|---|---|
| | | 3 | 4 | 5 | | |
| **Total** | | 109 | 87 | 14 | | |
| **Age (years)** | | 64.2±7.1 | 65.2±7.1 | 71.1±6.8 | F=5.964 | p=.003 |
| **TP T-cores N (%)** | | 9 (8.3) | 25 (28.7) | 7 (50.0) | $X^2$=21.781 | p<.001 |
| **Cancer volume in TP target cores (%)** | | 18.9±11.7 | 51.2±28.6 | 58.6±16.8 | F=7.056 | p=.002 |
| **Negative T-cores with positive S-cores N (%)** | | 27 (27.0) | 20 (32.3) | 2 (28.6) | $X^2$=.515 | p=.773 |
| **Negative T-cores with inflammation N (%)** | | 35 (35.0) | 21 (33.9) | 1 (14.3) | $X^2$=4.589 | p=.092 |
| | AI | 0 | 3 | 1 | $X^2$=12.932 | p=.053 |
| | CI | 21 | 12 | 0 | | |
| | ACI | 14 | 6 | 0 | | |
| | 1+ | 21 | 16 | 1 | $X^2$=11.579 | p=.073 |
| | 2+ | 14 | 3 | 0 | | |
| | 3+ | 0 | 2 | 0 | | |
| **Negative T-cores with ↑ stroma N (%)** | | 37 (37.0) | 25 (40.3) | 5 (71.4) | $X^2$=.705 | p=.753 |
| **Negative T-cores with ↑ glands N (%)** | | 30 (30.0) | 20 (32.3) | 0 (0.0) | $X^2$=5.236 | p=.082 |

N: sample size; TP: true-positive; T: target; AI: acute inflammation; CI: chronic inflammation; ACI: acute and chronic inflammation

**Conclusions:** Inflammation, increased stromal and glandular components are common cancer mimics in mpMRI prostate studies. Although the amount of glandular component seems to be the mechanism for mpMRI detection of TP lesions across all PI-RADS scores studied, the histologic features underlying negative lesions differ among PI-RADS groups. In this era of mpMRI, the best clinical practice for prostatic cancer detection should still be systematic with targeted biopsies, especially on patients with lesions of lower PI-RADS scores.

## 963 Post-Radiation Bladder Carcinomas (BCa): Analysis of Clinicopathologic Features Including Molecular Subtypes

Jitin Makker[1], Monish Aron[2], Leslie Ballas[2], Guang-Qian Xiao[3], Shivani Kandukuri[4], Siamak Daneshmand[2], Manju Aron[2]
*[1]Keck Hospital of USC and LAC-USC Medical Center, Los Angeles, CA, [2]Keck School of Medicine of University of Southern California, Los Angeles, CA, [3]Keck Medical Center of USC, Los Angeles, CA, [4]University of Southern California Keck School of Medicine, Los Angeles, CA*

**Disclosures:** Jitin Makker: None; Monish Aron: None; Leslie Ballas: None; Guang-Qian Xiao: None; Shivani Kandukuri: None; Siamak Daneshmand: None; Manju Aron: None

**Background:** Radiotherapy is a known risk factor for secondary malignancies within the radiation field. However, the clinical, pathologic and molecular features of secondary BCa following radiotherapy to the prostate or other pelvic malignancies has not been well characterized.

**Design:** Our cystectomy database was queried for patients who had pelvic radiotherapy prior to cystectomy (2000-2019). Pertinent clinical and pathologic findings were noted. Individual slides of invasive high-grade (HG) urothelial carcinoma (UCa) with available blocks were stained with GATA3 and CK5/6 and classified as luminal (LS; GATA3+/ CK 5/6 -) or basal (BS; GATA3-/CK 5/6 +). A positive cut off of > 20% staining as previously reported was used to subtype these tumors.

**Results:** 55 patients met inclusion criteria (3% of 1755 cases). 87% (48) were males and 13% (7) females, ranging in age from 62 - 90 years (mean: 74.9 years). The median time interval between radiation and cancer development was 8.25 years (2.4 - 43 years). 39 patients had external beam radiation,11 had brachytherapy, and 5 had both. The indication for radiation was prostate cancer in males and gynecologic malignancies in females. The tumor was located in the lateral wall in 35%, posterior wall in 24%, trigone/bladder neck in 23%, and dome in 11%. BCa location was unavailable in 5 cases.

98% (54/55) had UCa, with squamous cell carcinoma in 1 case. 96% (52/54) were HGUCa, with invasion in 83% (43), of which 50% (26) showed extravesical spread. 47% of the invasive HGUCa were conventional, 28% had divergent differentiation (DD), and 25% had variant histology(Figure1). Immunohistochemical stains(IHC) were performed in 25 cases of invasive HGUCa (Table1). In 72% cases accurate classification was possible. 52% cases including 80% conventional UC and all cases of micropapillary, clear cell and plasmacytoid variant showed LS. One case each of small cell carcinoma and rhabddoid UCa were negative for both markers. Of the 10 cases with DD, only 60% could be classified as either LS or BS.

**Table 1:** Immunohistological characterization into molecular subtypes (n=25)

| Histologic subtype | n | CK5/6+ GATA3- | CK5/6- GATA3+ | CK5/6+ GATA3+ | CK5/6- GATA3- | Molecular subtype |
|---|---|---|---|---|---|---|
| Conventional | 5 | - | 4/5 (80%) | 1/5 (20%) | - | LS |
| Variant | | | | | | |
| Micropapillary | 3 | - | 3/3 (100) | - | - | LS |
| Plasmacytoid | 1 | - | 1/1 (100%) | - | - | LS |
| Small cell | 1 | - | - | - | 1/1 (100%) | Unclassifiable |
| Clear cell | 1 | - | 1/1 (100%) | - | - | LS |
| Rhabdoid | 1 | - | - | - | 1/1 (100%) | Unclassifiable |
| Sarcomatoid | 3 | 2/3 (66.7%) | 1/3 (33.3%) | - | - | LS; BS |
| Divergent Differentiation | | | | | | |
| Squamous | 8 | 3/8 (37.5%) | 3/8 (37.5) | | 2/8 (25%) | LS; BS |
| Glandular | 2 | | | 1/2 (50%) | 1/2 (50%) | Unclassifiable |

Figure 1 - 963

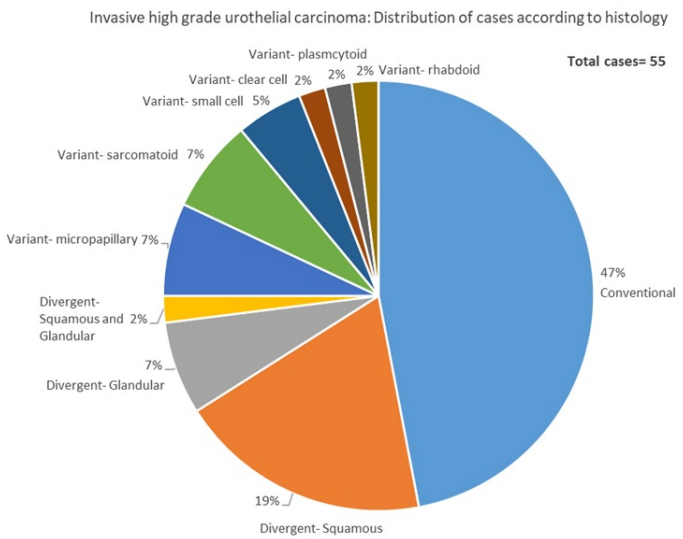

**Conclusions:** UCa are the most common cancers of the bladder in the post radiation setting with 50% showing extravesical spread. More than half of the UCa (53%) show divergent differentiation or variant histology. GATA3 and CK 5/6 are discriminatory in the molecular subtyping of a majority (72%) of UCa in the post-radiation setting, but could classify only 60% of cases of divergent differentiation; a possible reflection of the molecular heterogeneity of this subtype of UCa.

## 964 INSL3 is a Specific Biomarker for Leydig Cells, Leydig Cell Hyperplasia and Leydig Cell Tumors

Renuka Malenie[1], Jianhui Shi[1], Fan Lin[1], Patricia Kim[1], Haiyan Liu[1]
*[1]Geisinger Medical Center, Danville, PA*

**Disclosures:** Renuka Malenie: None; Jianhui Shi: None; Fan Lin: None; Patricia Kim: None; Haiyan Liu: None

**Background:** Insulin-like 3 (INSL3) is a peptide hormone, produced exclusively by Leydig cells in testis, and is responsible for the physiological testicular descent during embryonic development. There are few published studies investigating the expression pattern of INSL3 by immunohistochemistry (IHC) in normal Leydig cell, Leydig cell tumor (LCT) and hyperplasia (LCH). The current study investigated further to explore INSL3 expression by IHC in a series of Sex cord-stromal tumors (SCST), germ cell tumors (GCT) and normal (NL) tissues of ovary and testis, to assess the diagnostic utility of INSL3.

**Design:** Immunohistochemical evaluation of INSL3 (EPR20739, Abcam) was performed on tissue and tissue microarray (TMA) sections of 56 SCSTs, including ovarian fibroma/thecoma/fibrothecoma (23), Sertoli cell (2) and granulosa cell (13) tumors, ovarian LCT (5), and testicular LCT/LCH (13), 70 cases of testicular GCTs and 76 NL tissues of ovary (43) and testicle (33). The staining intensity was recorded as strong (S) or weak (W); staining distribution was graded as negative (<5% cell staining), 1+ (5-25%), 2+ (25-50%), 3+ (50-75%), and 4+ (>75%).

**Results:** The staining results are summarized in Table 1. INSL3 expression was observed in 100% (13/13) of testicular LCT/LCH (Fig.1), 80% (4/5) of ovarian LCTs, and Leydig cells in normal testicular stroma (33/33) (Fig.2), with the majority (72%, 36/50) being strong and diffuse. The staining intensity is strongest in Leydig cells of the normal testicle. INSL3 expression was not observed in GCTs (70) and other SCSTs including Sertoli cell tumor (2), granulosa cell tumor (13) and fibroma/thecoma/fibrothecoma (23).

| Tissue (N) | 1+ W/S | 2+ W/S | 3+ W/S | 4+ W/S | Pos.% (N) |
|---|---|---|---|---|---|
| TS, Ovarian LCT (5) | 0 | 0/1 | 0/3 | 0 | 80% (4/5) |
| Testicular LCT/LCH (13):<br><br>TS (3); TMA (10) | 0/1 | 0/4 | 3/5 | 0 | 100% (13/13) |
| TMA, Testicular GCT (70)<br><br>Mixed GCT (29)<br><br>Seminoma (25)<br><br>Yolk sac tumor (7)<br><br>Embryonal CA (9) | 0 | 0 | 0 | 0 | 0% (0/70) |
| TS, Granulosa Cell Tumor (10) and Mets (3) | 0 | 0 | 0 | 0 | 0% (0/13) |
| TS, Sertoli cell tumor/nodule (2) | 0 | 0 | 0 | 0 | 0% (0/2) |
| TS, Fibroma/Thecoma/Fibrothecoma (23) | 0 | 0 | 0 | 0 | 0% (0/23) |
| NL Testicle (33)<br><br>TS (4); TMA (29) | 0 | 1/1 | 2/7 | 1/21 | 100% (33/33) |
| NL Ovary (43)<br><br>TS (23); TMA (20) | 0 | 0 | 0 | 0 | 0% (0/43) |

Mets: metastasis; TS: tissue section.

Figure 1 - 964

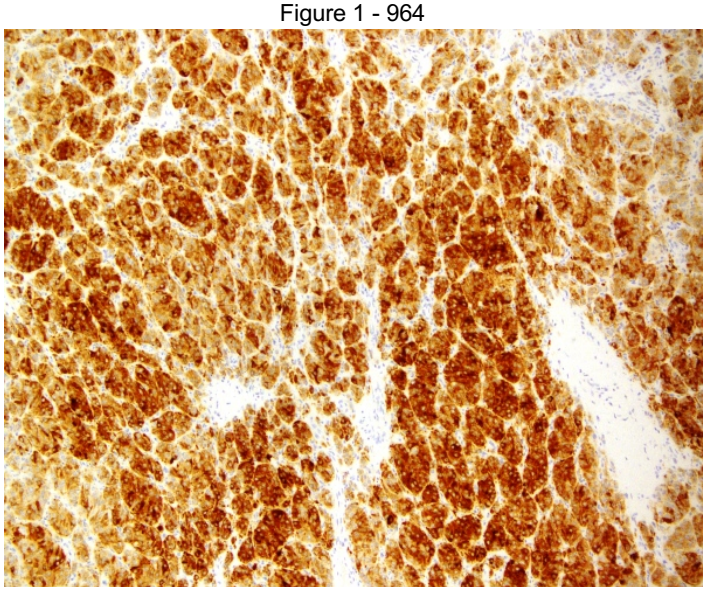

Figure 2 - 964

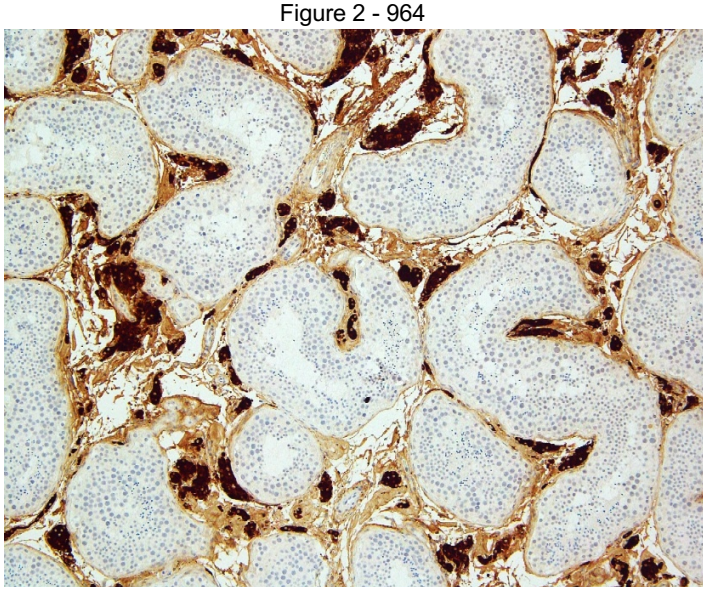

**Conclusions:** Our data demonstrated that INSL3 expression was only observed in NL Leydig cells, LCH and LCTs within the SCST group (total 56, 38 excluding LCT/LCH) and various GCTs of the testicle (70); therefore, INSL3 is a sensitive (98%, 50/51) and specific (100%, 0/108) marker for Leydig cell and LCT/LCH, can be used as a Leydig cell specific marker in distinguishing testicular and ovarian tumors.

## 965 3D Open-Top Light-Sheet (OTLS) Fluorescence Microscopy of Entire Prostate Core Biopsies Improves Diagnostic Accuracy

James Malleis[1], Adam Glaser[1], Soyoung Kang[1], Kaylene Pang[2], Lawrence True[3], Jonathan Liu[1], Nicholas Reder[1]
*[1]University of Washington, Seattle, WA, [2]University of Washington, Bellevue, WA, [3]University of Washington Medical Center, Seattle, WA*

**Disclosures:** James Malleis: None; Adam Glaser: *Consultant*, LightSpeed Microscopy; Soyoung Kang: None; Kaylene Pang: None; Lawrence True: *Stock Ownership*, Lightspeed Microscopy, Inc.; Jonathan Liu: *Stock Ownership*, LightSpeed Microscopy Inc.; Nicholas Reder: *Employee*, Lightspeed Microscopy, Inc.

**Background:** The distinction between Grade Group 1 (GG1) and GG2 prostate carcinoma is crucial for patient management. However, there is high variability among pathologists in distinguishing GG1 from GG2. Traditional H&E-stained 2D sections provide a static impression of this architecture, thus are limited in demonstrating the evolving 3D structure of these glands. Tangential sections of well-formed (GG1) cancer glands may lead to improper classification. In addition, foci of higher-grade cancer may be missed due to the limited sampling of traditional sections. We hypothesized that visualizing entire core biopsies in 3D would improve accuracy in diagnosis and grading.

**Design:** Ex vivo core needle prostate biopsies taken from radical prostatectomy specimens were clarified and stained with nuclear (TO-PRO3) and cytoplasmic (eosin) stains. A custom-built open-top light sheet (OTLS) microscope imaged the biopsies. These images were reconstructed in 3D and analyzed using the BigStitcher plug-in ImageJ. The entire thickness of the biopsy (~1-mm in diameter) was visualized, diagnosed, and graded in 100-micron increments of depth. A diagnosis and grade was assigned to each 100-micron thick volume of the biopsy, and differences between the 100-micron volumes within each biopsy were compared.

**Results:** 44 prostate needle core biopsies were examined. Clarification and staining required 24-48 hours, and imaging/data processing required 45 minutes for each biopsy. There were differences in diagnosis in 6/44 biopsies (14%). All differences in diagnosis resulted from deeper “virtual” sections showing carcinoma, though the superficial levels were benign. There were grading differences in 5/44 biopsies (11%). Of these cores with variable grade through the depth of the biopsy, the most common discrepancy was increased gland complexity distinguishing Gleason patterns 3 from 4. Intraductal carcinoma in an otherwise benign biopsy was identified in 1 core. Foci suspicious for lymphovascular invasion were identified in 3 cores.

**Conclusions:** Our findings suggest that 3D microscopy aids in the sampling and accurate grading and diagnosis of prostatic adenocarcinoma. In some cases, it was difficult to decipher subtle morphologic features that would aid in diagnosis/grading using OTLS images. Although technical improvements in staining, clearing, and imaging are needed, this pilot study shows the potential of 3D OTLS to enable improved prostate cancer diagnosis and grading.

## 966 Assessment of L1 Cell Adhesion Molecule (L1CAM) and Protein (2SC) Succination Immunohistochemical Profiles in Hereditary Leiomyomatosis and Renal Cell Carcinoma-Associated Renal Cell Carcinoma and Other Renal Subtypes

Rahul Mannan[1], Xiaoming (Mindy) Wang[2], Anya Chinnaiyan[3], Roshni Rangaswamy[4], Pankaj Vats[2], Yuping Zhang[3], Sathiya Pandi Narayanan[5], Aaron Udager[6], Fengyun Su[2], Xuhong Cao[2], Mahul Amin[7], Steven Smith[8], Kiril Trpkov[9], Jesse McKenney[10], Adeboye O. Osunkoya[11], Arul Chinnaiyan[12], Saravana Dhanasekaran[2], Rohit Mehra[2]

*[1]Michigan Medicine, University of Michigan, Ann Arbor, MI, [2]University of Michigan, Ann Arbor, MI, [3]Michigan Center for Translational Pathology, Ann Arbor, MI, [4]Michigan Center for Translational Pathology, Ypsilanti, MI, [5]University of Michigan Hospitals, Ann Arbor, MI, [6]University of Michigan Medical School, Ann Arbor, MI, [7]Methodist University Hospital, Memphis, TN, [8]Virginia Commonwealth University School of Medicine, Richmond, VA, [9]University of Calgary, Calgary, AB, [10]Cleveland Clinic, Cleveland, OH, [11]Emory University, Atlanta, GA, [12]Plymouth, MI*

**Disclosures:** Rahul Mannan: None; Xiaoming (Mindy) Wang: None; Anya Chinnaiyan: None; Roshni Rangaswamy: None; Pankaj Vats: None; Yuping Zhang: None; Sathiya Pandi Narayanan: None; Aaron Udager: None; Fengyun Su: None; Xuhong Cao: None; Mahul Amin: *Consultant*, Urogen; *Consultant*, Advanced Clinical; *Advisory Board Member*, Cell Max; *Advisory Board Member*, Precipio Diagnostics; Steven Smith: *Consultant*, Elsevier Publishing/Amirsys; Kiril Trpkov: None; Jesse McKenney: None; Adeboye O. Osunkoya: None; Arul Chinnaiyan: None; Saravana Dhanasekaran: None; Rohit Mehra: None

**Background:** Patients with hereditary leiomyomatosis and renal cell carcinoma- associated renal cell carcinoma (HLRCC- associated RCC) demonstrate germ-line *FH* gene mutation and increased susceptibility for leiomyomatosis. Apart from the known FH bi-allelic loss (with established clinical use of negative anti-FH antibody staining), details on genomic aberrations or additional biomarkers of this disease are not well characterized. We analyzed RCC data by next generation RNA sequencing (RNAseq) to identify and validate possible novel HLRCC-associated RCC biomarkers.

**Design:** RNAseq data from major RCC subtypes such as clear cell, papillary, and chromophobe RCC from TCGA and rare RCC subtypes were assembled to generate a pan-RCC transcriptomic dataset from more than 1000 RCC patients. Differential expression analysis identified L1CAM among the top 3 biomarkers of HLRCC-associated RCC. The FH deficiency in HLRCC- associated RCC leads to fumarate and succinate accumulation and both these TCA cycle intermediates are considered as oncometabolites. Succinate accumulation leads to the covalent modification of cysteine residues to S-(2- succinyl) cysteine (2SC) in several target proteins (termed protein succination). In this study we performed immunohistochemical (IHC) assessment of L1CAM and 2SC staining (using a new commercial anti-2SC antibody) on a RCC cohort for expression and localization. The 131 cases studied are detailed in the Table-1. Crucial control tissues such as paraganglioma (as positive control for L1CAM), normal kidney and HLRCC derived cell line, UOK262 pellet were also included.

**Results:** L1CAM demonstrated diffuse strong membranous expression in all HLRCC-associated RCC. The IHC expression of L1CAM was also focal/patchy in a small subset of cases from other RCC subtypes. Regarding 2SC, IHC showed diffuse nuclear and cytoplasmic expression in HLRCC-associated RCC cases, but also a limited to variable cytoplasmic expression in a small subset of other RCC subtypes. Among non-HLRCC cases that showed positivity with these two antibodies, staining was commonly mutually exclusive. (Table-1)

**Table-1:** Summary of comparative assessment of L1CAM and 2SC in the study cohort

| | L1CAM+/2SC+ | L1CAM+/2SC- | L1CAM-/2SC+ | L1CAM-/2SC- |
|---|---|---|---|---|
| ***Primary RCC Subtypes*** | | | | |
| **HLRCC[a]** | 9 | 0 | 0 | 0 |
| **CCRCC[b]** | 0 | 0 | 0 | 18 |
| **CHRCC[c]** | 2 | 3 | 2 | 13 |
| **EoCHRCC[d]** | 2 | 1 | 0 | 7 |
| **PRCC-1[e]** | 1 | 3 | 0 | 5 |
| **TRCC[f]** | 1 | 0 | 2 | 1 |
| **Oncocytoma** | 0 | 0 | 3 | 2 |
| **MTSCC[g]** | 1 | 1 | 0 | 4 |
| **CCPRCC[h]** | 0 | 2 | 0 | 3 |
| **PRCC-2[i]** | 0 | 1 | 0 | 1 |
| **Oncocytic-U[j]** | 0 | 0 | 0 | 5 |
| **RCC-U[k]** | 0 | 4 | 0 | 2 |
| ***Metastatic RCC Subtypes*** | | | | |
| **mCCRCC[l]** | 0 | 0 | 0 | 14 |
| **mCHRCC[m]** | 0 | 0 | 0 | 5 |
| **mPRCC-2[n]** | 0 | 1 | 0 | 0 |
| **mRCC-U[o]** | 0 | 2 | 0 | 2 |
| ***Miscellaneous*** | | | | |
| **PGPC[p]** | 2 | 0 | 0 | 0 |
| **Kidney (N)[q]** | 0 | 0 | 0 | 5 |
| **Cell Pellet[r]** | 1 | 0 | 0 | 0 |
| **Total** | 19 | 18 | 7 | 87 |

a-HLRCC-associated RCC; b-Clear cell RCC; c-Chromophobe RCC; d-Eosinophilic RCC; e-Papillary RCC-Type-1; f- MiT Translocation RCC; g- Mucinous tubular spindle cell carcinoma; h-Clear cell papillary RCC; i-Papillary RCC-Type 2; j-Oncocytic-unclassified; k-RCC-unclassified; l-Metastatic clear cell RCC; m-Metastatic Chromophobe RCC; n-Metastatic Papillary RCC; o-Metastatic RCC-Unclassified; p-Paraganglioma; q-Normal kidney;r-Cell pellet from HLRCC specific cell line UK0262

**Conclusions:** We observed strong membranous and cytoplasmic L1CAM expression in all HLRCC- associated RCC in our cohort. Nuclear and cytoplasmic expression of 2SC was also seen in all HLRCC- associated RCC. The reason for the expression of L1CAM and 2SC staining in a subset of other RCC subtypes remains to be further investigated, but possibly suggests a metabolic TCA cycle stress in these cases.

## 967 SPOP Mutated, MSI Positive and High TMB Prostate Carcinomas are Significantly Associates to Higher PDL-1 Expression

Maurizio Martini[1], Marco Dell'Aquila[1], Francesco Pierconti[1], Tonia Cenci[2], Sara Capodimonti[3], Luigi Maria Larocca[4]
*[1]Catholic University of Sacred Heart, Rome, Italy, [2]Catholic University, Roma, [3]Catholic University, Roma, Italy, [4]Fondazione Policlinico Universitario A. Gemelli, Rome, Italy*

**Disclosures:** Maurizio Martini: None; Marco Dell'Aquila: None; Francesco Pierconti: None; Tonia Cenci: None; Sara Capodimonti: None; Luigi Maria Larocca: None

**Background:** Despite the promising introduction of anti-PDL-1 therapy in advanced stage of prostate cancer it was reported limited success suggesting the need to improve the patient selection and to define the mechanisms of response. Recent molecular profiling studies identify a specific prostate carcinoma sub-type with inactivating SPOP gene mutation (prevalence of 6-15%). SPOP is a cullin-based E3 ubiquitin ligase that has a central role in the degradation of several proteins, and its inactivating mutations determine a significant upregulation of PDL-1 expression in neoplastic cells. In this study we investigate the SPOP mutations, the MSI and TMB in a cohort of prostate carcinoma patients, correlating our results with PDL-1 expression, with clinical and pathological features.

**Design:** We retrospectively selected 153 prostate cancer cohort, including a subset of 35 metastatic patients. We evaluated the PDL-1 expression with immunohistochemistry (anti-PDL-1 antibody, 22C3) using the TPS score (PDL-1 expression cutt-off≥ 1). We searched for SPOP mutations using an exone-sequencing. We also performed the MMR and the MSI analysis with immunohistochemistry and with EasyPGX® ready MSI kit (Diatech, Jesi, Italy) and analyzed the TMB using a TruSight Oncology 500 kit (Illumina, Milan, Italy).

**Results:** We found positive expression of PDL-1 in 21 out 153 samples (13,72%) and a significant association with metastatic disease (9 out 35 in metastatic and 12 out 118 non metastatic patients, p=0.0263) and high Gleason grade (16 out 55 with Gleason grade group of 4-5 versus 5 out 98 Gleason grade group of 2-3, p=0.0007). SPOP missense mutations with functional alteration were identified in 14 out 153 samples (9,15%): 12 samples had an exone 6 mutation and 2 had the exone 5 mutation. Six out 14 SPOP mutated samples showed a higher PDL-1 expression (p=0.0005) and a significant association with high Gleason grade group (12 out 55; p=0.0004). We also found that 4 patients had MSI positive phenotype (2,6%), while 5 cases had a high TMN (all MSI positive cases and one with MSI negative patient). Four out 5 patients with MSI positive or high TMB had a higher PDL-1 expression (p=0.0023) and a significant association with the high Gleason grade group (5 out 55; p=0.0073).

**Conclusions:** SPOP mutations and high TMB could be involved in the high PDL-1 expression of the prostate tumor, representing a possible and useful markers in the selection of prostate cancer patients who candidates for the immunotherapy.

## 968 Association of KIT Mutations with Concurrent RAS/MAPK Pathway Driver Alterations in Seminomatous and Non-Seminomatous Germ-Cell Tumors

Douglas Mata[1], Soo-Ryum Yang[1], Donna Ferguson[1], Ying Liu[1], Rohit Sharma[1], Hikmat Al-Ahmadie[1], David Solit[1], Darren Feldman[1], Satish Tickoo[1], Victor Reuter[1], Maria Arcila[1], Marc Ladanyi[1], Chad Vanderbilt[2]
*[1]Memorial Sloan Kettering Cancer Center, New York, NY, [2]Memorial Sloan Kettering Cancer Center, Denver, CO*

**Disclosures:** Douglas Mata: None; Soo-Ryum Yang: *Consultant*, Invitae; Donna Ferguson: None; Ying Liu: None; Rohit Sharma: None; Hikmat Al-Ahmadie: None; David Solit: *Consultant*, Pfizer; *Consultant*, Loxo Oncology; *Consultant*, Lilly Oncology; *Consultant*, Vivideon Oncology; *Consultant*, Illumina; Darren Feldman: None; Satish Tickoo: None; Victor Reuter: None; Maria Arcila: *Speaker*, biocartis; *Speaker*, Invivoscribe; Marc Ladanyi: None; Chad Vanderbilt: *Consultant*, Docdoc. ltd. (Singapore); *Consultant*, Paige AI; *Consultant*, OncoKB

**Background:** A subset of seminomatous and non-seminomatous GCTs (SGCT/NSGCTs) is defined by activating *KIT* mutations. Such mutations have potential therapeutic relevance in other solid tumors, as patients with *KIT*-mutant GISTs experience durable clinical benefit from TKIs. However, despite case reports of successful imatinib treatment in *KIT*-expressing, chemotherapy-refractory GCTs, clinical trials have been negative. This lack of efficacy has not been rigorously explored by considering underlying genomic alterations. Herein, we report on the mutational profile and clinical outcomes of a cohort of patients with *KIT*-mutated GCTs.

**Design:** Retrospective cohort study of all patients with *KIT*-mutant GCTs sequenced at this institution between March 2014 and August 2019. Tumors were assessed with a hybrid capture-based DNA NGS assay for targeted sequencing of up to 468 key cancer genes.

**Results:** Among 576 patients with GCTs, 5.9% (n = 34) had somatic *KIT* mutations, including 25 men with testicular GCTs, 7 men with mediastinal GCTs, and 2 women with ovarian dysgerminomas (Fig. 1). Among the 34 cases, 32 had 1, 1 had 2, and 1 had 3 *KIT* mutations. Exons 17 (64.9% [24/37]) and 11 (18.9% [7/37]) were most commonly affected (Table, Fig. 2). Overall, 95.1% (39/41) were curated in OncoKB as likely oncogenic mutations that may respond to TKIs in other tumor types. The most frequently mutated codons were D816 and N822 in 10 and 9 cases, respectively. *KRAS* was concurrently mutated in 8 cases and *NRAS* in 2. Copy-number gains in 12p (including *KRAS*, among other genes) were seen in 14 cases, supporting the presence of isochromosome 12p. No cases harbored additional RAS/MAPK pathway alterations (*e.g.*, mutations in *BRAF*, *HRAS*, *NF1*, or *MAP2K1/2*). In all, 76.5% (26/34) of patients had metastasis at any point and 94.1% (32/34) received chemotherapy. None received TKIs. At follow up, 85.3% (29/34) were free of disease, 8.8% (3/34) had disease, and 5.9% (2/34) had died due to disease.

| Type | N | Exon | Position | cDNA | Amino Acid |
|---|---|---|---|---|---|
| SGCT | 1 | 8 | 55589773 | c.1255G>A | p.D419N |
| SGCT | 1 | 9 | 55592202 | c.1526A>T | p.K509I |
| SGCT | 1 | 11 | 55593604 | c.1670G>C | p.W557S |
| SGCT | 1 | 11 | 55593649 | c.1715A>G | p.D572G |
| SGCT | 1 | 11 | 55593655 | c.1724_1726delACA | p.Q575del |
| SGCT | 3 | 11 | 55593661 | c.1727T>C | p.L576P |
| SGCT | 1 | 13 | 55594221 | c.1924A>C | p.K642Q |
| SGCT | 1 | 13 | 55594262 | c.1965T>G | p.N655K |
| SGCT | 1 | 17 | 55599320 | c.2446G>C | p.D816H |
| SGCT | 1 | 17 | 55599320 | c.2446G>T | p.D816Y |
| SGCT | 1 | 17 | 55599321 | c.2447A>C | p.D816A |
| SGCT | 4 | 17 | 55599321 | c.2447A>T | p.D816V |
| SGCT | 1 | 17 | 55599333 | c.2459A>G | p.D820G |
| SGCT | 1 | 17 | 55599333 | c.2459A>T | p.D820V |
| SGCT | 1 | 17 | 55599338 | c.2467_2469delTAT | p.Y823del |
| SGCT | 2 | 17 | 55599338 | c.2464A>T | p.N822Y |
| SGCT | 1 | 17 | 55599340 | c.2466T>A | p.N822K |
| SGCT | 3 | 17 | 55599340 | c.2466T>G | p.N822K |
| SGCT | 3 | 17 | 55599340 | c.2466T>A | p.N822K |
| SGCT | 1 | 17 | 55599341 | c.2467T>G | p.Y823D |
| SGCT | 1 | 17 | 55599342 | c.2468A>G | p.Y823C |
| SGCT | 1 | 18 | 55602664 | c.2485G>C | p.A829P |
| SGCT | 1 | 19 | 55602886 | c.2598_2603dupAAGCAG | p.S867_S868insRS |
| NSGCT | 1 | 11 | 55593603 | c.1669T>C | p.W557R |
| NSGCT | 3 | 17 | 55599321 | c.2447A>T | p.D816V |
| NSGCT | 2 | 17 | 55599338 | c.2464A>T | p.N822Y |
| NSGCT | 1 | 17 | 55599340 | c.2466T>G | p.N822K |

Figure 1 - 968

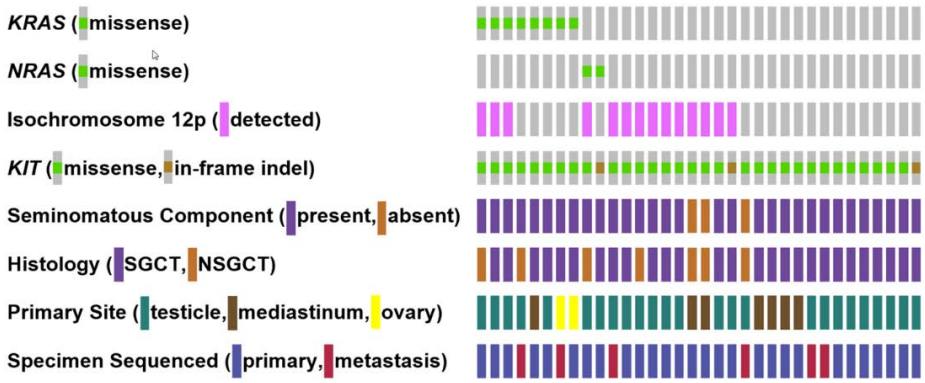


Figure 2 - 968

**Conclusions:** NGS analysis of GCTs can uncover TKI-responsive *KIT* mutations and associated genomic alterations. Approximately one third of *KIT*-mutated GCTs also harbor *KRAS* or *NRAS* mutations, which may explain the lack of efficacy of TKIs in many patients. TKIs may benefit patients with *KIT*-mutated GCTs without RAS/MAPK alterations. Alternately, dual MEK/KIT inhibitor therapy in *KIT*-mutated GCTs with concurrent RAS/MAPK alterations may be a plausible therapeutic strategy.

## 969 Clinical Trajectory of Prostatic Carcinoma with Aberrant Expression of P63 (PCAEP) on Active Surveillance: A Series of 6 Cases

Isaac McCool[1], Isabell Sesterhenn[2], Allen Burke[3], Adina Paulk[2]
*[1]Bethesda, MD, [2]Joint Pathology Center, Silver Spring, MD, [3]University of Maryland, Baltimore, MD*

**Disclosures:** Isaac McCool: None; Isabell Sesterhenn: None; Allen Burke: None; Adina Paulk: None

**Background:** PCAEP is a rare subtype of carcinoma which has shown a low-grade behavior in studies of prostatectomy specimens and is molecularly distinct from conventional prostatic adenocarcinoma. No study has described the clinical trajectory of PCAEP in patients who underwent active surveillance.

**Design:** We retrospectively identified 6 cases of PCAEP between 2011-2016 and recorded clinical features using electronic medical records. Slides and immunohistochemical studies were reviewed.

**Results:** Demographic data of the 6 patients are detailed in Table 1. 5/6 patients are alive at most recent follow up, with 1 patient deceased of unrelated causes. 5/6 patients are without subsequent genitourinary or other malignancies. 1 patient developed muscle-invasive urothelial carcinoma. 2/6 patients showed only PCAEP on biopsy; these patients did not show progression of disease on active surveillance. 3/5 patients showed progression of conventional prostatic carcinoma on active surveillance [grade group (GG)2 carcinoma in <5% of 1 core at 15 months post-diagnosis; GG2 carcinoma in 2 cores with seminal vesicle invasion at 10 months post-diagnosis; and GG1 carcinoma involving 5 cores at 3 months post-diagnosis] leading to definitive treatment (RP, n=1, radiation, n=2). No patients developed castration-resistant disease or GG3/higher disease (median follow up 55 months). 1 case illustrated lymphovascular space invasion by the PCAEP (Figure 1). Of note, 3/4 cases where ER-a immunostaining was performed showed at least focal expression (Figure 2).

**Table 1:** Demographic and clinical data of patients with PCAEP on active surveillance

| Study # | Age at Diagnosis (years), Race | Total Follow Up Time (months) | p63+ Tumor Location on Biopsy | ER IHC Staining | Association with Usual Prostatic Carcinoma/Grade Group on biopsy | Clinical Follow Up |
|---|---|---|---|---|---|---|
| **1** | 52, AA | 64.6 | Right base | N/A | No | Patient on surveillance. No susequent positive biopsies or evidence of progression of disease at last follow up. |
| **2** | 84, CA | 79.7 | Left base | Positive | Yes, GG2 and GG1 | Patient treated wtih Leuprolide 8 months after diagnosis. Patient developed muscle-invasive urothelial carcinoma. Dead of unrelated causes at 79.7 months following diagnosis. |
| **3** | 57, AA | 47.9 | Left apex | Focally positive | Yes, GG2 | 15 months after diagnosis, found to have GG2 on surveillance biopsy. Underwent radical prostatectomy which showed GG2 carcinoma involvinmg <5% of prostate. Patient without evidence of recurrence. |
| **4** | 67, AA | 57.2 | Left base | Negative | Yes, GG1 | 24 months after diagnosis, surveillance biopsy showed GG2 prostatic carcinoma. Patient was treated with Elegard anti-androgen therapy and radiation. Patient currently without evidence of recurrence at last follow up. |
| **5** | 73, AA | 76.3 | Left base | N/A | Yes, GG1 | Patient treated with radiation therapy at 13 months post diagnosis due to increased cores with GG1 carcinoma. No evidence of recurrence at last follow up. |
| **6** | 69, CA | 6.8 | Right apex | Focally positive | No | Patient on active surveillance. No evidnece of progression of disease at last follow up. |

AA= African American
CA= Caucasian
GG= Grade Group

Figure 1 - 969

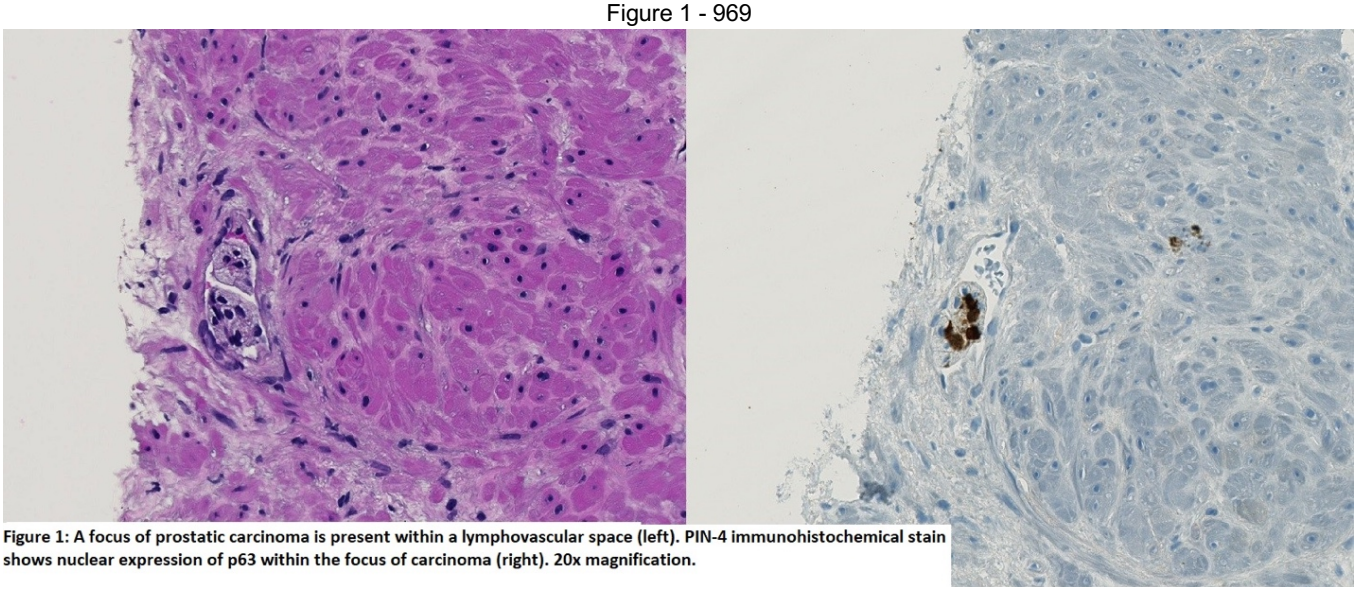

Figure 1: A focus of prostatic carcinoma is present within a lymphovascular space (left). PIN-4 immunohistochemical stain shows nuclear expression of p63 within the focus of carcinoma (right). 20x magnification.

Figure 2 - 969

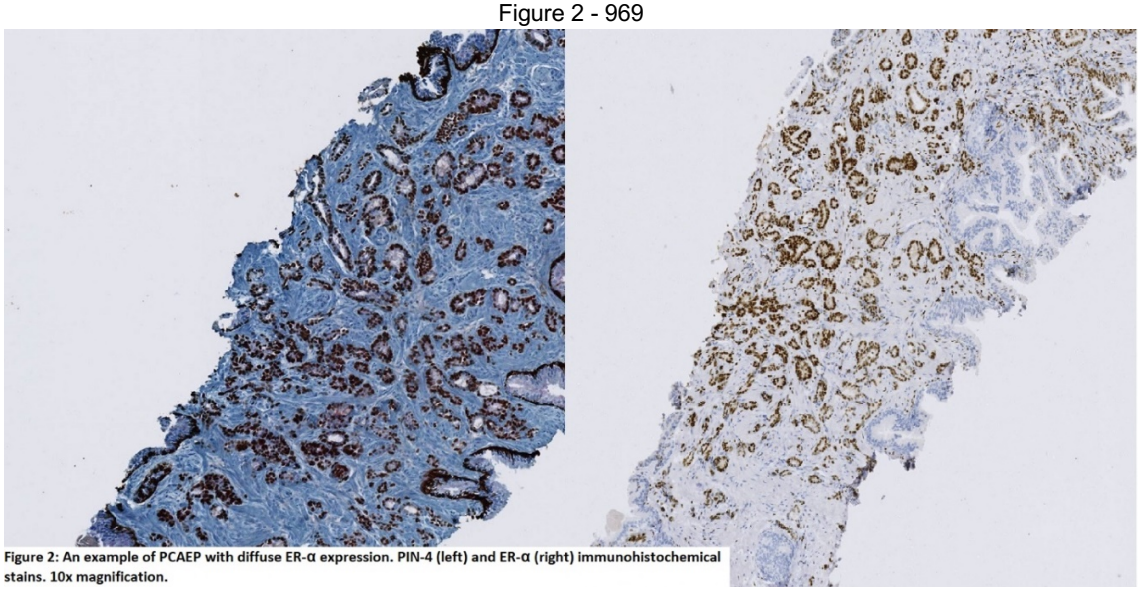

Figure 2: An example of PCAEP with diffuse ER-α expression. PIN-4 (left) and ER-α (right) immunohistochemical stains. 10x magnification.

**Conclusions:** In a small series, PCAEP behaves like low grade prostatic carcinoma on active surveillance. A high proportion of our cases showed immunohistochemical expression of ER, which has been seen in treated and high grade carcinomas. PCAEP may show lymphovascular invasion and may be associated with locally advanced disease.

## 970 Aberrant GATA-3 Staining in Prostatic Adenocarcinoma: A Potential Diagnostic Pitfall

Timothy McDonald[1], Jonathan Epstein[2]
*[1]Brigham and Women's Hospital, Boston, MA, [2]Johns Hopkins Medical Institutions, Baltimore, MD*

**Disclosures:** Timothy McDonald: None; Jonathan Epstein: None

**Background:** Distinguishing between poorly differentiated urothelial carcinoma and high grade prostatic adenocarcinoma is a common challenge in genitourinary pathology, particularly when the tumor involves the bladder neck or prostatic urethra. GATA-3 is thought to be a sensitive and relatively specific marker of urothelial carcinoma, however, there is scant data regarding it's staining in high grade prostatic adenocarcinomas. The aim of this study is to describe rare cases with strong aberrant GATA-3 staining in prostatic adenocarcinoma as a potential diagnostic pitfall.

**Design:** We identified 7 cases of prostatic adenocarcinoma with aberrant positive GATA-3 staining from 2015-2019 as part of a large consultation service at our institution. The cases were reviewed and evaluated by immunohistochemistry (IHC) for GATA-3 (Biocare, clone L50-823), NKX3.1, PSA and p501s (prostein).

**Results:** All 7 cases were Grade Group 5, six had a Gleason score of 5+5=10 and one 4+5=9. Four of the cases were from the prostate, 3 from the urinary bladder, and 1 from the prostatic urethra. All cases were morphologically typical of high grade prostatic adenocarcinoma, although were sent for consultation due to uncertainty in the diagnosis. GATA-3 positivity was strong, diffuse in 3 cases; strong, patchy in 1 case and strong, focal in 3 cases. All cases were positive for NKX3.1, 5 positive for p501s, and 5 positive for PSA (Table 1).

| Study Results | | | | | | |
|---|---|---|---|---|---|---|
| **Specimen** | **Gleason Score** | **GG** | **GATA-3** | **NKX3.1** | **p501s** | **PSA** |
| Prostatic urethra biopsy | 5+5=10 | 5 | + (strong, patchy) | + | + | + |
| Bladder biopsy | 5+5=10 | 5 | + (strong, focal) | + | - | - |
| Prostate Needle biopsy | 5+5=10 | 5 | + (strong, diffuse) | + | - | + |
| TURP | 5+5=10 | 5 | + (strong, diffuse) | + | + | + |
| Prostate Needle biopsy | 5+5=10 | 5 | + (strong, focal) | + | + | + |
| Bladder biopsy | 5+5=10 | 5 | + (strong, focal) | + | + | - |
| TURP | 4+5=9 | 5 | + (strong, diffuse) | + | + | + |

**Table 1.** GG = Grade Group, TURP = transurethral resection of prostate

**Figure 1.** A) Transurethral resection of prostate (TURP) specimen with high grade prostatic adenocarcinoma, Gleason score 5+5=10, Grade Group 5. B) Strong, diffuse positive staining for GATA-3. C) Strong, diffuse positive staining for NKX3.1

Figure 1 – 970

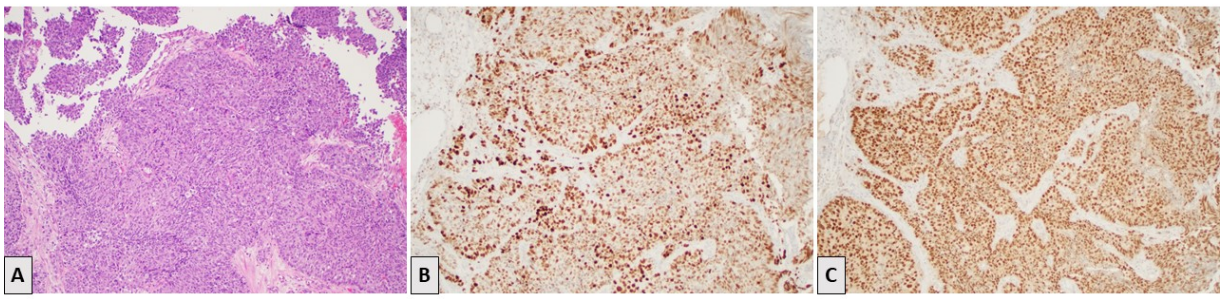


**Conclusions:** Poorly differentiated prostate adenocarcinoma can have pleomorphic giant cell features, and pseudopapillary or solid architecture, closely mimicking urothelial carcinoma. Clinically, the distinction between these two tumors can also be difficult. Proper diagnosis in these patients is essential as they have differing prognoses and clinical management. The current study describes that rare cases of prostatic adenocarcinoma can show focal or diffuse strong staining for GATA3. In order to avoid this diagnostic pitfall, undifferentiated carcinomas involving the prostate, bladder neck or trigone should be evaluated not only with GATA3 (which may label rare prostate cancers) and PSA (which can be negative in high grade prostate cancer), but also the prostate specific and more sensitive markers of NKX3.1 and p501s.

## 971 Aggressive Variant of Prostate Carcinoma - Clinicopathologic and Histopathologic Features

Charles Middleton[1], John Henegan[1], Varsha Manucha[1]
[1]*University of Mississippi Medical Center, Jackson, MS*

**Disclosures:** Charles Middleton: None; Varsha Manucha: None

**Background:** Aggressive variant of prostate cancer (AVPCa) is a rapidly progressive form of metastatic castrate resistant prostate cancer often involving visceral sites in the setting of low or modestly rising prostate specific antigen (PSA) levels. While the diagnosis of AVPCa can be suspected on clinical features, histologic confirmation and demonstration of the pathognomonic molecular signature of AVPCa is often made on biopsies from sites of metastases. The pathologic diagnosis is challenging given the limited size of the specimen, inconsistent morphology and variable immunohistochemistry (IHC) expression.

**Design:** We reviewed the clinicopathologic characteristics of 3 metastatic carcinomas of prostate origin with clinical suspicion for AVPCa, subsequently confirmed by demonstration of molecular signature ( loss of at least 2 of the following : RB , PTEN, p53) on the biopsy from the metastatic site. The morphologic features as well as IHC results on all three cases are reviewed.

**Results:** The three patients were 56, 59 and 62 years at the time of diagnosis. The PSA at the time of diagnosis was >100ng/ml in two patients and 7.1 ng/ml in the third patient. All three at the time of initial presentation had widespread osseous metastases. After a period ranging from 6-16 months of androgen deprivation therapy and initial fall of PSA levels, the three patients developed either new bone lesions or soft tissue masses. Subsequent biopsies of metastatic sites revealed a pure adenocarcinoma , a mixed squamous cell carcinoma and neuroendocrine carcinoma (cytology smears showed neuroendocrine component only, figures 1 and 2) and a neuroendocrine carcinoma with an intermixed glandular component . Excluding the patient with adenocarcinoma, the other two tumor specimens were negative for prostate specific markers . Neuroendocrine markers were expressed in 2 of three tumors (Table 1).

| Clinicopathologic features of the three cases of AVPCa | | | |
|---|---|---|---|
| | **Case 1** | **Case 2** | **Case 3** |
| Age (years)/race | 56/African American | 62/Caucasian | 59/Caucasian |
| Grade Group of acinar adenocarcinoma at the time of diagnosis | GG5 | NA | GG5 |
| Findings at time of presentation | | | |
| PSA | 261ng/ml | 1960 ng/ml | 7.1ng/ml |
| Multiple and diffuse osseous metastasis | present | present | present |
| Enlarged abdominal lymph nodes | present | absent | present |
| Therapy | Leuprolide and chemotherapy | Abiraterone and Leuprolide | Abiraterone/Enzalutamide and Leuprolide |
| Post treatment follow up | 10 months later – interval increase in osseous metastases, pelvic mass ; PSA, 2.5ng/ml | 6 months later – new bony metastases, PSA , 3-4ng/ml | 16 months later - extraosseous enlargement of tumor at bone metastatic sites; PSA , 0.20ng/ml |
| Site of subsequent biopsy | Iliac crest | Right humerus | Thoracic vertebra (T8) |
| Histologic diagnosis | Metastatic carcinoma with discreet squamous and neuroendocrine component | Metastatic adenocarcinoma | Metastatic carcinoma with intermixed neuroendocrine and glandular component |
| IHC | | | |
| Positive | Neuroendocrine component - CD56, synaptophysin, chromogranin<br><br>Squamous component – CK903, p63,p40 | NKX3.1, PSA, PSAP | Synaptophysin, TTF-1, Ki-67 -70% |
| Negative | PSA,PSAP, NKX3.1 | Synaptophysin, chromogranin, CD56, AE1/AE3,EMA,PAX8, CK7,CK20,GATA-3,AMACR,TTF-1 | CD56, NKX3.1, GATA3,chromogranin |
| IHC for molecular signature (PTEN/RB/p53) | Loss of PTEN and p53 | Loss of RB and PTEN | Loss of RB and PTEN |
| Follow up | Deceased 11 months after diagnosis | Alive at last follow up | Alive at last follow up |

Figure 1 - 971

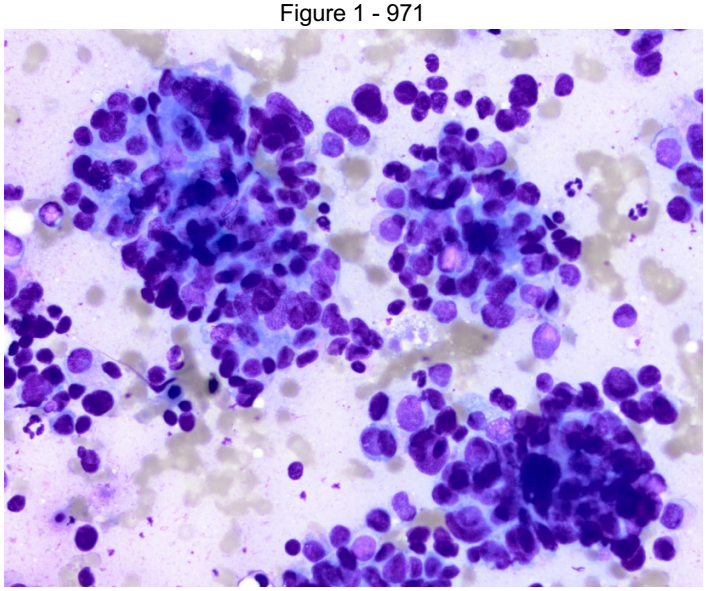

Figure 2 - 971

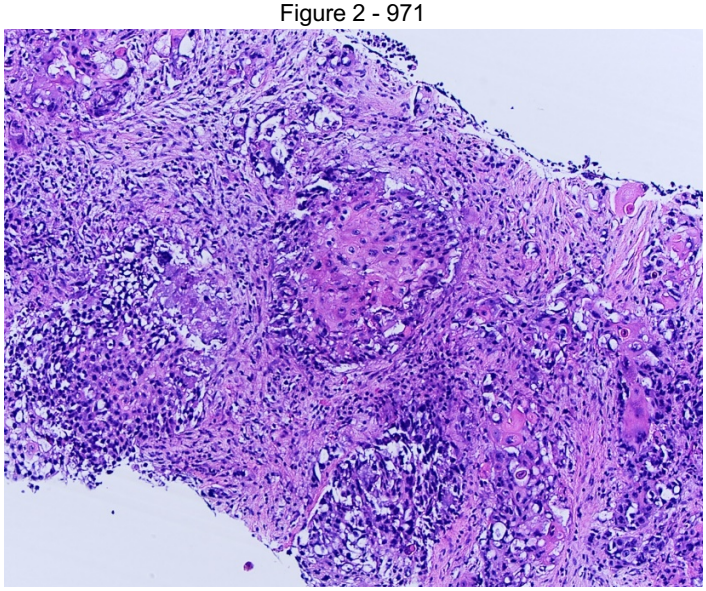

**Conclusions:** This series highlights that morphologic and clinical features of AVPCa are variable and may not be specific or sensitive enough for this diagnosis. Since molecular diagnosis will impact treatment selection, global testing for molecular AVPCa should be considered. Moreover, recognition of AVPCa as a distinct entity in WHO classification of prostate carcinomas will result in its increased awareness amongst pathologists.

## 972 Immunohistochemistry of Androgen Receptor and Rab27b in Non-Muscle-Invasive Bladder Cancer as Predictors of Sensitivity to Intravesical Bacillus Calmette-Guérin Immunotherapy

Taichi Mizushima[1], Takashi Kawahara[2], Ikuma Kato[3], Guiyang Jiang[4], Hiroshi Miyamoto[5]
*[1]University of Rochester, Rochester, NY, [2]University of Rochester, Yokohama, Kanagaea, Japan, [3]Yokohama City University, Yokohama, Kanagawa, Japan, [4]China Medical University, Shenyang, Liaoning, China, [5]University of Rochester Medical Center, Rochester, NY*

**Disclosures:** Taichi Mizushima: None; Takashi Kawahara: None; Ikuma Kato: None; Guiyang Jiang: None; Hiroshi Miyamoto: None

**Background:** Intravesical bacillus Calmette-Guérin (BCG) immunotherapy is quite effective in some of patients with bladder cancer, but others fail to respond to it for which underlying mechanisms are poorly understood. Interestingly, in a few studies, male patients have been shown to be less likely to respond to BCG therapy, compared with female patients. Meanwhile, our preliminary study in cell lines and mouse models has indicated that androgen receptor (AR) activity in bladder cancer correlates with sensitivity to BCG therapy presumably via modulating the expression of a GTPase Rab27b that contributes to the elimination of the bacteria from urothelial cells. The current study aims to determine the expression status of AR and Rab27b in bladder cancer tissues and its prognostic significance.

**Design:** We immunohistochemically stained for AR and Rab27b in non-muscle-invasive high-grade urothelial carcinoma specimens from patients who subsequently underwent intravesical BCG therapy. We then evaluated the relationship between the expression of each protein and patient outcomes.

**Results:** Positive signals of AR and Rab27b were detected predominantly in the nucleus and cytoplasm, respectively, of tumor cells. Overall, AR was immunoreactive in 13 (40.6%) of 32 cases, including 6 (30.0%) of 20 without recurrence versus 7 (58.3%) of 12 with recurrence ($P = 0.057$). Similarly, Rab27b was immunoreactive in 26 (81.3%) of 32 cases, including 14 (70.0%) of 20 without recurrence versus 12 (100%) of 12 with recurrence ($P = 0.018$). Kaplan-Meier analysis coupled with the log-rank test revealed that patients with AR-positive ($P = 0.024$) or Rab27b-positive ($P = 0.032$) tumor had a significantly higher risk of tumor recurrence following transurethral surgery.

**Conclusions:** Our results suggest that positivity of AR and Rab27b in bladder cancers is associated with resistance to intravesical BCG immunotherapy. Immunohistochemical detection of AR and/or Rab27b may thus be helpful in predicting response to BCG therapy in patients with non-muscle-invasive bladder tumor.

## 973 Spectrum of Neoplasms in the Setting of Polycystic Kidney Disease

Ashley Monsrud[1], Rayan Rammal[2], Lara Harik[3]
[1]Emory University, Atlanta, GA, [2]American University of Beirut, Beirut, Lebanon, [3]Emory University School of Medicine, Atlanta, GA

**Disclosures:** Ashley Monsrud: None; Rayan Rammal: None; Lara Harik: None

**Background:** Very few studies have described the spectrum of neoplasms arising in polycystic kidney disease (PCKD); most are in the form of single case reports. We present an institutional review of the variety of lesions and neoplasms encountered in PCKD patients.

**Design:** A review of the institutional database for PCKD patients was performed to include cases between years 2013-2019. Clinical, gross and histologic features were collected.

**Results:** Seventeen patients with PCKD were evaluated; 11 bilateral and 6 unilateral nephrectomies. The average age was 60 years (range, 40-71y). The M: F ratio was 1.42:1 with 10 males and 7 females. The mean weight was 2,280.5 grams (range, 625-5,400g) and mean size was 26.5cm (range, 18-40cm). A variety of benign and malignant neoplasms were seen. Benign lesions include 1) multiloculated cysts in all patients with a mean size of 9.7mm (range, 4-17mm) 2) papillary adenomas (PA) in 11 of 17 patients with a mean size of 3.78mm (range, 0.6-14mm) and 3) cystic papillary lesions (CPL) in 100% of cases with a mean size of 5.47mm (range, 2.5-16mm). CPL were defined as unilocular or multilocular cysts with papillary structures along and within the cyst wall with basal nuclei, lacking atypia. Malignant neoplasms present in 11 of 17 patients included: papillary renal cell carcinoma (RCC) n=4, mean size 4.3cm (range, 3.5-7.0cm), clear cell papillary RCC n=3, mean size 1.2cm (range, 0.7-2.1cm), unclassified RCC (one with microcystic architecture) n=2, measuring 0.5cm and 1.0cm, clear cell RCC n=2, measuring 1.6cm and 5.0cm, and chromophobe RCC n=1, size 3.0cm. One patient had bilateral clear cell RCC, and another patient had bilateral clear cell papillary RCC. One patient had two malignancies (papillary RCC and chromophobe RCC) in one kidney. Follow up average was 24 months (range, 1-61mos) and showed no recurrence or metastatic disease.

**Conclusions:** A variety of benign and malignant proliferations are encountered in the setting of PCKD. CPLs are frequently seen and described both in our review and other studies, but lack a defined nomenclature in current literature. We propose the term cystic papillary adenoma (CPA) for these CPLs. Diagnostic criteria should include the lack of nuclear atypia similar to PA. Since the bulk of CPA sizes are the cysts, in contrast to the non-cystic PA, a larger size criterion, such as up to 2 cm, should be acceptable.

## 974 Clinico-Pathologic Characteristics of Prostatic Adenocarcinoma Patients with Lymph Node Metastases

Ashley Monsrud[1], Meredith Kline[2], Alexandra Speak[2], Zhengjia Chen[3], Yuzi Zhang[4], Mehmet Bilen[2], Lara Harik[2]
*[1]Emory University, Atlanta, GA, [2]Emory University School of Medicine, Atlanta, GA, [3]Winship Cancer Institute, Atlanta, GA, [4]Department of Biostatistics and Bioinformatics, Emory University, Atlanta, GA*

**Disclosures:** Ashley Monsrud: None; Meredith Kline: None; Alexandra Speak: None; Zhengjia Chen: None; Yuzi Zhang: None; Mehmet Bilen: None; Lara Harik: None

**Background:** The histologic characteristics of patients with metastatic prostatic adenocarcinoma (PCA) to the lymph nodes (LN) should be further studied to investigate further risk stratification based on primary tumor and/or metastatic burden characteristics.

**Design:** A review of the institutional database, between years 2011-2018, for PCA patients with LN metastasis (Mets) was performed. Detailed clinical and histologic characteristics were collected. Patients with LN Mets less than or equal to 0.2 mm were defined as individual tumor cells (ITC), between 0.2 and less than or equal to 2 mm as Micrometastases (Micro). Chi-square test and/or Fisher exact test were used to test the association of binary or categorical factors with patients' status at last follow up (no evidence of disease (NED) vs biochemical recurrence (BCR)).

**Results:** One hundred patients were identified; average age=61years (44-84y); with a majority of white (n=72, 72%) followed by African American patients (n=22, 22%). The distribution of Grade Group (GG) was GG2(n=4), GG3(n=27), GG4(n=6) and GG5(n=62) with one patient with high grade neuroendocrine carcinoma, not gradable. The distribution of stage was pT2(n=2), pT3a (n=28), and pT3b (n=70) and pM1a (n=21). Patients with Gleason Score (GS) 7 (n=31, 31%) showed high rates of tertiary pattern 5 (TP5), defined as less than or equal to 5%, (n=22, 71%) and uniformly displayed PCA with cribriform architecture (n=31, 100%). PCA with cribriform architecture was present in 97 (97%) of cases. The majority of patients had bilateral extra-prostatic extension (n=67, 67%) and/or bilateral seminal vesicle invasion (n=44, 44%). Bladder neck invasion was noted in 30 patients (30%) (14 focal, 16 extensive). Only two patients died of disease at 30 and 35 months.

**Table 1.** Details the distribution of patient variables stratified by their follow up status into NED or BCR.

| Covariate | Status at last follow up | | p-value |
|---|---|---|---|
| | 0=NED (n=24) | 1=BCR (n=76) | |
| **Race, No. (%)** | | | |
| White | 19 (79.17) | 53 (69.74) | 0.544 |
| Black | 5 (20.83) | 17 (22.37) | |
| Asian | 0 (0.00) | 3 (3.95) | |
| Other | 0 (0.00) | 3 (3.95) | |
| **LN Mets, No. (%)** | | | |
| Loco-regional | 20 (83.33) | 59 (77.63) | 0.55 |
| Distant | 4 (16.67) | 17 (22.37) | |
| **Total Positive LN, No. (%)** | | | |
| 1-2 pos LN | 16 (66.67) | 36 (47.37) | 0.099 |
| More than 2 pos LN | 8 (33.33) | 40 (52.63) | |
| **ITC and Micro, No. (%)** | | | |
| Less than or equal to 2 mm | 16 (66.67) | 68 (89.47) | **0.0079** |
| More than 2 mm | 8 (33.33) | 8 (10.53) | |
| **LN Bilaterality, No. (%)** | | | |
| Unilateral | 9 (50.00) | 25 (37.88) | 0.353 |
| Bilateral | 9 (50.00) | 41 (62.12) | |
| Not available | 6 | 10 | |
| **Largest size of metastasis, No. (%)** | | | |
| Less than or equal to 1 mm | 6 (25.00) | 4 (5.26) | **0.005** |
| More than 1 mm | 18 (75.00) | 72 (94.74) | |
| **Extranodal Extension, No. (%)** | | | |
| Negative | 9 (39.13) | 17 (24.64) | 0.181 |
| Positive | 14 (60.87) | 52 (75.36) | |
| **Gleason Score, No. (%)** | | | |
| 7 | 10 (41.67) | 21 (28.00) | 0.153 |
| 8 | 2 (8.33) | 4 (5.33) | |
| 9 | 12 (50.00) | 50 (66.67) | |
| Not applicable | 1 | | |
| **Grade Group, No. (%)** | | | |
| 2 | 3 (12.50) | 1 (1.33) | 0.081 |
| 3 | 7 (29.17) | 20 (26.67) | |
| 4 | 2 (8.33) | 4 (5.33) | |
| 5 | 12 (50.00) | 50 (66.67) | |
| Not applicable | 1 | | |
| **Stage, No. (%)** | | | |
| pT2 | 1 (4.17) | 1 (1.32) | 0.305 |
| pT3a | 9 (37.50) | 19 (25.00) | |
| pT3b | 14 (58.33) | 56 (73.68) | |
| pT4 | 0 (0.00) | 0 (0.00) | |
| **Age** | | | |
| Mean(sd) | 59.71(6.74) | 62.00(7.36) | 0.178 |
| **Follow-up Time (months)** | | | |
| Mean(sd) | 22.40(13.05) | 29.84(22.14) | 0.122 |
| **Total No. LN** | | | |
| Mean(sd) | 27.67(18.15) | 26.38(20.12) | 0.781 |

Metastatic PCA were largely Grade Group 4 and 5, with Grade Group 2 and 3 being a minority; Patients with Grade Group 2 and 3 showed high rates of tertiary pattern 5, suggesting a need to incorporate the tertiary pattern 5 into the Gleason Score on prostatectomies.

Our findings confirm the high risk associated with cribriform pattern PCA.

Patients with ITC and/or Micro Mets showed a significantly higher percentage of NED.

**Conclusions:** Smaller metastatic foci (<1mm) are more likely to remain NED.

A trend was observed in patients with 1-2 positive LN showing lower rates of recurrence.

## 975 The Significance of Squamous Histology on Clinical and Pathologic Outcomes in Bladder Cancer: Pure Urothelial vs Urothelial with Squamous Differentiation vs Pure Squamous Cell Carcinoma

Kathleen Montgomery[1], Giovanna A Giannico[1], Soroush Rais-Bahrami[2], Prabin Thapa[3], Stephen Boorjian[3], Igor Frank[3], John Cheville[3], Jennifer Gordetsky[1]
*[1]Vanderbilt University Medical Center, Nashville, TN, [2]The University of Alabama at Birmingham, Birmingham, AL, [3]Mayo Clinic, Rochester, MN*

**Disclosures:** Kathleen Montgomery: None; Giovanna A Giannico: None; Soroush Rais-Bahrami: None; Prabin Thapa: None; Stephen Boorjian: None; Igor Frank: None; John Cheville: None; Jennifer Gordetsky: None

**Background:** It has been proposed that urothelial carcinoma (UC), urothelial carcinoma with squamous differentiation (UCSD), and pure squamous cell carcinoma (SCC) of the bladder differ in terms of risk factors, incidence, and prognosis. This study evaluates the clinical and pathologic characteristics of 1472 tumors from patients who underwent radical cystectomy for bladder cancer.

**Design:** After IRB approval, the Mayo Clinic Cystectomy Clinical Registry was queried for patients with SCC, UCSD or UC in their radical cystectomy specimen between 1980 and 2015. A urologic pathologist reviewed all cases for histologic features and a nurse abstractor obtained clinical data, including outcome information. Multivariate Cox regression was used to identify prognostic factors. Kaplan-Meier estimation was used to assess cancer-specific survival.

**Results:** Of 1472 cases, there were 1128 UC (77%), 220 UCSD (15%), and 124 pure SCC (8%). Bladder cancer was more common in men than women (80% v. 20%). However, a higher proportion of SCC and UCSD occurred in women (35% of SCC, 22% of UCSD, 18% of UC). Women were significantly more likely to be never smokers in all three cohorts (45% v. 16% in UC, 44% v. 12% in UCSD, 40% v. 17% in SCC), and were more likely to have a history of urinary tract infection (UTI) (35% v. 11% in UC, 31% v. 20% in UCSD, 50% v. 15% in SCC). Patients with UCSD or SCC were more likely to be heavy smokers (≥10 pack years) (p=0.046). A history of UTI was observed in 35% of SCC, 23% of UCSD, and 16% of UC (p=0.0003) and neurogenic bladder was present in 18% of SCC, 8% of UCSD, and 2% of UC (p<0.0001). Patients with UC had lower pathologic stage disease than patients with UCSD or SCC (28% of UC was ≤ pT1, compared to 8% of UCSD and 2% of SCC (p<0.0001); 44% of UC was pT3 or pT4, compared to 75% of UCSD and 73% of SCC (p<0.0001)). Overall survival (p=0.01) and cancer-specific survival (p=0.01) were improved in UC compared with UCSD and SCC. There was no significant difference in time-to-recurrence or risk of local recurrence or metastasis.

**Conclusions:** Our study indicates that UC, UCSD, and SCC are associated with different risk factors, gender distributions, and clinical outcomes. The proportion of women with SCC or UCSD was higher than proportion of women with UC. More patients with SCC or UCSD had an extensive smoking history or chronic irritative/inflammatory conditions. Additionally, patients with SCC or UCSD had a higher pathologic stage at cystectomy and worse outcomes than patients with UC.

## 976 Immunohistochemical Evaluation of the mTOR Pathway of Genetically Characterized Chromophobe Renal Cell Carcinomas: A Pilot Study of 20 Cases

Aurélien Morini[1], Tom Drossart[2], Marc-Olivier Timsit[3], Arnaud Mejean[4], Constance Thibault[5], Anne-Paule Gimenez-Roqueplo[3], Judith Favier[2], Nelly Burnichon[3], Virginie Verkarre[6]
*[1]Georges Pompidou European Hospital, Bussy Saint Georges, Ile de France, France, [2]Université Paris, PARCC, INSERM, Equipe Labellisée par la Ligue contre le Cancer, Paris, Ile de France, France, [3]APHP.5 Hôpital Européen Georges Pompidou; INSERM UMR970, Paris Descartes University, Paris, France, [4]APHP.5 Hôpital Européen Georges Pompidou; Paris Descartes University, Paris, France, [5]Assistance Publique - Hôpitaux de Paris (AP-HP.Centre), Georges Pompidou European Hospital, Paris, Ile de France, France, [6]Hôpital Européen Georges Pompidou, APHP, Paris, Ile de France, France*

**Disclosures:** Aurélien Morini: None; Tom Drossart: None; Marc-Olivier Timsit: None; Arnaud Mejean: None; Constance Thibault: *Consultant*, Pfizer; *Consultant*, Ipsen; Anne-Paule Gimenez-Roqueplo: None; Judith Favier: None; Nelly Burnichon: None; Virginie Verkarre: None

**Background:** The mammalian target of rapamycin (mTOR) pathway, which plays an important role in Renal Cell Carcinoma tumorigenesis and represents a potential target for therapy in advanced stage, has been poorly investigated in Chromophobe Renal Cell Carcinomas (ChRCC). Our objective was to evaluate the immunohistochemical analysis of the mTOR pathway as a predictive marker in ChRCC.

**Design:** From a large monocentric retrospective cohort of 274 ChRCC collected from 2001 to 2019, we selected 20 representative cases of nonmetastatic ChRCC for which we performed a combined genetic and immunohistochemical analysis.

Somatic and germline genetic analyses were performed by next generation sequencing using a in-house panel of 29 genes including *PTEN, MTOR, TSC1, TSC2, FLCN* (SeqCap EZ HyperCap, Roche®) on DNA extracted from 20 frozen tumors and matched blood samples.

Using a Tissue MicroArray (TMA) from FFPE samples of 20 tumors (2 spots/tumor) with matched non neoplastic renal parenchyma normal tissue, we performed immunohistochemistries with five antibodies against proteins interacting with mTOR pathway including Akt, Akt-P, p70S6K, p70S6K-P & 4EBP1-P. Expression was evaluated by a H-score (intensity (0 to +3) x percentage of labeled cells).

**Results:** Immunostaining of all mTOR proteins were low or absent, compared to normal renal tissue in all but two cases. The negative staining was correlated with the absence of genetic alteration in the mTOR pathway. A strong staining of the five mTOR proteins was observed in one patient with a germline variant of *TSC2* and in one tumor carrying a somatic *MTOR* mutation, respectively. The CD117 immunohistochemistry performed in the *MTOR*-mutated tumor allowed us to reclassify it as the emerging entity of low-grade oncocytic tumor.

**Conclusions:** This characterization of the mTOR pathway in a series of ChRCC showed its rare involvement in such renal carcinoma. However, this pilot study revealed an excellent correlation between Akt, Akt-P, p70S6K, p70S6K-P and 4EBP1-P expression and genetic alteration in the mTOR pathway. Moreover, it allowed the first identification of a *MTOR* mutation in a low-grade oncocytic tumor. A larger study on the whole cohort including metastatic ChRCC is ongoing to better evaluate the impact of the mTOR pathway alterations as prognosis marker. These preliminary results suggest that the targeted use of mTOR inhibitors should be relevant in ChRCC patients presenting a genetic alteration in the mTOR pathway.

## 977 Is There Utility in Screening for DNA Mismatch Repair Deficiency in Grade Group 5 Prostate Cancers?

Casey Morrison[1], Anh Le[2], Kyle Devins[3], Daniel Rader[3], Kara Maxwell[4], Lauren Schwartz[5]
*[1]The Hospital of the University of Pennsylvania, Philadelphia, PA, [2]Perelman School of Medicine at the University of Pennsylvania, Philadelphia, PA, [3]Hospital of the University of Pennsylvania, Philadelphia, PA, [4]University of Pennsylvania, Philadelphia, PA, [5]Perelman School of Medicine at the University of Pennsylvania, Bala Cynwyd, PA*

**Disclosures:** Casey Morrison: None; Anh Le: None; Kyle Devins: None; Lauren Schwartz: None

**Background:** Prostate cancer (PCa) is one of the most common malignancies in men. In PCa, the presence of Gleason pattern 5 is associated with a poor prognosis. Studies looking specifically at Gleason Score 9-10/Grade Group 5 PCa are few and often limited by a small sample size. The available data suggests that these high-grade PCas may be associated with higher rates of DNA mismatch repair (MMR) protein deficiency. This finding has implications for treatment options and Lynch syndrome screening, thus, we designed our study to investigate the rate of MMR deficiency in Gleason Score 9-10/Grade Group 5 PCas by immunohistochemistry.

**Design:** The institutional tumor tissue bank was retrospectively queried for cases of Gleason Score 9-10/Grade Group 5 PCa. A tissue microarray (TMA) was constructed and immunohistochemical stains for MLH1, PMS2, MSH2 and MSH6 were performed on the TMAs using standard lab practices. MMR protein expression was evaluated as either retained or lost (complete lack of nuclear staining) in tumor cells.

**Results:** Of 1,852 men identified with a confirmed history of PCa, 145 were graded as Gleason Score 9-10/Grade Group 5. Tissue from radical prostatectomy specimens were available for 68 cases. Five of the 68 (7.35%) cases showed complete loss of expression of at least one mismatch repair protein. One case (1.47%) showed loss of MLH1 and PMS2, two (2.94%) showed loss of MSH2 and MSH6, and two (2.94%) showed loss of MSH6 alone.

**Conclusions:** In our cohort of Gleason Score 9-10/Grade Group 5 PCas, the observed rate of MMR deficiency (7.35%) is greater than the previously reported rate across PCa Grade Groups (estimated at 0.5-1.5%). Our findings have significant management implications, suggesting that screening with MMR IHC should be considered in all Gleason 9–10/Grade Group 5 PCas. Screening would help identify patients and families who may benefit from germline testing for Lynch syndrome, as well as those who could qualify for treatment with checkpoint blockade immunotherapies in the case of recurrence or development of metastatic disease.

## 978 DLL3 RNAish: A Tissue-Based Biomarker for Targeted Therapy of Advanced Prostate Cancer

Samaneh Motanagh[1], Hussein Alnajar[2], Himisha Beltran[3], Aram Vosoughi[4], Verena Sailer[5], Olivier Elemento[6], Andrea Sboner[2], Juan Miguel Mosquera[2]
*[1]Lebanon, NH, [2]Weill Cornell Medicine, New York, NY, [3]Dana-Farber Cancer Institute, Harvard T.H. Chan School of Public Health, Boston, MA, [4]Yale University School of Medicine, New Haven, CT, [5]University Medical Center Schleswig-Holstein, Campus Lübeck and Research Center Borstel, Leibniz Lung Center, Borstel, Germany, [6]New York, NY*

**Disclosures:** Samaneh Motanagh: None; Hussein Alnajar: None; Himisha Beltran: *Grant or Research Support*, Abbvie Stemcentryx; Aram Vosoughi: None; Verena Sailer: None; Olivier Elemento: None; Andrea Sboner: None; Juan Miguel Mosquera: None

**Background:** Rovalpituzumab tesirine is a first-in-class antibody-drug conjugate directed against delta-like protein 3 (DLL3), a novel target expressed in more than 80% of patients with small-cell lung cancer (Rudin et al., Lancet Oncol 2017). We recently described that some

advanced castration-resistant prostate cancers (CRPC), mainly AR-negative with neuroendocrine differentiation, also express DLL3 (Puca et al., Sci Transl Med. 2019). The goal of this study was to optimize an RNA in situ hybridization (RNAish) assay to detect DLL3 expression.

**Design:** We studied 65 cases of CRPC: 22 with adenocarcinoma histology (CRPC-Adeno), 19 with neuroendocrine differentiation (CRPC-NE), and 24 with high-grade morphology. For assay optimization, DLL3 immunohistochemistry (IHC) and NanoString gene expression results were compared with DLL3 RNAish in a subset of cases including the H660 cell line (positive control). RNAish expression was quantified by image analysis HALO software (Indica Labs, Inc.).

**Results:** 8 out of 19 (42%) CRPC-NE, 5 out of 22 (23%) CRPC-Adeno and 1 out of 24 (4%) high-grade carcinoma showed DLL3 RNAish expression (Figure.1), 50% concordance NanoString values. 5 discrepant cases (1 CRPC-Adeno and 4 CRPC-NE) were negative for DLL3 RNAish.

Figure 1 - 978

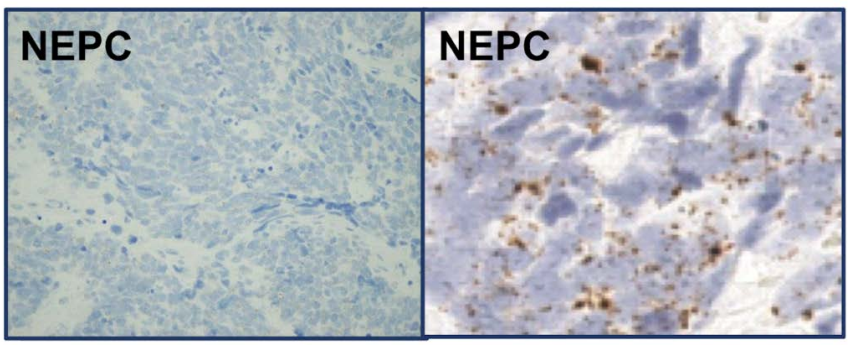


**Figure 1: RNAish image**

**Conclusions:** We optimized an RNAish assay to evaluate DLL3 expression – a therapeutic target - in CRPC. A signficant number of cases – especially CRPC-NE – overexpress DLL3. Future studies will establish the potential application of this assay as a potential predictive biomarker for CRPC patients who are candidates for DLL3 targeted therapy.

## 979 Comparison Between Pathologic Findings in Male and Female Patients Who Undergo Early Bladder Re-Resection for Urothelial Carcinoma: Potential Role for Risk Stratification

Patrick Mullane[1], Mehrdad Alemozaffar[1], Adeboye O. Osunkoya[1]
*[1]Emory University, Atlanta, GA*

**Disclosures:** Patrick Mullane: None; Mehrdad Alemozaffar: None; Adeboye O. Osunkoya: None

**Background:** Urothelial carcinoma (UCa) of the bladder is the sixth most common malignancy in the USA. Patients diagnosed with UCa with lamina propria (LP) invasion are particularly at risk for disease recurrence and progression to muscularis propria (MP) invasion. However, the comparison between the pathologic findings in male and female patients who undergo bladder re-resection for UCa has not been well characterized. In this study we compared the pathologic findings between male and female patients who underwent repeat transurethral resection of bladder tumor (TURBT) following a diagnosis of LP invasion at a major academic institution.

**Design:** We searched our Urologic Pathology files and expert consult cases of the senior author for patients who underwent repeat TURBT within 8 weeks of a diagnosis of UCa with LP invasion. Patients whose re-resections were delayed or had a prior diagnosis of UCa with MP invasion were excluded. Clincopathologic data was obtained.

**Results:** Eighty-nine consecutive patients were identified. Majority 58/89 (65%) were male and 31/89 (35%) were female. The mean age was 73 years (range: 51-92 years). On initial biopsy, female patients were less likely to have MP present (51.6% vs 62%) and less likely to have CIS (12.9% vs 36.2%). On re-resection, recurrence rates were comparable between female and male patients (58.1% vs 65.5%). However, recurrence of UCa with LP invasion was higher in male than female patients (34.5% vs 16.1%), while progression of UCa with MP invasion was higher in female than male patients (12.9% vs 6.9%).

**Conclusions:** Comparison of male and female patients undergoing early bladder re-resection following a diagnosis of UCa with LP invasion in our cohort identified important risk factors associated with patient gender. Female patients were less likely to have MP present on initial biopsy and had a higher proportion of disease progression on re-resection, despite the overall rate of recurrence being somewhat

similar to male patients. Our findings highlight the importance of adequate TURBT sampling, especially in female patients, and support a potential role for risk stratification in male and female patients with UCa of the bladder.

## 980 A Clinicopathologic Analysis of Patients Undergoing Early (<8 weeks) versus Late (>8weeks) Repeat Transurethral Resection of Bladder Tumor Following an Initial Diagnosis of Urothelial Carcinoma with Lamina Propria Invasion

Patrick Mullane[1], Mehrdad Alemozaffar[1], Adeboye O. Osunkoya[1]
*[1]Emory University, Atlanta, GA*

**Disclosures:** Patrick Mullane: None; Mehrdad Alemozaffar: None; Adeboye O. Osunkoya: None

**Background:** Repeat transurethral resection of bladder tumor (TURBT) for patients with urothelial carcinoma (UCa) with lamina propria (LP) invasion is recommended due to the risk of recurrence and upstaging to muscularis propria (MP) invasive disease. Early repeat TURBT within 8 weeks of initial biopsy may improve patient outcomes by facilitating disease clearance and accurate staging. Here, we compared the clinical and pathologic characteristics of patients with a new diagnosis of UCa with LP invasion who underwent early versus late repeat TURBT at a major academic institution.

**Design:** A search was made through our Urologic Pathology files and expert consult cases of the senior author for patients who received a new diagnosis of UCa with LP invasion and underwent at least one subsequent TURBT. Early repeat resection was defined as a repeat TURBT that was performed within 8 weeks of the initial diagnosis.

**Results:** One hundred consecutive cases were selected. Fifty nine patients underwent early repeat TURBT and 41 patients had delayed repeat TURBT. The mean age for early repeat TURBT was 72 years (range: 52-92 years) with 38/59 (64.4%) male and 21/59 (35.6%) female. The mean age for late repeat TURBT was 74 years (range: 52-95 years) with 26/41 (63.4%) male and 15/41 (36.6%) female. Elapsed time range to early repeat TURBT was 1-8 weeks and 9-121 weeks for late repeat TURBT. Patients with early repeat TURBT were less likely to have MP (61.0% vs. 73.2%), variant histology/divergent differentiation (16.9% vs. 31.7%), or multifocal disease (40.4% vs 61.3%) on initial biopsy. Recurrence rates were lower for patients with early repeat TURBT (62.7% vs. 80.5%) as was progression to MP invasive disease (6.8% vs. 12.2%).

**Conclusions:** In our cohort, early repeat TURBT was associated with lower rates of recurrence and progression to UCa with MP invasion. However, patients with multifocal disease, variant histology/divergent differentiation, or MP on initial biopsy were less likely to undergo early repeat TURBT. Our findings support early repeat TURBT for patients with UCa with LP invasion, and identify possible clinical and pathologic etiologies for the discrepant patient outcomes.

## 981 A Deep Learning System with Subspecialist-Level Accuracy for Gleason Grading Prostate Biopsies

Kunal Nagpal[1], Davis Foote[2], Fraser Tan[2], Yun Liu[3], Po-Hsuan Cameron Chen[2], David Steiner[4], Naren Manoj[5], Niels Olson[6], Jenny Smith[7], Arash Mohtashamian[8], Brandon Peterson[9], Mahul Amin[10], Andrew Evans[11], Joan Sweet[12], Carol Cheung[13], Theodorus Van Der Kwast[12], Ankur Sangoi[14], Ming Zhou[15], Robert Allan[16], Peter Humphrey[17], jason Hipp[18], Krishna Gadepalli[2], Greg Corrado[2], Lily Peng[2], Martin Stumpe[2], Craig Mermel[3]
*[1]Google, New York, NY, [2]Google, Mountain View, CA, [3]Google, Palo Alto, CA, [4]Stanford University School of Medicine, Redwood City, CA, [5]Toyota Technological Institute Chicago, Chicago, IL, [6]San Diego, CA, [7]Navy Medical Center San Diego, San Diego, CA, [8]Navy, San Diego, CA, [9]Naval Medical Center San Diego, San Diego, CA, [10]Methodist University Hospital, Memphis, TN, [11]Toronto General Hospital, Toronto, ON, [12]University Health Network, Toronto, ON, [13]University of Toronto, Toronto, ON, [14]El Camino Hospital, Mountain View, CA, [15]Tufts Medical Center, Boston, MA, [16]Tampa, FL, [17]Yale University School of Medicine, New Haven, CT, [18]Los Altos, CA*

**Disclosures:** Kunal Nagpal: *Employee*, Google; *Employee*, Google; Yun Liu: *Employee*, Google; *Employee*, Google; Po-Hsuan Cameron Chen: *Employee*, Google; David Steiner: *Employee*, Google; *Employee*, Google; Naren Manoj: None; Brandon Peterson: None; Mahul Amin: *Consultant*, Urogen; *Consultant*, Advanced Clinical; *Advisory Board Member*, CellMax; *Advisory Board Member*, Precipio Diagnostics; Carol Cheung: None; Theodorus Van Der Kwast: None; Ankur Sangoi: None; Ming Zhou: None; Robert Allan: None; Peter Humphrey: None; Craig Mermel: *Employee*, Google LLC; *Employee*, Google LLC

**Background:** For prostate cancer, the biopsy's Gleason score and its derived Grade Group (GG) play a pivotal role in determining patient management. However, Gleason grading exhibits significant interobserver variability, leading to a pressing need for decision support tools to improve the accuracy and consistency of Gleason grading in routine clinical practice. This study evaluates a deep learning system's (DLS) accuracy in Gleason grading hematoxylin-and-eosin stained diagnostic prostate biopsies.

**Design:** The DLS was evaluated using 757 biopsies from three institutions in the United States. A multi-institutional panel of six genitourinary specialist pathologists (average years of experience: 25) determined the reference standard GG: two specialists first reviewed each biopsy, and a third subspecialist helped to resolve disagreements. To reduce diagnostic uncertainty, the subspecialists had

access to immunohistochemistry and multiple sections for every biopsy. The breakdown within these biopsies was: 34% non-tumor; 33% GG1; 16% GG2; 9% GG3; and 8% GG4-5.

**Results:** In categorizing each biopsy as one of non-tumor, GG1, GG2, GG3, or GG4-5, the DLS's accuracy was 77.8% (95%CI 74.9-80.7), significantly higher than a cohort of 19 general pathologists: mean accuracy 71.8% (95%CI 69.1-74.3, p<0.001). Differences were more pronounced on tumor-containing biopsies (69.8% DLS accuracy vs. 57.8% pathologists), with the DLS less frequently "overgrading" at important clinical thresholds: GG1-GG2 (11.6% vs. 25.9%) and GG2-GG3 (8.2% vs. 29.2%). DLS:subspecialist concordances were similar to inter-subspecialist concordances, and both were higher than inter-general-pathologist concordances (mean concordance on tumor-containing biopsies: 64.7% DLS:subspecialist vs. 66.3% inter-subspecialist vs. 52.3% inter-general-pathologist). In sub-analyses, the DLS performed similarly on biopsies from an independent data source not used for DLS development (n=324).

**A**

| Subspecialist-determined reference standard | DLS (n=757 reviews across 757 biopsies) | | | | |
|---|---|---|---|---|---|
| | Non-tumor | GG1 | GG2 | GG3 | GG4-5 |
| Non-tumor | 31.4% | 0.8% | 0.0% | 0.7% | 0.7% |
| GG1 | 3.2% | 25.9% | 3.6% | 0.1% | 0.1% |
| GG2 | 0.4% | 4.9% | 9.5% | 1.2% | 0.1% |
| GG3 | 0.3% | 0.4% | 2.2% | 4.9% | 1.5% |
| GG4-5 | 0.0% | 0.0% | 0.0% | 2.0% | 6.2% |

**B**

| Subspecialist-determined reference standard | Pathologists (n=2239 reviews across 757 biopsies) | | | | |
|---|---|---|---|---|---|
| | Non-tumor | GG1 | GG2 | GG3 | GG4-5 |
| Non-tumor | 32.3% | 0.8% | 0.0% | 0.0% | 0.0% |
| GG1 | 3.5% | 20.3% | 7.0% | 0.9% | 0.4% |
| GG2 | 0.2% | 3.5% | 8.1% | 3.7% | 1.2% |
| GG3 | 0.2% | 0.2% | 1.2% | 4.0% | 3.7% |
| GG4-5 | 0.1% | 0.0% | 0.1% | 0.9% | 7.0% |

**Table 1.** Breakdown of classifications by the deep learning system (DLS, A) and pathologists (B) relative to the genitourinary subspecialists-determined reference standard. Each row represents the biopsies graded by subspecialists as one of 5 categories: non-tumor, and Grade Groups (GG) 1, 2, 3, and 4-5. Each cell indicates what percentage of all reviews corresponded to that category for the DLS (A) or the general pathologists (B). The diagonal values (in bold) represent correct classifications relative to the reference standard; the region below the diagonal thus represents undergrading (grading more conservatively than subspecialists); and the region above the diagonal right region represents overgrading (grading more aggressively than subspecialists). DLS overcalls of biopsies without tumor as GG3-5 were generally on small regions (eFigure 3 in the Supplement) that are unlikely to mislead pathologists using the DLS as a decision support tool by also reviewing the gland-level predictions.

Figure 1 - 981

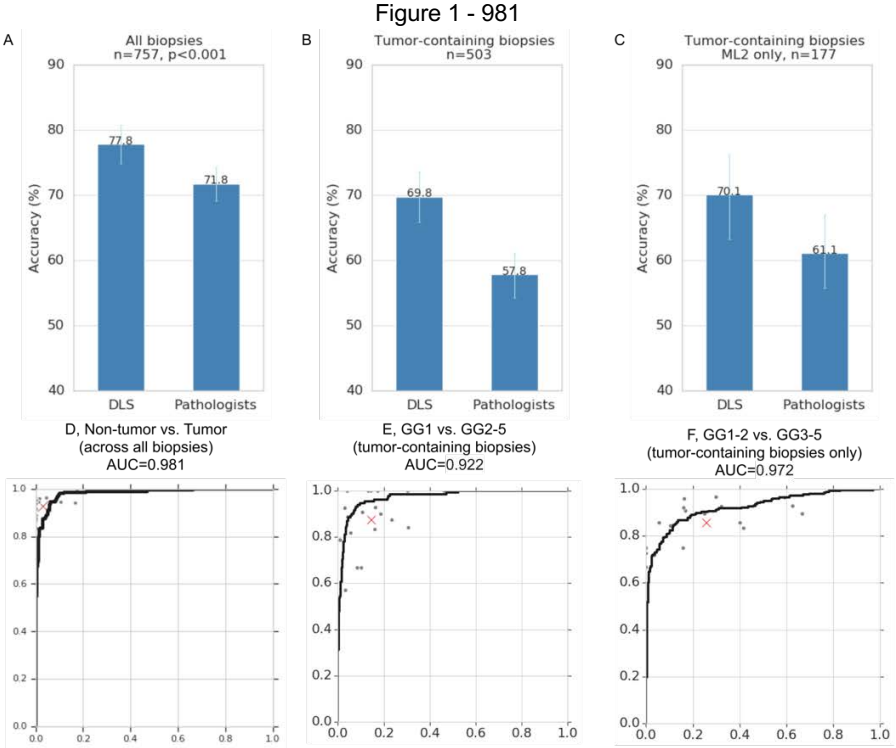


**Figure 1. Validation set performance for Gleason grading and tumor detection. A**, blue bars indicate the accuracy of the DLS and the mean accuracy among a cohort of 19 pathologists for categorizing each biopsy as one of 5 categories: non-tumor (NT), and Grade Groups (GG) 1, 2, 3, and 4-5. Error bars represent the 95% confidence interval for the DLS or the pathologist cohort, respectively **B,** Accuracy on tumor-containing biopsies. **C,** Accuracy on tumor-containing biopsies from the independent data source ML2 (that was not used in DLS development). Accuracy of pathologists excludes pathologists who provided fewer than 20 reviews on ML2 (comparison to all pathologists are presented in eTable 3 in the Supplement). **D-F**, receiver operating characteristic curves of sensitivity and specificity of the DLS (blue line) for the specified slides in comparison with individual pathologists (gray dots) and the average of the pathologists (red cross). The curves plot the performance at three clinically important cutoffs: NT versus tumor (**D**); GG1 versus GG2-5 on tumor-containing slides (**E**); and GG1-2 versus GG3-5 on tumor-containing slides (**F**).

**Conclusions:** The DLS was significantly more accurate than general pathologists at Gleason grading prostate biopsies, and the DLS-subspecialist agreement was similar to inter-subspecialist agreement. Future research is necessary to evaluate the impact of using the DLS as a decision support tool in clinical workflows to improve the consistency of prostate cancer grading for therapy decisions.

## 982 CD44 Methylation Levels and Prostate Cancer Biologic Phenotype: Epigenetic Modulation in a Series of Hormonally Treated and Non-Treated Patients

Gabriella Nesi[1], Ilaria Galli[1], Calogero Saieva[2], Laura Ottini[3], Raffaella Santi[4]
*[1]University of Florence, Florence, Italy, [2]Molecular and Nutritional Epidemiology Unit, Cancer Research and Prevention Institute (ISPO), Florence, Italy, [3]Sapienza, University of Rome, Rome, Italy, [4]Florence, Italy*

**Disclosures:** Gabriella Nesi: None; Ilaria Galli: None; Calogero Saieva: None; Laura Ottini: None; Raffaella Santi: None

**Background:** Epigenetic changes, particularly DNA methylation, have been reported to promote the development and progression of prostate cancer (PCa). Compared with normal prostate tissue, PCa samples from patients treated with androgen-deprivation therapy (ADT) show hypermethylation of several genes primarily implicated in PCa progression. These genes are promising biomarkers which could predict castration-resistant disease, although no DNA methylation signature specifically related to treatment has yet been identified.

**Design:** A series of 90 cases of radical prostatectomies was retrospectively analyzed. Forty-six patients had surgery alone (non-treated) and 44 received ADT prior to surgery (treated). All PCa cases were characterized for the main clinico-pathologic features, i.e. age at diagnosis, pTNM classification, Gleason score and margin status. Endothelial expression of CD31 and LYVE-1 was assessed immunohistochemically. Staining hot spot areas were used to evaluate microvessel density (MVD) with a semi-quantitative scoring system. Promoter methylation analysis of genes involved in hormonal (*AR*, *ESR1*, *ESR2*) and tumor progression (*RASSF1*, *APC*, *CD44*, *CDH1*, *BCL2*, *ZEB1*) pathways was performed. Biomolecular studies were conducted by pyrosequencing and methylation levels estimated by calculating average methylation for each gene. The mRNA expression of significantly differentially methylated genes was investigated by quantitative Real-Time PCR (qRT-PCR) using a TaqMan pre-designed assay.

**Results:** ADT was associated with LYVE1 (p<0.001) and CD31 (p=0.04) expression; correlation between stage and increased MVD (p=0.026) was also observed. Median *CD44* methylation levels were significantly higher in non-treated patients (p=0.0005). For the other genes analyzed, no significant differences emerged. In non-treated cases, *CD44* methylation levels inversely correlated with CD31 expression (p=0.02). No association between *CD44* methylation levels and pathologic variables was seen in either group. *CD44* gene expression levels were significantly lower in the non-treated group (p=0.01). A significant relationship was found between methylation levels and mRNA expression of *CD44* using the Pearson product-moment correlation (r=-0.22; p=0.046).

**Conclusions:** Our results suggest that ADT contributes to the development of a more aggressive PCa phenotype through increased MVD. Furthermore, CD44 promoter methylation is proposed as a candidate molecular marker of PCa progression.

## 983 Radical Prostatectomy Findings in Glomeruloid Pattern Prostate Cancer with Transition to Cribriform Architecture: Comparison with Other Cribriform Growth Patterns

Sarah Ni Mhaolcatha[1], Susan Prendeville[1]
[1]*Cork University Hospital, Cork, Ireland*

**Disclosures:** Sarah Ni Mhaolcatha: None; Susan Prendeville: None

**Background:** The presence of cribriform architecture, including invasive and intraductal growth patterns, has been associated with adverse outcomes in prostate cancer (PCa). The glomeruloid subtype of PCa comprises cribriform structures with one or two points of attachment which sometimes shows transition to lumen-spanning cribriform architecture; however, the prognostic significance of this growth pattern has not been fully determined. This study evaluated glomeruloid growth with cribriform transition at radical prostatectomy (RP) and compared with other types of cribriform architecture.

**Design:** Completely embedded radical prostatectomy specimens (n=285) were reviewed for the presence of cribriform architecture and grouped as follows: i) Glomeruloid growth with at least focal transition to lumen-spanning cribriform areas (GLOM/CR) ii) Intraductal carcinoma (IDC) with or without invasive cribriform carcinoma (IDC/CR) iii) invasive cribriform carcinoma without IDC (CR ONLY). Each group was correlated with pathologic outcome at RP.

**Results:** The cohort included 33 GLOM/CR; 52 IDC/CR and 59 CR ONLY (Table 1). The IDC/CR group had the greatest association with adverse pathologic features at RP including presence of non-organ confined disease, seminal vesicle invasion (SVI) and lymph node metastasis (LN+). The rate of non-organ confined disease and SVI was significantly different between GLOM/CR and IDC/CR groups but not between GLOM/CR and CR ONLY groups.

| RP FIndings | GLOM CR | CR/IDC | CR ONLY | P value [1] | P value [2] | P value [3] |
|---|---|---|---|---|---|---|
| **Grade Group** | | | | | | |
| **2** | 22 (67%) | 22 (42%) | 28 (47%) | | | |
| **3** | 9 (27%) | 23 (44%) | 25 (42%) | | | |
| **4** | 2 (6%) | 3 (6%) | 4 (7%) | | | |
| **5** | 0 | 4 (8%) | 2 (4%) | | | |
| **Organ-confined disease (pT2)** | | | | | | |
| **Yes** | 17 (52%) | 13 (25%) | 26 (44%) | p=0.03 | p=0.02 | p=0.52 |
| **No** | 16 (48%) | 39 (75%) | 33 (56%) | | | |
| **SVI** | | | | | | |
| **Yes** | 2 (6%) | 13 (25%) | 7 (12%) | p=0.04 | p=0.03 | p=0.37 |
| **No** | 31 (94%) | 39 (75%) | 52 (88%) | | | |
| **LN+** | 2 (6%) | 10 (19%) | 2 (3%) | p=0.014 | p=0.09 | p=0.56 |

1: Across all 3 groups

2: Between GLOM/CR and IDC/CR groups

3: Between GLOM/CR and CR ONLY groups

**Conclusions:** Cribriform growth with IDC showed the greatest association with adverse pathologic findings at RP. The glomeruloid pattern showing transition to cribriform architecture showed more favorable features compared to cases with IDC but was similar to cases with invasive cribriform carcinoma only. Additional evaluation of the spectrum of cribriform architecture may further refine the prognostic significance of individual growth patterns.

## 984 The Clinical Impact of Extraprostatic Extension and Bladder Neck Invasion in Patients with pT3b Prostate Cancer Undergoing Radical Prostatectomy

Numbereye Numbere[1], Pratik Gurung[2], Yuki Teramoto[2], Zhiming Yang[2], Hiroshi Miyamoto[2]
*[1]University of Rochester Medical Center, Pittsford, NY, [2]University of Rochester Medical Center, Rochester, NY*

**Disclosures:** Numbereye Numbere: None; Pratik Gurung: None; Yuki Teramoto: None; Zhiming Yang: None; Hiroshi Miyamoto: None

**Background:** The presence of seminal vesicle invasion by prostate cancer (pT3b disease) has been associated with poor patient outcomes. However, the significance of T3a lesions [i.e. extraprostatic extension (EPE), bladder neck invasion (BNI)] in pT3b disease remains poorly understood. In the present study, we aim to compare radical prostatectomy (RP) findings and long-term oncologic outcomes in men with pT3b prostate cancer with versus without EPE/BNI.

**Design:** We assessed consecutive patients who had undergone RP between 2009 and 2018. Within our Surgical Pathology database, we identified a total of 248 patients with pT3b disease without undergoing neoadjuvant therapy.

**Results:** EPE or BNI was found in 231 (93%) or 43 (17%) of the cases, respectively. Compared to cases without EPE [EPE(-)], the presence of EPE [EPE(+)] was associated with higher rates of BNI (19% vs. 0%, $P = 0.088$), positive surgical margin (SM) (39% vs. 13%, $P = 0.035$), and lymphovascular invasion (LVI) (30% vs. 6%, $P = 0.047$), as well as larger estimated tumor volume (mean: 18.8 vs. 9.5 cc, $P < 0.001$). There were no significant differences in Grade Groups (GGs), pN status, or preoperative prostate-specific antigen (PSA) level between EPE(-) and EPE(+) cases. Similarly, compared to cases without BNI [BNI(-)], the presence of BNI [BNI(+)] was associated with higher rates of EPE (100% vs. 83%, $P = 0.088$), positive SM (93% vs. 34%, $P < 0.001$), LVI (44% vs. 25%, $P = 0.015$), and lymph node metastasis (56% vs. 34%, $P = 0.010$), as well as higher PSA level (21.86 vs. 10.40 ng/mL, $P = 0.033$) and larger tumor volume (31.4 vs. 15.4 cc, $P < 0.001$). The rates of GG 3-5 (91% vs. 83%, $P = 0.257$), GG 4-5 (58% vs. 40%, $P = 0.028$), and GG 5 (53% vs. 32%, $P = 0.009$) were also higher in BNI(+) cases than in BNI(-) cases. Kaplan-Meier analysis coupled with log-rank test revealed that patients with BNI had a significantly higher risk of biochemical recurrence (BCR) following RP (defined as a single PSA of ≥0.1 ng/mL), compared with BNI(-) cases ($P = 0.049$). However, there were no significant associations between EPE and BCR as well as between EPE or BNI and cancer-specific mortality.

**Conclusions:** The presence of EPE and/or BNI in pT3b prostate cancer was found to be associated with worse histopathologic features in RP specimens. BNI was also associated with the risk of BCR. Pathologists may thus need to report the presence or absence of pT3a lesions in RP specimens showing seminal vesicle invasion.

## 985 The Clinical Impact of Unilateral vs. Bilateral Invasion of the Seminal Vesicle in Patients with Prostate Cancer Undergoing Radical Prostatectomy

Numbereye Numbere[1], Pratik Gurung[2], Yuki Teramoto[2], Zhiming Yang[2], Hiroshi Miyamoto[2]
*[1]University of Rochester Medical Center, Pittsford, NY, [2]University of Rochester Medical Center, Rochester, NY*

**Disclosures:** Numbereye Numbere: None; Pratik Gurung: None; Yuki Teramoto: None; Zhiming Yang: None; Hiroshi Miyamoto: None

**Background:** The presence of seminal vesicle invasion (SVI) by prostate cancer has been associated with poor patient outcomes, but clinical significance of unilateral (Uni) versus bilateral (Bil) involvement remains poorly understood. The present study aims to compare radical prostatectomy (RP) findings and long-term oncologic outcomes in men with prostate cancer showing Uni-SVI or Bil-SVI.

**Design:** We assessed consecutive patients who had undergone RP between 2009 and 2018. Within our Surgical Pathology database, we identified a total of 248 patients with pT3b disease without undergoing neoadjuvant therapy.

**Results:** Of the 248 cases, 139 (56%) and 109 (44%) exhibited Uni-SVI and Bil-SVI, respectively. The rates of Grade Group (GG) 3-5 (90% vs. 81%, $P = 0.043$), GG 4-5 (55% vs. 33%, $P < 0.001$), and GG 5 (47% vs. 27%, $P = 0.002$) were significantly higher in Bil-SVI cases than in Uni-SVI cases. Additionally, Bil-SVI was associated with higher rates of bladder neck invasion (27% vs. 10%, $P < 0.001$), positive surgical margin (51% vs. 26%, $P < 0.001$), lymphovascular invasion (38% vs. 21%, $P = 0.004$), and lymph node metastasis (48% vs. 30%, $P = 0.003$), as well as higher preoperative prostate-specific antigen (PSA) level (14.84 vs. 10.45 ng/mL, $P = 0.062$) and larger estimated tumor volume (mean: 24.3 vs. 13.3 cc, $P < 0.001$). Similarly, when the histopathologic features of the tumors at the foci of SVI were compared, Bil-SVI was associated with higher rates of GG 3-5 (93% vs. 65%, $P < 0.001$), GG 4-5 (74% vs. 46%, $P < 0.001$), GG 5 (32% vs. 13%, $P = 0.001$), and cribriform morphology (46% vs. 32%, $P = 0.037$), as well as a greater dimension of the tumors [mean: 0.78 (mean of both sides) vs. 0.67 cm, $P = 0.034$]. Kaplan-Meier analysis coupled with log-rank test revealed that patients with Bil-SVI had a significantly higher risk of biochemical recurrence (BCR) following RP (defined as a single PSA of ≥0.1 ng/mL) ($P = 0.040$), but not cancer-specific mortality ($P = 0.377$), compared with Uni-SVI patients. GG at SVI foci was also associated with the risk of BCR (GG 2 vs. GG 3-5, $P = 0.009$; GG 2-3 vs. GG 4-5, $P = 0.013$) or cancer-specific mortality (GG 2-4 vs. GG 5, $P = 0.079$).

**Conclusions:** Bilateral seminal vesicle involvement in prostate cancer was found to be associated with worse histopathologic features in RP specimens and poorer prognosis. These findings suggest that pathologists may need to report Uni-SVI versus Bil-SVI, as well as histopathologic findings at SVI such as Gleason score, in RP specimens.

## 986 Identification of Protein Profiles by Mass Spectrometry Associated with Development of Castration-Resistant Prostate Cancer

Anne Offermann[1], Marie Christine Hupe[2], Mirjam Polzer[3], Jutta Kirfel[4], Axel Merseburger[5], Timo Gemoll[6], Sven Perner[7]
*[1]Pathology of the University Hospital Schleswig-Holstein, Campus Lübeck, Lübeck, Schleswig-Holstein, Germany, [2]University Hospital Schleswig-Holstein, Luebeck, Germany, [3]Pathology of the University Hospital Schleswig-Holstein, Campus Luebeck, Luebeck, Germany, [4]Institute of Pathology, University Hospital UKSH, Luebeck, Germany, [5]University Hospital Luebeck, Luebeck, Germany, [6]University of Luebeck and University Medical Center Schleswig-Holstein, Campus Luebeck, Luebeck, SH, Germany, [7]University Medical Center Schleswig-Holstein, Leibniz Center for Medicine and Biosciences, Luebeck, Germany*

**Disclosures:** Anne Offermann: None; Marie Christine Hupe: None; Mirjam Polzer: None; Jutta Kirfel: None; Axel Merseburger: None; Timo Gemoll: None; Sven Perner: None

**Background:** Patients suffering from advanced prostate cancer (PCa) are routinely treated with androgen deprivation therapy (ADT). Initially, the treatment leads to tumor regression and decline of serum PSA levels for an indefinite period of time. However, after this initial therapy response patients develop castration-resistant PCa (CRPC) defining the most aggressive type of PCa. There are currently no biomarkers predicting individual response to ADT, and only limited therapy options for the treatment of CRPC. Aim of this study was to identify novel molecular structures associated with the development of CRPC.

**Design:** Hormone-naïve PCa tissue from 50 patients obtained by radical prostatectomy or transurethral resection were used for protein isolation followed by mass spectrometry (MS) to identify the most abundant peptides in primary PCa. All patients received ADT during the observation period. Early relapse was defined as development of CRPC within the first year of ADT. The log2 fold change values were calculated between different patient groups and statistically tested using student t-test.

**Results:** A total of 111 proteins were identified to be significant differentially expressed between tumor tissues from patients who developed CRPC and patients who did not, and 141 proteins between patients who developed an early or late progress under ADT. The most differentially expressed proteins are involved in processes of (I) cellular metabolism including up-regulation of Apoliproteins and CYP enzymes, both associated with deregulation of cholesterol homeostasis, in patients who developed early CRPC, (II) angiogenesis as well as (III) immune modulators. Within the latter, we observed a striking up-regulation of several immunoglobulins in patients with early progress. Supervised clustering allowed significant patient stratification into protein expression profiles predicting success of ADT.

**Conclusions:** In the current study, we identified a protein expression pattern on hormone-naïve PCa tissue that associates with early development of CRPC. Deregulation of metabolic modulators may foster PCa cells to grow and survive under androgen deprivation. Up-regulation of immunoglobulins by cancer cells that has been recently reported as pro-tumorigenic mechanism might also be involved in the progression of PCa to lethal CRPC. Conclusively, further advancements of our results will provide predictive markers for the response to widely used ADT as well as therapeutic targets for the treatment of CRPC.

## 987 Metastatic Prostatic Adenocarcinoma to the Brain and Spinal Cord: A Contemporary Clinicopathologic Analysis of 31 Cases

Oluwaseun Ogunbona[1], Abigail Goodman[2], Adeboye O. Osunkoya[3]
*[1]Emory University School of Medicine, Atlanta, GA, [2]Emory University Hospital, Atlanta, GA, [3]Emory University, Atlanta, GA*

**Disclosures:** Oluwaseun Ogunbona: None; Abigail Goodman: None; Adeboye O. Osunkoya: None

**Background:** Metastatic prostatic adenocarcinoma (PCa) to lymph nodes and bone is well documented in the literature, however, only case reports and small series of metastatic PCa to the brain and spinal cord have been published.

**Design:** We identified 31 cases of metastatic PCa to the brain and spinal cord from our Neuropathology and Urologic Pathology files, including consultation cases of the senior author.

**Results:** Mean patient age at diagnosis was 66 years (range: 51 to 87 years). Fourteen (45%) cases involved the brain and 17 (55%) cases involved the spinal cord. Of the 14 cases involving the brain, 7 (50%) were metastasis to the temporal lobe, 3 (21%) to the occipital lobe, 2 (14%) to the frontal lobe, 1 (7%) to the parietal lobe. Two of the 3 occipital lobe cases involved another location (parietal and frontal lobes). One case involved the dura on the left side of the brain, 1 case involved the pituitary and was initially diagnosed as a pituitary adenoma on frozen section, and another case involved the cerebellum and was designated as a cerebellar cyst on imaging. Nine of the 14 (64%) cases were on the right side of the brain including cerebellum, in contrast to 4 (29%) cases on the left side. The spinal cord lesions involved the thoracic region in 13 of 17 (76%) cases. The cervical and lumbar spinal cord were each involved in 2 (12%) cases. The sacral

spinal cord was involved in 1 (6%) case that also involved the lumbar spinal cord. The vast majority of the cases (87%) were a single mass within the brain and spinal cord. All patients had one or more metastases to other sites including lymph nodes, bone, bladder, perirectal/perianal tissue, penis, lung, liver, and adrenal gland. Follow-up was available in 15 cases with a mean duration of 18 months (range: 1 to 130 months). Seven patients died of disease, 5 patients are alive with disease, and 3 patients have had no evidence of residual disease following resection.

**Conclusions:** This is one of the largest studies to date of metastatic PCa to the brain and spinal cord. Metastatic PCa should be considered in the differential diagnosis of a solitary brain or spinal cord mass in male patients. Both clinicians and pathologists should be aware that late brain metastases may occur, even over a decade after the initial diagnosis of PCa.

## 988 T-cell Infiltration in Metastatic Upper Tract Urothelial Carcinoma as a Determinant of Response to Immunotherapy

Kentaro Ohara[1], Bhavneet Bhinder[1], Kenneth Eng[2], Evan Fernandez[1], Aram Vosoughi[3], Shaham Beg[1], David Wilkes[1], Brian Robinson[1], Francesca Khani[1], Rohan Bareja[4], Andrea Sboner[1], Olivier Elemento[5], Bishoy Faltas[1], Juan Miguel Mosquera[1]
*[1]Weill Cornell Medicine, New York, NY, [2]Englander Institute for Precision Medicine, Brooklyn, NY, [3]Yale University School of Medicine, New Haven, CT, [4]Englander Institute for Precision Medicine, New York, NY, [5]New York, NY*

**Disclosures:** Kentaro Ohara: None; Bhavneet Bhinder: None; Kenneth Eng: None; Evan Fernandez: None; Aram Vosoughi: None; Shaham Beg: None; David Wilkes: None; Brian Robinson: None; Francesca Khani: None; Rohan Bareja: None; Andrea Sboner: None; Olivier Elemento: None; Bishoy Faltas: *Advisory Board Member*, Immunomedics; *Grant or Research Support*, Eli Lilly; Juan Miguel Mosquera: None

**Background:** Upper tract urothelial carcinoma (UTUC) is a distinct clinicopathological entity with an aggressive behavior. Our group recently characterized the T-cell depleted immune contexture of primary UTUC (pUTUC). Little is known about the biological differences with metastatic UTUC (mUTUC). We analyzed whole exome sequencing (WES) and RNA-seq data from our Precision Medicine cohort.

**Design:** 26 patients with UTUC were enrolled in our clinical trial. Paired pUTUC and mUTUC were obtained from 7 patients. WES and RNA-seq data from 24 pUTUCs (17 renal pelvis, 7 ureter) and from 16 mUTUCs (10 distant organs, 4 lymph nodes and 2 local recurrences) were compared. We analyzed RNA-seq data to evaluate the immune cell composition. To this end, we conducted hierarchical consensus clustering of 170 immune related genes across both our cohort and urothelial carcinoma of the bladder (UCB) from TCGA.

**Results:** All primary tumors were diagnosed as high-grade UTUC. The most recurrently altered gene in mUTUC was *TP53* (50%). *RAF1* (38% vs 4%, P=0.01, Fisher's exact test) and *PPARG* (38% vs 8%, P=0.04) were more frequently altered in mUTUC. The differences of both tumor mutational burden (TMB) (median, 2.4/Mb vs 1.3/Mb) and microsatellite instability (MSI) scores (median, 0.07 vs 0.08) between mUTUCs and pUTUCs were not statistically significant. No tumors were MSI-H. Seven mUTUCs showed the T-cell depleted phenotype, and 2 mUTUCs showed the T-cell inflamed subtype. Interestingly, one mUTUC patient whose tumor had a prominent high T-cell infiltration score even with low MSI-sensor and low-TMB scores had extreme response to immune checkpoint inhibitor therapy resulting in sustained complete remission for 5 years.

**Conclusions:** This study confirms that the majority of UTUC tumors are T-cell depleted. The genomic and immunophenotypic features were similar between primary and metastatic UTUC. However, a minority of UTUC tumors with T-cell inflamed subtype represent outliers that may be extreme responders to immunotherapy even in absence of high-TMB or microsatellite instability. Further studies to better characterize the underlying mechanisms in these patients are ongoing.

## 989 Comparison of MP-MRI/US Fusion-Guided Biopsy and Standard US-Guided Biopsy in the Detection of Prostate Cancer: An Institutional Experience

Kelly Olson[1], Samuel Hubbard[2], David Jarrard[2], Wei Huang[2]
*[1]University of Wisconsin-Madison School of Medicine and Public Health, Madison, WI, [2]University of Wisconsin, Madison, WI*

**Disclosures:** Kelly Olson: None; Samuel Hubbard: None; Wei Huang: *Primary Investigator*, Dhristi, Inc (PathomIQ); *Stock Ownership*, Dhristi, Inc

**Background:** The advent of multiparametric magnetic resonance imaging (MP-MRI) enables imaging-based identification of prostate cancer (PCa), leading to the development of targeted MRI/ultrasound (US) fusion biopsy (targeted) platforms. Studies suggest that targeted and standard biopsy combined is superior to standard biopsy alone in detecting clinically significant PCa. Questions were raised about the necessity of performing concurrent standard biopsy if targeted biopsy was also performed, as targeted alone is more cost effective. We examined the data of targeted and standard biopsies at our institution.

**Design:** Four hundred and forty prostate biopsy cases from 2017 to 2019 were sequentially selected. Pathology reports and clinical notes were reviewed to find targeted (lesion) biopsy and standard (non-lesion) biopsy cases. All targeted biopsy cases in this study had

concurrent standard biopsy. PCa was stratified into three categories: low, intermediate and high risk. Low risk on biopsy was defined as Gleason score 6 or low-volume Gleason score 3+4 (<50% of any core containing cancer and <33% of standard biopsy cores positive for cancer). Intermediate risk was defined as Gleason score 3+4 with 50% or more of any core positive for cancer or 33% or more of standard biopsy cores positive for cancer. High-risk tumors were Gleason score 4+3 or greater cancers. The PCa detection rates between these two methods were studied and compared. Fisher exact test was used for statistical analysis.

**Results:** Our data showed that targeted biopsy with concurrent standard biopsy was significantly better in the detection of PCa (63.2%) than standard biopsy (51.5%) ($p<0.05$), but not superior in detecting high risk PCa (35% vs 45.5% for targeted and standard biopsy, respectively; $p>0.05$). Examining the biopsy results of lesion site(s) vs non-lesion sites separately in those positive cases identified by targeted fusion biopsy, our data showed that targeted (lesion) biopsy with concurrent standard biopsy was superior to targeted (lesion) biopsy or standard (non-lesion) biopsy alone. Targeted biopsy without concurrent standard biopsy could also miss low risk (8%) and high risk (2%) PCa, but to a lesser degree than standard biopsy alone, which missed low, intermediate and high risk PCa at 8%, 5% and 7%, respectively (Table 1).

**Table 1.** A Close Look of Positive Cases Identified by Target Biopsy with Concurrent Standard Biopsy

| Case (n) | Lesion(s) (L) | | Non-Lesion(s) (NL) | | Grade Group | PCa Risk | | |
|---|---|---|---|---|---|---|---|---|
| | Dx | Rate (%) | Dx | Rate (%) | | Low n(%) | Intermediate n(%) | High n(%) |
| 12 | PCa | 90 | Neg | 20 | | 5 (8) | 3 (5) | 4 (7) |
| 7 | PCa | | PCa | 80 | L > NL | | | |
| 26 | PCa | | PCa | | L = NL | | | |
| 9 | PCa | | PCa | | L < NL | | | |
| 6 | Neg | 10 | PCa | | | 5 (8) | 0 | 1 (2) |

**Conclusions:** Compared to standard biopsy, MP-MRI/US fusion-guided biopsy had higher detection rate of PCa but not high-risk PCa. Targeted fusion biopsy alone could also miss clinically significant PCa.

## 990 Metastatic Carcinoma Suggestive of Urothelial Carcinoma in the Absence of Known High-Stage Urothelial Carcinoma: Analysis of Clinical and Pathologic Parameters

Ifeoma Onwubiko[1], Shannon Rodgers[2], Oluwayomi Oyedeji[1], Kanika Taneja[1], Oudai Hassan[1], Nilesh Gupta[1], Sean Williamson[1]
*[1]Henry Ford Health System, Detroit, MI, [2]Henry Ford Hospital, Detroit, MI*

**Disclosures:** Ifeoma Onwubiko: None; Shannon Rodgers: None; Oluwayomi Oyedeji: None; Kanika Taneja: None; Oudai Hassan: None; Nilesh Gupta: None; Sean Williamson: None

**Background:** Urothelial carcinoma that is pT2 or higher is known to be an aggressive disease. However, we have encountered occasional biopsies of metastatic carcinoma with features suggestive of urothelial carcinoma in patients who have no known high-stage primary tumor.

**Design:** We searched our pathology database for reports indicating metastatic carcinoma with findings suggesting urothelial carcinoma. Clinical and pathologic data were reviewed to identify patients without a known high-stage primary tumor.

**Results:** Search identified 272 specimens showing metastatic carcinoma suggestive of urothelial carcinoma. Of these, 14 patients had no known primary tumor of pT2 or higher on comprehensive pathology and electronic medical record review, including 10 (71%) pT1, 3 (21%) carcinoma in situ, and 2 (14%) pTa. A substantial number (n=8, 57%) had tumors of the renal pelvis (n=5), ureter (n=1), or prostatic urethra (n=2). Metastatic sites included the lungs (n=4), liver (n=4), bone / soft tissue (n=3), brain (n=2), and lymph nodes (n=2). Unique patients included one with a renal pelvis high-grade papillary urothelial carcinoma concurrent with multiple sites of clear cell adenocarcinoma thought to be also of urinary tract origin. Another patient had prominent inflammatory / myxoid changes surrounding the ureter that was resected to relieve obstruction; however, no carcinoma was sampled in this specimen.

**Conclusions:** A high proportion of patients with metastatic carcinoma suggestive of urothelial carcinoma in the absence of a high-stage primary tumor (pT2 or higher) have had a primary tumor in uncommon sites, including the renal pelvis, prostatic urethra, or ureter (57%). This raises the possibility that current staging parameters and pathologic evaluation for non-bladder primary tumors are not entirely adequate for assessing their risk.

## 991 Response to Immune Checkpoint Therapy and Clinical Outcome is Not Related to Proportion of Sarcomatous Component in Sarcomatoid Renal Cell Carcinoma

Diana Oramas[1], TaeBeom Kim[2], Ken Chen[1], Priya Rao[1], Pheroze Tamboli[1], Jose Karam[1], Daniel Shapiro[1], Kanishka Sircar[1]
*[1]The University of Texas MD Anderson Cancer Center, Houston, TX, [2]The University of Texas MD Anderson Cancer Center, Pearland, TX*

**Disclosures:** Diana Oramas: None; TaeBeom Kim: None; Ken Chen: None; Priya Rao: None; Pheroze Tamboli: None; Daniel Shapiro: None; Kanishka Sircar: None

**Background:** Renal cell carcinoma with sarcomatoid features (sRCC) is an advanced, treatment resistant phenotype of RCC that is associated with a very poor prognosis. Recent studies have shown promising responses to immune checkpoint therapy in sRCC and also that the sarcomatous component of this tumor has a higher immunohistochemical expression of PD-1/PD-L1 compared to the epithelioid component. Therefore, in the current study we aim to determine the overall survival (OS) of patients with sRCC treated with immunotherapy according to the percentage of the sarcomatous component.

**Design:** We retrospectively identified a cohort of 33 cases with sRCC treated with immunotherapy at MD Anderson Cancer Center between 2013 to 2017.The diagnosis and percentage of sarcomatous component was confirmed by genitourinary pathologists. We abstracted patient demographics, cancer and treatment-specific data such as stage, percentage of sarcomatous component, and type of treatment. Our outcome measure was OS in the whole cohort and stratified by percentage of sarcomatous component. We divided percentage of sarcomatous component into 2 groups: ≥ 50% and ≤ 50%. Patients were categorized as responders and non-responders to immunotherapy. OS follow up, time to death and time to progression from diagnosis date were completed for all patients. All analyses were conducted in R using survival package.

**Results:** The patient demographics and clinicopathologic data for the sRCC cohort are summarized in Table 1. Out of the 33 patients, 14 (42.4%) died during the study period. The OS in the whole cohort was 3.13 years (95% CI: 2.65 – NA). Although the proportion of patients surviving at the end of the study period was higher among those with ≥ 50% sarcomatous component, the analysis did not reach statistical significance (62.5% vs 42%, p = 0.39) (Figure 1). In a sensitivity analysis restricted to T3 and T4 tumors, our results did not change.

**Table 1. Demographic and Cancer Treatment Results**

| | **≤50% (n=22)** | **≥50% (n=11)** | **Overall (n=33)** |
|---|---|---|---|
| **Age**<br>Mean (SD) | 62.8 (12.1) | 60.6 (9.41) | 60.4 (11.1) |
| **Race**<br>White<br>Non-white | 17 (77.3%)<br>5 (22.7%) | 8 (72.7%)<br>3 (27.3%) | 25 (75.8%)<br>8 (24.2%) |
| **Gender**<br>Male<br>Female | 14 (63.6%)<br>8 (36.4%) | 7 (63.6%)<br>4 (36.4%) | 21 (63.6%)<br>12 (36.4%) |
| **Stage AJCC 8th edition**<br>T1<br>T2<br>T3<br>T4 | 1 (4.5%)<br>2 (9.1%)<br>16 (72.7%)<br>3 (13.6%) | 0 (0%)<br>0 (0%)<br>11 (100%)<br>0 (0%) | 1 (3.0%)<br>2 (6.1%)<br>27 (81.8%)<br>3 (9.1%) |
| **Survival time in years**<br>Mean (SD)<br>Median (Min, Max) | 2.46 (1.30)<br>2.41 [0.534, 5.76] | 2.89 (1.65)<br>3.09 [0.663, 5.42] | 2.60 (1.42)<br>2.56 [0.534, 5.76] |

Figure 1 - 991

**Overall Survival by Percentage of Sarcomatous Component.**

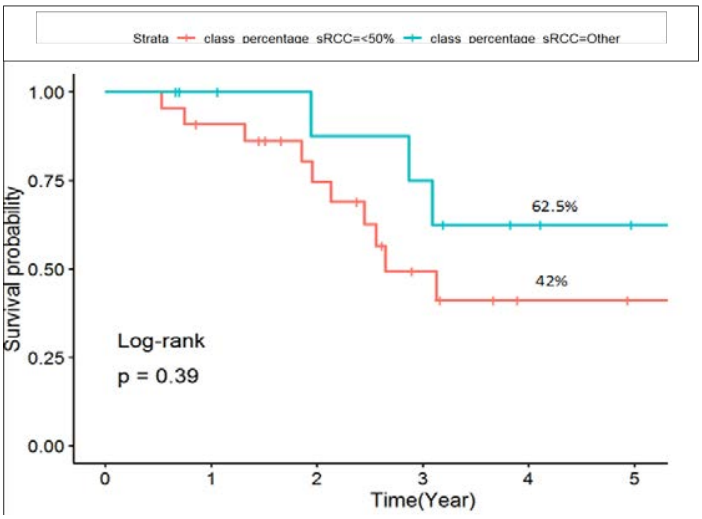


**Conclusions:** Our findings suggest that response to immune checkpoint blockade and associated survival in sRCC are not correlated to the intratumoral fraction of the histological sarcomatous component. However, larger validation studies are indicated to establish the role of histologic intratumoral heterogeneity as markers of response to immune therapies.

## 992 Multifocality of Prostate Cancer and Implication for Focal Therapy

Domenika Ortiz[1], Oleksii Iakymenko[2], Isabella Lugo[3], Ivan Nemov[4], Oleksandr Kryvenko[4]
*[1]University of Miami Miller School of Medicine/Jackson Memorial Hospital, Miami, FL, [2]Jackson Memorial Hospital, Miami, FL, [3]University of Miami, Davie, FL, [4]University of Miami Miller School of Medicine, Miami, FL*

**Disclosures:** Domenika Ortiz: None; Oleksii Iakymenko: None; Isabella Lugo: None; Ivan Nemov: None; Oleksandr Kryvenko: None

**Background:** Prostate cancer is often multifocal. Separate tumor nodules (TN) in the same gland can have different Grade Group (GG) and tumor volume (TV). We investigate how often the highest TV, highest grade, highest Gleason pattern4 (GP4) percentage (for GG2 & 3), extraprostatic extension (EPE), seminal vesicle invasion (SVI), and positive surgical margin (M+) do not occur in the same TN at radical prostatectomy (RP).

**Design:** 1,306 continuous entirely submitted RPs performed from 2014-2019 were reviewed. TNs were considered spatially separate if they were ≥3 mm apart in a plane of section or ≥4 mm on adjacent sections. Each TN was graded, staged, and its volume assessed. We documented GP4% for GG2 & 3 TNs.

**Results:** 1,272 treatment naïve RPs were included. The median age was 63 y (range, 38-85) and median PSA levels was 6.4 ng/ml (range, 0.3-181.9). We excluded cases with extensive bilateral (74/5.8%) and 1 TN (260/20.4%) leaving 938 (73.7%) cases with ≥2 TNs with (mean, 4.5; range, 2-7). In 13/195 (6.7%) GG1 RPs, EPE occurred always in the largest TN; 18 (9.2%) had M+, which 1 case occurred in the smaller TN; no SVI was present. In 95/743 (12.8%) GG2-5 RPs, highest grade TN was not the largest. EPE was present in 351 (47.2%) RPs in the largest and highest grade TN; 12 (1.6%) RPs also had EPE in the smaller lower grade TN; 19 (2.6%) RPs had EPE only in the smaller lower grade TN. 39 (5.2%) RPs had intraprostatic incision in the highest grade and 12 (1.6%) in the lower grade TN. 165/743 had M+ in the dominant TN (1 in dominant and secondary). 19 had M+ in secondary TN (12 in the area of intraprostatic incision and 7 in EPE). SVI was present in 69/71 (9.3%) RPs in TN with highest grade and volume, and 2 (0.3%) in highest grade but lower volume. 226 RPs had ≥2 TNs with GG2 or higher: 2 TNs – 171, 3 TNs – 50; 4 TNs – 4, 5 TNs – 1. The dominant TN was bilateral in 46 (20.4%); primary and secondary TNs were bilateral in 155 (68.6%); 25 (11%) had unilateral primary and secondary TNs. Among these, 88 (39%) had GG2 and 57 (25.2%) GG3 in the dominant TN. 19/88 GG2 and 2/57 GG3 cases had smaller TN with the same GG and higher GP4%.

**Conclusions:** Although the largest grade and volume do not coincide in the same TN in 12.8% of multifocal disease cases, the adverse RP outcomes occur only in 2.9% in smaller TN. 30% of RPs have ≥2 TNs with significant GG (2-5). Of these only 11% can be suitable for unilateral focal therapy and 15% of GG2&3 case have lower volume TN with higher GP4%.

## 993 An Optimized and Validated Chromogenic "8-Color" Multiplex Immunohistochemical Process for T-Cell Subtyping in the Prostate Cancer Tumor Microenvironment

Busra Ozbek[1], Onur Ertunc[1], Andrew Erickson[2], Igor Damasceno Vidal[1], Gunes Guner[3], Jessica Hicks[4], Tracy Jones[4], Angelo De Marzo[1]

*[1]Johns Hopkins University, Baltimore, MD, [2]University of Oxford, Oxford, United Kingdom, [3]Baltimore, MD, [4]Johns Hopkins University School of Medicine, Baltimore, MD*

**Disclosures:** Busra Ozbek: None; Onur Ertunc: None; Andrew Erickson: None; Igor Damasceno Vidal: None; Gunes Guner: None; Jessica Hicks: None; Tracy Jones: None; Angelo De Marzo: None

**Background:** Multiplex immuno-staining is important for immuno-oncology studies in which co-localization of multiple antigens on the same cell is often required to phenotype specific immune cell populations. While newer technologies are emerging, two main approaches are being widely deployed. The first is multiplex immunofluorescence using tyramide-based dyes (e.g. Opal™ Staining Kits from AKOYA Biosciences), that requires fluorescent slide scanning and spectral unmixing, and the second is iterative staining using chromogenic IHC (PMID: 28380359). Iterative chromogenic IHC provides advantages such as the ability to use standard brightfield whole slide scanners (PMID: 28380359). However, workflows for image handling are in flux and this approach has not been applied to prostate cancer tissues.

**Design:** FFPE slides were used for sequential IHC consisting of cycles of staining, scanning, chromagen dissolution and heat-induced antibody removal. Using this approach, we validated and optimized an IHC panel consisting of PD-1, CD3, CD8, CD4, FOXP3, P63, CK8 and hematoxylin, providing 8 eight-pseudo colors per slide. Slides were scanned using either a Roche/Ventana DP200 or a Hamamatsu XR. Scanned whole slide images were registered and pseudo-fluorescent layers were created using the HALO™ image analysis platform (Indica Labs). The High-Plex FL algorithm was used for cell identification and specific cell-type counting in regions of interest (ROI).

**Results:** We first compared HALO™ cell counting to manual cell counting for ROI across different standard slides from prostatectomies; results were concordant for CD3 ($R^2=0.8$, $p=0.001$), CD8 ($R^2=0.92$, $p<0.001$), CD4 ($R^2=0.86$, $p<0.001$), and FOXP3 ($R^2=0.84$, $p<0.001$). To ensure that iteratively stained slides did not lose immunogenicity, and hence result in procedure induced reductions in cell numbers, iteratively stained prostate tissue microarray slides were compared with serial sections of adjacent singleplex chromogenically stained slides for CD3, CD8, and FOXP3. The number of cells positive in multiplex IHC correlated with singleplex for CD3 ($R^2=0.87$, $p<0.001$), CD8 ($R^2=0.94$, $p<0.001$), CD4($R^2=0.96$, $p<0.001$), and FOXP3($R^2=0.74$, $p<0.001$).

Figure 1 - 993

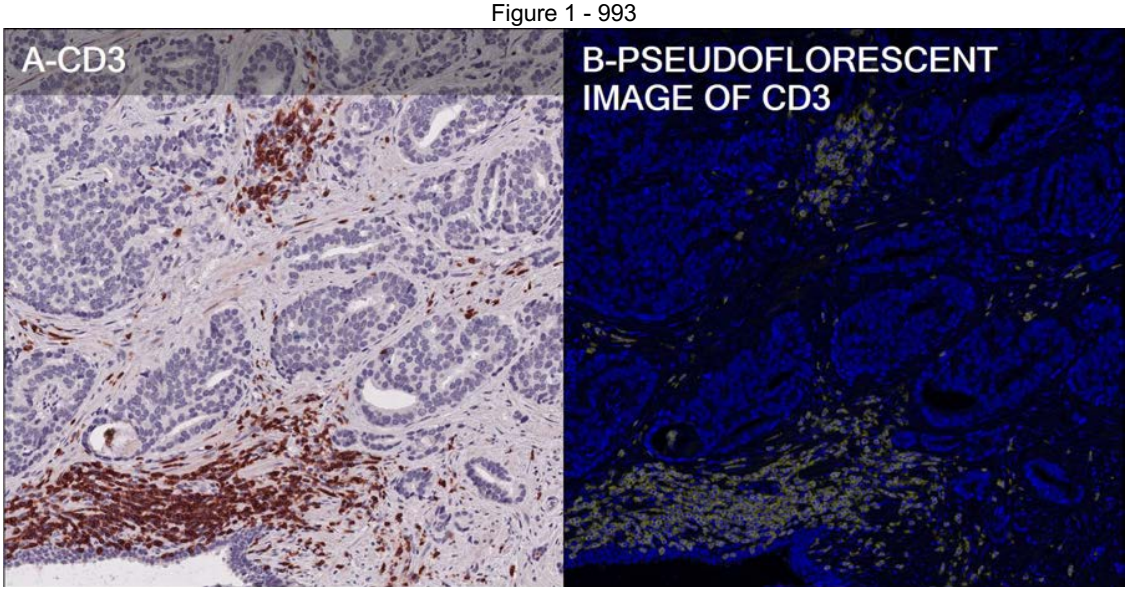

Figure 2 - 993

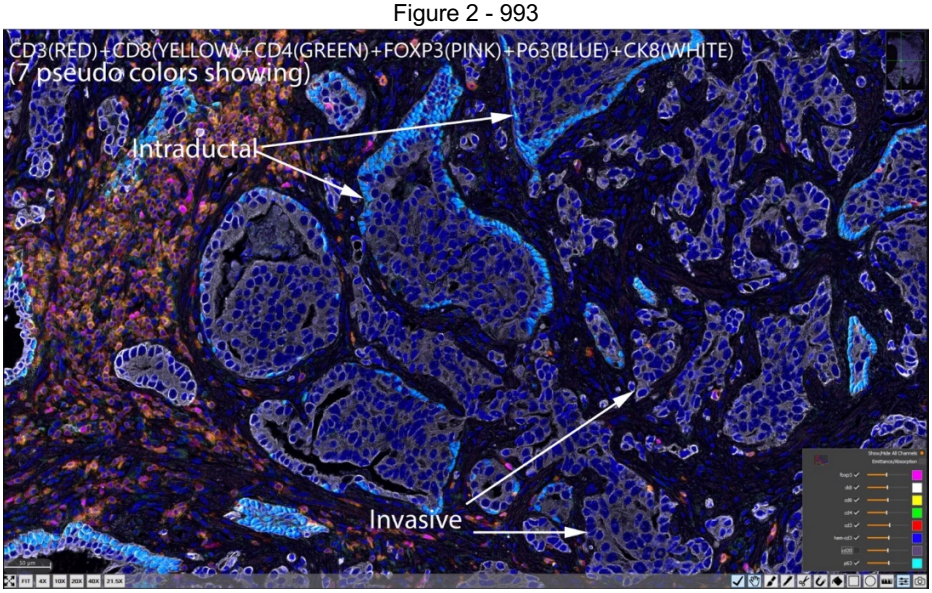


**Conclusions:** We optimized and validated a chromogenic multiplex IHC assay using 7 antibodies for T-Cell subtyping in immuno-oncology studies in prostate cancer, and implemented a digital image processing workflow using commercially available software (HALO™). This approach can be applied to any set of IHC markers.

## 994 Coexistence of Angiomyolipomas and Renal Cell Neoplasms in Non-Tuberous Sclerosis Patients: Study of a Series of 38 Cases

Angel Panizo[1], Francisco J Queipo[2], Luiz M Nova[1], Tamara Zudaire[1], Irene Fernández[1], Maria Zelaya[1], Gregorio Aisa[3], Rosa Guarch[1]

*[1]Complejo Hospitalario de Navarra, Pamplona, Navarra, Spain, [2]Hospital San Jorge, Huesca, Aragón, Spain, [3]Complejo Hospitalario de Navarra, Pamplona, Spain*

**Disclosures:** Angel Panizo: None; Francisco J Queipo: None; Luiz M Nova: None; Tamara Zudaire: None; Irene Fernández: None; Maria Zelaya: None; Gregorio Aisa: None; Rosa Guarch: None

**Background:** Most cases of angiomyolipomas (AML) are sporadic; however, they are extremely common in tuberous sclerosis complex (TSC). Concurrent renal cell neoplasms (RCN) and AML are rare: very few studies have addressed this association outside of TSC. The aim of this study was to investigate the clinicopathological features of concurrent AML and RCN in non-TSC patients.

**Design:** We searched the pathology files at our institutions for partial/radical nephrectomy, or autopsy specimens from 1980 to 2019: non-TSC patients with coexistent, precedent, or subsequent RCN and AML. Clinical data were extracted from medical records. Macroscopic and H&E sections of each neoplasm were reviewed. RCNs were classified according to the 2016 WHO criteria, and staged according AJCC 8th Ed. IHC with melanocytic markers was performed. AML were assessed for size, subtype, and topographic relationship with the RCN.

**Results:** A total of 121 AML were identified (8 cases in TSC). Of 113 AML, we identified 38 cases (33.6%) with RCN in non-TSC patients. Age range was 35-90 yrs. (mean: 64.2 yrs.): 21 males and 17 women. The mean size of the RCN was 5.3 cm (range: 1.3-12.5 cm). The RCN included 13 ccRCCs, 8 ChRCCs, 8 oncocytomas, 3 urothelial carcinomas, 2 papillary RCCs, 2 TFE3 RCCs, 1 mucinous tubular and spindle-cell RCC, and 1 unclassified RCC. 25 RCN were intrarenal (19 pT1; 6 pT2), 12 pT3 and 1 pTis urothelial carcinoma. In 23 cases, neoplasms occurred synchronously in the right kidney, in 13 in the left, in 1 they were bilateral, and in 1 the left RCN preceded a contralateral right AML. In 25 cases, AML and RCN were located far in different areas of the kidney. The mean size of the AMLs was 0.8 cm (range: 0.1-3.4 cm). All but four patients had a single AML, and 6 cases had two RCN. Histologically, 16 AMLs were triphasic, 9 adipocytic-predominant, 7 epithelioid-predominant, and 6 leiomyomatous-predominant. Follow-up information was available in 31 cases (median follow-up 38 months; range 2-284 months): 23 patients were alive without disease, 3 alive in progression, 3 died of disease, and 2 died without disease.

Figure 1 - 994

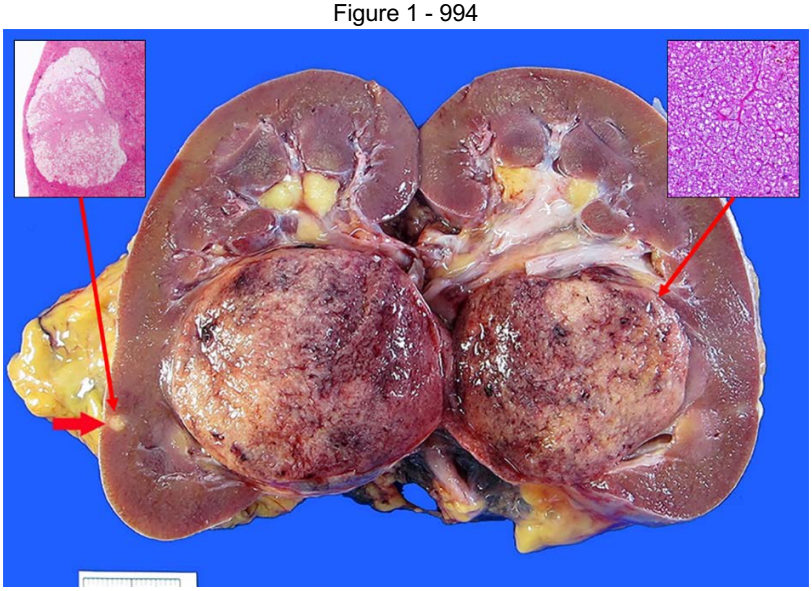

Figure 2 - 994

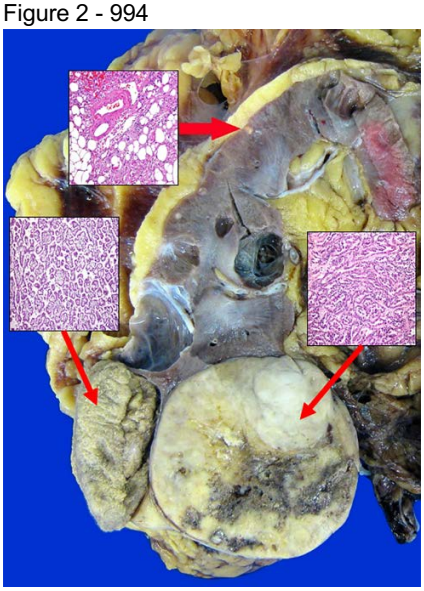

**Conclusions:** The coexistence of RCN with AML in non-TSC is a rare event: 38 cases in our study, rendering the largest series to date of this unique association. Clear-cell RCC was the most common RCN associated with AML. Interestingly, chromophobe RCC and oncocytoma were the second most common RCN identified (eight cases each). AMLs associated with RCNs in non-TSC patients were predominantly non-epithelioid.

## 995 Sarcomatoid Urothelial Carcinoma: Contemporary Analysis of 93 Cases with Emphasis in Patients with pT1 Tumors who Underwent Early Cystectomy

Vamsi Parimi (Parini)[1], Kara Lombardo[2], Andres Matoso[2]
*[1]Johns Hopkins University School of Medicine, Elkridge, MD, [2]Johns Hopkins Medical Institutions, Baltimore, MD*

**Disclosures:** Vamsi Parimi (Parini): None; Kara Lombardo: None; Andres Matoso: None

**Background:** Sarcomatoid urothelial carcinoma (SUC) is an unusual variant that bears poor prognosis. Guidelines recommend consideration for early cystectomy (RC) in patients with SUC and pT1 tumors. We studied clinicopathologic parameters associated with prognosis including 6 patients with pT1 tumors who underwent RC.

**Design:** A retrospective review identified 93 patients who were diagnosed as SUC between 1993 and 2018. H&E were reviewed by expert GU pathologists (VP and AM) and tumor size, size of sarcoma component and percent of sarcoma were annotated. T-test and Spearman correlation tests were used to assess clinicopathologic outcomes.

**Results:** Median age was 70 yrs; male:female ratio was 3.5:1. In 30% cases, biopsy/TURB did not identify SUC. Twelve patients did not undergo definitive surgical resection. The remaining 81 underwent the following resection procedures: RC= 13, partial cystectomy= 4, cystoprostatectomy= 59, and anterior exenteration= 5. Of 93, 27% were 100% sarcomatoid, and 73% were mixed with conventional UC; 12% of SUC showing chondroid, osteoid and rhabdoid differentiation; rest were non-specific spindle cell phenotype. Average size of total tumor and SUC component was 6cm (SD ± 3.7cm) and 4.5cm (SD ± 3.7cm) respectively. The distribution of SUC by T stage (pretreatment) was 6%, 31%, 41% and 17% (T1, T2, T3 and T4); 5% were unknown. The average OS was 30 months (range 1-198 months). The mean OS without RC was shorter (8.3 months; $p<0.05$). The mean SUC tumor size at RC among patients receiving no neoadjuvant chemotherapy (NAC) vs NAC was 4.6 and 2.8 cm respectively (T-test, $p>0.05$). There were 6 patients with pT1 tumors with an average age of 68 years and were all males. Four patients had SUC associated with papillary UC, one with flat carcinoma in-situ and one with squamous cell carcinoma. Two pT1 patients received NAC and both had no residual tumor at RC. Four of six patients were alive at an average follow-up of 49 months (1 with metastatic disease, 3 with no evidence of disease), 1 died of disease (patient with small cell carcinoma) and 1 was lost to follow-up.

**Conclusions:** Our data suggests that neither size of tumor nor percent of the sarcomatoid component correlate with survival. Despite the small number of patients with pT1 tumors, they seem to have better survival after cystectomy suggesting that early radical surgery in these patients could be beneficial. NAC also correlated with better outcomes.

## 996 Urothelial Carcinoma with Small Cell Carcinoma Component: Comparison of Pure Small Cell Carcinoma versus Mixed Small Cell Carcinoma with Invasive Conventional Urothelial Carcinoma

Vamsi Parimi (Parini)[1], Kara Lombardo[2], Andres Matoso[2]
*[1]Johns Hopkins University School of Medicine, Elkridge, MD, [2]Johns Hopkins Medical Institutions, Baltimore, MD*

**Disclosures:** Vamsi Parimi (Parini): None; Kara Lombardo: None; Andres Matoso: None

**Background:** Small Cell Urothelial Carcinoma (SCUC) is a rare and there has not been a study comparing pure small cell carcinoma versus small cell carcinoma mixed with conventional invasive urothelial carcinoma.

**Design:** A retrospective review of the institutional pathology database was performed to identify 44 patients from 2011 and 2019. H&E slides were reviewed by two expert GU pathologists (VP and AM) and grouped into PSCC and MUSCC. Descriptive statistics comparing clinicopathologic outcomes were performed using T-test, Chi-Square and Spearman correlation tests. Univariable and multivariable Cox regression analyses tested the size of SUC on recurrence, cancer-specific mortality (CSM), and overall mortality (OM) after accounting for all available confounders.

**Results:** There were 21 patients with PSCC and 23 with MUSCC. Median age was 68 yrs in PSCC and 66 years in MUSCC; male: female ratio is 6:1 in PSCC and 4.8:1 in MUSCC. All except 1 patient in PSCC and all except 2 patients in MUSCC received neoadjuvant chemotherapy (NAC). 8/21 (38%) of PSCC and 7/23 (30.4%) of MUSCC had distant metastasis at diagnosis. 13/21 (62%) in PSCC and 16/23 (70%) in MUSCC underwent radical cystectomy (RC). The overall size of the tumor in the cystectomy specimens was similar (3.65 and 3.47 cm). The non-small cell component within MUSCC included urothelial and sarcomatoid (n=2), squamous carcinoma (n=1), and conventional urothelial carcinoma (n=20). The pathologic stage at RC were similar in both groups with only one complete response in each group and the majority were ypT2 and ypT3 tumors. RC lymph nodes were positive in 5/13 (38%) PSCC and in 4/16 (25%) of MUSC. After cystectomy, 6 PSCC and 8 MUSCC patients developed distant metastasis. The overall survival was similar in both groups (average months of survival is 23 in PSCC and 28 in MUSCC; p=0.09).

**Conclusions:** Our data emphasis the overall poor prognosis of small cell carcinoma of the bladder and shows that cases that are pure small cell carcinoma have similar prognosis than those with tumors that are mixed with conventional invasive urothelial carcinoma. These results argue against reporting percent of the small cell carcinoma component in the urinary bladder.

## 997 A Molecular Comparison of Intraductal Carcinoma of the Prostate, Associated Invasive High Grade Prostatic Carcinoma, and Lymph Node Metastases by Copy Number Alteration Analysis

Kyung Park[1], Brian Robinson[2], Mai Ho[3], Kartik Viswanathan[4], Swarna Gogineni[5], Juan Miguel Mosquera[2], Christopher Barbieri[3], Tamara Lotan[6], Massimo Loda[2], Susan Mathew[2], Alain Borczuk[2], Francesca Khani[2]
*[1]NYU Langone Health, New York, NY, [2]Weill Cornell Medicine, New York, NY, [3]Weill Cornell Medical College, New York, NY, [4]New York-Presbyterian Hospital/Weill Cornell Medical Center, New York, NY, [5]New York-Presbyterian/Weill Cornell, Foresthills, NY, [6]Johns Hopkins School of Medicine, Baltimore, MD*

**Disclosures:** Kyung Park: None; Brian Robinson: None; Mai Ho: None; Kartik Viswanathan: None; Swarna Gogineni: None; Juan Miguel Mosquera: None; Christopher Barbieri: None; Tamara Lotan: None; Massimo Loda: None; Susan Mathew: None; Alain Borczuk: None; Francesca Khani: None

**Background:** Intraductal carcinoma of the prostate (IDC-P) is considered a harbinger of aggressive disease and is associated with poor clinical prognosis. It is believed to represent retrograde spread of high grade invasive carcinoma into the prostatic ductular system, although there is minimal molecular evidence to support this theory. We aimed to further study the molecular evolution of IDC-P and how it relates to invasive carcinoma and tumor metastases.

**Design:** Radical prostatectomy specimens where the dominant tumor nodule had an abundant IDC-P component (>20%) were identified. Cases were reviewed by GU pathologists to annotate areas of IDC-P and high grade ($\geq$ Grade Group 3) invasive carcinoma (HGIC) in ten selected cases. Five cases also had lymph node metastases. DNA was extracted from each macrodissected area and subjected to copy number alteration (CNA) analysis using the OncoScan Assay (Affymetrix). CNA was performed using the Oncoscan Nexus Express software v3.0. FISH was utilized to validate particular key findings with centromeric probes for chromosomes 8, 10, and 12.

**Results:** Similar 8p and 10q losses were seen in both the IDC-P and high grade invasive carcinoma in all 10 cases, and 8q gains were also seen in both areas in 7 cases. In 3 of 10 cases, the IDC-P component showed copy number gains spanning the entire genome in the regions without chromosomal losses, and in one of these cases, the HGIC area showed similar whole genome gains. In addition, those non-amplified regions of chromosomal loss are common to the HGIC and IDC-P components, including both deletion and uniparental disomy. In 2 of 5 cases, the lymph node metastases also showed a copy number profile that was more similar to IDC-P than it was to HGIC, including one case with whole genome gain. Whole genome gains were further validated by FISH, which showed a mixed population of cells containing a range of 2-5 copies of each of the selected chromosomes.

**Conclusions:** IDC-P and invasive high grade carcinoma are clonally related, as evidenced by similar focal chromosomal gains and losses. Whole genome gains are seen in IDC-P, and share the same loss pattern with HGIC. This suggests a clonal evolution from invasive carcinoma to IDC-P in some cases. The copy number alteration pattern of the lymph node metastases is sometimes more similar to IDC-P than it is to HGIC, suggesting that the tumor clones present within IDC-P have metastatic potential.

## 998 Comprehensive Genomic Profiling Identifies Frequent Recurrent NF2 Genomic Alterations in Advanced Papillary Renal Cell Carcinoma

Carmen Perrino[1], Melissa Stanton[2], Benedito Carneiro[3], Shaolei Lu[4], Jon Chung[5], Siraj Ali[6], Evgeny Yakirevich[7], Jeffrey Ross[8]
*[1]Sharon, MA, [2]Mayo Clinic Arizona, Phoenix, AZ, [3]Brown University, Alpert Medical School, Lifespan Cancer Institute, Providence, RI, [4]Alpert Medical School of Brown University, Providence, RI, [5]Foundation Medicine, Inc., Cambridge, MA, [6]Cambridge, MA, [7]Rhode Island Hospital, Providence, RI, [8]Upstate Medical University, Syracuse, NY*

**Disclosures:** Carmen Perrino: None; Melissa Stanton: None; Benedito Carneiro: None; Shaolei Lu: None; Jon Chung: *Employee*, Foundation Medicine; *Stock Ownership*, Roche; Siraj Ali: *Employee*, Foundation Medicine; *Advisory Board Member*, INcysus Therapeutics; *Consultant*, Takeda; Evgeny Yakirevich: None; Jeffrey Ross: *Employee*, Foundation Medicine

**Background:** *Neurofibromatosis type 2 (NF2)* gene is a tumor suppressor gene involved in tumor cell proliferation, growth, and apoptosis. Frequent genomic alterations (GAs) in *NF2* have recently been described in aggressive kidney tumors, including collecting duct carcinoma (29%), sarcomatoid RCC (19%), and unclassified RCC (19%). We queried whether *NF2* GAs are present in clinically advanced cases of papillary RCC (PRCC).

**Design:** Comprehensive genomic profiling (CGP) was performed on FFPE samples from 285 cases of clinically advanced PRCC. Tumor mutational burden (TMB) was determined on 0.8 to 1.1 Mbp of sequenced DNA and microsatellite instability (MSI) was determined on 114 loci. PD-L1 expression in tumor cells (Dako 22C3) was measured by IHC.

**Results:** Thirty seven (13%) PRCC cases featured *NF2* GAs (92% short variant [SV] mutations, 5% copy number changes, 3% gene rearrangements). The age and gender were similar in both *NF2*mut and *NF2*-wild type (*NF2*WT) PRCCs (Table). All *NF2*mut cases were stage IV, 92% had histologic features of PRCC type 2, and 6 (16%) exhibited sarcomatoid differentiation (10-80% of tumor). Twenty-one *NF2*mut samples used for CGP were metastatic biopsies and 16 were primary kidney tumors. Other than the potentially targetable *NF2* status, the frequencies of both currently not targetable and targetable GAs were similar in both groups. Among the most frequent GAs, PRCC *NF2*mut had 17% *FH* GAs versus 9% in *NF2*WT cases. Among the other potentially targetable GAs, the *NF2*WT PRCC cases had a significantly higher frequency of *MET* GAs equally divided into SV mutations and amplifications, while no *MET* GAs were identified in *NF2*mut tumors. Rare targetable GAs in *BRCA1* and *PIK3CA* were identified in both groups and GAs in *ERBB2* and *BRAF* were found in *NF2*WT cases only. There were no MSI-high cases and the TMB was low with almost no cases featuring TMB > 10mut/Mb in either the *NF2*mut or *NF2*WT group. PD-L1 IHC staining was relatively low in both groups, although *NF2*WT featured 11% of cases with PD-L1 high expression versus 0% in *NF2*mut group (p=0.01).

| | PRCC NF2 Mutated | | PRCC NF2 Not Mutated | |
|---|---|---|---|---|
| Cases | 37 | | 247 | |
| Gender | Male 76%; Female 24% | | Male 74%; Female 26% | |
| Median Age/Range (years) | 60 (23-78) | | 63 (22-88) | |
| GA/tumor | 3.1 | | 2.7 | |
| Most Frequently Altered Genes | *NF2*<br>*CDKN2A*<br>*CDKN2B*<br>*FH*<br>*SETD2*<br>*TERT*<br>*BAP1*<br>*SDHA* | 100%<br>29%<br>18%<br>17%<br>13%<br>9%<br>8%<br>6% | *TERT*<br>*CDKN2A*<br>*CDKN2B*<br>*MET*<br>*SETD2*<br>*FH*<br>*ARID1A*<br>*PBRM1*<br>*SMARCB1*<br>*TP53* | 23%<br>19%<br>13%<br>11%<br>9%<br>9%<br>9%<br>9%<br>9%<br>7% |
| Potential Targeted Therapy Impacting Alterations | *NF2*<br>*BRCA1*<br>*PIK3CA*<br>*NF1* | 100%<br>3%<br>3%<br>3% | *MET*<br>*PIK3CA*<br>*BRAF*<br>*ERBB2*<br>*BRCA1* | 11%<br>5%<br>3%<br>3%<br>2% |
| MSI High Status | 0% | | 0% | |
| TMB Median (mut/Mb) | 2.6 | | 2.6 | |
| TMB > 10 mut/Mb | 0% | | 1% | |
| TMB > 20 mut/Mb | 0% | | 0.4% | |
| PD-L1 IHC Low | 19% | | 7% | |
| PD-L1 IHC High | 0% | | 11% | |

**Conclusions:** Recurrent *NF2* GAs are present in 13% of advanced PRCCs and could represent a potential therapeutic target. Alterations in *NF2* and *MET* genes are mutually exclusive. Based on low TMB and low PD-L1 expression, *NF2*mut cases are not likely candidates for immunotherapy.

## 999 Oncocytic Papillary Renal Cell Carcinoma: Morphologic and Immunohistochemical Analysis of Three Distinct Genetic Subgroups

Kristyna Pivovarcikova[1], Reza Alaghehbandan[2], Petr Grossmann[3], Kvetoslava Michalova[4], Bohuslava Saskova[5], Pavla Rotterova[6], Joanna Rogala[7], Michal Michal[3], Ondrej Hes[8]
*[1]Biopticka Laborator Plzen, Plzen, West Bohemia, Czech Republic, [2]Royal Columbian Hospital, University of British Columbia, New Westminster, BC, [3]Biopticka laborator s.r.o., Plzen, Czech Republic, [4]Biopticka Laborator Ltd., Plzen, Czech Republic, [5]Biopticka Laborator Plzen, Plzen, Czech Republic, [6]Biopticka laborator s.r.o., Pilsen, Czechia, Czech Republic, [7]Wroclaw, Lower Silesia, Poland, [8]Biopticka laborator s.r.o., Plzen, Plzensky kraj, Czech Republic*

**Disclosures:** Kristyna Pivovarcikova: None; Reza Alaghehbandan: None; Petr Grossmann: None; Kvetoslava Michalova: None; Bohuslava Saskova: None; Pavla Rotterova: None; Joanna Rogala: None; Michal Michal: None; Ondrej Hes: None

**Background:** Neoplasms with oncocytic features are known in various organs (i.e., thyroid gland, adrenal gland, parotid gland, kidney etc.). Oncocytic cell is defined as a cell in which its cytoplasmic is packed with mitochondria. Oncocytic papillary renal cell carcinoma (OPRCC) is a provisional entity in current WHO 2016, but the entity is still poorly understood and the key diagnostic features have not yet been determined. The aim of this study was to investigate and define morphological, immunohistochemical or molecular genetic features for this entity.

**Design:** We analyzed 34 OPRCCs in adult patients. Cases were divided into 3 distinct groups according to their chromosomal copy number variation pattern (CNV) as follows: 1) OPRCC with CNV identical to renal oncocytoma (10 cases), 2) OPRCC with gains of chromosomes 7 and 17 (7 cases), and 3) OPRCC with variable CNV (17 cases). All OPRCCs were analyzed by morphology and immunohistochemistry, followed by *CCND1* gene analysis.

**Results:** Clinical and demographic data (i.e., age, gender, tumor stage) between the three groups were similar. All tumors showed papillary/tubulopapillary architecture lined by oncocytic cells (confirmed by antimitochondrial antigen antibody (MIA)). There were no significant differences in architectural or cytologic tumor grade among all cases, but immunohistochemical profile was variable. All cases were positive for MIA and vimentin. Immunoreactivity for CK7, CK20, AMACR, cyclin D1, GATA3, and carboanhydrase IX was variable across the three groups. All tumors were negative for CD117, TFE3, HMB45, and Melan A. No correlation between immunoprofile and CNV status was found. Rearrangement of *CCND1* was found in 1 case, gain of *CCND1* in 3 cases. Further, immunohistochemical staining with cyclin D1 did not correlate with the genetics results.

**Conclusions:** Although all OPRCCs (in three groups) were relatively morphologically similar (confirmed by MIA and vimentin with oncocytic cells arranged in papillary/tubulopapillary patterns), the extended immunohistochemical profile found to be highly variable across the three groups as well as within each group. Also morphologic and immunohistochemical features did not correspond with particular CNV. Abnormalities in *CCND1* gene did not have impact on biologic behavior either. In order to further understand this potentially aggressive variant of PRCC, it is necessary to establish seminal features and key diagnostic criteria for this neoplasm.

## 1000 Mixed Epithelial and Stromal Tumor Family - Refining the Diagnostic Criteria by Morphologic and Immunohistochemical Study of 36 Cases

Kristyna Pivovarcikova[1], Kiril Trpkov[2], Reza Alaghehbandan[3], Joanna Rogala[4], Kvetoslava Michalova[5], Pavla Rotterova[6], Bohuslava Saskova[7], Maria Pané Foix[8], Michal Michal[9], Ondrej Hes[10]

*[1]Biopticka Laborator Plzen, Plzen, West Bohemia, Czech Republic, [2]University of Calgary, Calgary, AB, [3]Royal Columbian Hospital, University of British Columbia, New Westminster, BC, [4]Wroclaw, Lower Silesia, Poland, [5]Biopticka Laborator Ltd., Plzen, Czech Republic, [6]Biopticka laborator s.r.o., Pilsen, Czechia, Czech Republic, [7]Biopticka Laborator Plzen, Plzen, Czech Republic, [8]Hospital Universitari de Bellvitge, L'Hospital de Llobregat, Barcelona, Spain, [9]Biopticka laborator s.r.o., Plzen, Czech Republic, [10]Biopticka laborator s.r.o., Plzen, Plzensky kraj, Czech Republic*

**Disclosures:** Kristyna Pivovarcikova: None; Kiril Trpkov: None; Reza Alaghehbandan: None; Joanna Rogala: None; Kvetoslava Michalova: None; Pavla Rotterova: None; Bohuslava Saskova: None; Maria Pané Foix: None; Michal Michal: None; Ondrej Hes: None

**Background:** Mixed epithelial and stromal tumor (MEST) and adult cystic nephroma are presumed to represent different ends of the spectrum of kidney neoplasms, designated as MEST family (MESTF) in the WHO 2016 classification. The morphologic criteria to differentiate MESTF from similar lesions demonstrating “multilocular cyst” (MC) morphology remain to be clarified. Therefore, we compared a cohorts of MESTF and MC to try to refine the discriminating diagnostic criteria.

**Design:** We evaluated 36 MESTF and 19 MC, which were defined as multicystic lesions, composed of thin hypocellular septa covered by flat, hobnail and/or atrophic epithelium. We performed a morphologic analysis and immunohistochemistry (IHC).

**Results:** MESTF group: 35 females and 1 male, with mean age of 54. 1 years (range: 25-74), mean tumor size 7.7 cm (range 1-25). Mullerian-type (MT) stroma was found in 28 cases (in 13 cases only focal); however, 8 MESTF cases showed hypocellular collagenous stroma. Hobnail epithelium was present in all cases, and 13 cases showed MT epithelium (Fig 1). On IHC, the stromal component in all cases was positive for estrogen receptors (ER), progesterone receptors (PR), and CD56; CD10 was positive in 29 (80.5%) cases, and WT1 in 10 (28%) cases. Epithelial cells were reactive for PAX8 in all cases.

MC group: 11 males and 7 females (no clinical information for 1 case). Mean age was 53 years (range 34-79), mean tumor size 3.1 cm (range 0.2-12.5). MT stroma was not identified in any of the cases, while hobnail epithelium was found in 11 (58%) cases (Fig 2). 10 (53%) cases were positive for ER (in 4 focally) and 8 (42%) cases were positive for PR (in 7 focally). WT1, CD56 and CD10 stained the stroma in 5 (26%), 10 (53%), and 1 (5%) case, respectively. Epithelial component stained for both WT1 and CD56 in 3 (16%) cases, PAX8 in 19 (100%), and CD10 in 10 (53%) cases.

Figure 1 - 1000

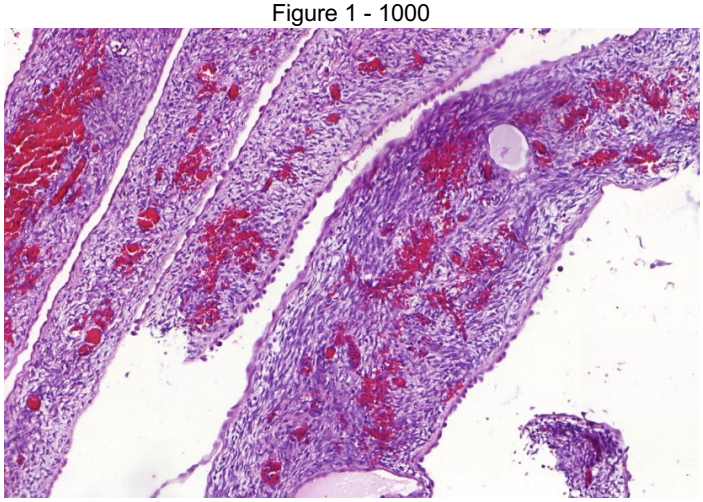

Figure 2 - 1000

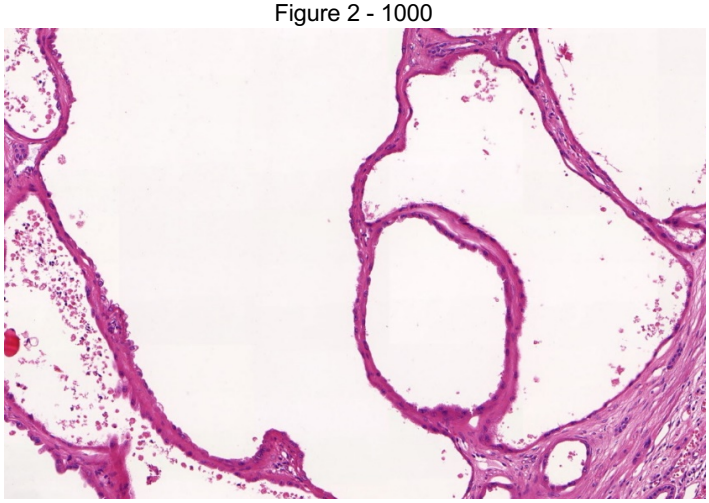

**Conclusions:** Presence of MT stroma appears to be the key diagnostic feature for identifying MESTF. In the cases where the stroma is not prominent, presence of other MT elements (such as epithelium) may help in establishing the diagnosis. IHC may also aid in differentiating MESTF, as majority of these cases are reactive for ER, PR, and CD10. In contrast, these markers were rarely positive in MC. MESTF also

appears to arise almost exclusively in females, which supports the hypothesis that true MESTF are tumors of Mullerian differentiation that are found extremely rarely in men.

## 1001 Urothelial Carcinoma with Trophoblastic Differentiation: A Clinicopathologic Analysis of 15 Cases with Clinical Follow Up

Christopher Przybycin[1], Jesse McKenney[1], Jane Nguyen[1], Rajal Shah[2], Saleem Umar[3], Ie-Ming Shih[4], Roni Cox[5]
*[1]Cleveland Clinic, Cleveland, OH, [2]University of Texas Southwestern Medical Center, Plano, TX, [3]Lake Worth, FL, [4]Johns Hopkins Hospital, Baltimore, MD, [5]Cleveland, OH*

**Disclosures:** Christopher Przybycin: None; Jesse McKenney: None; Jane Nguyen: None; Rajal Shah: None; Saleem Umar: None; Ie-Ming Shih: None; Roni Cox: None

**Background:** Trophoblastic differentiation, including choriocarcinomatous differentiation, has been described in carcinomas arising in multiple organs, including stomach, breast, colon, and lung, as well as the bladder. As prior descriptions of urothelial carcinoma with trophoblastic features are limited to case reports, we compiled a large series of this uncommon tumor (the majority from a single institution) with analysis of the morphological spectrum, application of trophoblast stains not previously studied, and detailed clinical follow up.

**Design:** All H&E slides were reviewed by two study pathologists (CP and RC), noting tumor grade, pT stage, presence of trophoblastic differentiation, and other types of divergent differentiation. Immunohistochemical stains for human chorionic gonadotropin (HCG) and Hydroxyl-δ-5-steroid dehydrogenase (HSD3B1-a trophoblast-specific marker) were performed on cases with available blocks. Clinical history, demographics, and follow up were obtained from the medical record.

**Results:** 15 cases were identified, including 13 bladder tumors (86%), 1 ureteral tumor (7%), and 1 prostatic urethral tumor (7%). Patients included 12 males (80%) and 3 females (20%) with a mean age of 65 (range 44-89). Bladder tumors included 4 pT1 tumors, 6 pT2, 1 pT3a, and 2 pT3b tumors. The ureteral tumor was pT3; the urethral tumor was pT1. Two types of trophoblastic differentiation were identified: 1.Urothelial carcinoma with syncytiotrophoblasts, defined as tumor giant cells with a clustered syncytium of nuclei (6 cases, 40%), and 2.Choriocarcinomatous differentiation, defined as a biphasic proliferation of cytotrophoblasts capped by syncytiotrophoblasts, (9 cases, 60%). The proportion of trophoblastic differentiation ranged from 5% to 100% (mean 53%). Other divergent differentiation included squamous (1 case), glandular (2 cases), lipoid (2 cases), and chordoid/myxoid, (1 case). 11 of the 13 stained cases (85%) were positive for HCG; 13 were positive for HSD3B1 (100%). Follow up (mean 34 months; 2-120 months), available in 13 patients, demonstrated distant metastases in 6 cases (46%) [4 patients with choriocarcinomatous differentiation, 2 patients with syncytiotrophoblasts] and death of disease in 3 cases (19%) [2 with choriocarcinomatous differentiation, 1 with syncytiotrophoblasts].

**Conclusions:** Trophoblastic differentiation in urothelial carcinoma is associated with significant metastatic potential and death from disease. We present the largest series of such tumors to date.

## 1002 HPV Status and World Health Organization 2016 Classification of Penile Squamous Cell Carcinoma and Penile Intraepithelial Neoplasia: 206 Cases from a Single, Contemporary, Western Cohort of Patients with Emphasis on the “Discordant Cases"

Costantino Ricci[1], Luiza Dorofte[2], Tania Franceschini[3], Mattia Riefolo[1], Francesca Giunchi[4], Michelangelo Fiorentino[5], Sabina Davidsson[6], Gabriella Lillsunde-Larsson[7]
*[1]S.Orsola-Malpighi Hospital, University of Bologna, Bologna, Italy, [2]Department of Laboratory Medicine, Faculty of Medicine and Health, Örebro University, Örebro, Sweden, [3]Bologna, Italy, [4]S.Orsola-Malpighi Hospital, Bologna, Italy, [5]Department of Pathology, Sant'Orsola-Malpighi University Hospital, University of Bologna, Bologna, Italy, [6]Örebro University, Faculty of Medicine and Health, Örebro, Sweden, [7]School of Health Sciences, Örebro University, Örebro, Sweden*

**Disclosures:** Costantino Ricci: None; Luiza Dorofte: None; Tania Franceschini: None; Mattia Riefolo: None; Francesca Giunchi: None; Gabriella Lillsunde-Larsson: None

**Background:** Penile squamous cel carcinoma (pSCC) cancer has been considered a rare tumour in the western world. Although some conflicting results, the most recent meta-analyses report an increase in its incidence and in the percentage of HPV(+) cases in numerous western countries. This scenario mirrors what observed for HPV(+) oropharynx cancer and could be explained by changes in sexual practice and in exposure of men to HPV. In this study, we analyzed pathological features and HPV-DNA prevalence in a contemporary, western pSCC cohort.

**Design:** This study enrolled 206 patients with pSCC from Örebro University. DNA was extracted from paraffin-embedded tumor tissue samples, and HPV-DNA genotyping were performed using PCR method Anyplex II HPV28. In a subset of cases, HPV-DNA was also assessed in penile intraepithelial neoplasia (PeIN), lymph node metastasis (LnM) or both (51%, 11.6% and 18.9%). All the cases have been histologically re-classified according to the WHO 2016 classification of pSCC.

**Results:** HPV-DNA was detected in 92/206 (44.7%) pSCC, 78/141 (55.3%) PeIN and 28/61 LnM (45.9%), respectively. HPV16 was the predominant type, representing 78.3% for pSCC, 79.5% for PeIN and 96.4% for LnM. In 7.8% of the cases, more than a HPV genotype has been detected in the same specimen or in different specimens of the same patients. Curiously, we found 8.5% of cases (14/164) with discordance of HPV-DNA detection in different specimens from the same patient (pSCC, PeIN and/or /LnM). In HPV(+) pSCC the predominant histologic subtype was "warty" (41.3%); in HPV(-) pSCC it was "usual" (65.8%). For PeIN, "warty" was the predominant subtype in HPV(+) PeIN (39.7%) and "differentiated" in HPV(-) PeIN (79.4%). For pSCC, we observed disagreement between histology and HPV status in 23.8% of cases: 13.1% HPV(+)/Non-HPV-related histology and 10.7% HPV(-)/HPV-related histology.

**Conclusions:** HPV-DNA was observed in a relevant portion of pSCC and PeIN in our case series, confirming an increasing role of HPV in the pathogenesis of this disease. These results are particularly relevant, as they reflect the current epidemiological trend in the western world. Future studies are needed to clarify the exact role of HPV in cases with discordance between histology and HPV status and in cases with disagreement of HPV detection in different specimens from the same patient (pSCC, PeIN and/or LnM).

## 1003 Molecular Heterogeneity within Brain Metastatic Prostate Cancer: A Multicenter Study of 50 Patients

Antonio Rodriguez[1], Dilara Akhoundova Sanoyan[2], Alison Ferguson[3], Sina Maletti[4], Senija Selimovic-Hamza[5], Federico Comoglio[6], Rémy Bruggmann[6], Ekkehard Hewer[5], Vera Genitsch[5], Achim Fleischmann[7], Elisabeth Rushing[8], Holger Moch[9], Lukas Bubendorf[10], Rainer Grobholz[11], Ingeborg Fischer[12], Wolfram Jochum[13], Laurence de Leval[14], Gieri Cathomas[15], Salvatore Piscuoglio[16], Silke Gillessen Sommer[17], Mark Rubin[5]

*[1]Institute of Pathology, University of Bern, Liebefeld, Switzerland, [2]Department of Oncology, University Hospital Zurich, Zurich, Switzerland, [3]Precision Oncology; Ludwig Cancer Centre, University of Lausanne, Bern, Switzerland, [4]Precision Oncology, Department for BioMedical Research (DBMR), University of Bern, Bern, Switzerland, [5]University of Bern, Bern, Switzerland, [6]Interfaculty Bioinformatics Unit, University of Bern, Bern, Switzerland, [7]Institut fur Pathologie Kantonsspital, Munsterlingen, Switzerland, [8]University Hospital of Zurich, Zurich, Switzerland, [9]University Hospital Zürich, Zurich, Switzerland, [10]University Hospital Basel, Basel, Switzerland, [11]Aarau, AG, Switzerland, [12]Institute of Pathology, Cantonal Hospital Aarau, Aarau, Switzerland, [13]St. Gallen, Switzerland, [14]University Hospital of Lausanne, Lausanne, Vaud, Switzerland, [15]Institut fur Pathologie, Liestal, Switzerland, [16]University of Basel, Basel, BS, Switzerland, [17]IOSI, Bellinzona, Canton Ticino, Switzerland*

**Disclosures:** Antonio Rodriguez: None; Dilara Akhoundova Sanoyan: None; Alison Ferguson: None; Sina Maletti: None; Senija Selimovic-Hamza: None; Federico Comoglio: None; Rémy Bruggmann: None; Ekkehard Hewer: None; Vera Genitsch: None; Achim Fleischmann: None; Elisabeth Rushing: None; Holger Moch: *Speaker*, Roche; *Grant or Research Support*, Roche; *Advisory Board Member*, Definiens; *Advisory Board Member*, Bristol Myers; Lukas Bubendorf: None; Rainer Grobholz: None; Ingeborg Fischer: None; Wolfram Jochum: None; Laurence de Leval: None; Gieri Cathomas: None; Salvatore Piscuoglio: None; Silke Gillessen Sommer: *Consultant*, Sanofi, Orion, Roche; *Speaker*, Janssen; Mark Rubin: None

**Background:** Brain metastases (BM) of prostate cancer (PCa) represent a rare event, mostly in the setting of metastatic castration prostate cancer (mCRPC). However, its diagnosis seems to be increasing, most likely due to prolonged survival with the advent of novel treatment options. To date there is no large-scale study focusing on its molecular landscape and its potential intratumoral heterogeneity.

**Design:** From50 patients across Switzerland we collected FFPE-tissue from BM, matched PCa and benign tissue (BT). Using established protocols based on morphological and immunohistochemical (IHC) analyses (i.e., ERG/P53/PTEN), we selected, when present, heterogeneous intratumoral regions of interest (ROIs) in both BM and PCa. ROIs underwent next generation sequencing (targeted DNA/RNA and WES). Additional cores were taken for tumor microarray construction (Fig. 1). Proteomics analyses using CRPC panels will be conduct in *situ* through GeoMx (Nanostring). Finally, clinical data will be correlated with obtained data.

**Results:** Preliminary data comprises morphological and IHC features from the first 24 patients: 24 BM (56 ROIs, 8 of them heterogeneous (14%)); 15 matched PCa (37 ROIs, 25 of them heterogeneous (68%)).IHC was assessed on 35 ROIs within PCa and on 46 ROIs within BM. PCa showed Gleason scores 7-10 ($\bar{x}$=9.1). Intraductal carcinoma was present in 7 ROIs (19%). No neuroendocrine or ductal carcinoma morphology was observed. IHC analyses revealed: 1) P53 positivity (³50%) or entire negativity in 25 ROIs (71%), (2) ERG positivity in 10 ROIs (29%) and 3) the absence of PTEN expression: cytoplasmic in 26 ROIs (74%); nuclear in 100%.BM demonstrated three ROIs with an overlapping morphology between conventional adenocarcinoma and neuroendocrine differentiated carcinoma. IHC-staining showed, 1) p53 positivity (³50%) or entire negativity in 36 ROIs (78%), 2) ERG positivity in 29 ROIs (63%) and 3) the absence of PTEN expression: cytoplasmic in 35 ROIs (76%) and nuclear in 100% (Tab 1). Concurrent P53 positivity (³50%) or entire negativity, ERG positivity and PTEN negativity (cytoplasmic and nuclear) was found in 4 ROIs (11%) within PT and in 22 ROIs (48%) within BM.

| | MORPHOLOGY | | | | | IHC | | | | |
|---|---|---|---|---|---|---|---|---|---|---|
| | N (ROIs) | GS ($\bar{x}$) | ISUP-grade ($\bar{x}$) | IDC (%) | NED (%) | N (ROIs) | P53 (0 or ≥50) (%) | ERG positivity (%) | PTEN-n negativity (%) | PTEN-c negativity (%) |
| **PT** | 37 | 9,1 | 4,7 | 19 | 0 | 35 | 71 | 29 | 100 | 74 |
| **BM** | 56 | 9,5* | NA | NA | <1 | 46 | 78 | 63 | 100 | 76 |

*PT= primary tumors; BM= brain metastases; ROIs= regions of interest; GS= Gleason Score; IDC= intraductal carcinoma; NED=neuroendocrine differentiation; PTEN-n= nuclear*

*expression; PTEN-c= cytoplasmic expression; *Reminiscent of Gleason Score; NA: not applicable.*

Figure 1 - 1003

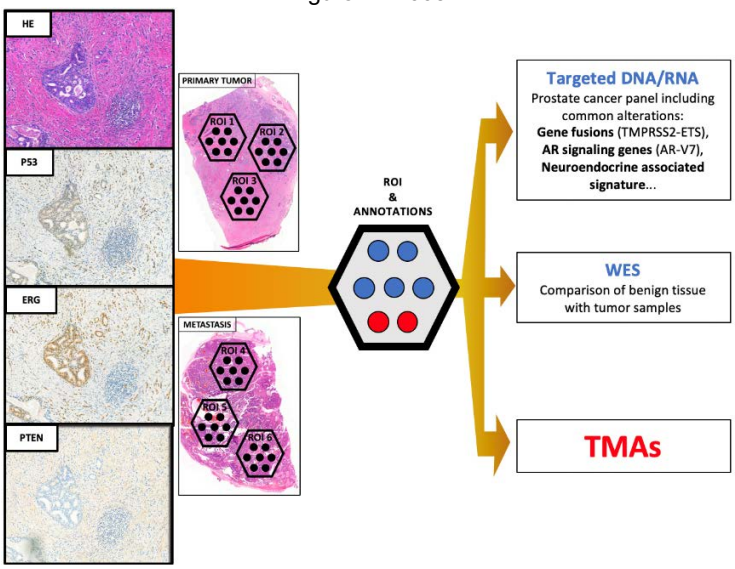


**Conclusions:** All PCa showed high-grade morphology with greater intratumoral heterogeneity than in paired BM. Concurrent P53 (0% or ³50%), ERG positivity and PTEN negativity was more common in BM than in PT. Completed analysis with tumor evolution and heterogeneity maps will be presented.

## 1004 PDL1 Expression in Lymph Node Metastases Associated Immune Cells Predicts Survival in Locally Advanced Urothelial Bladder Carcinoma

Antonio Rodriguez[1], Vera Genitsch[2], Christian Herrmann[3], Marc Furrer[4], Roland Seiler[4], Achim Fleischmann[5]
*[1]Institute of Pathology, University of Bern, Liebefeld, Switzerland, [2]University of Bern, Bern, Switzerland, [3]Krebsregister Ostschweiz, St Gallen, Switzerland, [4]Department of Urology, Inselspital, Bern, Switzerland, [5]Institut fur Pathologie Kantonsspital, Munsterlingen, Switzerland*

**Disclosures:** Antonio Rodriguez: None; Vera Genitsch: None; Christian Herrmann: None; Marc Furrer: None; Roland Seiler: None; Achim Fleischmann: None

**Background:** Information about the prognostic significance of PDL1 expression in muscle invasive bladder cancer (MIBC) is limited and there are no data on inter- and intrapatient tumor heterogeneity. Better knowledge hereof might elucidate its pathobiological role and variations in clinical response to anti-PDL1 therapies.

**Design:** 125 patients with urothelial MIBC underwent cystectomy and extended pelvic lymphadenectomy with curative intent between 1986 and 2015 and were followed according to a prospective standard protocol. All patients had lymph node metastases upon pathological examination (90 ≥ two) and 48 patients received adjuvant chemotherapy. Tissue microarrays were constructed with four samples from each primary tumor and two from each metastasis. PDL1 expression was assessed by immunohistochemistry (SP263 Ventana) as a continuous variable separately for tumor (TC) and associated immune cells (IC) according to the Ventana guidelines. For overall survival (OS) analyses, (a) separate mean values were calculated for each MIBC and its entire metastatic component and (b) these values were categorized as low (<5%), moderate (5-20%) or high (>20%). Statistical analyses were done with Stata® version 15.

**Results:** Inter- and intrapatient heterogeneity of PDL1 expression is shown in Fig.1. No expression in TC and IC of the MIBC is present in 58% and 23%, respectively; however, their metastatic components are PDL1 positive in 22% (TC) and 86% (IC), respectively. PDL1 expression in IC and TC is higher in the metastatic component, but this is only significant for IC (p=0.007) and the correlation is low in IC and moderate in TC (Spearman: 0,269 vs. 0,596).

Cox regression analyses corrected for the major risk factors age and chemotherapy status show that PDL1 expression in IC of the metastatic component is the most robust predictor of OS when tested together with all PDL1 expressing tumor components. Kaplan-Meier curves reveal no significant survival difference between patients with low and moderate PDL1 levels (p=0.864) but a significantly better outcome in case of high PDL1 expression (p=0.007) (Fig2).

Figure 1 - 1004

Figure 1: Parallel coordinates plots show PDL1 expression levels in the different corresponding tumor components of all patients in their immune and tumor cells.

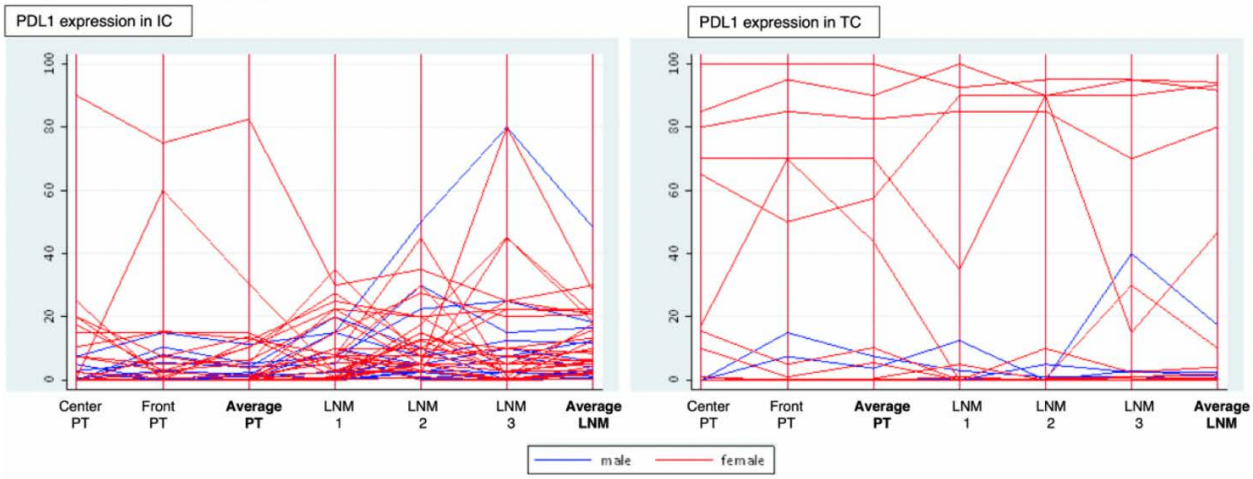


*PT=Primary tumor; LNM=Lymph node metastasis; IC=Immune cells; TC= Tumor cells.*

Figure 2 - 1004

Figure 2: Kaplan Meier curves adjusted for the significant risk factors age and chemotherapy status.

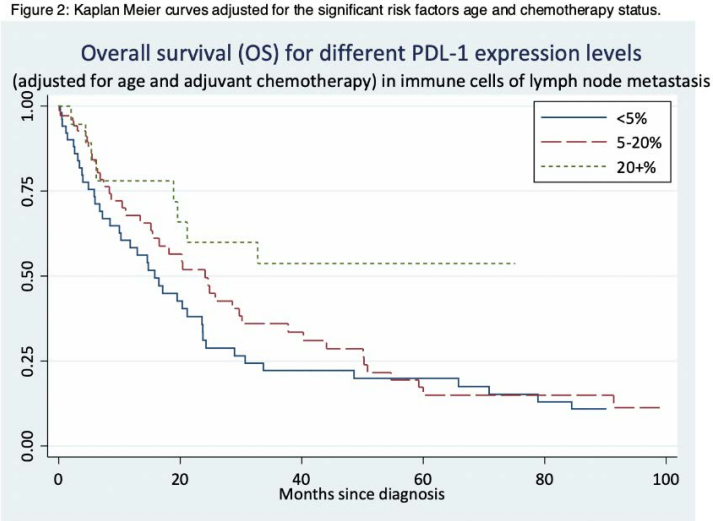


**Conclusions:** PDL1 expression in metastasizing MIBC may differ substantially intratumoral and intermetastatic in a given patient, what might explain variations in treatment effects. The favorable long-term outcome for patients with high PDL1 levels might indicate that PDL1 is a marker of strong cytotoxic local immune response as suggested in other tumors.

## 1005 Neuroendocrine Features in Treated and Metastatic Prostatic Adenocarcinoma

Jenny Ross[1], Xunda Luo[1], Xiaoqi Lin[2], Ximing Yang[2]
*[1]Northwestern University Feinberg School of Medicine, Chicago, IL, [2]Northwestern University, Chicago, IL*

**Disclosures:** Jenny Ross: None; Xunda Luo: None; Xiaoqi Lin: None; Ximing Yang: None

**Background:** As long-term survival in patients with prostatic adenocarcinoma improves, mechanisms of progression will gain increasing interest. There is speculation that patients with treated prostatic adenocarcinoma progress to neuroendocrine carcinoma, but it is unknown whether contemporary treatment modalities result in selection of tumor cell clones with neuroendocrine features.

**Design:** Four tissue microarray blocks (two containing prostatic primary tumors, one with prostatic primaries and corresponding metastases, and one with predominantly treated prostatic primaries) were evaluated for immunostaining with synaptophysin, chromogranin, and neuron-specific enolase. Any distinct immunostaining in tumor cells stronger than background was considered positive; a handful of strongly positive cells was considered negative because such result most likely demonstrated resident benign neuroendocrine cells.

**Results:** Overall, treated prostatic cancers showed only mild increase in frequency of neuroendocrine immunostaining. When stratified by treatment type (androgen suppression (AS), radiation, or combined treatment), radiation had more cases with neuroendocrine features than AS or combination therapy: average of 0.4 of 5 pure radiation-treated cases, average of 0.167 of 20 androgen suppression cases, and average of 0.083 of 4 combined radiotherapy/AS. Duration and latency of treatment did not yield sufficient data for stratification.

The metastatic group, however, showed a marked increase in expression of neuroendocrine markers in the metastases as compared to the primary and the grouped non-treated primary tumors: an average 38.3% in metastatic cases as opposed to average of 22.5% in variously treated cases and average of 15.2% in combined non-treated cases.

| | Primary tumors | Metastatic tumors | Treated tumors |
|---|---|---|---|
| Synapto | 11 / 74 (18.8%) | 8 / 15 (53.3%) | 10 / 34 (29.4%) |
| Chromo | 8 / 81 (8.88%) | 5 / 15 (33%) | 4 / 34 (11.8%) |
| NSE | 14 / 78 (17.9%) | 4 / 14 (28.6%) | 9 / 34 (26.4%) |
| Average | 15.20% | 38.30% | 22.50% |

**Conclusions:** Based on this limited data, there is increased neuroendocrine immunostaining in metastatic prostatic adenocarcinoma; however, neuroendocrine immunostaining in primary location is only mildly increased. Expanded examination of these cohorts is needed.

## 1006 Automated Cancer Detection of Transurethral Resection of Prostate Images Using Deep Neural Networks Trained on Prostate Needle Biopsies

Han Suk Ryu[1], Hyeyoon Chang[2], Tae-Yeong Kwak[3], Joonyoung Cho[2]
*[1]Seoul National University College of Medicine/Hospital, Seoul, Korea, Republic of South Korea, [2]Deep Bio Inc., Seoul, Korea, Republic of South Korea, [3]Deep Bio Inc., Guro-gu, Korea, Republic of South Korea*

**Disclosures:** Han Suk Ryu: None; Hyeyoon Chang: *Employee*, DeepBio Inc; Tae-Yeong Kwak: *Employee*, Deep Bio Inc.; Joonyoung Cho: *Employee*, Deep Bio Inc.

**Background:** Transurethral resection of the prostate (TURP) is the most common form of surgical treatment of benign prostatic hyperplasia. The probability of detecting incidental prostate cancer on the TURP specimen were rates of 4.1–16.7%. TURP specimens usually consist of a large number of small tissue fragments. All TURP specimens should be examined carefully so as not to miss any cancer that may be present. In this study, we diagnosed 250 TURP whole slide images (WSIs) using a deep neural network (DNN) model intended to diagnose prostate needle biopsies.

**Design:** The 250 TURP glass slides, one slide per patient, were collected and scanned into WSIs using an Aperio AT2 digital slide scanner (Leica Biosystems Imaging, Inc., Vista, CA, United States). Automated analysis for cancer detection was performed using the DNN model originally developed to diagnose prostate cancer. The model was trained with thousands of prostate needle biopsy WSIs, whose cancer lesions were annotated by experienced pathologists.

The detection performance was evaluated on the original hospital diagnosis, which was confirmed by an experienced pathologist with reviewing all the glass slides. The accuracy, sensitivity, specificity, and positive predictive value (PPV) were measured.

**Results:** A total of 90 malignant and 160 benign WSIs were included in this study. Of the 90 malignant WSIs, 89 contained prostate adenocarcinoma and 1 contained urothelial carcinoma. There were no cases of disagreement between the hospital's original diagnosis and the pathologist's review.

The model's detection accuracy, sensitivity, specificity, and PPV were 0.652, 0.978, 0.469, and 0.509 respectively. The representative images of the model's analyses are shown in Fig. 1. The model failed to detect cancer in tissue areas with cautery or coagulative artifacts. (Fig. 2A and B) Diffuse inflammatory areas and disrupted glands with a detachment of epithelial cells from the basement membrane were falsely diagnosed malignant. (Fig. 2C and D)

Figure 1 - 1006

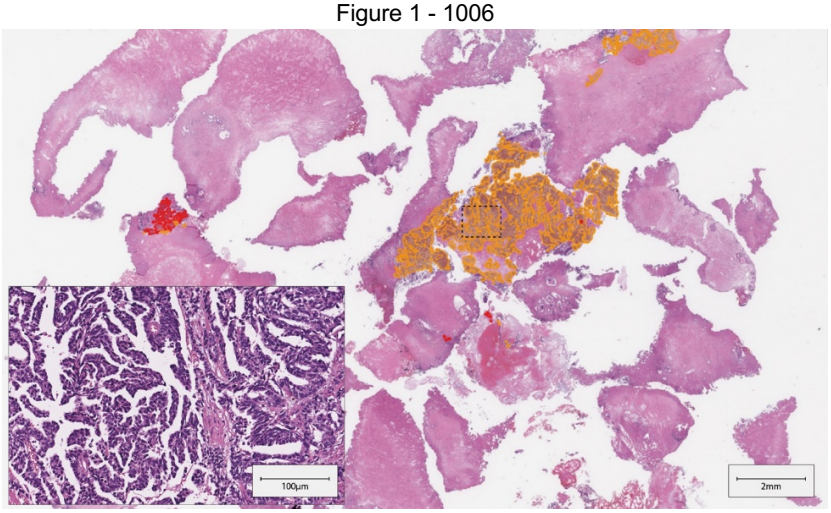


Figure 2 - 1006

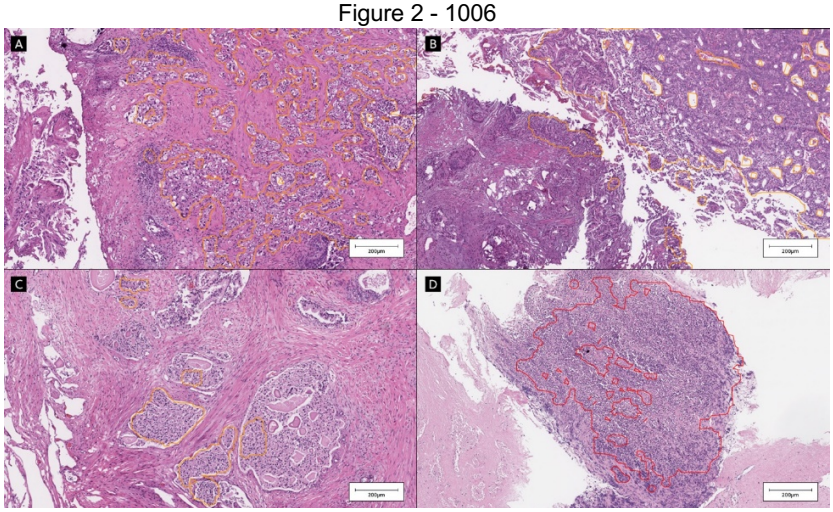


**Conclusions:** In this study, we performed an automatic diagnosis of TURP WSIs by translationally applying a DNN model which was developed for the diagnosis of prostate needle biopsy. The false positive rate was high because some of the tissue artifacts that were not observed in biopsy samples were in TURP specimens. We expect our model which has high sensitivity could assist the pathologist in diagnosing TURP specimens in the screening phase through additional training for inflammation and lesions with tissue artifact.

## 1007 p53 Pathway Activation in Papillary Renal Cell Carcinoma Correlates with the Biological Subtype

Rola Saleeb[1], George Yousef[2], Yuan Gao[3], Vidya Beharry[4], Marly Mikhail[5], Samir Al Bashir[6], Kiril Trpkov[7]
*[1]St Michael's Hospital/ University of Toronto, Toronto, ON, [2]Hospital for Sick Children, Toronto, ON, [3]Eastern Health/Memorial University, St. John's, NL, [4]St. Michael's Hospital, Toronto, ON, [5]International Baccalaureate, Oakville, ON, [6]Jordan University of Science & Technology, Irbid, Jordan, [7]University of Calgary, Calgary, AB*

**Disclosures:** Rola Saleeb: None; George Yousef: None; Yuan Gao: None; Vidya Beharry: None; Marly Mikhail: None; Samir Al Bashir: None; Kiril Trpkov: None

**Background:** *TP53* mutational status and p53 expression have been the subject of scrutiny in many cancer subtypes. Mutational events of *TP53* are extremely rare in renal cell carcinoma. Few previous studies have correlated p53 expression to prognosis in renal cell carcinoma. The pathogenesis of p53 protein expression without an associated mutational event is poorly understood. However, the exact correlation of p53 expression in papillary renal cell carcinoma (PRCC) and its association with different PRCC subtypes and outcome have not been previously studied.

**Design:** PRCC tissue microarray of 80 cases was subtyped using the proposed PRCC classification (Saleeb et al *AJSP* 2017) and it was evaluated using p53, quantified by image analysis. P53 associated gene signature (n=23) was selected from the literature. Next generation sequencing of 9 PRCCs was performed. Gene expression was also studied in another 80 cases selected from the cancer genome atlas

(TCGA) PRCC cohort (n=281), which was also assessed for *TP53* mutational events. Clinicopathologic information was gathered and statistical analysis was performed using Graphpadprism8.

**Results:** Control normal kidney showed no p53 staining. In contrast, PRCC showed a range of p53 expressions (figure 1). PRCC type 1 had the lowest mean expression, while types 2 and 3 had significantly higher p53 expression when compared to the normal kidney (p=0.011 and 0.045 respectively) (figure 2). Only 2% of PRCCs had *TP53* mutations. Genes involved in the mitotic checkpoint (*CENPE, CENPF, ANAPC7, CDCA8, KIF2C*) were commonly mutated in PRCC and were more frequent in types 2 and 3 than in type 1. The expression of p53 signature genes was also largely abnormal in PRCC type 2, compared to type 1. Univariate analysis didn't reveal a significant relationship between p53 expression and the overall survival. Only the PRCC subtype maintained its significance on multivariate analysis (table).

| Multivariate analysis parameters (OS) | P value |
|---|---|
| PRCC subtype (1&4 vs 2&3) | 0.0157* |
| Age | 0.8565 |
| Tumor size | 0.6523 |
| WHO/ISUP Grade | 0.5038 |
| Pathological Stage | 0.2835 |
| Necrosis (< 20% or > 20%) | 0.4338 |
| P53 expression (digital quantification) | 0.7941 |

Figure 1 - 1007

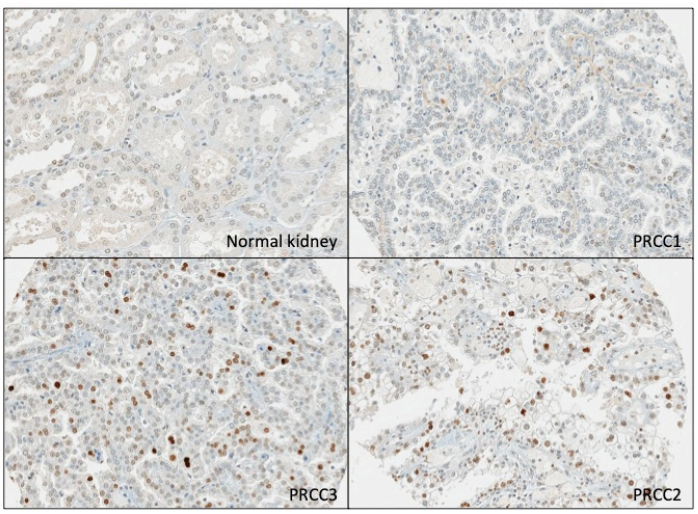


Figure 2 - 1007

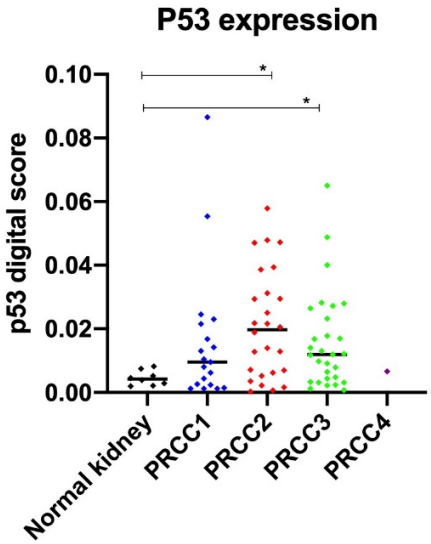


**Conclusions:** P53 expression is more frequently increased in PRCC subtypes 2 and 3, but the mechanism of p53 increased expression is not related to *TP53*mutation. Genes known to be associated with p53 mutational status are also commonly implicated in the PRCC subtypes that show higher p53 expression. It is possible that the activation of other cell cycle genes, through genetic or epigenetic mechanisms, influences the p53 effect in the PRCC. While P53 is not directly predictive of survival, it appears that it can act as an indicator of the underlying biological subtype.

## 1008 Expression of Mismatch Repair Proteins (MSH2, MSH6, MLH1, and PMS2), c-Myc, PTEN and ERG in Prostate Adenocarcinoma in Patients Under 50 Years: Correlation with Grade Groups and Biochemical Recurrence

Iryna Samarska[1], Ruud Clarijs[2], Axel zur Hausen[1], Jonathan Epstein[3]
*[1]Maastricht University Medical Centre+, Maastricht, Limburg, Netherlands, [2]Zuyderland Medical Centre, Sittard-Geleen, Limburg, Netherlands, [3]Johns Hopkins Medical Institutions, Baltimore, MD*

**Disclosures:** Iryna Samarska: None; Ruud Clarijs: None; Axel zur Hausen: None; Jonathan Epstein: None

**Background:** One in 350 men under 50 years is diagnosed with prostate cancer (PCa).

**Design:** We identified 44 cases of PCa in men diagnosed under the age of 50 years (age range 41-50) from 2004-2019 in our database. Clinical data were collected retrospectively from medical records and immunohistochemistry (IHC) was performed. Data on tumor grade,

primary treatment and initial PSA value were available in all 44 patients. Data on follow-up, family history, biochemical recurrence were available in 42 patients. IHC was performed on 40 prostate cancer cases of which the blocks were available.

**Results:** Clinicopathological data are summarized in Table 1. Only 5/42 (11.9%) patients had a positive family history for PCa. The 32/44 patients (72.7%) were diagnosed with Grade group 1 and 2 PCa. Biochemical and/or local recurrence was found in 12/44 (27.3%) patients. Lymph node metastases were found in 5/44 patients (11.4%), and distant metastases in 2/44 (4.5%) men. The expression of mismatch repair proteins (MSH2, MSH6, MLH1, and PMS2) was retained in all 39 successfully stained cases. PTEN loss was found in 12/40 (30%), c-Myc expressed in 20/40 (50%), and ERG expressed in 33/40 (82.5%) tumors (Table 1). In cases with and without biochemical recurrence (BCR), PTEN loss was found 5/12 (41.6%) and 7/28 (25.0%), respectively (p>0.05); c-Myc expression was seen in 8/12 (66.6%) and in 12/28 (42.8%), respectively (P>0.05); and ERG expression was present in 9/12 (75%) and 24/28 (85.7%), respectively (p>0.05). PTEN loss, ERG and c-Myc expression were compared between groups with and without biochemical recurrence by Cox regression and the p-value were 0.08 for PTEN loss, 0.4 for ERG and 0.9 for c-Myc expression (Figure 1).

**Table 1.** Clinicopathological characteristics, MMR, PTEN, ERG and c-Myc expression.

| *Patient characteristics* | |
|---|---|
| *Age, yr, median (range)* | *48.2 (41-50)* |
| *Follow-up, mo, median (range)* | *60 (1-168)* |
| *PSA level, ng/dl, median (range)* | *6.6 (1.6-170)* |
| *T stage, % (no.)* | |
| *T1a* | *2.3 (1/44)* |
| *T1c* | *11.4 (5/44)* |
| *T2a* | *9.1 (4/44)* |
| *T2b* | *4.5 (2/44)* |
| *T2c* | *43.2 (19/44)* |
| *T3a* | *27.3 (12/44)* |
| *T4* | *2.3 (1/44)* |
| *Biochemical recurrence, % (no.)* | *28.6 (12/42)* |
| *Local recurrence, % (no.)* | *14.3 (6/42)* |
| *Lymph node metastases, % (no.)* | *11.9 (5/42)* |
| *Bone or visceral organ metastases, % (no.)* | *4.8 (2/42)* |
| *Tumor Grade, % (no.)* | |
| • *Grade group 1* | *34.1 (15/44)* |
| • *Grade group 2* | *38.6 (17/44)* |
| • *Grade group 3* | *13.6 (6/44)* |
| • *Grade group 4* | *4.5 (2/44)* |
| • *Grade group 5* | *9.0 (4/44)* |
| *Primary treatment, % (no.)* | |
| • *Resection* | *75 (33/44)* |
| • *Brachytherapy/radiotherapy* | *15.9 (7/44)* |
| • *AS* | *4.5 (2/44)* |
| • *HIFU* | *2.3 (1/44)* |
| • *Hormone therapy* | *2.3 (1/44)* |
| *ERG expression, % (no.)* | |
| • *Grade group 1* | *92.3 (12/13 available blocks)* |
| • *Grade group 2* | *81.3 (13/16 available blocks)* |
| • *Grade group 3* | *66.7 (4/6)* |
| • *Grade group 4-5* | *80.0 (4/5 available blocks)* |
| *c-Myc expression, % (no.)* | |
| • *Grade group 1* | *61.5 (8/13 available blocks)* |
| • *Grade group 2* | *43.8 (7/16 available blocks)* |
| • *Grade group 3* | *33.3 (2/6)* |
| • *Grade group 4-5* | *60.0 (3/5 available blocks)* |
| *PTEN loss, % (no.)* | |
| • *Grade group 1* | *23.1 (3/13 available blocks)* |
| • *Grade group 2* | *31.3 (5/16 available blocks)* |
| • *Grade group 3* | *33.3 (2/6)* |
| • *Grade group 4-5* | *40.0 (2/5 available blocks)* |

Figure 1 - 1008

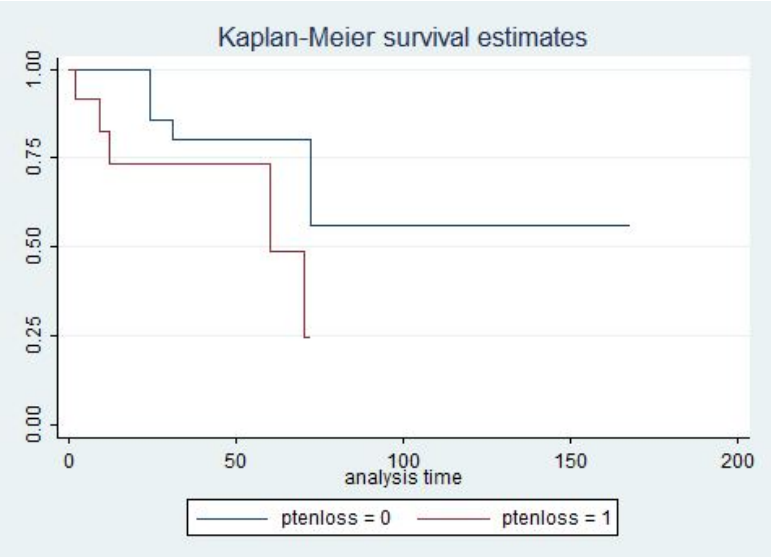


**Conclusions:** *Early onset prostate cancer in our patient cohort revealed retained expression of MMR proteins, which does not support an association of these early onset prostate cancer in patients under 50 years in the context of Lynch syndrome. Expression of ERG and c-Myc were the most common immunochemical findings irrespective of the tumor grade. Biochemical recurrence was not statistically associated with c-Myc, ERG, and PTEN expression. Although the differences in PTEN loss were not significantly different, this could have been due to low number of cases and further studies with larger numbers of patients are needed.*

## 1009 Both Percentage of Gleason Pattern 4 and Total Length of Gleason Pattern 4 Outperform Other Clinicopathological Parameters in Predicting Postoperative Adverse Pathological Findings among Intermediate Risk Gleason Score 3+4=7 Cancers

Shun Sato[1], Takahiro Kimura[2], Hajime Onuma[1], Shin Egawa[3], Hiroyuki Takahashi[4]
*[1]The Jikei University School of Medicine, Minato-ku, Tokyo, Japan, [2]Jikei University School of Medicine, Tokyo, Japan, [3]The Jikei University School of Medicine, Tokyo, Japan, [4]The Jikei University School of Medicine, Minatoku, Tokyo, Japan*

**Disclosures:** Shun Sato: None; Hajime Onuma: None

**Background:** Recently, subclassification of intermediate risk prostate cancers (IR-PC) has been discussed and several criteria have been proposed because those with favorable outcome can be potential active surveillance candidates. The latest National Comprehensive Cancer Network (NCCN) guideline, which is most frequently used worldwide, adopts clinical T (cT) stage, Gleason score (GS), serum PSA level and percentage of positive cores in biopsy as parameters for defining favorable IR-PC. Other pathological prognostic parameters such as percentage of Gleason pattern 4 (%GP4) and presence of cribriform pattern are not included. In this research, we evaluated predictive value of those clinicopathological parameters in GS 3+4=7 IR-PC.

**Design:** A total of 228 IR-PC cases who were diagnosed as GS 3+4=7 cancer at biopsy, and subsequently underwent radical prostatectomy (RP) between 2009 and 2019, were adopted. The cT stage, serum PSA level, percentage of positive cores in biopsy, presence of cribriform pattern, highest %GP4, total length of GP4 (GP4-TL) and percentage of GS7 cores to total cores retrieved were compared for the predictive value of postoperative adverse pathological findings (AP). The highest %GP4 was defined as the largest %GP4 among all cores in each case. The GP4-TL was calculated by "sum of (cancer length x %GP4) of each core" (mm). The AP was defined as GS upgrade to 4+3=7 or higher, pT3b cancer, or positive lymph node metastasis. The predictive value of each parameter was analyzed by univariate logistic regression analysis. Area under the curve (AUC) was compared between highest %GP4 and GP4-TL using receiver operating characteristic (ROC) curve.

**Results:** In this cohort, the AP was observed in 54 cases (23.7%). The results of the univariate logistic regression analysis are shown in the Table. By the univariate logistic regression analysis, only highest %GP4 and GP4-TL were independent predictive factors of AP. The AUC for the highest %GP4 and GP4-TL were similar (0.674 vs. 0.618), and statistical significance was not shown (p=0.0581).

| Parameters | Odds Ratio (95% CI) | P-Value |
|---|---|---|
| Serum PSA level | 1.030 (0.944-1.120) | 0.5140 |
| cT stage (1c+2a vs. 2b+2c) | 1.35 (0.4820-3.760) | 0.7520 |
| % of positive cores | 0.997 (0.982-1.010) | 0.7500 |
| Cribriform pattern | 1.43 (0.671-3.040) | 0.355 |
| Highest %GP4 | 1.05 (1.0200-1.070) | 0.0001 |
| GP4-TL | 1.160 (1.010-1.320) | 0.0309 |
| % of GS7 cores | 1.020 (0.991-1.050) | 0.191 |

**Conclusions:** The results of this research suggest that the highest %GP4 and GP4-TL in biopsy specimens are strong predictive parameters of AP in GS 3+4=7 IR-PC.

## 1010 ETS2 Loss of Expression in Prostate Cancer

Laura Segales Tana[1], Josep Lloreta-Trull[2], Nuria Juanpere-Rodero[3], Marta Lorenzo[3], Lluís Fumadó[3], Lluís Cecchini[3], Silvia Hernández-Llodrà[1]
*[1]Universitat Pompeu Fabra, Barcelona, Spain, [2]Hospital del Mar, Parc de Salut Mar, Universitat Pompeu Fabra, Barcelona, Spain, [3]Hospital del Mar-Parc de Salut Mar-IMIM, Barcelona, Spain*

**Disclosures:** Laura Segales Tana: None; Josep Lloreta-Trull: None; Nuria Juanpere-Rodero: None; Marta Lorenzo: None; Lluís Fumadó: None; Lluis Cecchini: None; Silvia Hernández-Llodrà: None

**Background:** Chromosomic rearrangements involving *TMPRSS2* and *ERG* have been reported as a relevant feature in prostate cancer (PrCa), and induce *ERG* overexpression in more than 90% of cases. This alteration can result from direct fusion or complex rearrangement. The former is produced through deletion of the chromosomal region between *TMPRSS2* and *ERG* on chromosome 21, that contains the *ETS2* gene, and has been associated with high-risk PrCa. However, the role of the interstitial gene *ETS2* loss in the pathogenesis of PrCa is poorly characterized.

**Design:** mRNA expression of *ERG* and *ETS2* was analyzed by qPCR in 87 PrCa. *GADPH* was the control gene; 3 benign frozen prostate samples were used to normalize gene thresholds. *ERG* overexpression cut-off was $^{2}$(-DDCt) ≥ 2.6, while *ETS2* loss was considered for $^{2}$(-DDCt) ≤ 0.40. Presence of the *TMPRSS2-ERG* rearrangement was assessed by PCR. Fusion variants were characterized through Sanger direct sequencing.

**Results:** Loss of *ETS2* expression was found in 32.2% of PrCa, and *ERG* overexpression in 55.2%. The *TMPRSS2-ERG* fusion was identified in 62.1% of cases, and the T1:E4 variant was present in all of them. Thirty-three PrCa had a single fusion, while 21 cases harbored two co-occurring variants, combining T1:E4 with T1-3:E4 in 20 tumors, and with T1:E2 in one. As expected, there was a very high correlation between *ERG* overexpression and the *TMPRSS2-ERG* fusion (P<0.00001). Loss of *ETS2* expression was associated with *ERG* overexpression (P=0.0008), and with the *TMPRSS2-ERG* rearrangement (P=0.0017). In fact, *ETS2* loss of expression was found in 45.5% of tumors with single T1:E4, 42.8% of tumors with two co-occurring variants, but in 12.1% of the non-fused cases (P=0.0072). Additionally, we found *ETS2* loss of expression in 16.7% GG1, 32.1% GG2, 63.2% GG3, 22.2% GG4, and 14.3% GG5 tumors (P=0.0143). *ETS2* loss of expression showed a trend to be associated with high tumor stage (P=0.0672), as it was detected in 18.5% pT2, while in 38.3% pT3-4 tumors. Finally, the loss of *ETS2* was not associated with PSA recurrence (P=0.7054), and did not add prognostic information to the *TMPRSS2-ERG* rearrangement (P=0.6806).

**Conclusions:** *ETS2* loss of expression is present in a high percentage of prostate tumors, and is associated with *ERG* overexpression and *TMPRSS2-ERG* rearrangement. Interestingly, *ETS2* loss of expression is more frequent in GG3 and pT3-4 tumors, but it is not related to PrCa PSA recurrence.

(FIS/Carlos III/FEDER/PI15/00452, Spanish Ministry of Health).

## 1011 Gleason Score 3+4=7 Prostate Cancer with Minimal Pattern 4 Identified in Prostate Needle Biopsy Barely has Worse Pathological Outcomes

Antonio Serrano[1], Jonathan Melamed[2], Qinghu Ren[3], Hongying Huang[1], Kyung Park[1], Abdallah Flaifel[4], Fangming Deng[5]
*[1]NYU Langone Health, New York, NY, [2]NYU, New York, NY, [3]New York University Langone Medical Center, New York, NY, [4]NYU School of Medicine, New York, NY, [5]New York University Medical Center, New York, NY*

**Disclosures:** Antonio Serrano: None; Jonathan Melamed: None; Qinghu Ren: None; Hongying Huang: None; Kyung Park: None; Abdallah Flaifel: None; Fangming Deng: None

**Background:** Recent clinical guidelines for management of prostate adenocarcinoma are aimed at expanding active surveillance (AS) to include men with intermediate-risk (Gleason score 3+4=7) disease on needle biopsy (NB). However, studies reported a large portion of

men with Gleason 3+4=7 prostate cancer on biopsy, that harbored adverse surgical pathologic findings. It remains unclear which subset of intermediate-risk patients with Gleason score 7 cancers can be safely treated with AS. In this study we investigate whether the percentage of Gleason pattern 4 in NB with Gleason score 7 cancers is an indicator for stratifying risk.

**Design:** We retrospectively reviewed our electronic record database for patients that underwent core NB over a 6-year period. We included NB with Gleason score 3+3=6 (G336), 3+4=7 with <5% Gleason pattern 4 (G4%<5) and 3+4=7 with 6-49% maximum Gleason pattern 4 (G4%6-49); all cases had corresponding radical prostatectomy (RP) within 6 months of the biopsy. We defined adverse pathology (AP) as any RP with Gleason score equal to or greater than 4+3=7 and/or stage T3 or higher. We compare AP outcomes in final follow-up RP of three NB groups: G336, G4%<5 and G4%6-49.

**Results:** A total of 289 NB with corresponding radical prostatectomies were identified. The breakdown of Gleason groups is shown in Table 1.

GS336 has an AP rate of 26.6%, while G4<5% an AP rate of 20%. In comparison, the group of patients with G4%6-49 exhibited a 42% rate of AP (Table 1). A Chi-square test performed comparing AP of G4%<5 and G%6-49 is statistically significant p= .0237 (Figure 1). Conversely, there is no statistical difference between the rate of AP in G4<5% and G336, p= 0.46. G336 and G4%<5 were aggregated into a new group G%0-5 with an AP rate of 25.2% compared to G%6-10 AP rate 39.6%, p= 0.0576 (Figure 2). G4%6-10 and G4%11-49 had comparable rates of AP, 39.6% and 43.1%, respectively (p=0.681).

| Gleason Group | | | |
|---|---|---|---|
| | 3+3=6 (N=109) | G4%<5 (N=30) | G4%6-49 (N=150) |
| Adverse Pathology | 26.60% | 20.00% | 42.00% |
| Gleason Grade Group ≥ 3 | 11.00% | 3.33% | 12.00% |
| T Stage ≥ 3 | 17.40% | 16.67% | 37.33% |

Figure 1 - 1011

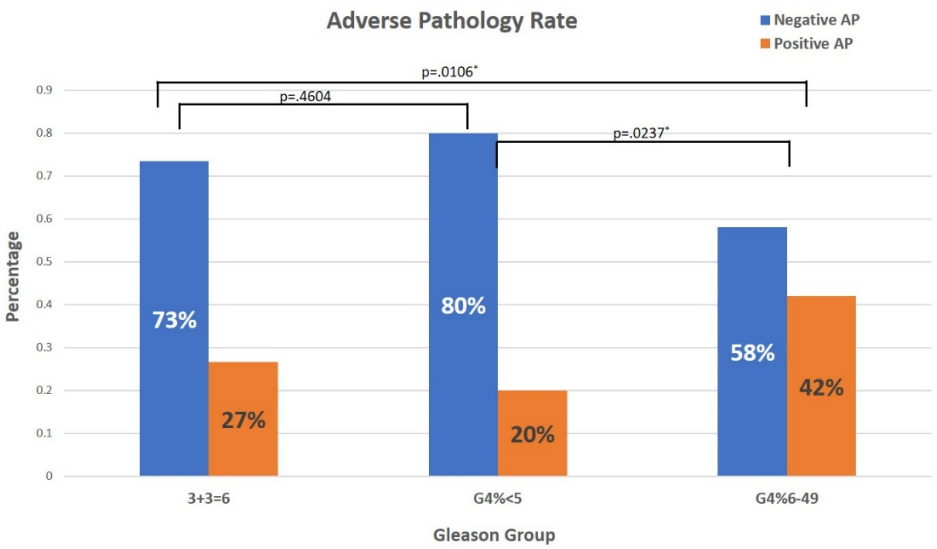

Figure 2 - 1011

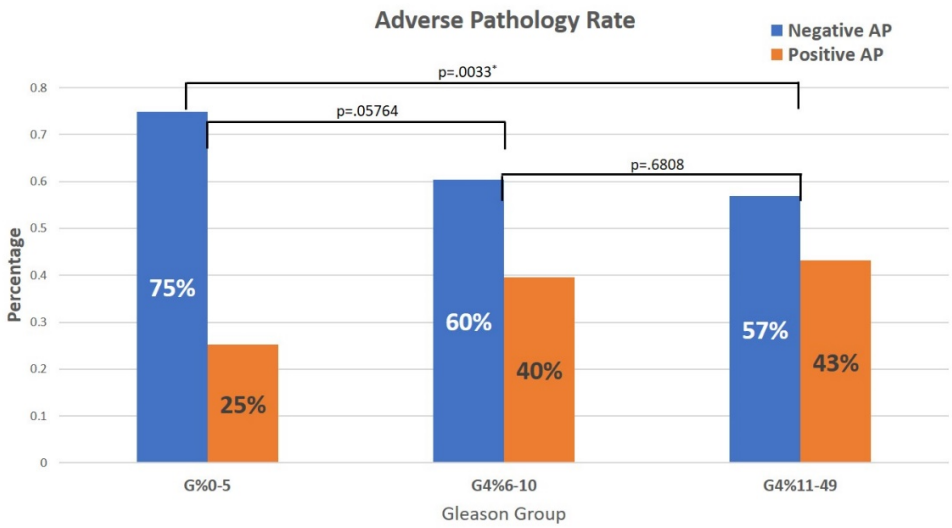


**Conclusions:** Currently there is a paradigm shift amongst pathologist and the significance of minimal percentage pattern 4 on prostate biopsies. Our current data supports the recent literature publications that <5% maximal Gleason pattern 4 on a single core has a similar rate of adverse pathological outcomes as Gleason score 3+3=6 and can be considered for AS.

Although we did not detect a statistical difference between the rate of AP between G4%0-5 and G4%6-10, the data is beginning to approach statistical significance and warrants further risk stratification.

## 1012 Effects of Immune Checkpoint Inhibitors on Histopathology of Renal Cell Carcinoma

Sasan Setoodeh[1], Christopher Przybycin[2], Roy Elias[1], Brian Rini[2], James Brugarolas[3], Payal Kapur[3]
*[1]UTSW Medical Center, Dallas, TX, [2]Cleveland Clinic, Cleveland, OH, [3]University of Texas Southwestern, Dallas, TX*

**Disclosures:** Sasan Setoodeh: None; Christopher Przybycin: None; Roy Elias: None; Brian Rini: *Grant or Research Support*, Pfizer; *Consultant*, Merck; *Consultant*, Roche; *Consultant*, BMS; James Brugarolas: *Advisory Board Member*, Bethyl Laboratories; *Consultant*, Arrowhead; *Consultant*, Exelixis; Payal Kapur: None

**Background:** Immune checkpoint inhibitors (ICI), including the PD1 inhibitor, Nivolumab, alone or in combination with the CTLA4 inhibitor, Ipilimumab, are increasingly being used in advanced renal cell carcinoma (RCC). The goal of this study was aimed to evaluate their histopathologic effects.

**Design:** 12 patients with post-ICI nephrectomy, including 8 conventional CCRCC, 1 sarcomatoid CCRCC, 1 PRCC, 1 TFE-B RCC, and 1 with complete response, were selected from our institutional Kidney Cancer Program database and were compared to 10 random nephrectomies without neo-adjuvant therapy. Clinical characteristics were comparable to non-ICI patients. Viable tumors and non-neoplastic background kidney were evaluated for several histopathologic features as tabulated (table). The morphologic findings were compared with 6 ICI treated CCRCCs from The Cleveland Clinic using scanned images. IHCs for PD-L1, PD-1, CD3, CD4, CD8, and CD163 were performed.

**Results:** 3 patients had 12 or more cycles of ICI and had prior therapies (TKI or mTOR pathway inhibitor). 9 cases had only 1-2 cycle of ICI pre-nephrectomy. 7 cases had received only Nivolumab and 5 cases had received combination of Nivolumab and Ipilimumab. One case (case 1) showed complete response with no residual viable tumor. Most CCRCCs showed: 1) reduction/shrinkage of tumor cell cytoplasm and nucleus (reminiscent of ISUP/WHO grade 1), 2) fibrin deposition in vessel walls and capillary endothelial hyperplasia, endothelialitis and fibrosis, 3) prominent fibrous scaring and collagenization suggesting therapy effect. These features were also observed in the Cleveland Clinic cases but not seen in any of the ICI naive cases reviewed. PRCC and TFE-B RCC cases did not show these features. The sarcomatoid case showed prominent dense fibrosis, inflammation, vascular fibrin deposition and endothelialitis. PD-L1 circumferential tumor cell staining was <1% in 29% and >5% in 71% of cases. Prominent CD8+ TILs were seen in 43% of cases. 17% were negative for CD163+ macrophages.

Figure 1 - 1012

| Histologic findings | Case 1 | Case 2 | Case 3 | Case 4 | Case 5 | Case 6 | Case 7 | Case 8 | Case 9 | Case 10 | Case 11 | Case 12 |
|---|---|---|---|---|---|---|---|---|---|---|---|---|
| Viable tumor | | | | | | | | | | | | |
| Histologic classification | N/A | Sarc CCRCC | CCRCC | CCRCC | CCRCC | CCRCC | TFEB RCC | CCRCC | PRCC | CCRCC | CCRCC | CCRCC |
| Architectural pattern | | | | | | | | | | | | |
| Vascular-rich | N/A | - | + | + | - | + | - | + | - | + | + | + |
| Vascular-poor | N/A | + | - | - | + | - | + | - | + | - | - | - |
| Tumor necrosis | + | + | - | - | - | - | + | + | + | - | - | - |
| Dense fibrosis | + | + | + | + | + | - | - | - | - | + | + | - |
| Inflammation | | | | | | | | | | | | |
| Peritumoral | L, mild | L P, mod | L, mild | L, mild | L, mod | L, mod | L, mild | L, mild | L, mild | L, mild | L, mod | L, severe |
| Intratumoral | L H, mod | N L P, mod | L, mild | L, mod | L H, mod | L, mild | L, mild | L, mild | L, mild | L H, mild | L, mod | L, mild |
| Follicle formation | - | - | - | + | - | - | - | - | + | - | - | + |
| Vascular changes | | | | | | | | | | | | |
| Endothelial proliferation | N/A | + | + | + | + | + | - | + | - | + | + | + |
| Endothelialitis/vasculitis | N/A | + | + | + | + | + | - | - | - | - | - | - |
| Fibrin deposition | N/A | + | + | + | - | + | - | + | - | + | + | + |
| BM thickening | N/A | + | + | + | + | - | - | + | - | - | + | - |
| Epithelial changes | | | | | | | | | | | | |
| Cytoplasmic shrinkage | N/A | + | + | + | - | + | - | + | - | + | + | + |
| Nuclear diminution | N/A | + | + | + | - | + | - | + | - | + | + | + |
| Non-neoplastic kidney | | | | | | | | | | | | |
| Tubular atrophy | + | + | + | + | + | - | - | + | - | + | - | + |
| Interstitial fibrosis | + | + | + | + | + | - | - | + | - | + | - | + |
| BM thickening | + | + | - | - | - | - | - | - | - | - | - | - |
| Inflammation | L | + | L | L, focal | L | - | L | L | L | L | L, focal | L |
| Glomerulosclerosis | + | - | - | - | - | - | - | - | - | - | - | - |

Table 1. Histologic findings

Sarc: sarcomatoid, L: lymphocytes, P: plasma cells, N: neutrophils, H: histiocytes, mod: moderate

**Conclusions:** Our study describes novel findings as effects of ICI on RCC histopathology. The most specific findings for ICI treated CCRCCs were vascular changes including fibrin deposition in vessel walls and capillary endothelial hyperplasia which are particularly of interest considering the recent observation of better responses to ICI and VEGF inhibitors in combination. Due to the shrinkage in nuclear size, the tumors will likely be under graded post ICI therapies.

## 1013 Comprehensive Histopathologic and Genomic Evaluation of Eosinophilic Variant of Chromophobe Renal Cell Carcinoma

Sasan Setoodeh[1], Suneetha Chintalapati[2], Alana Christie[3], Yunguan Wang[4], Liwei Jia[1], Wang Tao[1], James Brugarolas[5], Payal Kapur[5]

*[1]UTSW Medical Center, Dallas, TX, [2]University of Texas Southwestern Medical Center, Irving, TX, [3]University of Texas Southwestern Medical Center, Dallas, TX, [4]UTSW Medical Center, Irving, TX, [5]University of Texas Southwestern, Dallas, TX*

**Disclosures:** Sasan Setoodeh: None; Suneetha Chintalapati: None; Alana Christie: None; Yunguan Wang: None; Liwei Jia: None; Wang Tao: None; James Brugarolas: *Advisory Board Member*, Bethyl Laboratories; *Consultant*, Arrowhead; *Consultant*, Exelixis; Payal Kapur: None

**Background:** WHO classifies chromophobe renal cell carcinoma (ChRCC) in to classic (c-ChRCC) and eosinophilic (e-ChRCC) variants; however, e-ChRCC morphologically closely resemble renal oncocytomas (RO). To better understand these entities we aimed to compare the clinicopathological and molecular characteristics of e-ChRCC with c-ChRCC, RO, and oncocytic papillary RCC (OPRCC).

**Design:** Oncocytic tumors with available fresh tissue and/or tissue microarray (TMA) were selected from our institutional Kidney Cancer Program database. Morphologic criteria for e-ChRCC included presence of diffuse oncocytic cytoplasm with at least focal area showing perinuclear clearing and nuclear membrane irregularities. Oncocytic tumors showing nuclear membrane irregularities or significant binucleation but with no identifiable perinuclear halos were categorized as RON. TMAs were stained for CD117, CK7, CK20, Melan-A, TFE3, Cathepsin-k, SDHB, and FH. Whole exome sequencing, SNP array and RNA-sequence analysis were performed (some genomic data published previously).

**Results:** 14 e-ChRCC, 41 c-ChRCC, 72 RO, 7 OPRCC, and 10 RON cases were identified. RO and e-ChRCC were seen in slightly older age patients compared to c-ChRCC (65.4 and 67.7 vs 55.9 years respectively). E-ChRCCs were smaller than c-ChRCC (5.4 vs 8.3 cm) and closer to the size of ROs (4.6 cm). Sarcomatoid morphology, nodal disease and stage 4 were identified only in c-ChRCC (3.1%, 6.3%, and 3.1% respectively). No TFE3+, SDHB- or FH- cases were identified. CD117 was negative in 9% of cases. 3 cases showed both CK20 and Melan-A staining, 2 of which were CD117 negative. Cases without classic IHC pattern were reviewed and a spectrum of morphologies and overlapping with newly described oncocytic tumors (HOT and LOT) were noted. Genomics were available on 36 c-ChRCC, 12 e-ChRCC, 35 RO (including 4 RON), and 7 OPRCC cases. SNP arrays revealed no alterations in all e-ChRCC, few copy number losses of chromosome 1 in RO, and frequent multiple copy number losses in c-ChRCC. No p53 or PTEN mutation was seen in e-ChRCC. Principal component analysis showed clustering of e-ChRCC in between RO and c-ChRCC (figure). OPRCCs clustered away from oncocytic tumors.

Figure 1 - 1013

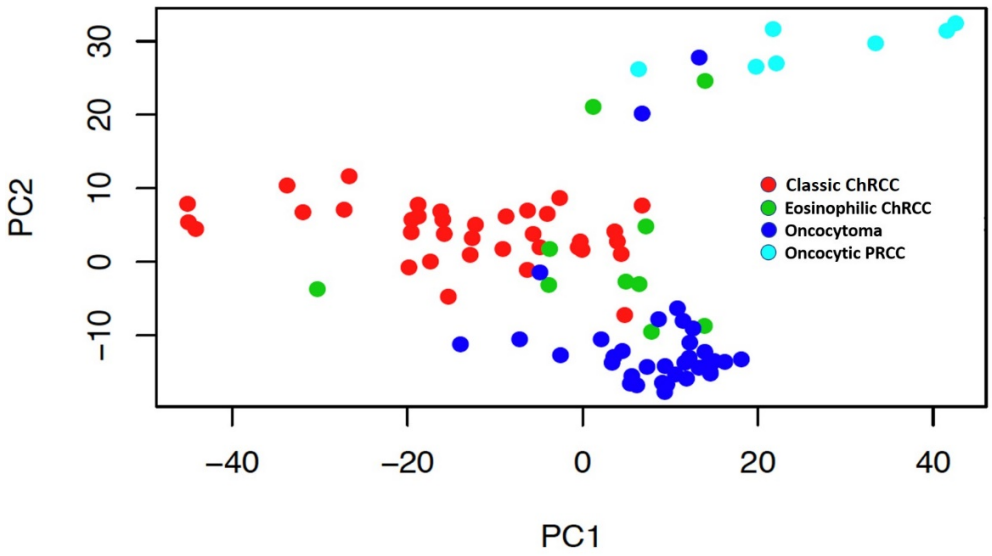


**Conclusions:** The histopathologic findings with the support of genomic data suggest that e-ChRCC may belong to a spectrum of renal oncocytic tumors with RO and c-ChRCC on different ends. Clinically aggressive tumors largely seem to be restricted in the classic variant.

## 1014 End Stage Renal Disease (ESRD) and Associated Tumors and Cysts

Abhishek Shah[1], Priti Lal[2], Lauren Schwartz[3], Matthew Palmer[2], Norge Vergara[1], Anupma Nayak[4]
*[1]Hospital of the University of Pennsylvania, Philadelphia, PA, [2]University of Pennsylvania, Philadelphia, PA, [3]Perelman School of Medicine at the University of Pennsylvania, Bala Cynwyd, PA, [4]Perelman School of Medicine at the University of Pennsylvania, Philadelphia, PA*

**Disclosures:** Abhishek Shah: None; Priti Lal: None; Lauren Schwartz: None; Matthew Palmer: None; Norge Vergara: None; Anupma Nayak: None

**Background:** Individuals with acquired cystic kidney disease (ACKD) in the setting of ESRD have a high risk for developing renal neoplasms, particularly ACKD-associated RCC (ACKD-RCC). ACKD-RCC is a well-recognized entity now; however, there is limited data published on the pathology of acquired cysts suggesting them as putative precursors of these tumors. Herein, we present our experience with ESRD kidneys, with comprehensive analysis of associated tumors and cysts.

**Design:** Cases were retrieved from pathology archives of Hospital of the University of Pennsylvania (2000-2018) using the key word "ESRD." H&E and IHC slides were reviewed to confirm the tumor diagnosis. Cysts were categorized as simple, atypical or ACDK-RCC-like cysts. Clinical history was reviewed from EMR. Next gen sequencing was performed on a small group of tumors (results pending).

**Results:** Of the 59 cases with ESRD (30-75 yrs), 55 were classified of having ACKD. 41/59 had 1 or > associated tumors (60 tumors) (size, 0.4 - 14cm). ACDK-RCC was the most common dominant tumor (25, 61%), followed by clear cell tubulopapillary (4, 10%), clear cell RCC (4; 10%), papillary type 1 RCC (5; 12%), papillary type 2 RCC (1, 2%), papillary adenoma (1, 2%) and oncocytoma (1, 2%). Of 25 cases of ACDK-RCC, 6 had b/l tumors and 19 had additional other tumors. 16 ACDK-RCCs exhibited microcystic/sieve pattern with mix of eosinophilic & clear cells with vacuolated cytoplasm and 12 had papillary type 2 features. Oxalate was identified in 20 cases. Of note, 18/25 ACDK-RCCs had ACDK-RCC-like cysts, 3 had atypical cysts, and 1 had both ACDK-RCC-like and atypical cysts in the background kidney. 33/41 cases had h/o hemo or peritoneal dialysis (range <1 to 20 yrs), 7 had no h/o dialysis and in 1 hx was not available. All 25 cases with ACDK-RCC received dialysis. 26/41 were African American, 13 Caucasian, and 2 with unknown race. Of the remaining non-tumor cases, 11 cases had cysts (4, atypical cysts and 7, multiple simple cysts). 2 of 59 ESRD cases did not have tumor or cysts. Follow up was available in 41 patients, including 13 deceased pts secondary to multiple comorbidities. 1 case had<

**Conclusions:** Our data shows that ACDK-RCC represents more than half of the tumors developing in ESRD. H/o dialysis and African American race are potential risk factors for developing ACDK-RCC, as well as other renal tumors. ACDK-RCC-like cysts are possible precursors of ACDK-RCC. Results of molecular study are pending and will be presented later.

## 1015 Renal Cell Carcinoma with Leiomyomatous Stroma Harbor Somatic Mutations of TSC1, TSC2, mTOR, and/or TCEB1: Clinicopathologic and Molecular Characterization of 18 Sporadic Tumors Supports a Distinct Entity

Rajal Shah[1], Bradley Stohr[2], Zheng Jin Tu[3], Yuan Gao[4], Christopher Przybycin[5], Jane Nguyen[5], Roni Cox[6], Fariborz Kolvear[7], Michael Weindel[8], Daniel Farkas[5], Kiril Trpkov[7], Jesse McKenney[5]

*[1]University of Texas Southwestern Medical Center, Plano, TX, [2]University of California San Francisco, San Francisco, CA, [3]Robert J. Tomsich Pathology & Laboratory Medicine Institute, Cleveland Clinic, Cleveland, OH, [4]Eastern Health/Memorial University, St. John's, NL, [5]Cleveland Clinic, Cleveland, OH, [6]Cleveland, OH, [7]University of Calgary, Calgary, AB, [8]Ann Arbor, MI*

**Disclosures:** Rajal Shah: None; Bradley Stohr: None; Zheng Jin Tu: None; Yuan Gao: None; Christopher Przybycin: None; Jane Nguyen: None; Roni Cox: None; Daniel Farkas: None; Kiril Trpkov: None; Jesse McKenney: None

**Background:** Renal cell carcinoma with (angio) leiomyomatous stroma (RCCLMS) is included as a provisional entity in the 2016 WHO classification of renal epithelial neoplasms. The debate remains whether it represents a distinct tumor entity or a heterogeneous group of RCCs presenting with similar morphology.

**Design:** We analyzed clinicopathologic, immunohistochemical, and molecular characteristics of 18 sporadic RCCs that met the provisional criteria, which included diffuse CK7 expression. Five cases from the initial cohort of 23 potential RCCLMSs were reclassified as clear cell RCC (CCRCC) based on morphology and CK7 expression pattern. To investigate their mutational and copy number alterations, we used a 170 gene solid tumor panel in 14 RCCLMS and 5 control CCRCCs. Additionally, 4 RCCLMS, suspicious for chromosome 8 copy number loss, were further analyzed by a 479 gene panel that included *TCEB1*.

**Results:** The mean patient age was 52 years (range, 33-69) with male: female ratio of 1:2. The average tumor size was 2.26 cm (range, 1.1-4.5). Microscopically, the distinctive feature included neoplastic nodules of elongated and often branching tubules, lined by cells with voluminous and mostly clear cytoplasm (100%). The nodules were separated by focal to prominent smooth muscle stroma. Additional features included: biphasic pattern of collapsed acini surrounding tubules with voluminous cytoplasm (50%), variable papillary architecture (39%), peritumoral lymphoid aggregates (39%), and hemosiderin-laden macrophages (33%). All (100%) RCCLMSs were pT1; 78% and 22% were WHO/ISUP grade 2 and 3, respectively. All patients with available follow-up were alive and without disease progression after a mean of 25.2 months (range, 1-58). RCCLMS showed a diffuse CK7, CAM5.2 and CD10 positivity in all cases. The molecular results showed recurrent mutations in all RCCLMS: *TSC1* (4), *TSC2* (4), *mTOR* (6), or *TCEB1* (2). Of 2 RCCLMSs with chr. 8 loss, one showed a hotspot *TCEB1* mutation without TSC/mTOR mutations, and one showed a previously undescribed 3-bp in-frame *TCEB1* deletion, along with a truncating *TSC1* mutation.

Figure 1 - 1015

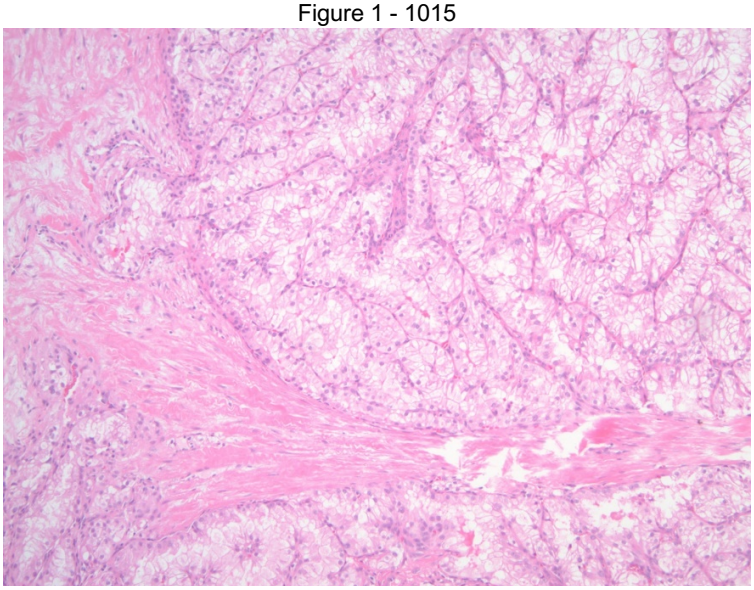

**Conclusions:** All evaluated RCCLMS harbored mutations of *TSC1*/*TSC2, mTOR*, and/or *TCEB1*, consistent with a hyperactive mTOR complex. Our results support the hypothesis that sporadic RCCLMS represents a counterpart of the similar RCC found in tuberous sclerosis complex (TSC) patients. RCCLMS represents a novel, emerging RCC subtype, distinct from both clear cell and clear cell-papillary RCC.

## 1016 Hexokinase 2 and its Subcellular Localization Detect Exfoliated Tumor Cells in Urine for Diagnosing and Grading Bladder Cancer

Qihui Shi[1], Peihua Lu[2], Jun Wu[3], Zhuo Wang[1], Jie Chen[4]
*[1]Fudan University Shanghai Medical College, Shanghai, China, [2]Wuxi People's Hospital Affiliated to Nanjing Medical University, Wuxi, Jiangsu, China, [3]Shanghai General Hospital, Shanghai Jiao Tong University School of Medicine, Shanghai, China, [4]Shanghai Jiao Tong University, Shanghai, China*

**Disclosures:** Zhuo Wang: None; Jie Chen: None

**Background:** Bladder cancer is among the most common tumors with a high recurrence rate necessitating high sensitive and noninvasive diagnosis and surveillance. Cystoscopy as an invasive procedure is the most effective means of detecting bladder cancer. Urine cytology is a noninvasive method for detecting high grade tumors, but remains limited utility in diagnosing low grade tumors. Molecular techniques such as BTA stat, NMP22 and UroVysion FISH suffer from insufficient sensitivity or specificity.

**Design:** We developed a cell-based Hexokinase 2 (HK2) immunoassay to detect exfoliated tumor cells (ETCs) engaging in elevated glycolysis in urine for high sensitive and noninvasive detection of bladder cancer, especially low-grade tumors. The cutoff of HK2 activity for identifying high glycolytic ETCs was generated from large-scale single-cell sequencing of urine-derived cells from 7 bladder cancer patients. Single-cell sequencing characterized the genome-wide copy number alternations and oncogenic driver mutations that determine the malignancy of cells, leading to establishment of the definition of high glycolytic ETCs ($HK2^{+}/CD45^{-}/DAPI^{+}$). The HK2 assay was then tested with a group of patients (n=107) including urothelial carcinoma patients and patients with other genitourinary disorders for evaluating diagnostic accuracy.

**Results:** We detected considerably higher high glycolytic ETCs in urothelial carcinoma patients versus the negative control group [37.5 (10.25-150.5) vs 0 (0-0) ETCs/10mL; P<0.0001). The diagnostic sensitivity, specificity, positive predictive value and negative predictive value were 89%, 88%, 82% and 94%, respectively. The subcellular HK2 localization was found to be associated with the grades of urothelial carcinoma, leading to 75% of overall accuracy in grading urothelial carcinoma.

Figure 1 - 1016

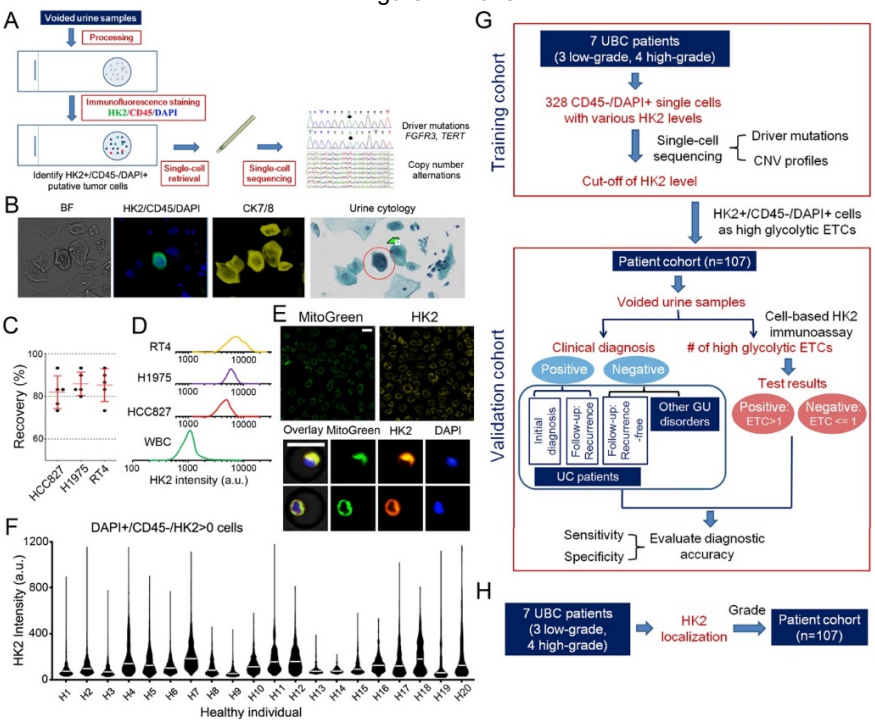

Figure 2 - 1016

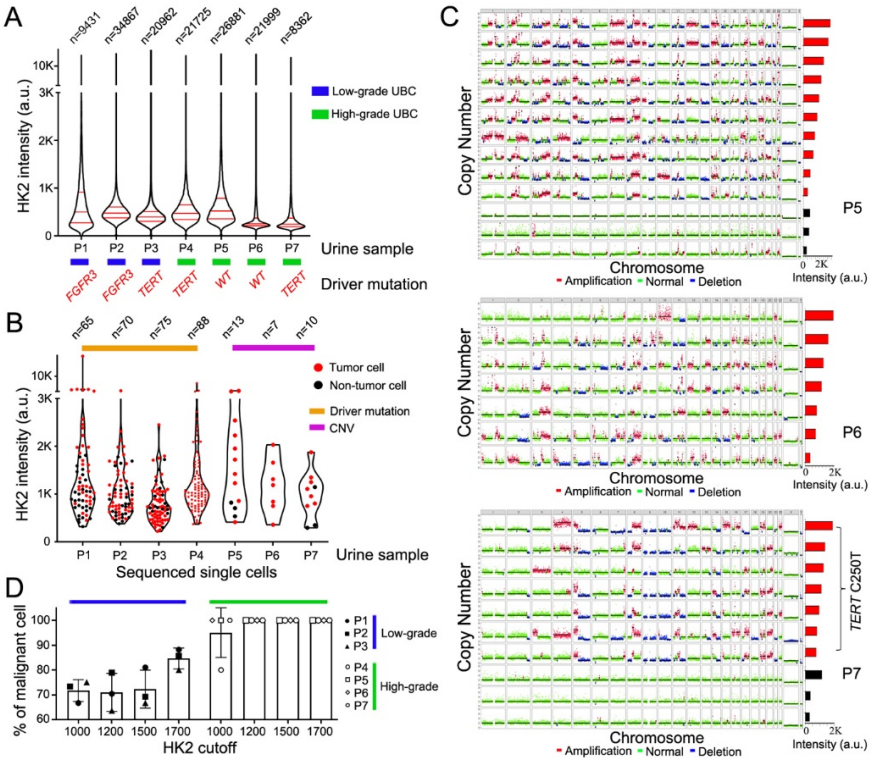


**Conclusions:** A novel urine-based, noninvasive metabolic assay has been developed for diagnosing and grading bladder cancer with potential clinical utility as a complement for cytology.

## 1017 Post-Transplant Bladder Carcinomas Associated with Oncogenic Polyomavirus Latent Infection

Luisa Sofía Silva Alcoser[1], Ana Aula Olivar[2], Mario Giner Pichel[1], Javier Hernandez-Losa[3], Stefania Landolfi[4], Santiago Ramon Y Cajal[1], Ines de Torres[5], Maria Eugenia Semidey-Raven[1]

*[1]Vall d'Hebron University Hospital, Barcelona, Spain, [2]Vall d'Hebron University Hospital (HUVH), Barcelona, Spain, [3]1. Hospital Universitari Vall d'Hebron. 2. VHIR. 3. CIBERONC, Barcelona, Spain, [4]1. Vall d'Hebron University Hospital; 2. CIBERONC, Barcelona, Spain, [5]Vall d'Hebron Campus and Autonomous University of Barcelona (UAB), Barcelona, Spain*

**Disclosures:** Luisa Sofía Silva Alcoser: None; Ana Aula Olivar: None; Mario Giner Pichel: None; Javier Hernandez-Losa: None; Stefania Landolfi: None; Santiago Ramon Y Cajal: None; Ines de Torres: None; Maria Eugenia Semidey-Raven: None

**Background:** Transplant recipients have known to have increased risk of malignancies due to immunosuppression, activation of oncogenic viruses, and chronic stimulation of immune system. Polyomavirus infection, latent or active, can favor cell proliferation, immune evasion and downregulation of apoptosis through its viral oncoproteins integrating in human genome. The urinary tract could be a target for carcinomas secondary to polyomavirus infection in immunosupressed (transplant) patients.

**Design:** Patients with post-transplant bladder carcinoma diagnosis were retrospectively reviewed between years 1999-2018 in our center. Clinical histories, biochemical, and histological findings were reviewed in each case. Immunohistochemistry (IHC, SV40) and polyomavirus PCR detection were performed in all cases.

**Results:** A series of 16 post-transplant patients were found with subsequent diagnosis of bladder carcinoma, of which 11 cases (69%) correspond to renal transplants, 3/liver (19%), 1/ pulmonary (6%) and 1/renopulmonary (6%). The average age of presentation was 59 years (47-72) with a mean time of 7y (1-28) after transplantation. Histologic high-grade tumors were observed in 75% of the cases, including 8 urothelial carcinomas (6 usual, 1 nested and 1 micropapillary), 2 squamous carcinomas, 1 adenocarcinoma and 1 mesonephric carcinoma. There were 4 (25%) low grade urothelial carcinomas. SV40 IHC technique was positive in 4 cases (25%): mesonephric carcinoma, micropapillary urothelial carcinoma and in two usual high-grade urothelial carcinomas. Study with PCR technique resulted positive in 5 cases (31.25%) corresponding to SV40+ tumors and one high-grade urothelial carcinoma SV40 negative case. Serum polyomavirus levels were measured in 6 asymptomatic patients, positive in 2 of them (SV40+, PCR+). Recurrence was seen in 2 cases (7 cases globally) associated with Polyomavirus infection and 1/6 (SV40+PCR+) patient died of the disease in the follow up.

**Conclusions:** There is a high incidence of polyomavirus latent infection (31,25%) in patients with bladder carcinomas after transplantation, frequently aggressive high grade carcinomas. Detection should be made with IHC/PCR in the tumor. Post-transplant patients with serum viremia(+) should aware clinicians of oncogenic effects and propose modifications in immusuppression/treatment of the disease. Polyomavirus infection could be a mechanism with new therapeutic targets in the treatment of bladder carcinomas associated with transplantation/Polyomavirus+.

## 1018 Urothelial Dysplasia: Diagnostic Value in Clinical Practice 20 Years since the 1998 WHO/ISUP Consensus

Steven Smith[1], Jesse McKenney[2], Gladell Paner[3], Hikmat Al-Ahmadie[4], Manju Aron[5], Daniel Berney[6], John Cheville[7], Maurizio Colecchia[8], Eva Compérat[9], Isabela da Cunha[10], Donna Hansel[11], Ondrej Hes[12], Michelle Hirsch[13], Rafael Jimenez[7], Seema Kaushal[14], Naoto Kuroda[15], James Kench[16], Oleksandr Kryvenko[17], Antonio Lopez-Beltran[18], Daniel Luthringer[19], Cristina Magi-Galluzzi[20], Rohit Mehra[21], Santosh Menon[22], Priya Rao[23], Ankur Sangoi[24], Luciana Schultz[25], Jeffry Simko[26], Bradley Stohr[26], Puay Hoon Tan[27], Toyonori Tsuzuki[28], Murali Varma[29], Sean Williamson[30], Ming Zhou[31], Debra Zynger[32], Holger Moch[33], George J. Netto[20], Lawrence True[34], Jae Ro[35], Kiril Trpkov[36], Rodolfo Montironi[37], John Srigley[38], Peter Humphrey[39], Jonathan Epstein[40], Victor Reuter[4], Mahul Amin[41]

*[1]Virginia Commonwealth University School of Medicine, Richmond, VA, [2]Cleveland Clinic, Cleveland, OH, [3]The University of Chicago, Chicago, IL, [4]Memorial Sloan Kettering Cancer Center, New York, NY, [5]Keck School of Medicine of University of Southern California, Los Angeles, CA, [6]Queen Mary University of London, London, United Kingdom, [7]Mayo Clinic, Rochester, MN, [8]Fondazione IRCCS Istituto Nazionale Tumori Milano, Milan, Italy, [9]Tenon Hospital, Paris, France, [10]Rede D'OR - São Luiz, São Paulo, SP, Brazil, [11]Oregon Health & Science University, Portland, OR, [12]Biopticka laborator s.r.o., Plzen, Plzensky kraj, Czech Republic, [13]Brigham and Women's Hospital, Boston, MA, [14]All India Institute of Medical Sciences, New Delhi, Delhi, India, [15]Kochi Red Cross Hospital, Kochi City, Kochi, Japan, [16]Royal Prince Alfred Hospital, Sydney, NSW, Australia, [17]University of Miami Miller School of Medicine, Miami, FL, [18]Champalimaud Clinical Center, Lisbon, Portugal, [19]Cedars-Sinai Medical Center, West Hollywood, CA, [20]The University of Alabama at Birmingham, Birmingham, AL, [21]University of Michigan, Ann Arbor, MI, [22]Tata Memorial Hospital, Mumbai, India, [23]The University of Texas MD Anderson Cancer Center, Houston, TX, [24]El Camino Hospital, Mountain View, CA, [25]Instituto de Anatomia Patológica, Anatomia Patologica Rede D'Or, Santa Barbara dOeste, SP, Brazil, [26]University of California San Francisco, San Francisco, CA, [27]Singapore General Hospital, Singapore, Singapore, [28]Aichi Medical University Hospital, Nagakute, Aichi, Japan, [29]University Hospital of Wales, Cardiff, Wales, United Kingdom, [30]Henry Ford Health System, Detroit, MI, [31]Tufts Medical Center, Boston, MA, [32]The Ohio State University Medical Center, Columbus, OH, [33]University Hospital Zürich, Zurich, Switzerland, [34]University of Washington Medical Center, Seattle, WA, [35]Houston Methodist Hospital, Houston, TX, [36]University of Calgary, Calgary, AB, [37]University Politecnica delle Marche/Medicine, Ancona, Italy, [38]Trillium Health Partners - Credit Valley Hospital, Mississauga, ON, [39]Yale University School of Medicine, New Haven, CT, [40]Johns Hopkins Medical Institutions, Baltimore, MD, [41]Methodist University Hospital, Memphis, TN*

**Disclosures:** Steven Smith: *Consultant*, Elsevier Publishing/Amirsys; Jesse McKenney: None; Gladell Paner: None; Hikmat Al-Ahmadie: None; Manju Aron: None; John Cheville: None; Maurizio Colecchia: None; Eva Compérat: None; Isabela da Cunha: None; Ondrej Hes: None; Michelle Hirsch: None; Rafael Jimenez: None; Seema Kaushal: None; Naoto Kuroda: None; Oleksandr Kryvenko: None; Daniel Luthringer: None; Cristina Magi-Galluzzi: None; Rohit Mehra: None; Santosh Menon: None; Priya Rao: None; Ankur Sangoi: None; Luciana Schultz: None; Jeffry Simko: None; Bradley Stohr: None; Puay Hoon Tan: None; Toyonori Tsuzuki: None; Murali Varma: None; Sean Williamson: None; Ming Zhou: None; Debra Zynger: None; George J. Netto: None; Lawrence True: None; Jae Ro: None; Kiril Trpkov: None; Rodolfo Montironi: None; Peter Humphrey: None; Jonathan Epstein: None; Victor Reuter: None; Mahul Amin: *Consultant*, Urogen; *Consultant*, Advanced Clinical; *Advisory Board Member*, Cell Max; *Advisory Board Member*, Precipio Diagnostics

**Background:** In the 1980-90s, flat neoplastic urothelial lesions were categorized as mild, moderate, and severe dysplasia, and urothelial carcinoma in situ (CIS). Three subsequent WHO classifications have condensed these lesions into urothelial dysplasia and CIS, with CIS including many lesions with moderate to severe dysplasia. Many suggest ‘dysplasia’ is infrequent in diagnostic specimens, but little is known of the use of this term in contemporary practice.

**Design:** We surveyed 45 academic uropathologists practicing in 12 countries on their diagnostic practices regarding 'dysplasia'. Deidentified responses to both specific questions regarding diagnostic practice and opinions regarding dysplasia diagnosis in prior and future practice were tabulated.

**Results:** Most respondents diagnosed dysplasia (82%) in the past 10 years, though many noted rarity of usage. Of those who have diagnosed dysplasia (N=37), 38% had done so in a *de novo* setting, although the majority (86%) made the diagnosis in the setting of antecedent urothelial neoplasm. Further, 31% have diagnosed dysplasia in the upper tract, 39% have diagnosed multifocal dysplasia, 56% diagnosed it with concurrent CIS or papillary neoplasm, and 33% used IHC to assess dysplasia *versus* CIS. Of those who did not diagnose dysplasia (N=8, 18%), all have reported the possibility of dysplasia in biopsies labeled ‘atypical’. Most (83%) consider dysplasia a relevant concept in the pathogenesis of urothelial neoplasms and nearly all (91%) support greater study. Only a minority (11%) could identify any important work supporting dysplasia as a distinct entity in two decades. Overall, nearly half of the participants were for (56%) or against (44%) prospective use of ‘dysplasia’ in practice.

**Conclusions:** Among academic uropathologists, there is striking variation in the use of ‘urothelial dysplasia’ across diagnostic settings. Most who use the term use it in biopsies with prior or concurrent urothelial neoplasia; some avoid the term, preferring ‘atypia’ for lesions

falling short of CIS. This discrepancy confirms need for a diagnostic term for lesions with features believed neoplastic but insufficient to designate as CIS. The decrease in urologic pathologists who favor future use of 'dysplasia' diagnosis (56%) compared to those reporting prior use of the term (84%) may signal the opportunity to promulgate improved terminology to communicate diagnostic concern and uncertainty. Future study will be needed to inform recommended follow-up and management.

## 1019 Multispectral Deep UV Microscopy: Utility in Prostate Cancer

Soheil Soltani[1], Ashkan Ojaghi[1], Adeboye O. Osunkoya[2], Francisco Robles[3]
*[1]Georgia Institute of Technology, Atlanta, GA, [2]Emory University, Atlanta, GA, [3]Georgia Institute of Technology and Emory University, Atlanta, GA*

**Disclosures:** Soheil Soltani: None; Ashkan Ojaghi: None; Adeboye O. Osunkoya: None; Francisco Robles: None

**Background:** Although the Gleason score (Grade group) continues to be one of the most reliable indicators of tumor aggressiveness in prostate cancer (PCa), it has important limitations including intra- and inter-observer variability in some cases, and inability to assess the molecular and subcellular structural composition of the tumor cells. We developed a quantitative, label-free multispectral deep ultraviolet (UV) microscopy technique to study PCa tissue sections, in order to identify the rich endogenous molecular composition of tissues with subcellular resolution.

**Design:** Ten cases of PCa with variable Gleason scores (Grade Groups) were selected. Unstained slides were obtained. A plasma-driven broadband light source (Energetiq, EQ-99X) that provides a continuous spectrum from 200 nm to around 2 μm was utilized. For each acquisition, only one wavelength was selected using a bandpass filter (bandwidth=10nm). The incoming beam was relayed to the samples using an off-axis parabolic mirror. The transmitted light was collected using a Thorlabs (LMU-40X-UVB) UV objective and detected using a UV camera (PCO. Ultraviolet) with a biconvex lens (f=150 mm). A schematic of the setup is shown in fig.1.

For each area of interest, a multispectral data cube was taken at four different wavelengths by rotating a filter wheel to choose the corresponding wavelength (220, 255, 280 and 300 nm). Acquisition time was 100ms for each wavelength with a field of view of ~300μm X 300μm and resolution of ~250 nm.

**Results:** Analysis of the samples from the 10 patients showed clear morphological and molecular differences from each region of interest with different degrees of tumor aggressiveness (Gleason scores/Grade groups). The summary of data analysis and two representative colorized images are shown in fig.2.

Figure 1 - 1019

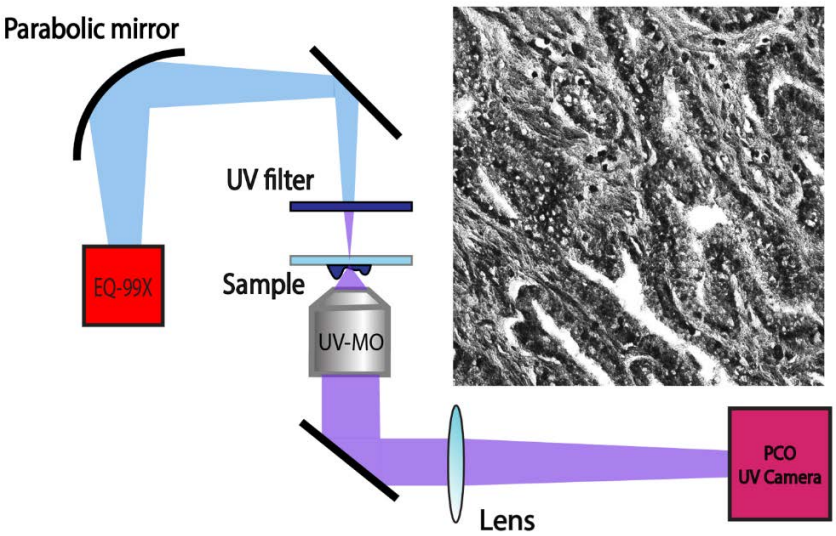

Figure 2 - 1019

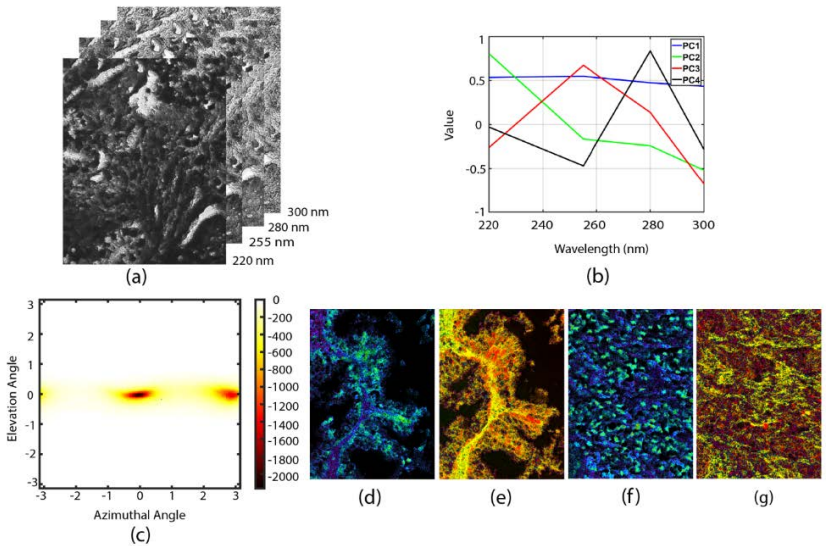


**Conclusions:** Our multispectral deep UV microscopy technique uses distinct spectral features of biomolecules in the UV spectrum to provide unique molecular and structural quantitative information of PCa samples. Samples with different Gleason scores (Grade groups) have district molecular and structural composition as determined with deep-UV microscopy. This approach is fast, inexpensive, and has high-spatial resolution, and thus could be used to study phenotypes of aggressive PCa, and help improve diagnostic accuracy and prognosis.

## 1020 CCDC170 as a Candidate for Prostate Cancer Predisposition Gene Variants in a Korean Family with Hereditary Prostate Cancer

Ji-Youn Sung[1], Hangyeol Kim[2], Sang Hyub Lee[1], Inho Park[3]
*[1]Kyung Hee University, Seoul, Korea, Republic of South Korea, [2]Seoul, Korea, Republic of South Korea, [3]SD Genomics, Seoul, Korea, Republic of South Korea*

**Disclosures:** Ji-Youn Sung: None; Hangyeol Kim: None; Sang Hyub Lee: None; Inho Park: None

**Background:** Prostate cancer (CaP) is one of the most common cancers in men, and the incidence rate of CaP is the highest in developed countries. The family history of CaP is one of the established risk factors for the disease apart from environment and ethnicity. To date, several genetic variants such as mutations of *BRCA2* and *HOXB13* have been suggested to affect the development of CaP. However, most genetic studies on CaP were conducted on Western patients. Few studies have been conducted on the associations between CaP and genetic variations in Asians.

**Design:** We sequence whole exoomes of 9 family members including 3 prostate cancer patients of the pedigree shown in Fig. 1. The exomes were captured with the Agilent SureSelect Human All Exon V6 and sequenced with paired-end sequencing (2 x 150 bp) using the NextSeq (Illumina). The sequence reads were mapped to the human reference genome (hg38) with bwa-mem (0.7.17-r1188) followed by joint variant calling with the best practice proposed by the GATK team. We predicted functional effect of each variant on genes and proteins with SnpEff (ver. 4.3), and annotated the population frequency of each variant with the following well known databases: dbSNP, ExAC, TopMed, and 1000 genomes phase3. To reflect ethnic specificity, we also included KRGDB as a population frequency database.

**Results:** There were 3 variants mapped to known herreditary cancer predisposition genes which is defined as genes whose variants have been reported as pathogenic or likely pathogenic for CLDN matched with "cancer" or "prostate" from ClinVar database (as of 2018-12-02). According to the pedigree, the variants observed in all the three affected samples are further filtered with the condition of absence of variant in all the samples in unknown-sibling groupo. This yields 41 high impact or moderate impact variants. To further investigate the rare variant. we calculated the distance between those variants and GWAS catalogue SNPs. Within 10,000 bp distance, there was a pair of rare variants of GWAS SNP. The frame0shift deletion of CCDC170 is located near rs3757318, known to increase risk of breast cancer.

Figure 1 - 1020

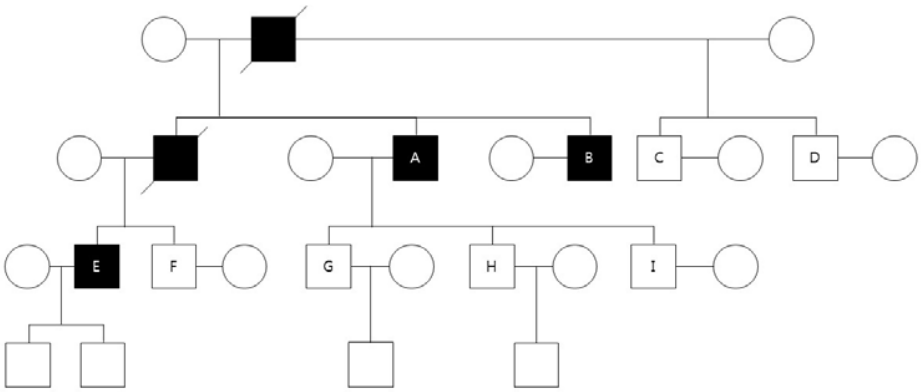


**Conclusions:** Since we could not detect pathogenic or likely pathogenic variant among well-established hereditary cancer genes, we might suggest a frameshift mutation in the CCDC170 as the most promising novel candidate in the family by considering its known association to breast cancer.

## 1021 Persistent Challenges in Nuclear Grading of Clear Cell Renal Cell Carcinoma

Kanika Taneja[1], Sean Williamson[1]
*[1]Henry Ford Health System, Detroit, MI*

**Disclosures:** Kanika Taneja: None; Sean Williamson: None

**Background:** The World Health Organization (WHO) and International Society of Urological Pathology (ISUP) grading system for renal cell carcinoma now focuses on nucleolar prominence as the main criterion. We aimed to investigate how this system is implemented in certain scenarios.

**Design:** An online survey was circulated via e-mail to a group of genitourinary pathology specialists (GU) and shared publicly via social media (including via Twitter and 3 Facebook pathology groups, 2 focusing on urologic pathology and 1 large general surgical pathology group). The survey included a mixture of descriptive questions and images.

**Results:** In total, 91 responses were received from non-trainee pathologists, 77 self-identified as GU and 14 as non-GU. The vast majority reported using the ISUP/WHO system rather than Fuhrman (92% GU, 79% non-GU). Most reported not requiring nucleoli to be eosinophilic when determining visibility (77% GU and 72% non-GU). Most indicated that nucleoli visualized at high magnification at all (40×, composing an entire high-power field), would be considered grade 2, even if nucleoli are not eosinophilic / large (67% GU and 57% non-GU). Distinguishing grade 2 from 3 (10× magnification) yielded a similar response with 63% GU and 61% non-GU. When shown a photomicrograph taken at 40× magnification with visible but relatively small basophilic nucleoli (Figure A), most reported grade 2 (93% GU and 79% non-GU). For an image with more prominent nucleoli described as visible at 10×, 82% of GU and 71% non-GU reported grade 3. Respondents estimated using grade 1 in 5% or less of resection cases (73% GU, 57% non-GU, with one-third estimating 2% of cases or less). For multinucleated cells with bland individual nuclei (Figure B), most (84% GU, 86% non-GU) would not consider this grade 4.

Figure 1 - 1021

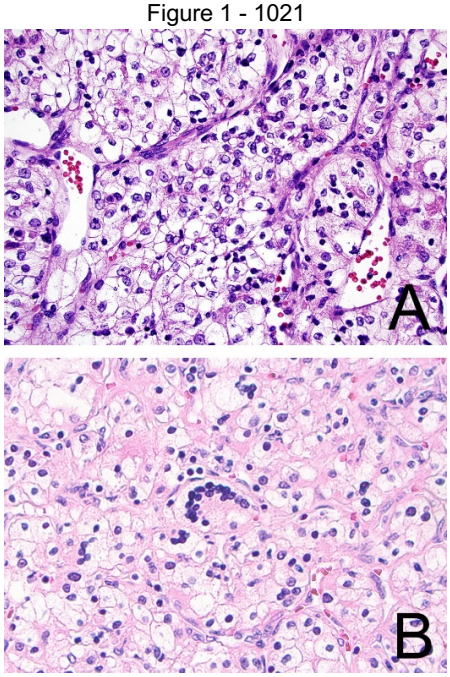


**Conclusions:** The ISUP/WHO grading system for renal cell carcinoma has gained relatively widespread acceptance; however, some uncertainty remains regarding the degree of nucleolar prominence that warrants a higher grade. Despite the official descriptions requiring nucleoli to be eosinophilic, most pathologists do not require this in practice. Most respondents estimate that they use grade 1 very rarely. It is not entirely clear how tumor cells with multiple, non-bizarre nuclei should be handled, although most do not consider this inherently grade 4.

## 1022 Glycogen Synthase Kinase-3 Beta (GSK-3β) Expression, Tumor Mutational Burden (TMB) and PD-L1 Tumor Proportion Score (TPS) in Bladder Cancer

Fabio Tavora[1], Ali Amin[2], Carmen Perrino[3], Cleto Dantas Nogueira[4], Marclesson Alves[5], Vinicios Alves da Silva[6], Dragan Golijanin[7], Andre de Souza[7], Howard Safran[8], Wafik El-Deiry[9], Benedito Carneiro[1]

*[1]Brown University, Alpert Medical School, Lifespan Cancer Institute, Providence, RI, [2]Lifespan, Providence, RI, [3]Sharon, MA, [4]Fortaleza, CE, Brazil, [5]Federal University of Ceará, Fortaleza, CE, Brazil, [6]Argos Laboratory / Messejana Heart and Lung Hospital, Fortaleza, CE, Brazil, [7]Brown University Lifespan Academic Medical Center, Providence, RI, [8]Brown University, Lifespan Cancer Institute, Providence, RI, [9]Brown University, Providence, RI*

**Disclosures:** Fabio Tavora: None; Ali Amin: None; Carmen Perrino: None; Cleto Dantas Nogueira: None; Marclesson Alves: None; Vinicios Alves da Silva: None; Howard Safran: None; Benedito Carneiro: None

**Background:** Glycogen Synthase Kinase-3 beta (GSK-3β) regulates diverse cellular functions including metabolic activity, signaling and structural proteins. GSK-3β phosphorylates target pro-oncogenes such as C-myc and regulates programmed cell death-ligand 1 (PD-L1) expression in T cells (Taylor A *et al.* 2016). GSK-3β nuclear expression has been associated with high-grade morphology, metastasis, and poor prognosis (Ougolkov 2006). Small molecule selective GSK-3β inhibitors such as 9-ING-41 with significant pre-clinical antitumor activity in a broad spectrum of malignancies is clinical development (NCT03678883). This study investigated the correlation between GSK-3β expression and other clinically relevant molecular features of bladder cancer.

**Design:** We retrospectively evaluated genomic sequencing data and expression of PD-L1 and GSK-3β by immunohistochemistry in 18 specimens of advanced stage bladder cancer and complemented the study with the evaluation of a second cohort of 140 bladder urothelial carcinoma with tissue microarrays from 102 cystectomies and 38 transurethral resections of bladder tumors.

**Results:** Of the 140 cases of the TMA, 90.7% showed cytoplasmic positivity for GSK-3β, with a positive correlation with high-grade tumors ($p<0.001$). Low-grade tumors showed a lower histologic score overall and did not show nuclear positivity. All urothelial carcinomas with squamous differentiation (n=16) expressed GSK-3β and had the highest histologic scores. Eighteen cases were submitted to next-generation sequencing (NGS). Tumor mutational burden available in 11 cases ranged from 2,9 to 13mut/mb. All tumors were microsatellite stable. Sixteen (88%) showed cytoplasmic positivity for GSK-3β with a histologic score (intensity x percentage) ranging from 40 to 280. PD-L1 was positive in 9 cases, with two tumors having high expression of PD-L1 (>50%). These two cases were the only ones showing intense nuclear expression of GSK-3β.

**Conclusions:** Cytoplasmic expression of GSK-3β was identified in 90% of urothelial carcinomas and correlated with high-grade tumors. Urothelial carcinomas with squamous differentiation had a distinctly high expression of GSK-3β. Nuclear GSK-3β expression was observed in tumors with high expression of PD-L1.

## 1023 Glycogen Synthase Kinase-3beta Fusions and Mutations in Prostate Cancer

Fabio Tavora[1], Brittany Borden[2], Marclesson Alves[3], Andre de Souza[4], Howard Safran[5], Carmen Perrino[6], Ali Amin[7], Francis Giles[8], Dragan Golijanin[4], Wafik El-Deiry[9], Benedito Carneiro[1]
*[1]Brown University, Alpert Medical School, Lifespan Cancer Institute, Providence, RI, [2]Alpert Medical School of Brown University, Providence, RI, [3]Federal University of Ceará, Fortaleza, CE, Brazil, [4]Brown University Lifespan Academic Medical Center, Providence, RI, [5]Brown University, Lifespan Cancer Institute, Providence, RI, [6]Sharon, MA, [7]Lifespan, Providence, RI, [8]Developmental Therapeutics Consortium, Chicago, IL, [9]Brown University, Providence, RI*

**Disclosures:** Fabio Tavora: None; Brittany Borden: None; Marclesson Alves: None; Howard Safran: None; Carmen Perrino: None; Ali Amin: None; Francis Giles: *Employee*, Actuate Therapeutics; Benedito Carneiro: None

**Background:** Glycogen synthase kinase-3 beta (GSK3b) regulates cancer relevant cellular processes and represents a potential therapeutic target. It phosphorylates target pro-oncogenes such as C-Jun and C-myc and regulates nuclear NF-kB transcriptional activity. GSK3b is upregulated in prostate cancer cells and GSK3b inhibitors reduced prostate cancer cell growth. Defining the landscape of GSK3b gene alterations in prostate cancer can reveal potential pathological subgroups relevant for treatment with GSK3b inhibitors in clinical development.

**Design:** We queried the CBioportal cancer genomics database to investigate the *GSK3b* genomic alterations in human samples of prostate cancer and to compare with the current molecular taxonomy. The database contains datasets of published cancer studies, including more than 4800 prostate cancer samples. After listing the *GSK3b* genomic alterations, we searched for other genomic data involving the main genes previously described in prostate cancer data (*TP53, PTEN, ERG, ETV1/4, FLI1, SPOP, FOXA1 and IDH1*)

**Results:** There was a total of 4638 patients with prostate cancer (4868 samples) in 19 studies. GSK3b alterations were identified in 7% of the cases. The most prevalent alteration was copy number variations (CNV) in 59 samples (YY%; 52 amplifications, 7 homozygous deletions), including primary, metastatic, castration-resistant and neuroendocrine tumors. There were 2 cases with frameshift deletions involving the locus E211Dfs*17, four cases with R167* nonsense mutations, and other mutations in single cases. The AR gene was the most common mutated gene, present in 5 samples. *SPOP* mutations were present in 4 samples (F125L, F133L, F133L, K129E). Other genes associated with the AR pathway (ZBTB16, ZBTB3, ZBTB49) were present in one sample each. In addition, there were 2 samples with FOXA1 mutations.

**Conclusions:** GSK3b molecular alterations were present in 7% of cases of prostate cancer. The most frequent molecular alteration was CNV but mutations and deletions were also observed. Understanding the genomic landscape of *GSK3b* gene alterations in prostate cancer will be important to guide the clinical development of novel GSK3b inhibitors and define relevant molecular subgroups potentially sensitive to these inhibitors.

## 1024 Nuclear Localization of Gsk-3β Protein Correlates with PTEN Loss and Worse Pathologic Outcomes Post-Prostatectomy

Fabio Tavora[1], Tamara Lotan[2], Daniela Correia Salles[3], Igor Costa[4], Vinicios Alves da Silva[5], Carmen Perrino[6], Ali Amin[7], Francis Giles[8], Dragan Golijanin[9], Brittany Borden[10], Howard Safran[11], Wafik El-Deiry[12], Benedito Carneiro[1]
*[1]Brown University, Alpert Medical School, Lifespan Cancer Institute, Providence, RI, [2]Johns Hopkins School of Medicine, Baltimore, MD, [3]Johns Hopkins Medical Institutions, Baltimore, MD, [4]Argos Laboratory, Fortaleza, CE, Brazil, [5]Argos Laboratory / Messejana Heart and Lung Hospital, Fortaleza, CE, Brazil, [6]Sharon, MA, [7]Lifespan, Providence, RI, [8]Developmental Therapeutics Consortium, Chicago, IL, [9]Brown University Lifespan Academic Medical Center, Providence, RI, [10]Alpert Medical School of Brown University, Providence, RI, [11]Brown University, Lifespan Cancer Institute, Providence, RI, [12]Brown University, Providence, RI*

**Disclosures:** Fabio Tavora: None; Tamara Lotan: *Grant or Research Support*, Ventana/Roche; Daniela Correia Salles: None; Igor Costa: None; Vinicios Alves da Silva: None; Carmen Perrino: None; Ali Amin: None; Francis Giles: *Employee*, Actuate Therapeutics; Brittany Borden: None; Howard Safran: None; Benedito Carneiro: None

**Background:** Glycogen synthase kinase 3ß (GSK-3β) regulates cancer-relevant cellular processes and represents a potential therapeutic target. Nuclear accumulation of GSK-3β is associated with high-grade tumors, metastatic potential, and poor prognosis (Ougolkov 2006). GSK-3β is upregulated in prostate cancer cells and GSK-3 inhibitors reduced prostate cancer cell growth. Defining subgroups of prostate cancer associated with high expression of GSK-3 might be relevant for selection for treatment with GSK-3β inhibitors in clinical development, including 9-ING-41, a small molecule potent selective GSK-3β inhibitor in phase 1/2 clinical trial (NCT03678883).

**Design:** This project aimed to investigate the association between GSK-3β expression, the molecular subtypes of prostate cancer and pathologic outcomes after radical prostatectomy (RP). A total of 140 men who underwent RP were included. GSK-3β expression was

assessed by semi-quantitative and automated analyses and correlated with ERG and PTEN that were assessed using validated immunohistochemistry assays in tissue microarrays. A histologic score (h-score) from 0-300 was established measuring GSK-3β positive cells by a genitourinary pathologist and automated detection on digitized scanned image using QuPath software.

**Results:** Cytoplasmic GSK-3β positivity was seen in the majority of tumors (n=110; 78%), but the nuclear expression of GSK-3β was detected in only 8 cases (5.7%). ERG expression and PTEN loss were observed in 52% (71/140) and 42%, respectively. There was a significant correlation between automated detection of GSK-3β positive tumor cells and pathologist evaluation (kappa agreement of 0.82). The GSK-3β h-score correlated with higher Gleason grade, extraprostatic extension (pT3a). The molecular subgroup more commonly positive for GSK3ß was PTEN intact/ERG positive. Interestingly, the 8 cases with nuclear localization of GSK3ß had higher Gleason score (no grade group-1/Gleason 6 cases), higher pathologic stage (5 stage 3 and 1 patient with positive nodal disease N1), and all but one had PTEN loss.

**Conclusions:** GSK3ß-positive prostate tumors are associated with higher-grade tumors displaying a distinct molecular subtype (PTEN intact/ERG positivity). Tumors with nuclear expression of GSK-3β were associated with PTEN loss and adverse pathologic outcomes.

## 1025 Limited Adenocarcinoma of the Prostate on Needle Core Biopsy: Is Accurate Grading Critical?

Yuki Teramoto[1], Phoenix Bell[1], Pratik Gurung[1], Zhiming Yang[1], Hiroshi Miyamoto[1]
*[1]University of Rochester Medical Center, Rochester, NY*

**Disclosures:** Yuki Teramoto: None; Phoenix Bell: None; Pratik Gurung: None; Zhiming Yang: None; Hiroshi Miyamoto: None

**Background:** Grading small foci of prostate cancer on needle core biopsy (Bx) is often difficult. Meanwhile, up-grading in radical prostatectomy (RP) specimens is relatively common, especially in Bx with Grade Group (GG) 1 tumor. The primary aim of this study is to assess the clinical significance of accurate grading for limited prostatic adenocarcinoma on Bx.

**Design:** We studied consecutive patients undergoing sextant prostate needle Bx (≥12 cores) followed by RP from 2008-2017. Within our Surgical Pathology database, we identified 296 men who met the inclusion criteria for only 1 core involvement of adenocarcinoma on Bx. Cases showing discontinuous tumor foci separated by intervening benign tissue, or carcinoma detected on target Bx, were excluded.

**Results:** The linear lengths of tumor involvement in these Bxs were: <1-mm (L0-1, n=115); ≥1/<2-mm (L1-2, n=82); ≥2/<3-mm (L2-3, n=33); and ≥3-mm (L3-, n=66). Bx GGs in the L0-1/L1-2/L2-3/L3- groups were up- or down-graded on RP in 43%/37%/45%/36% of cases, respectively. Thus, the rates of up/down-grading on RP were not significantly different among groups. pT3 disease was more often found in Bx GG2-4 cases (all: 24% vs 9%, $P$<0.001; <3-mm: 18% vs 8%, $P$=0.0495) than in Bx GG1 cases as well as in Bx GG3-4 cases (all: 27% vs 12%, $P$=0.015) than in Bx GG1-2 cases. Estimated tumor volume was also significantly larger in Bx GG2-4 cases (all, $P$<0.001; <1-mm, $P$<0.001; <2-mm, $P$=0.002; <3-mm, $P$<0.001; 1-2-mm, $P$=0.012). Kaplan-Meier analysis and log-rank test revealed higher risks of biochemical recurrence (BCR) after RP in men with Bx GG2-4 ($P$<0.001), GG3-4 ($P$<0.001), GG4 ($P$<0.001), L3- GG2-4 ($P$=0.035), L3- GG3-4 ($P$<0.001), or L3- GG4 ($P$<0.001) tumor. Only 2 (0.9%) patients with Bx <3-mm tumor had a BCR. Additionally, when tumor length on Bx was compared (i.e. <1-mm vs ≥1-mm, <2-mm vs ≥2-mm, <3-mm vs ≥3-mm), there were statistically significant differences in RP GG (GG1-2 vs GG3-4; all comparisons), pT stage (2 vs 3; all comparisons), surgical margin status (<1-mm vs ≥1-mm, <3-mm vs ≥3-mm), tumor volume (all comparisons), and BCR (<1-mm vs ≥2-mm, <3-mm vs ≥3-mm), but not pN stage.

**Conclusions:** GG and tumor length on prostate Bx appear to have an impact on pT stage, tumor volume, and/or BCR risk, while there are no significant differences in the rate of under/over-grading among the groups classified based on the Bx tumor length. These results suggest that pathologists may still need to make maximum efforts to grade relatively small prostate cancer on needle core Bx.

## 1026 Evaluation of a Direct-to-Digital Histology Method for Rapid Primary Diagnosis of Prostate Biopsies

Richard Torres[1], Eben Olson[1], Darryl Martin[1], Preston Sprenkle[2], Robert Homer[3], Michael Levene[4], Sudhir Perincheri[5], Peter Humphrey[2]
*[1]Yale School of Medicine, New Haven, CT, [2]Yale University School of Medicine, New Haven, CT, [3]Yale University School of Medicine, Hamden, CT, [4]Applikate Technologies, Weston, CT, [5]Yale University, New Haven, CT*

**Disclosures:** Richard Torres: *Stock Ownership*, Applikate Technologies, LLC; Eben Olson: *Stock Ownership*, Applikate Technologies; Robert Homer: None; Michael Levene: *Employee*, Applikate Technologies, LLC; Sudhir Perincheri: None; Peter Humphrey: None

**Background:** The low prostate diagnostic concordance rate could benefit from remote access to image data by specialist pathologist consultants, but digital adoption has been hampered by associated labor and cost plus imaging artifacts which likely reduce accuracy. Whole slide imaging (WSI) also does not address numerous drawbacks associated with processing itself. Multiphoton microscopy (MPM) obtains optical rather than physical sections from fluorescently stained uncut, unembedded prostate biopsies which can closely recreate physical H&E slides while addressing problems of WSI and histology processing, but practical implementation has been perceived to be a

challenge. Here we describe an initial clinical validation of a new MPM system for primary diagnosis on intact prostate biopsies that implements recent advances in image quality and acquisition speed potentially enabling practical application as a substitute for physical slide preparation.

**Design:** Prostate core biopsy specimens from 20 consented individuals with a high or moderate likelihood of prostatic adenocarcinoma based on pre-biopsy MRI. Sample preparation involved a previously-described two-step process involving a combined alcohol dehydration/staining step followed by clearing for refractive index matching. The imaging system is a prototype multiphoton microscope system designed for fast image capture at high resolution and at depth. Visualization software (Stackstreamer) developed for the efficient histologic review of multi-level image stacks was used for pathologist evaluation. Subsequently embedded and physically sectioned slides were visualized under wide-field microscopy as well as with WSI for comparative evaluation.

**Results:** Specimens collected showed full range of diagnostic Gleason grades. Prostate specimens that were imaged same day of biopsy (n = 9) had primary diagnostic images available within < 3 hours of time of biopsy, markedly faster than standard processing. Digital slices derived from multiphoton imaging were virtually indistinguishable from digitized physical slices (figure 1), with no clinically relevant differences recognized other than fewer cutting artifacts. Primary diagnostic interpretation by the MPM digital method showed improved concordance with final reference diagnosis, fewer immunohistochemistry requests, and longer measurable core and carcinoma length.

Figure 1 - 1026

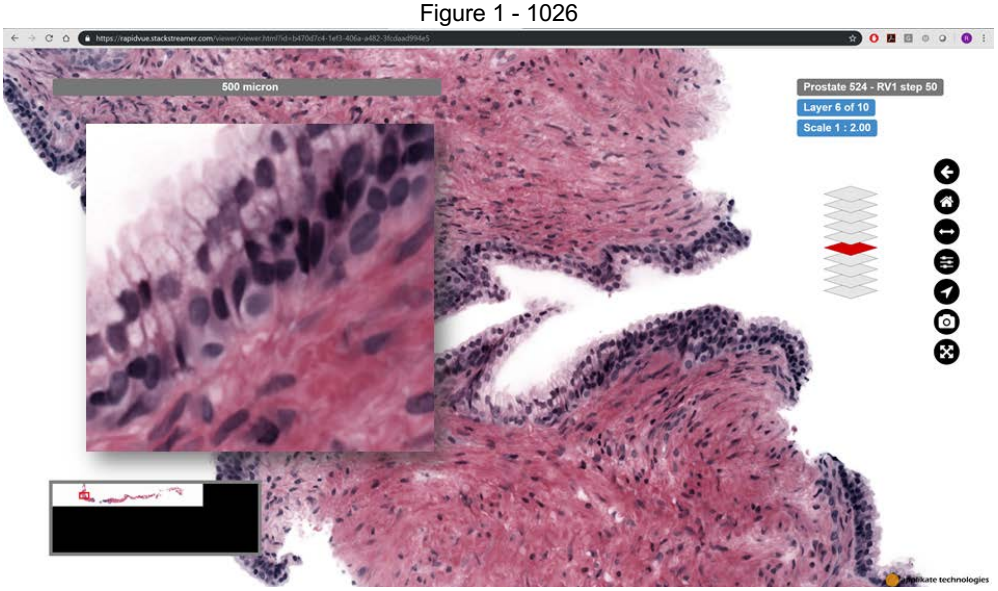


**Conclusions:** Findings justify clinical integration of MPM for further clinical validation as an alternative to standard tissue processing and WSI.

## 1027 Differential Expression of PRAME in Testicular Germ Cell Tumors

Aimi Toyama[1], Yan Zhou[1], Paari Murugan[1], Faqian Li[1], Lihong Bu[1]
[1]*University of Minnesota, Minneapolis, MN*

**Disclosures:** Aimi Toyama: None; Yan Zhou: None; Paari Murugan: None; Faqian Li: None; Lihong Bu: None

**Background:** The accurate identification of testicular germ cell tumor (GCT) is essential to the clinical team in tailoring treatment in this era of personalized medicine. PRAME (preferentially expressed antigen in melanoma), a tumor-associated antigen in the family of cancer testis antigens, has been previously shown to regulate pluripotency and suppress somatic/germ cell differentiation in seminomas. High nuclear expression of the antigen has been demonstrated in pure seminomas, whereas it was absent in embryonal carcinomas (EC). This suggests that PRAME immunohistochemical (IHC) stains have the potential to be a useful diagnostic marker in the detection of seminomas. To better understand its utility, we retrospectively studied PRAME IHC staining in both pure and mixed testicular GCTs.

**Design:** Within our institution database, we searched for testicular GCTs from 2005 to 2018, yielding a total of 132 cases (76 seminomas, 9 teratomas, 7 EC, 1 yolk sac tumor (YST), 1 choriocarcinoma (CC), and 38 mixed GCTs). Among these, 60 cases were evaluated that had slides available to review as well as a representative block for staining with PRAME antibody. Cases with artifacts such as folding and loss of tissue were excluded. Only 12 cases of pure seminomas were randomly chosen to match the number of mixed seminomas that were available for staining. For analysis, nuclear staining was considered positive, and the results were reviewed by two pathologists.

**Results:** All cases of pure seminoma (12/12) showed positive nuclear staining with PRAME. Similarly, all seminomatous components within mixed GCTs (11/11) showed nuclear positivity. EC, both in pure (0/5) and as a component of a mixed GCT (0/24), showed negative PRAME staining. Teratomas, both in pure (0/5) and as a component of a mixed GCT (0/12), also showed negative staining. Only one case of pure CC was identified and stained positive (1/1) for PRAME, although within mixed GCTs, the CC component stained negative in all 5 cases (0/5). Staining of YST yielded notable results, with the only pure case (1/1) as well as 4/14 (25.6%) of mixed cases staining positive, whereas 10/14 (71.4%) of mixed cases showed absent staining. In all cases reviewed where GCNIS was present, the GCNIS component was positive (26/26).

**Conclusions:** With high PRAME IHC staining in seminomas and variable expression in CC and YST, PRAME may have diagnostic utility as a marker for identifying seminomatous components within mixed GCTs and distinguishing them from EC and teratoma components.

## 1028 Well Differentiated Neuroendocrine Tumors of Lower Urinary Tract

Aline Tregnago[1], Yuly Ramirez[2], Daniela Correia Salles[3], Maria Del Carmen Rodriguez Pena[4], Marie-Lisa Eich[5], Jonathan Epstein[3], George J. Netto[4]
*[1]Centro de Patologia Medica, Caxias Do Sul, RS, Brazil, [2]Bogotá, D.C., Colombia, [3]Johns Hopkins Medical Institutions, Baltimore, MD, [4]The University of Alabama at Birmingham, Birmingham, AL, [5]University Hospital Cologne, Cologne, NRW, Germany*

**Disclosures:** Yuly Ramirez: None; Daniela Correia Salles: None; Maria Del Carmen Rodriguez Pena: None; Marie-Lisa Eich: None; Jonathan Epstein: None; George J. Netto: None

**Background:** Primary well differentiated neuroendocrine tumors (WD-NET) of the lower urinary tract (LUT) are very rare. Although they have been considered potentially malignant neuroendocrine neoplasms, most of the previously reported cases were associated with favorable outcome. Only 13 histologically well documented cases of pure carcinoid tumors of the bladder and 2 of the prostatic urethra have been reported in the literature.

**Design:** Surgical pathology electronic medical records were searched in 1 institution for all diagnosis of “carcinoid” tumor of LUT, including consultation cases, between 1984 and 2016. We identified 10 primary WD-NET. All cases were reviewed by a genitourinary pathologist. Immunohistochemical (IHC) analysis for synaptophysin, chromogranin and Ki-67 was performed in all cases. NKX3.1 and PSA was applied in one case. Follow up data was obtained.

**Results:** A total of 10 cases were identified, 8 arising in the bladder, 1 in the prostatic urethra and 1 in a female urethra. Patients included 6 male and 4 female and ranged in age from 45 to 73 years (mean 61). The 8 urinary bladder cases were located in the trigone and bladder neck regions.

Microscopically, all the lesions were confined to the lamina propria. Tumor architecture was prominently pseudoglandular with acinar and cribriform structures and focal solid areas. Cystitis cystica et glandularis (CCG) was identified in 5 cases. Cytologically, typical WD-NET morphology was displayed. Mitotic activity was rare to absent and no necrosis was identified.

Neuroendocrine differentiation was confirmed by IHC. Synaptophysin and chromogranin were diffusely positive in all cases. Differential diagnosis of prostate cancer was raised in 1 case and resolved with negative PSA and NKX3.1. Ki-67 proliferation index was 2% or less (see table). There was no evidence of residual disease or recurrence in any patient. Follow up ranged from 1 to 11 months.

| Case | Age (y) / Sex | Location | Ki-67 index |
|---|---|---|---|
| 1 | 60/F | Bladder | <1% |
| 2 | 45/M | Bladder | 1% |
| 3 | 58/M | Bladder | 1% |
| 4 | 59/M | Bladder | 1% |
| 5 | 56/M | Prostatic urethra | <1% |
| 6 | 72/F | Bladder | <1% |
| 7 | 73/M | Bladder | 2% |
| 8 | 64/F | Urethra | 2% |
| 9 | 69/F | Bladder | 1% |
| 10 | 54/M | Bladder | 2% |

LP: lamina propria

**Conclusions:** Ten new cases of WD-NET are described. All cases had benign biologic behavior on follow-up. The tumors share typical morphologic features with WD-NET of other sites, with notable pseudo-glandular architecture and association with CCG.

## 1029 To Stage or not to Stage: Determining the True Clinical Significance of Biopsy Tract Seeding of Renal Cell Carcinoma in Perinephric Fat

Aida Valencia-Guerrero[1], Esther Oliva[2], Chin-Lee Wu[3], Shulin Wu[1], Travis Rice-Stitt[4], Peter Sadow[2], Adam Feldman[1], Kristine Cornejo[1]
*[1]Massachusetts General Hospital, Boston, MA, [2]Massachusetts General Hospital, Harvard Medical School, Boston, MA, [3]Massachusetts General Hospital, Newton Center, MA, [4]Massachusetts General Hospital, Somerville, MA*

**Disclosures:** Aida Valencia-Guerrero: None; Esther Oliva: None; Chin-Lee Wu: None; Shulin Wu: None; Travis Rice-Stitt: None; Peter Sadow: None; Adam Feldman: *Grant or Research Support*, Myriad genetics; Kristine Cornejo: None

**Background:** Perinephric fat invasion (PFI) is a key component of renal cell carcinoma (RCC) staging, but there is limited data pertaining to biopsy tract seeding (BTS), resulting in perinephric fat involvement (BTS-P). The aim of the study is to correlate clinical outcomes with pathologic stage to determine whether BTS-P alone should be considered as a criterion to upstage to pT3a.

**Design:** We searched the pathology files from 2005-2015 and identified 283 renal biopsies with subsequent nephrectomies for RCC of which 33 cases contained PFI. Each case was reviewed to determine the presence of BTS-P, other forms of invasion (e.g. non-BTS-P perirenal, hilar/sinus fat, renal vein) and compared this to survival outcomes. Due to a limited cohort, a meta-analysis of our data combined with previous reports from the literature was also performed.

**Results:** 10 (30%) of 33 tumors with PFI showed BTS-P as the only finding but were otherwise pT1 tumors of which 6 (60%) patients were alive without disease (AWOD) (mean follow-up 77.5 months), 3 were lost to follow-up (LTF) and 1 died of other disease (DOOD). 8 (80%) of 10 tumors were papillary RCC (PRCC), 1 clear cell papillary RCC and 1 clear cell RCC (CCRCC). Two patients with PRCCs also showed BTS-P and true perirenal fat invasion of which 1 was LTF and 1 is AWOD at 107 months. 9 (42%) of 21 patients with tumors with true invasion are AWOD (mean follow-up 96.6 months), 7 (33%) died of disease (DOD), 4 were LTF and 1 DOOD. Kaplan-Meier survival curves revealed the cancer specific survival (CSS) is significantly worse in patients with true invasion (*p=0.044)* than in those with BTS-P as the sole finding.

Our meta-analyses revealed a total of 38 resections with histologically proven BTS and follow-up data, of which 18 (47%) tumors were otherwise pT1 tumors with BTS-P alone and were mainly PRCCs (n=16; 89%). None (0%) of these patients DOD, in comparison to the 20 (53%) patients with tumors containing true invasion, of which 9 (45%) DOD. The Kaplan-Meier survival curve demonstrated the CSS is significantly better in patients with BTS alone than in those with true invasion (*p=0.016*).

**Conclusions:** Patients containing tumors with BTS-P alone was associated with significantly better outcomes when compared to those with true invasion and was more commonly seen in PRCC. The results suggest BTS-P alone should not be upstaged to pT3. Additional studies are needed to corroborate the significance of our observations.

## 1030 Origin of Germ Cell Tumors: Presence of Somatic Transformation and Role of Dedifferentiation in Mature Teratomas

Shikhar Vyas[1], Miao Zhang[2], Shi-Ming Tu[1]
*[1]The University of Texas MD Anderson Cancer Center, Houston, TX, [2]The University of Texas MD Anderson Cancer Center, Bellaire, TX*

**Disclosures:** Shikhar Vyas: None; Miao Zhang: None; Shi-Ming Tu: *Advisory Board Member*, Janssen Biotech

**Background:** Testicular germ cell tumor is a highly curable disease. However, it is lethal for a small percentage of young patients who are otherwise healthy, especially in cases of somatic transformation. The need for better understanding of the disease and better treatment is urgent. In the post chemotherapy setting, we frequently observe metastatic teratoma with concurrent somatic transformation, suggesting the presence of cancer stem cells (CSCs). Herein we utilize paired mature metastatic teratoma and somatic transformation material from the same patients to test this hypothesis.

**Design:** We identified 10 post-chemotherapy patients with metastatic mature teratoma with paired somatic transformation (Table 1.) H&E slides were circled for teratoma and somatic transformation components for microdissection. Unstained slides were utilized for genomic DNA and RNA, library prep, and capture for whole genome sequencing and RNAseq. The T200 target-capture deep sequencing data was aligned to human references assembly hg19. Raw RNA sequencing data was analyzed using STAR aligner. Fresh frozen tumor samples were collected for cell culture.

**Results:** Sequencing data is available for 7 of 10 patients. We detected a total of 58 genes harboring mutations in any of the 14 tumor samples. Among them, 24 genes indicated within-pair discordance. Testing against the null hypothesis that discordance in either direction to be the same amount, the “within patient mutation agreement” from the mutation matrix based on 58 genes, a subset of T200 genes, where at least one mutation was detected in any of the samples was between 86 to 95%, suggesting a high concordance. The denominator we used for this calculation is 58. If we used 202, the number of genes tested on T200v0, the % agreement would be even higher. Primary

cell culture growth and testing (flow cytometry, xenografts) are ongoing, with preliminary cell surface stem-ness markers (SSEA3, TRA1-60, Cripto-1, CD90, CD133, CD44) results indicating successful isolation of CSC in 3 of 3 prospective cases.

| Case no. | Age | Clinical stage | Primary Tumor | Metastasis site | Metastastic Tumor |
|---|---|---|---|---|---|
| 1 | 21 | IIIC | ST | RPLN | T + adenocarcinoma |
| 2 | 42 | IIIB | ST | RPLN | T + carcinoma/sarcoma |
| 3 | 23 | IB | ES | RPLN | T + PNET |
| 4 | 20 | IIIB | EYST | RPLN | T + sarcoma |
| 5 | 27 | IIIB | ECYT | Lung | T + adenocarcinoma |
| 6 | 24 | IIIA | EYST | Mediastinum | T + rhabdomyosarcoma |
| 7 | 27 | IIIC | EYST | RPLN | T + angiosarcoma |
| 8 | 18 | IIIB | EYT, PNET | Lung | T + sarcoma/adenocarcinoma |
| 9 | 48 | IA | EYT | RPLN | T + Rhabdomyosarcoma |
| 10 | 27 | III | S | Mediastinum | T + sarcoma |

Table 1, T, Teratoma; PNET, primitive neuroectodermal tumor; LN, Lymph node; RPLN, retroperitoneal lymph node; “ST” = seminoma; “ES” = embryonal carcinoma, seminoma; “EYST” = embryonal carcinoma, yolk sac tumor, seminoma, teratoma; “ECYT” = embryonal carcinoma, choriocarcinoma, yolk sac tumor, teratoma

**Conclusions:** We demonstrate that metastatic teratoma and their corresponding somatic transformations have very similar, if not identical, genetic profiles, confirming that they have a common clonal origin. Furthermore, there is no evidence for acquisition of genetic mutations that lead to dedifferentiation of teratoma. Primary cell culture indicates the presence of CSC isolated from metastatic mature teratoma, with ongoing testing of more samples to support this hypothesis.

## 1031 Molecular Profiling of Urothelial Carcinoma with and without Variant Histology from Primary and Metastatic Sites

Dandan Wang[1], Siamak Daneshmand[2], Anne Schuckman[2], Hooman Djaladat[2], Doan Lai[3], Kyle Hurth[2], Guang-Qian Xiao[4]
*[1]University of Southern California, Los Angeles, CA, [2]Keck School of Medicine of University of Southern California, Los Angeles, CA, [3]Oklahoma City, OK, [4]Keck Medical Center of USC, Los Angeles, CA*

**Disclosures:** Dandan Wang: None; Kyle Hurth: None; Guang-Qian Xiao: None

**Background:** Various histologic subtypes of urothelial carcinoma (UC) differ significantly in biologic and clinical behavior. Similarly, UC of different original sites can have different pathologic and clinical profile. The underlying mechanisms are not well understood. The aim of this study was to investigate the molecular genomic profile in UC from different primary and metastatic sites as well as of different histologic variants using next generation gene sequencing (NGS).

**Design:** UC cases collected from 36 unselected patients at our institution over a 2-year period had NGS test, including 14 from low urinary tract (LUT) (12 bladder, 2 urethra), 7 from upper urinary tract (UUT) (7 kidney, 3 ureter), 9 lymph node metastases and 6 distant metastases (liver, lung and bowel/soft tissue). There were 15 conventional UCs (c-UC), 9 squamous differentiation (UC-s), 4 glandular differentiation (UC-g), 4 micropapillary type (m-UC), 2 small cell carcinomas, 1 nested UC and 1 sarcomatoid UC. For each case, over 300 genes were assessed for potential genomic alterations.

**Results:** UUT-UCs seem to have a higher tumor mutation burden (TMB) than LUT-UCs. With the exception of 1 UUT- UC with high microsatellite instability (MSI), all the other UCs had a stable MSI. The genetic profiles in each site and variant groups are illustrated in figures 1 and 2.

Figure 1 - 1031

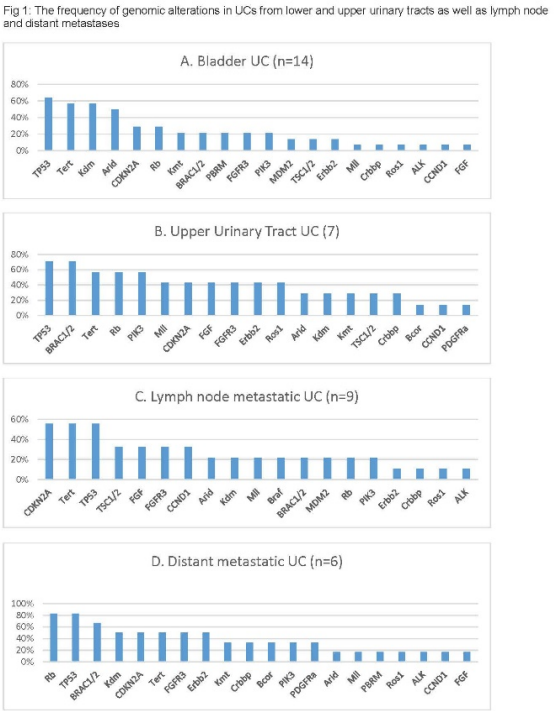


Figure 2 - 1031

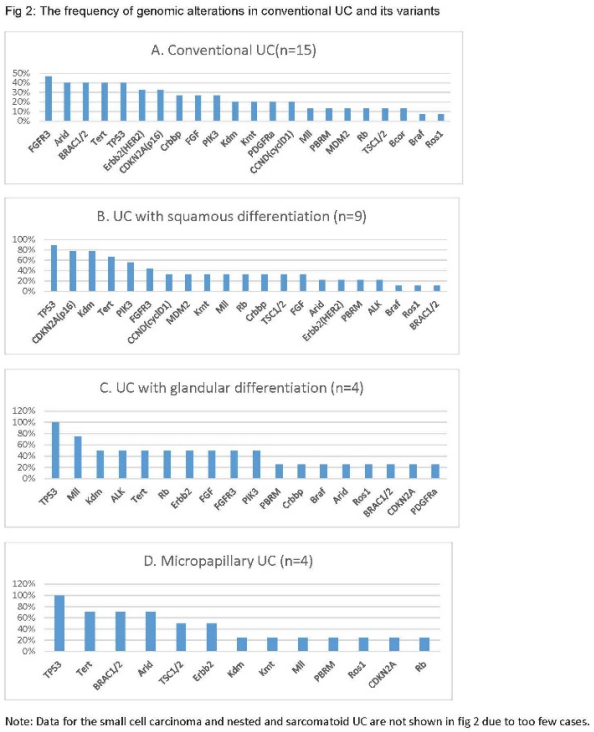


**Conclusions:** 1) Alterations of TP53 and TERT were common in UC subtypes, primary and metastatic UCs. 2) Alterations of FGFR3 and PI3K cell growth pathways were common in all histologic UC variants except m-UC. PIK3 mutations were more frequent in UUT-UC than LUT-UC. 3) BRAC1/2 mutation was more common in distant metastasis and UUT-UC than LUT-UC and more frequent in c-UC and m-UC than UC-s and UC-g. 4) ARID mutations were more common in c-UC and m-UC than UC-s and UC-g. Histone modulators KDM mutation occurred more frequently in UC-s. MLL mutation was more common in UUT-UC and UC-g than other UCs. 5) The CDKN2A (encoding p16) mutation was high in UC-s. 6) The frequent alteration in ERBB2 (encoding Her2/Neu) in m-UC and UC-g was compatible with their luminal subtype. Collectively, although with limited sample size, we found differential genomic alterations for specific UC histology variant and UC site-related may imply different underlying pathogenesis and the identification of many presently drug-targetable gene mutations (e.g. FGFR3, ERBB2, BRAC, MLL) appears promising for future targeted and individualized therapy for this frequently fatal disease.

## 1032 Renal Cell Carcinoma with "Gonadal Sex-cord Stromal tumor-like" Features: Analysis of 5 Cases of Novel Renal Entity

Gang Wang[1], Mahul Amin[2], Petr Grossmann[3], Malcolm Hayes[4], Arndt Hartmann[5], Abbas Agaimy[6], Jose Lopez[7], Ondrej Hes[8]
*[1]BC Cancer Vancouver Centre, Vancouver, BC, [2]Methodist University Hospital, Memphis, TN, [3]Biopticka laborator s.r.o., Plzen, Czech Republic, [4]BC Cancer Agency, Vancouver, BC, [5]Institut fur Pathologie, Erlangen, Germany, [6]Universitätsklinikum Erlangen, Germany, Erlangen, Germany, [7]Hospital de Cruces-Osakidetza, Barakaldo, Bizkaia, Spain, [8]Biopticka laborator s.r.o., Plzen, Plzensky kraj, Czech Republic*

**Disclosures:** Gang Wang: None; Mahul Amin: *Consultant*, Urogen; *Consultant*, Advanced Clinical; *Advisory Board Member*, Cell Max; *Advisory Board Member*, Precipio Diagnostics; Petr Grossmann: None; Malcolm Hayes: None; Arndt Hartmann: None; Abbas Agaimy: None; Jose Lopez: None; Ondrej Hes: None

**Background:** Renal tumors are one of the most diverse group of tumors in pathology. Six new entities were included in the latest WHO 2016 and many emerging and important entities have been described since. Here we describe a series of distinct renal tumors occurring in adult patients.

**Design:** Five cases with histologic features hitherto not described in any of the established or recently described renal cell carcinomas, and with a striking resemblance to gonadal sex cord stromal tumors were retrieved from consultation files of authors (5 institutions). Tumors were analyzed using morphologic, immunohistochemical and molecular genetic methods using the available paraffin tissue.

**Results:** Patients were 2 males and 3 females aged 56-82 years (mean 72 years, median 74 years); tumor size ranged from 0.9 to 3.6 cm (mean 3 cm). Four tumors were organ confined (pT1a) while one case had focal perinephric invasion (pT3a). No aggressive behavior was noted [follow up period ranged from 1 to 60 months (median 14 months)]. Microscopically, all the tumors were composed of loose or compact tubular structures with elongated or angulated shapes (Fig 1). The tumor cells were cylindrical or cuboidal, with pale eosinophilic cytoplasm, irregular nuclear membranes and WHO/ISUP grade 2-3 nuclei. The stroma showed focal or prominent collagen deposition with prominent basement membrane-like material (4 of 5 cases) (Fig 2). None of cases showed coagulative necrosis; one case contained focal foamy macrophages. In all of the cases, the tumor cells were positive for PAX8, CD10, vimentin, and retained positivity for FH, and SDHB. Cathepsin K and AMACR were variably positive. Tumors were negative for HMB45, Melan A, TFE3, SF1, inhibin, calretinin, ER, PR. CD117, OCT3/4, SAL4, ALK, and WT1. FISH or tumor sequencing studies showed no abnormalities in TFE3, TFEB, and FH genes. In both male cases, loss of Y chromosome was found.

Figure 1 - 1032

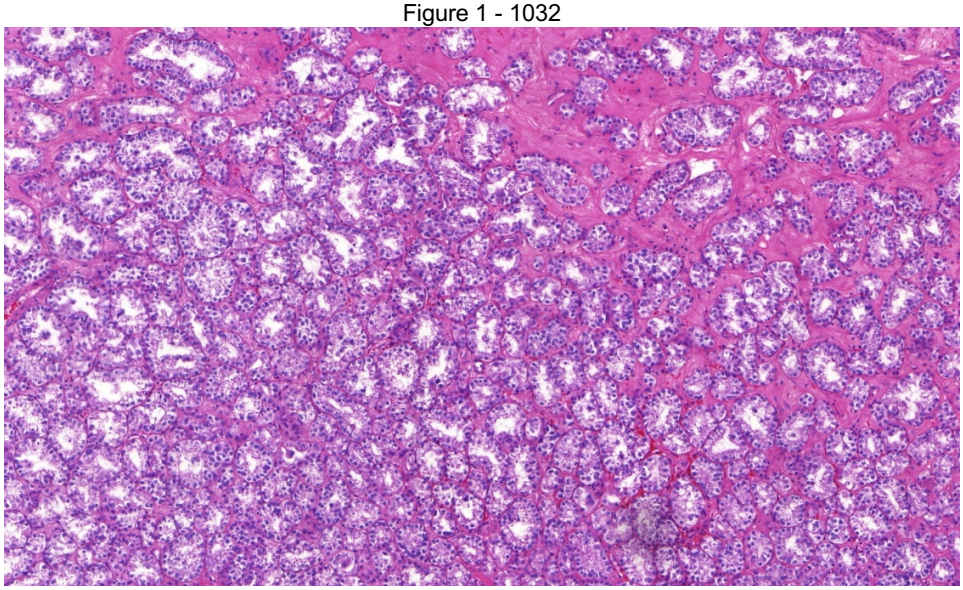

Figure 2 - 1032

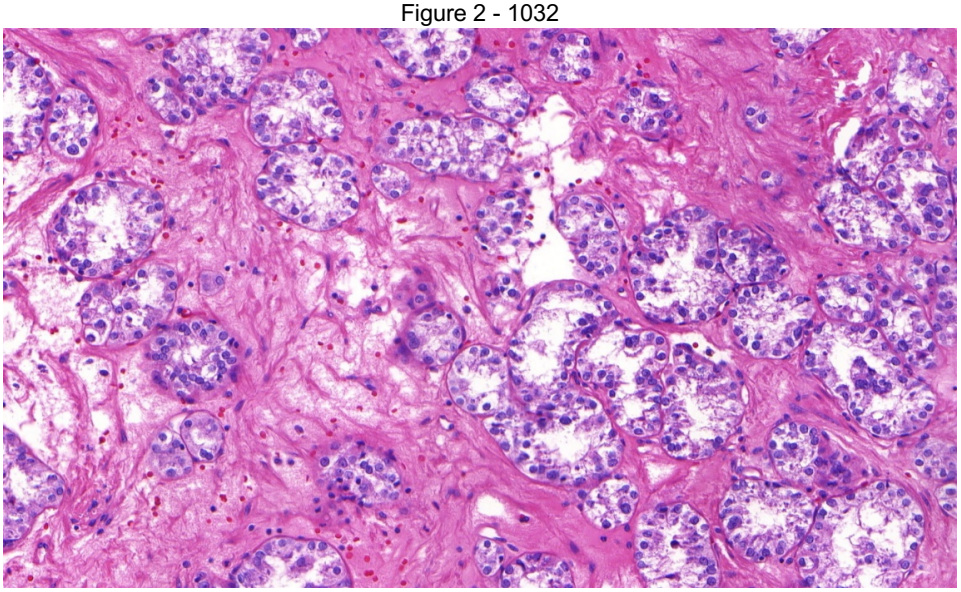

**Conclusions:** Herein we expand the clinico-pathologic diversity of renal cell carcinomas occurring in adults by describing a series of novel tumors resembling gonadal sex-stromal tumor. Tumors are characterized by tubular growth pattern, presence of dense stroma, and tubules filled by mostly multilayered weakly eosinophilic cells resembling Sertoli cells. Mimicry with gonadal stromal tumors is only at the morphological level with negativity for markers related to sex cord stromal derivation. In the relatively short follow up, these tumors appear to have indolent behavior.

## 1033 Novel Biomarker for MiT Family Translocation Renal Cell Carcinoma

Xiaoming (Mindy) Wang[1], Sounak Gupta[2], Yuping Zhang[3], Rahul Mannan[4], Stephanie Skala[1], Roshni Rangaswamy[5], Anya Chinnaiyan[3], Fengyun Su[1], Xuhong Cao[1], Thomas Giordano[6], Hong Xiao[1], Lina Shao[1], Bryan Betz[7], Noah Brown[1], Jesse McKenney[8], Satish Tickoo[9], Pedram Argani[10], Victor Reuter[9], Arul Chinnaiyan[11], Saravana Dhanasekaran[1], Rohit Mehra[1]

*[1]University of Michigan, Ann Arbor, MI, [2]Mayo Clinic, Rochester, MN, [3]Michigan Center for Translational Pathology, Ann Arbor, MI, [4]Michigan Medicine, University of Michigan, Ann Arbor, MI, [5]Michigan Center for Translational Pathology, Ypsilanti, MI, [6]University of Michigan Medicine, Ann Arbor, MI, [7]University of Michigan Medical School, Ann Arbor, MI, [8]Cleveland Clinic, Cleveland, OH, [9]Memorial Sloan Kettering Cancer Center, New York, NY, [10]Johns Hopkins Hospital, Ellicott City, MD, [11]Plymouth, MI*

**Disclosures:** Xiaoming (Mindy) Wang: None; Sounak Gupta: None; Yuping Zhang: None; Rahul Mannan: None; Stephanie Skala: None; Roshni Rangaswamy: None; Anya Chinnaiyan: None; Fengyun Su: None; Xuhong Cao: None; Thomas Giordano: *Consultant*, Interpace Diagnostics; Hong Xiao: None; Lina Shao: None; Bryan Betz: None; Noah Brown: None; Jesse McKenney: None; Satish Tickoo: None; Pedram Argani: None; Victor Reuter: None; Arul Chinnaiyan: None; Saravana Dhanasekaran: None; Rohit Mehra: None

**Background:** MiT family translocation renal cell carcinoma (TRCC) is caused by recurrent aberrations in the melanocyte inducing transcription factor (MITF) family genes *TFE3* or *TFEB*. TRCC demonstrate morphologic features that may overlap with clear cell RCC (CCRCC), papillary RCC (PRCC), and clear cell papillary RCC (CCPRCC). Currently, FISH assays are utilized to assist TRCC diagnosis; development of additional reliable chromogenic biomarkers would be helpful for routine clinical testing.

**Design:** We performed integrative analysis of RNAseq data to compare TRCC transcriptome to that of other RCC subtypes and benign kidney. We identified *TRIM63* gene as the top candidate biomarker highly expressed in TRCC, but not in other major RCC subtypes or normal kidney. We assessed *TRIM63* expression by RNA *in situ* hybridization (RNA-ISH) in a discovery cohort, including 16 TRCC, 10 CCRCC, 12 PRCC, 5 CCPRCC, 26 chromophobe RCC (ChRCC), 5 mucinous tubular and spindle cell RCC (MTSCC), 3 HLRCC-associated RCC, 1 SDH-deficient RCC, 2 hybrid oncocytic tumors (HOT), 5 metastatic CCRCC, and 6 metastatic ChRCC. We next evaluated *TRIM63* expression in a validation cohort. After excluding QC failures, *TRIM63* expression was tested in 22 FISH confirmed TRCC cases, and 38 renal tumors morphologically suspicious for TRCC (34 FISH negative, 4 FISH indeterminate). Genomic data was available for correlative assessment through clinical sequencing and/or *TFE3/TFEB* FISH.

**Results:** In the discovery cohort, 14/16 TRCC (87.5%) demonstrated high *TRIM63* expression; 2 TRCC cases showed limited/focal expression. We observed limited/focal *TRIM63* expression in 1 CCRCC and 1 metastatic ChRCC cases, no transcripts were detected in the other renal tumor subtypes listed above or adjacent normal kidney. In the validation cohort, 60/64 cases passed RNA-ISH assay QC. 21/22 (95%) TRCC cases were positive for *TRIM63* RNA-ISH. In addition, 6/34 (17.6%) FISH negative cases and 1/4 FISH indeterminate cases were positive for *TRIM63*; additional sequencing and/or copy number analysis will be needed to determine whether these FISH-negative, RNA-ISH positive cases harbor MIT family gene aberrations.

| | Discovery Cohort | | Validation Cohort | | |
|---|---|---|---|---|---|
| | FISH + cases | FISH - cases | FISH + cases | FISH - cases | FISH indeterminate cases |
| RNA-ISH + cases | 14/16[#] ( 88%) | 0/75 (0%) | 21/22[$] (95%) | 6/34 (18%) | 1/4 (25%) |
| RNA-ISH - cases | 2*/16 (12%) | 75[^]/75 (100%) | 1[%] /22 (5%) | 28/34 (82%) | 3/4 (75%) |

[#] 16 FISH+ TRCC cases in the discovery cohort include 11 TFE3 translocation, 4 TFEB amplification, and 1 TFEB translocation molecular subtypes

* limited/focal expression in 2 TRCC cases (1 TFE3 translocation and 1 TFEB amplification)

[^] focal expression in 2 cases (1 CCRCC and 1 metastatic ChRCC)

[$] 22 FISH+ or sequencing based TRCC cases in the validation cohort include 11 TFE3 translocation, 4 TFEB amplification, and 7 TFEB translocation molecular subtypes

[%] 1 of 11 cases from collaborative institutions (TFEB amplification) is negative for TRIM63 RNA-ISH

**Conclusions:** Based on this study, *TRIM63* is overexpressed specifically in TRCC. The *TRIM63* RNA-ISH assay results correlate with the sequencing based MiT family genomic aberrations and *TFE3/TFEB* FISH assay in the majority of cases; hence, TRIM63 RNA-ISH is a chromogenic assay which could be potentially utilized either as standalone or a companion diagnostic tool.

## 1034 Evaluation of Potential Targeted Therapy and Molecular Subtype in Large Nested Variant of Urothelial Carcinoma (LNUC)

Veronika Weyerer[1], Markus Eckstein[2], Eva Compérat[3], Hendrik Juette[4], Nadine Gaisa[5], Yves Allory[6], Robert Stoehr[7], Bernd Wullich[8], Morgan Roupret[9], Arndt Hartmann[10], Simone Bertz[11]
*[1]University Hospital Erlangen, Friedrich-Alexander Universität Erlangen-Nürnberg, Erlangen, Bavaria, Germany, [2]Friedrich-Alexander-Universität Erlangen-Nürnberg, Erlangen, Bavaria, Germany, [3]Tenon Hospital, Paris, France, [4]Institute of Pathology, University Hospital Bochum, Bochum, Germany, [5]RWTH Aachen University, Aachen, Northrhine Westfalia, Germany, [6]Curie Institute, St-Cloud, Ile de France, France, [7]Institute of Pathology, University Hospital, Erlangen, Erlangen, Germany, [8]Department of Urology and Pediatric Urology, University Hospital Erlangen, Erlangen, Bavaria, Germany, [9]Service d'Urologie, Hôpital La pitié-Salpetrière, Sorbonne University, Paris, France, [10]Institut fur Pathologie, Erlangen, Germany, [11]University Hospital Erlangen, Erlangen, Germany*

**Disclosures:** Veronika Weyerer: None; Markus Eckstein: *Consultant*, AstraZeneca; *Consultant*, Janssen-Cilag; *Consultant*, GenomicHealth; Eva Compérat: None; Hendrik Juette: *Speaker*, Roche, MSD, BMS; *Advisory Board Member*, BMS, Ipsen; Nadine Gaisa: None; Robert Stoehr: None; Bernd Wullich: None; Morgan Roupret: None; Arndt Hartmann: None; Simone Bertz: None

**Background:** Urothelial bladder cancer (UBC) frequently presents with distinct histomorphological features and rare histologic subtypes have been defined. Since 2016 large nested urothelial carcinoma (LNUC) has been included within the World Health Organization Classification among the nested type. Little is known about the biology and molecular background of this specific variant. However, limited reports with mainly small case numbers confirm the fully malignant and life-threatening behavior despite the bland morphological appearance. In this study we evaluated new therapeutic options including *FGFR3* mutational status and PD-L1 assessment as well as frequency of *TERT* promoter mutations and the molecular subtype of LNUC by using a limited immunohistochemical marker panel.

**Design:** 26 cases diagnosed as LNUC were collected and reviewed. DNA was extracted after manual microdissection of the tumor, including separation of morphologically differing areas. SNaPshot analysis of the hot spot regions of the *FGFR3* and *TERT* promoter gene were performed. Immunohistochemical analysis including basal and luminal markers were stained in order to elucidate the molecular subtype. Additionally, PD-L1 staining was assessed.

**Results:** Of 26 cases, 18 were pure LNUC, 12 showed an additional exophytic (non-invasive) papillary-like component, six presented areas of classical nested type variant and three a component of conventional UBC. 17/18 evaluable pure LNUC were *FGFR3*-mutated with a 100% concordance among the papillary-like component. No *FGFR3* mutation was found in 5/5 LNUC, if combined with classical nested type UBC. *TERT* promoter mutations were detected in 66.7 % pure and 78.9 % mixed LNUC. Immunohistochemistry revealed a luminal phenotype for LNUC; none was PD-L1 positive.

**Conclusions:** Pure LNUC is a prime example of a luminal, *FGFR3* mutated and PD-L1 negative tumor. In contrast, LNUC combined with classical nested type seems to represent a different molecular pathway with no *FGFR3* mutation detected. Regarding those unique molecular features, our findings are of particular interest since *FGFR*-pan inhibitors are currently tested in clinical trials.

## 1035 Distal Tubular Hyperplasia: A Novel Form of Renal Tubular Proliferation Distinct from Papillary Adenoma

Sean Williamson[1], Khaleel Al-Obaidy[2], Steven Smith[3], Carrie Phillips[2], Christopher Przybycin[4], David Grignon[2]
*[1]Henry Ford Health System, Detroit, MI, [2]Indiana University School of Medicine, Indianapolis, IN, [3]Virginia Commonwealth University School of Medicine, Richmond, VA, [4]Cleveland Clinic, Cleveland, OH*

**Disclosures:** Sean Williamson: None; Khaleel Al-Obaidy: None; Steven Smith: *Consultant*, Elsevier Publishing/Amirsys; Carrie Phillips: None; Christopher Przybycin: None; David Grignon: None

**Background:** Papillary adenoma is the only established incipient or preneoplastic lesion in the current classification of renal cell neoplasms. However, we have occasionally encountered a more diffuse proliferation in the setting of chronic renal disease that appears different from papillary adenoma, warranting further study.

**Design:** Renal specimens showing an unusual proliferation of tubules were retrieved from the authors' archives and studied for clinical and pathologic parameters and immunohistochemical profile. A series of end-stage renal disease specimens from one of the institutions was retrospectively reviewed to establish incidence.

**Results:** In total, 12 specimens were retrieved showing this tubular proliferation diffusely (n=7) or focally (n=5). Eight were identified from a series of 177 end-stage renal disease specimens from one institution (5%), of which 5 were focal (3%) and 3 diffuse (2%). Eight patients had concurrent renal cell tumors including clear cell (n=4), papillary (n=3), clear cell papillary (n=1), or acquired cystic kidney disease (n=1) renal cell carcinoma (and papillary adenomas, n=5). Four occurred with no neoplasm. All patients had end-stage renal disease, 1 being an explanted allograft; however, there was no definite commonality to the patients' renal disease. In most (n=9), the predominant pattern was indentation of chronic inflammation into renal tubules forming small polypoid structures (Figure A); however, 3 patients had predominantly

hyperplastic epithelium with less conspicuous inflammation in the cores (Figure B). In 7 patients both patterns were appreciable at least focally, whereas the remainder (with focal, minimal lesions) had only the inflammatory pattern. Immunohistochemistry was consistently positive for cytokeratin 7, high molecular weight cytokeratin (sometimes weak), and GATA3. Staining for alpha-methylacyl-CoA racemase (AMACR) was negative or weak, dramatically less intense than that of papillary neoplasms or proximal tubules. CD3 and CD20 showed a mixture of B and T lymphocytes in the inflammatory areas.

Figure 1 - 1035

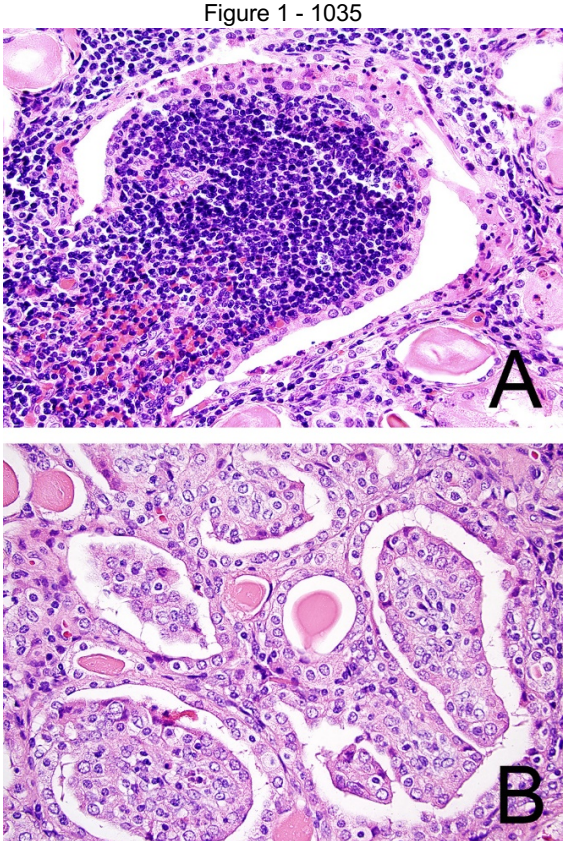


**Conclusions:** We describe a novel form of renal tubular proliferation that differs from papillary adenoma in that it shows weak or negative AMACR immunoreaction and in some cases is widely dispersed in sampled renal parenchyma. Based on consistent staining for high molecular weight cytokeratin and GATA3, this appears to be a proliferation of distal tubules, with both inflammatory and hyperplastic patterns.

## 1036 Diagnosis of All 12 Needle Cores within an Hour of a Prostate Biopsy Procedure

Weisi Xie[1], Nicholas Reder[1], Funda Vakar-Lopez[1], Jonathan Liu[1], Adam Glaser[1], Lawrence True[2]
*[1]University of Washington, Seattle, WA, [2]University of Washington Medical Center, Seattle, WA*

**Disclosures:** Weisi Xie: None; Nicholas Reder: *Employee*, Lightspeed Microscopy; Funda Vakar-Lopez: None; Jonathan Liu: *Stock Ownership*, LightSpeed Microscopy Inc.; Adam Glaser: *Consultant*, LightSpeed Microscopy; Lawrence True: *Stock Ownership*, Lightspeed Microscopy, Inc.

**Background:** A challenge for pathologists is providing an accurate diagnosis in a timely manner, enabling the surgeon to communicate findings shortly after the biopsy, thereby minimizing patient anxiety. However, such a rapid diagnosis is limited by current lab practice, which is labor-intensive and time-consuming. In addition, sampling, which consumes tissue, is limited to a few thin sections. To address these shortcomings we developed a 50-min work flow for nondestructive 3D pathology of 12 prostate core needle biopsies. We assessed the performance of this method.

**Design:** Sets of needle core biopsies were obtained ex-vivo from a set of radical prostatectomies. After brief fixation in formaldehyde, the biopsies were clarified in TDE, stained with fluorophore DRAQ5, and imaged using an open-top light-sheet (OTLS) microscope, which has a resolution equivalent to a 20X light microscope objective. Three GU pathologists independently diagnosed OTLS images of 44 biopsies, recording turnaround times. The biopsies were subsequently routinely processed and stained with H&E dyes. Whole slide (WS) scans of

the biopsies were diagnosed by the 3 pathologists who were blinded to the correlation between OTLS and WS H&E images. These diagnoses were compared with the OTLS diagnoses.

**Results:** Using the WS scans of H&E sections as the gold standard, the consensus-based accuracy of pathologists (PATH 1, 2, 3) in distinguishing benign from cancer was 91% (Table 1). Overall free-marginal inter-method kappa between OTLS and H&E diagnoses was 0.82. Turnaround time averaged 35 seconds per biopsy (range 4 - 145 seconds). Time to prepare, digitally process and diagnose 12 core biopsies averaged ~44.5 minutes. There was no discernible effect of the protocol on the histological quality of the tissue or on immunoreactivity for anti-keratin antibodies.

| Table 1 | Path 1 | Path 2 | Path 3 | Consensus |
|---|---|---|---|---|
| Accuracy | 0.91 | 0.91 | 0.77 | 0.91 |
| Sensitivity | 0.70 | 0.60 | 0.90 | 0.70 |
| Specificity | 0.97 | 1.00 | 0.97 | 0.97 |
| Positive Predictive Value | 0.88 | 1.00 | 0.50 | 0.88 |
| Negative Predictive Value | 0.92 | 0.89 | 0.96 | 0.92 |

**Conclusions:** Using an OTLS microscope and a tissue processing method that minimized light scattering, 3 pathologists could diagnose sets of 12 prostate biopsies within an hour of receipt, achieving an average accuracy of 91%. Since the procedure, which provides images and does not consume any tissue, had no discernible effect on tissue quality or immunoreactivity, the entire biopsy of all biopsies can be used for subsequent molecular studies. Our system promises to provide clinicians and patients rapid, timely accurate diagnoses while using minimal lab resources and consuming no tissue.

## 1037 Extent of Prostate Cancer at Radical Prostatectomy - the Accuracy of Visual Assessment in Routine Clinical Practice

Natalia Yanchenko[1], Isabella Lugo[2], Oleksii Iakymenko[3], Ivan Nemov[4], Andre Pinto[5], Merce Jorda[4], Oleksandr Kryvenko[4]
*[1]Dedham, MA, [2]University of Miami, Davie, FL, [3]Jackson Memorial Hospital, Miami, FL, [4]University of Miami Miller School of Medicine, Miami, FL, [5]University of Miami, Miami Beach, FL*

**Disclosures:** Natalia Yanchenko: None; Isabella Lugo: None; Oleksii Iakymenko: None; Ivan Nemov: None; Andre Pinto: None; Oleksandr Kryvenko: None

**Background:** Tumor volume (TV) is a variable linked to adverse radical prostatectomy (RP) outcomes and biochemical recurrence. Pathologists are expected to estimate the extent of carcinoma in RP. Visual assessment (VA) of the gland involvement by carcinoma with reporting of percentage of gland involved is the most common method used in clinical practice. This percentage may be used in retrospective cohorts to calculate tumor volume knowing gland weight. There is no studies assessing the accuracy of VA compared with measured TV.

**Design:** 1,273 entirely submitted RPs from 2014-2019 were reviewed. We first derived average gross prostate section thickness (3.74 mm) from 50 RPs. 1 gram of prostate weighed without seminal vesicles was considered equal to 1 cm3. Total tumor area (TTA) was calculated as follows: tumor was mapped on a histological slides, scanned in a background of 1 mm2 grid, and total number of square millimeter was manually calculated. TV was calculated by the formula: TTA × 3.74 × 1.12, shrinkage factor. The correlation between VA and measured TV was assessed with Pearson correlation coefficient generally and for 4 pathologists rotating on GU service.

**Results:** In 114 (9%) cases pathologists did not report the percentage of gland involvement. In the rest 1,159 cases, 189 (16%) pathologists underestimated the TV and 970 (84%) overestimated it. In 533 (46%) RPs pathologists' VA was within the range of 2.5% above or below measured TV (that equals an error of 0.00–2.67 cm3 of TV). 248 (21%) VAs were within 2.5-5% above or below measured TV (0.48–5.99 cm3 of TV error). 199 (17%) VAs were within 5-10% above or below measured TV (1.17–9.00 cm3 of TV). 179 (15%) VA were within >10% above or below measured TV (1.76–85.7 cm3 of TV). It was strong correlation between VA and measured TV in the whole practice ($R = 0.86$, $p<0.01$), as well as in each of 4 pathologists ($R = 0.80$; 0.84; 0.84; 0.88, $p<0.01$). The discrepancy between VA and measured TV was higher in bigger tumors and tumors involving a higher percentage of gland ($R = 0.60$ and 0.87 respectively, $p<0.01$). However, this discrepancy did not significantly correlate with gland volume and only weakly positively correlated ($R=0.18$, $p<0.05$) with the tumor grade.

**Conclusions:** Visual assessment is a relatively accurate method for the estimation of TV in RP in semi-subspecialty group. Significant overestimation of tumor burden is more common in larger tumors of any tumor grade and those involving higher gland percentage.

## 1038 Preoperative and Radical Prostatectomy Findings in Men with Different Prostate Gland Weight

Natalia Yanchenko[1], Isabella Lugo[2], Ivan Nemov[3], Oleksii Iakymenko[4], Oleksandr Kryvenko[3]
*[1]Dedham, MA, [2]University of Miami, Davie, FL, [3]University of Miami Miller School of Medicine, Miami, FL, [4]Jackson Memorial Hospital, Miami, FL*

**Disclosures:** Natalia Yanchenko: None; Isabella Lugo: None; Ivan Nemov: None; Oleksii Iakymenko: None

**Background:** Previous studies suggested a more favorable pathological outcomes in radical prostatectomies (RP) with larger size glands. However, major shift towards active surveillance in patients with low-risk prostate cancer altered the population subjected to RP. Herein we compare preoperative and RP findings in a large cohort of men in respect to their prostate weight (PW).

**Design:** 1,306 consecutive entirely submitted RPs were reviewed. Preoperative findings, American Urological Association (AUA) cancer risk stratification, and RP findings were compared between men with PW < 40 g, 40-60 g, and > 60g.

**Results:** We excluded cases with treated cancer, 26; peripheral gland adenosis, 1; vanishing cancer, 5; no PW, 1; carcinoid, 1; small cell carcinoma, 1; only intraductal cancer at biopsy at Grade Group (GG) 4 at RP, 1. In 1,270 cohort 538 had PW <40 g, 456 – 40-60 g, and 276 >60g. With increasing gland size, men were older (60.8 vs 62.4 vs 64.9), heavier (84.8 vs 88.3 vs 90.5), had higher BMI (27.5 vs 28.4 vs 29), higher PSA (7.9 vs 9.3 vs 10.8) and lower PSA density (0.25 vs 0.19 vs 0.13). Proportion of low and high-risk cancer increased with increased PW, p=0.003 (Table). At RP, the GG incidence paralleled that of preoperative AUA risk stratification with more lower and higher grades and lesser GG3 with increasing PW (Table). Tumor volume increased with gland size (2.1 vs 2.4 vs 3.0, p=0.001) but percentage of gland involvement decreased (6.8 vs 4.8 vs 3.7, p<0.001). Smaller glands had more frequent extraprostatic extension (47.2 vs 46.9 vs 38.7%, p=0.033) but there was no difference in incidence of intraprostatic incision (5.8 vs 4.6 vs 4.7%, p=0.67), positive surgical margin (28.3 vs 27.9 vs 23.9%, p=0.27), or seminal vesicle invasion (11.9 vs 9.4 vs 13.4%, p=0.22)

| **Risk** | < 40 (500) | 40-60 (434) | > 60 (267) | |
|---|---|---|---|---|
| Low | 164 (32.8) | 150 (34.6) | 102 (38.2) | 0.003 |
| Intermediate | 235 (47) | 184 (42.4) | 87 (32.6) | |
| High | 101 (20.2) | 100 (23) | 78 (29.2) | |
| **Outcome** | | | | |
| RP GG | < 40 (538) | 40-60 (456) | > 60 (276) | |
| 1 | 91 (16.9) | 78 (17.1) | 73 (26.4) | <0.001 |
| 2 | 218 (40.5) | 195 (42.8) | 79 (28.6) | |
| 3 | 104 (19.3) | 72 (15.8) | 31 (11.2) | |
| 4 | 9 (1.7) | 14 (3.1) | 17 (6.2) | |
| 5 | 116 (21.6) | 97 (21.3) | 76 (27.5) | |

**Conclusions:** Similar to prior studies, there is a slightly higher likelihood of extraprostatic extension in smaller glands while other staging parameters were not significantly different. Despite higher tumor volume with increasing PW, PSA density could not adequately assess this measure and in fact significantly declined with increasing PW. Although proportion of GG1 cancer was higher in men with PW > 60, this cohort had the higher pre and postoperative proportion of GG4-5 disease. The latter fining may be more influential on long term biochemical recurrence free survival than a more favorable RP pT staging in these men.

## 1039 Homozygous Loss of CDKN2A/B and Complex Genomic Alterations Observed in Locally Advanced/Metastatic Mucinous Tubular and Spindle Cell Carcinoma (MTSCC)

Chen Yang[1], Robert Cimera[1], Judy Sarungbam[1], Hikmat Al-Ahmadie[1], Anuradha Gopalan[1], S. Joseph Sirintrapun[1], Samson Fine[1], Satish Tickoo[1], Victor Reuter[1], Yanming Zhang[1], Ying-Bei Chen[1]
*[1]Memorial Sloan Kettering Cancer Center, New York, NY*

**Disclosures:** Chen Yang: None; Robert Cimera: None; Judy Sarungbam: None; Hikmat Al-Ahmadie: None; Anuradha Gopalan: None; S. Joseph Sirintrapun: None; Samson Fine: None; Satish Tickoo: None; Victor Reuter: None; Yanming Zhang: None; Ying-Bei Chen: None

**Background:** MTSCC is a rare subtype of renal epithelial neoplasm with characteristic chromosomal alterations and typically low-grade histologic features. However, a small subset of cases has been reported to exhibit high-grade features and/or aggressive clinical behavior. We aimed to investigate the histologic and molecular features of locally advanced/metastatic MTSCC (LAM-MTSCC).

**Design:** We retrospectively identified 26 consecutive patients with MTSCC based on institution database search and pathologic re-review, consisting of 8 cases of LAM-MTSCC (pT3 or N1 or M1) and 18 localized tumors. We examined genome-wide molecular alterations using a single nucleotide polymorphism (SNP) array (n=18) and a targeted next-generation sequencing (NGS) platform (n=5). Nine available samples (primary/metastatic) from 6 LAM-MTSCC patients were analyzed.

**Results:** Patients with LAM-MTSCC were 6 female (75%) and 2 male (25%) with median age of 66 years (range 56-71). Median tumor size was 11 cm (range 3-14). At nephrectomy, 4 cases (50%) were pT3 while the remainder (50%) were localized. All 8 patients developed metastasis and common sites included lymph node (4, 50%), bone (4, 50%), and retroperitoneum (3, 38%). Four patients died of disease (50%). Necrosis, rhabdoid/sarcomatoid, lymphovascular invasion, single file infiltration, and high mitotic index were associated with LAM-MTSCCs (all $p < 0.05$). LAM-MTSCCs shared typical MTSCC genomic profiles with loss of chromosomes 1, 4, 6, 8, 9, 13, 14, 15, and 22, supporting their being considered as MTSCC. However, additional complex genomic alterations were identified, including loss of 1p (6/6), 3p (4/6), and 17p (2/6). In a case where we compared the lymph node metastasis with renal primary by SNP array, the metastasis showed additional loss of chromosomes 10, 11, 19, complex loss of 1p, 3p, 3q, 5q, 7q, 17p, and gain of 5p, 17q, 20, indicative of clonal evolution. Noticeably, homozygous loss of *CDKN2A/B* (*TP16*) was observed in 2 (33%) LAM-MTSCCs and none of the localized MTSCCs. Focal gain of *MET* and *EGFR* were noted in one case. Oncogenic mutations of *NF2*, *KMT2C*, *EP300*, and *FBXW7* were detected in one case each.

**Conclusions:** MTSCC with high-grade features and aggressive clinical behavior may have progressed through clonal evolution. *CDKN2A/B* deletion and additional complex genomic abnormalities may contribute to this process. Evaluating for adverse histologic features seen in the tumor may help stratify patients for treatment and prognosis.

## 1040 A Novel High Frequent Single Nucleotide Polymorphism Site of CDH23 in Clear Cell Renal Cell Carcinoma with Sarcomatoid Differentiation Based on Whole Exome Sequencing

Wenjuan Yu[1], Yujun Li[1]
[1]*The Affiliated Hospital of Qingdao University, Qingdao, Shandong, China*

**Disclosures:** Wenjuan Yu: None; Yujun Li: None

**Background:** Clear cell renal cell carcinoma (CCRCC) with sarcomatoid differentiation (CCRCCS) displays high invasive behavior and poor prognosis. However, until now, the molecular mechanisms of sarcomatoid transformation had not been well elucidated. We aimed to elucidate the molecular mechanisms of sarcomatoid transformation, and search for novel pathogenic genes and therapeutic targets for CCRCCS.

**Design:** Whole exome sequencing was separately performed on matched carcinomatous-sarcomatoid elements from 5 specimens with CCRCCS. Among the candidate mutant genes, a nonsynonymous single nucleotide polymorphism (SNP) site of Cadherin 23 (CDH23) was further studied by Sanger sequencing in expanded 40 specimens with CCRCCS and 50 specimens with CCRCC. Meanwhile, the protein expression of CDH23 was detected, and the association between its variation and a series of clinicopathological features were investigated as well.

**Results:** Carcinomatous and sarcomatoid elements shared most somatic single nucleotide variants (SSNVs) showed by whole exome sequencing. Sarcomatoid element had a higher overall SSNVs burden than carcinomatous element. Among the mutant genes, a high frequent mutation in CDH23 (rs3802711) occurred simultaneously in 3 groups of sarcomatoid element and 2 groups of carcinomatous element resulting in amino acid substitution in the high conserved calcium-binding sites of the extracellular cadherin domain mediating the functions of cadherins. SWISS-MODEL revealed the three-dimensional structure of the mutation region of CDH23 was absolutely different from that of the wild type protein. In the expended 90 specimens, CDH23 SNP (rs3802711) is a high frequency mutation site in CCRCCS, which was much higher than that in CCRCC. Cox multivariate analysis indicated CDH23 SNP (rs3802711) genotype are the independent prognostic factor affecting the overall survival of renal cell carcinomas. CDH23 protein was negatively or weakly expressed in most CCRCCS specimens with CDH23 mutation.

| **Groups** | | | **SNP of CDH23** | | $x^2$ | ***P*** |
|---|---|---|---|---|---|---|
| | | | **rs3802711(A)** | **Wild type(G)** | | |
| CCRCCS | | 40 | 22 | 18 | 11.88 | 0.001 |
| CCRCC | | 50 | 10 | 40 | | |
| **CCRCCS** | | | | | | |
| Gender | male | 30 | 16 | 14 | 0.135 | 0.714 |
| | female | 10 | 6 | 4 | | |
| Age(years) | ≤63 | 20 | 9 | 11 | 1.616 | 0.204 |
| | ＞63 | 20 | 13 | 7 | | |
| Diameter(cm) | ≤8.0 | 24 | 11 | 13 | 2.037 | 0.154 |
| | ＞8.0 | 16 | 11 | 5 | | |
| Metastasis | No | 22 | 10 | 12 | 1.800 | 0.180 |
| | Yes | 18 | 12 | 6 | | |
| TNM stage | I- II | 19 | 8 | 11 | 2.431 | 0.119 |
| | III-IV | 21 | 14 | 7 | | |

Figure 1 - 1040

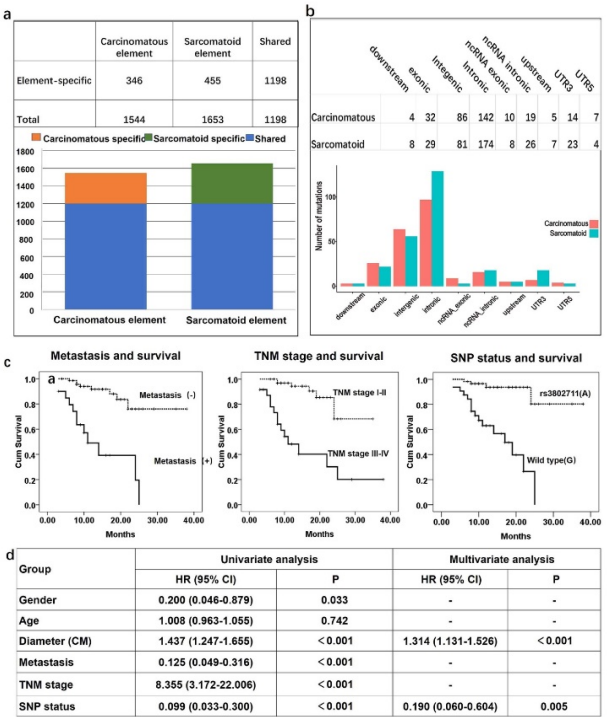


| Group | Univariate analysis | | Multivariate analysis | |
|---|---|---|---|---|
| | HR (95% CI) | P | HR (95% CI) | P |
| Gender | 0.200 (0.046-0.879) | 0.033 | - | - |
| Age | 1.008 (0.963-1.055) | 0.742 | - | - |
| Diameter (CM) | 1.437 (1.247-1.655) | <0.001 | 1.314 (1.131-1.526) | <0.001 |
| Metastasis | 0.125 (0.049-0.316) | <0.001 | - | - |
| TNM stage | 8.355 (3.172-22.006) | <0.001 | - | - |
| SNP status | 0.099 (0.033-0.300) | <0.001 | 0.190 (0.060-0.604) | 0.005 |

Figure 2 - 1040

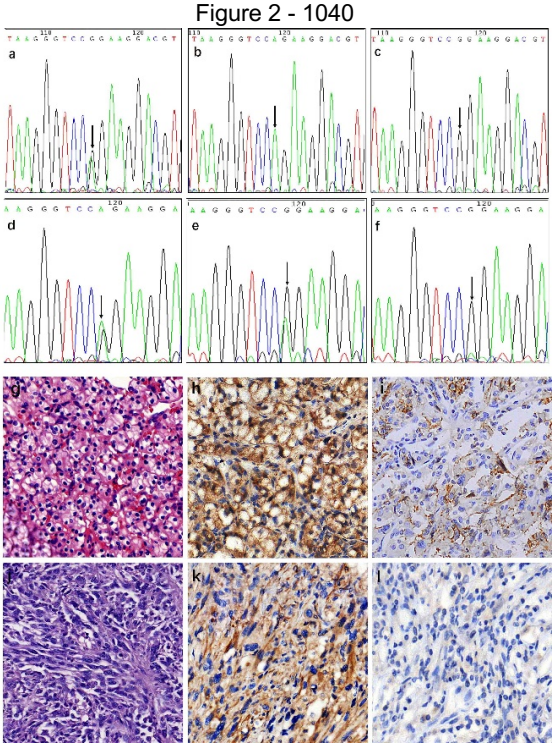


**Conclusions:** We for the first time found CDH23 mutation (rs3802711) was a high genetic risk factor for CCRCCS. CDH23 mutation (rs3802711) could impair the expression of CDH23 protein and disturb its function in cellular adhesion, indicating CDH23 probably played an important role in sarcomatoid transformation in CCRCCS. Also, we provided a new prognostic evaluation factor and potential target therapeutic site for CCRCCS.

## 1041 Aggressive Variant Prostate Cancer in Men with Hormone Naïve, de novo Metastatic Prostate Cancer (M1PC)

Miao Zhang[1], Ana Aparicio[2], Xuemei Wang[2], Brian F Chapin[2], Patricia Troncoso[2]
*[1]The University of Texas MD Anderson Cancer Center, Bellaire, TX, [2]The University of Texas MD Anderson Cancer Center, Houston, TX*

**Disclosures:** Miao Zhang: None; Ana Aparicio: None; Xuemei Wang: None; Brian F Chapin: *Grant or Research Support*, Janssen Pharmaceuticals; *Consultant*, Blue Earth Diagnostics; Patricia Troncoso: None

**Background:** Prostate cancer (PC) is biologically heterogeneous and clinically characterized as either *androgen-responsive* or *androgen-indifferent (aggressive variant, AVPC),* based on sensitivity to androgen signaling inhibition and sensitivity to platinum-based chemotherapy. AVPC shares clinical characteristics with small cell PC, but includes tumors with non-small cell morphology sharing a common molecular profile. Tissue based immunohistochemistry (IHC) for the androgen receptor (AR), AR variant Arv7, and tumor suppressor genes (Tp53, RB1 and PTEN) can be used to predict sensitivity (AR+, Arv7-) or resistance (>= 2 combined defects in tumor suppressor genes) to androgen ablation. Clinically, AVPC occurs most commonly following androgen ablation in patients (pts) with a long history of PC. This study evaluates the frequency of AVPC in pts with hormone naïve, *de novo* M1PC.

**Design:** We evaluated the AVPC molecular signature by IHC in biopsies of primary tumor and metastases at baseline (BL) and 6 months post-hormonal ablation treatment (pHAT), in a cohort presenting with *de novo* metastatic prostatic adenocarcinoma enrolled in a prospective clinical trial (NCT01751438) evaluating the role of local therapy in this patient population.

**Results:** Of the 119 pts enrolled, 169 prostate specimens (81 BL, 88 pHAT) and 46 metastases (10 BL, 36 pHAT) were available for IHC. The median age at diagnosis was 64 yrs (41-83); median PSA 30 ng/ml (0.4-4196). The Gleason score was 8-10 in 78% of pts. The majority of the pts were Caucasian (86%). Tumor suppressor gene alterations at BL/pHAT included Tp53 positivity (35.5%, n=27 / 21.7%, n=18), loss of RB1 (18.8%, n=15 / 8.3%, n=7) and homogeneous PTEN loss (40.3%, n=29 / 50%, n=37). Two or more tumor suppressor gene alterations (AVPC signature) were present in 25.3% (n=19) of the BL and 14.5% (n=12) of the pHAT primary tumor samples. ARv7 positivity was identical at BL and pHAT in the primary tumor (12.5%), was undetected in BL metastases, and present in 22% of pHAT metastases.

**Conclusions:** In this first prospective study to address the frequency of clinically relevant molecular subtypes of PC in *de novo* M1PC, the AVPC signature was detected in 25.3% of prostatic adenocarcinomas, similar to that observed in metastatic castration-resistant PC. The presence of this molecular subset should be considered in the evaluation of novel therapies. Although available data suggest the prognostic value of the AVPC signature, longer follow-up is required to evaluate its predictive value.

## 1042 Utility of Isochromosome 12p in Modern Treatment Era

Miao Zhang[1], Shi-Ming Tu[2], Michael Hwang[2]
*[1]The University of Texas MD Anderson Cancer Center, Bellaire, TX, [2]The University of Texas MD Anderson Cancer Center, Houston, TX*

**Disclosures:** Miao Zhang: None; Shi-Ming Tu: *Advisory Board Member*, Janssen Biotech; Michael Hwang: None

**Background:** Isochromosome 12p (i(12p)) has been used to define tumor of germ cell origin. When testicular germ cell tumor (GCT) develops somatic-type malignancy in metastasis, it may pose diagnostic challenge especially when there is no concomitant GCT component. Detection of i(12p) could help in such situation in the appropriate clinical context. However, the diagnostic value of detecting i(12p) in secondary somatic malignancy after testicular GCT is unclear. We aimed to study the prevalence of i(12p) on various types of somatic malignancies in patients with a history of testicular GCT.

**Design:** We identified 45 patients with documented testicular GCT and had diagnoses of malignancies with non-GCT morphology between 2011 and 2017. Unstained slides were selected for fluorescence in situ hybridization (FISH) of i(12p). The histopathologic findings and clinical history of these 45 cases were evaluated and analyzed. Patient's non-neoplastic tissue acquired during surgery was utilized as control.

**Results:** Our cohort consisted of 45 male patients with diagnosis of testicular GCT at a mean age of 41 yrs (range 20-68 yrs). A second malignancy was diagnosed at a mean age of 59 yrs (range 34-86 yrs) and an average interval of 18 yrs (range 0-57 yrs) after the diagnosis of testicular GCT. 7 of 29 cases (16%) were tested positive for i(12p) including two patients with clinical presentation consistent with somatic transformation of GCT (Case 5 and 6). The clinical histories of these seven patients were summarized in table 1. Non-tumor tissue from two patients were tested as control and both were negative for i(12p).

| Case | Age<br><br>Testicular GCT | Age<br><br>Second malignancy | Diagnosis<br><br>Testicular GCT | Diagnosis<br><br>Second malignancy |
|---|---|---|---|---|
| 1 | 51 | 57 | Regressed GCT | Retroperitoneum, high-grade sarcoma |
| 2 | 31 | 54 | Unknown | Liver, metastatic colorectal adenocarcinoma |
| 3 | 28 | 34 | Seminoma | Gluteal mass, leiomyosarcoma |
| 4 | 39 | 39 | Embryonal+Yolk sac | Pancreas, neuroendocrine tumor |
| 5 | 45 | 62 | Embryonal+Teratoma+Seminoma | Retroperitoneum, carcinoma with glandular features |
| 6 | 39 | 54 | Seminoma | Scapula, sarcomatoid carcinoma |
| 7 | 51 | 56 | Seminoma | Urinary bladder, papillary urothelial carcinoma, high grade |

**Conclusions:** In our cohort, FISH for i(12p) is positive in 16% of patients with somatic malignancy occurred after testicular GCT. Morphologically, these somatic malignancies were identical to those of patients without history of GCT. Although a positive result for i(12p) may support a diagnosis of GCT with somatic transformation in some cases, clinical behavior suggests that some tumors may actually represent a second primary malignancy unrelated to the testicular GCT. Therefore, a positive result for i(12p) should be interpreted with caution and should correlate with clinical presentation.

## 1043 The Composite Grade Group Score of Biopsies is a Better Predictor of Grade Group Score in the Prostate and Overgrades Fewer Prostate Cancers than does the Highest Grade Group Score

Xiaotun Zhang[1], Funda Vakar-Lopez[2], Nicholas Reder[2], Maria Tretiakova[2], Lawrence True[3]
*[1]University of Washington, Bothell, WA, [2]University of Washington, Seattle, WA, [3]University of Washington Medical Center, Seattle, WA*

**Disclosures:** Xiaotun Zhang: None; Funda Vakar-Lopez: None; Nicholas Reder: *Employee*, Lightspeed Microscopy; Maria Tretiakova: None; Lawrence True: None

**Background:** The treatment recommended to patients with prostate cancer (PCa) is largely based on tumor volume and Gleason grade in the diagnostic biopsies. By convention, the highest Gleason score among the biopsy cores is one of the most important decision-making parameters. An assumption of this practice is that the biopsies sample different tumor nodules and that the highest Gleason score represents a distinct "tumor". Consequently, the highest grade tumor is thought to best represent the biologic potential of the cancer. We questioned this assumption, hypothesizing that the composite grade of cancer in spatially adjacent cores would best reflect the grade of cancer in the prostate, and, thus, better represent the biologic potential of the tumor. In this study, we compared the highest Grade Group score (HGG) and Composite Grade Group score (CGG) in biopsies with the final Grade Group score in paired radical prostatectomy specimens (RGG).

**Design:** Four GU pathologists in our institution have provided a Gleason score and Grade Group score for each biopsy and an overall composite Gleason score and Grade Group score over the past 3 years. The CGG considers all Gleason patterns in spatially adjacent biopsies, presuming that they sample the same tumor. We collected data from patients who had prostate biopsies and a subsequent radical prostatectomy (RP) at our institution for 378 sequential RPs. We regarded the RGG as the gold standard Grade Group score.

**Results:** Of 378 patients (age range 41-78 y/o, median 63 y/o), the HGS undergraded 19% of prostate cancers and overgraded 15%. Conversely, the CGG undergraded 21% of prostate cancers and overgraded 9%. Table 1 shows the summary of each Grade Group.

| Grade Group | % HGG under-graded | % CGG under-graded | % HCG over-graded | % CGG over-graded |
|---|---|---|---|---|
| 1 | 60% | 57% | 0% | 0% |
| 2 | 14% | 16% | 0% | 0% |
| 3 | 7% | 14% | 35% | 14% |
| 4 | 11% | 9% | 63% | 55% |
| 5 | 0% | 0% | 38% | 39% |

**Conclusions:** Based on our data we concluded that (1) either method of grading undergrades approximately 20% of prostate cancers, and (2) that the Highest Grade Group score overgrades approximately twice as many cancers as does the Composite Grade Group score. We recommend that the Composite Grade Group score be used as the standard prostate cancer grading method to more accurately predict the grade of cancer in the prostate.

## 1044 BAF53B is Upregulated in Prostatic Carcinoma with Neuroendocrine Phenotype by REST Gene Suppression

Xiaotun Zhang[1], Lisha Brown[2], Mark Labrecque[3], Ilsa Coleman[4], Bryce Lakely[3], Daniel Lin[2], Eva Corey[3], Peter Nelson[3], Lawrence True[2], Colm Morrissey[3]
*[1]University of Washington, Bothell, WA, [2]University of Washington Medical Center, Seattle, WA, [3]University of Washington, Seattle, WA, [4]Fred Hutchinson Cancer Research Center, Seattle, WA*

**Disclosures:** Xiaotun Zhang: None; Lisha Brown: None; Mark Labrecque: None; Ilsa Coleman: None; Bryce Lakely: None; Daniel Lin: None; Eva Corey: None; Peter Nelson: None; Lawrence True: None; Colm Morrissey: None

**Background:** Emerging evidence suggests that neuroendocrine differentiation in prostate cancer (NEPC) frequently arises from castration-resistant prostatic adenocarcinoma (CRPC). However, the mechanism is still under investigation. Our group and others have shown that splicing of the REST transcript by SRRM4 inactivates the REST protein, thereby promoting the neuroendocrine phenotype in CRPC. The loss of REST activity increases REST-repressed messages and could directly regulate BAF53A and BAF53B, components of the SWI/SNF chromatin remodeling complex that governs neuronal gene expression [3]. In this study, our objective was to characterize the role of BAF53B in therapy related NEPC.

**Design:** Expression of chromogranin A (CHGA), synaptophysin (SYP), androgen receptor (AR), NKX3.1, prostate-specific antigen (PSA) and BAF53B was analyzed by immunohistochemical stain (IHC) in 124 CRPC metastases from 34 patients and in 24 LuCaP prostate cancer (PC) patient-derived xenografts (PDX). RNA sequencing (RNAseq) was performed on 98 CRPC metastasis specimens and 24 LuCaP PDXs. REST expression was suppressed by siRNA (siREST) in PC cell lines, and the cells were analyzed by RNAseq.

**Results:** Co-expression of CHGA and SYP in >30% of tumor cells was observed in 18 of 124 metastases (7 patients); 16 of the 18 metastases were AR-/PSA-/NKX3.1-. The rest 2 metastases were AR+/PSA+/NKX3.1+, consistent with the amphicrine phenotype. BAF53B was highly expressed in 13 of the 18 metastases and the remaining 5 sites were negative.

BAF53B was also detected in four metastases (4 patients) where the tumor cells expressed either SYP or CHGA, but not both. Interestingly, 1 metastasis with adenocarcinoma phenotype displayed BAF53B positivity. Correlation coefficient analysis demonstrated a strong association of BAF53B with SYP (0.54) and CHGA (0.67), and a moderate reverse association with AR (-0.29).

RNAseq of NEPC revealed an increased expression of *ACTL6B* gene that encodes the BAF53B protein. The *SRRM4* gene was also upregulated. Additionally, *ACTL6B* expression was increased in PC cell lines after siREST treatment.

**Conclusions:** To our knowledge, this is the first study of *ACTL6B*/BAF53B in prostatic carcinoma. Our data have shown that 1) BAF53B is highly expressed in prostatic cancers with neuroendocrine differentiation; and 2) Suppression of *REST* causes upregulation of BAF53B and neuroendocrine markers. These findings may help to explain the underlying mechanisms driving neuroendocrine differentiation in CRPC.

## 1045 Prediction by a Genomic Classifier of Unfavorable Disease in Low Grade Prostate Cancer

Yani Zhao[1], Fangming Deng[2], Hongying Huang[3], Jonathan Melamed[4], Kyung Park[3], Qinghu Ren[5]
*[1]Forest Hills, NY, [2]New York University Medical Center, New York, NY, [3]NYU Langone Health, New York, NY, [4]NYU, New York, NY, [5]New York University Langone Medical Center, New York, NY*

**Disclosures:** Yani Zhao: None; Fangming Deng: None; Hongying Huang: None; Jonathan Melamed: None; Kyung Park: None; Qinghu Ren: None

**Background:** Low risk prostate cancers are amenable to active surveillance which can reduce harmful overtreatment of indolent disease. However there is great variability of criteria in urological practice for determination of active surveillance candidacy. The quantity of Gleason pattern 4 is an important prognostic parameter and may influence treatment decisions. A genomic classifier, the Oncotype DX Genomic Prostate Score has been used to predict both clinical risk and tumor aggressiveness in patients diagnosed on biopsy with low risk prostate cancer (Grade group (GG) 1 and 2). This study investigated whether Genomic Prostate Score (GPS) can predict unfavorable disease and correlates with percentage of Gleason pattern 4 in low grade prostate cancer.

**Design:** We searched our surgical pathology database for prostate biopsies with Oncotype DX Genomic Prostate Score reports (2016-2019). Oncotype Dx was performed on the single core with worst disease (core with longest tumor and/or maximum percentage of pattern 4). Biopsy results including Gleason Score and length of the tumor and percentage of pattern 4 from the core submitted for Oncotype test were recorded. Follow-up repeat biopsy or prostatectomy, if performed, were also retrieved for review of Gleason Score. Oncotype GPS score and related clinical information were analyzed in the study.

**Results:** 306 prostate biopsy cases with Oncotype DX test report were included in the study. Among these cases, 124 cases were originally diagnosed as GG1 (Gleason Score 3 + 3) and 182 cases were GG2 (3 + 4). The average GPS in GG 2 is significantly higher than GG1 (28.52 ± 11.80 vs 17.88 ± 9.35, $p < 0.0001$). Forty cases in GG1 had follow up repeat biopsy or prostatectomy. Twenty cases were upgraded to GG2. Cases with higher GPS score are more likely to upgrade to GG2 (23.10 ± 10.13 vs 16.55 ± 8.22, $p < 0.05$) in follow up repeat biopsy or prostatectomy. In GG1 group, GPS score correlated with the maximum tumor length and tumor percentage ($p < 0.01$). In GG2, patients with Gleason pattern 4 greater than 30% received higher GPS score than patients with pattern 4 less than 30% ($p < 0.05$). GPS significantly correlated with percentage of Gleason pattern 4 but not length of pattern 4, length of tumor, PSA level or PSA density.

**Conclusions:** In GG1, Oncotype Dx GPS can predict the likelihood of unfavorable disease at follow up repeat biopsy or prostatectomy. In GG2, GPS score correlated with percentage of pattern 4, supporting its role as an auxiliary tool for clinical risk classification.

## 1046 Kidney Involvement by Hematological Neoplasms: Clinico-Radiological and Pathological Spectrum of 27 Cases

Tamara Zudaire[1], Luiz M Nova[1], Irene Fernández[1], Yessica P Rodriguez[1], Rosa Guarch[1], Marta Montes[1], Angel Panizo[1]
*[1]Complejo Hospitalario de Navarra, Pamplona, Navarra, Spain*

**Disclosures:** Tamara Zudaire: None; Luiz M Nova: None; Irene Fernández: None; Yessica P Rodriguez: None; Rosa Guarch: None; Marta Montes: None; Angel Panizo: None

**Background:** Kidney involvement in hematological neoplasms (HN) is a common finding at autopsy. However, most HN have not any clinical or radiological evidence of renal involvement, therefore it is rarely diagnosed. A percutaneous kidney biopsy (PKB) is usually required to detect the infiltration. Very few cases of HN diagnosed by PKB have been reported.

**Design:** We retrospectively analyzed a cohort of patients with HN and biopsy-proven (PKB or nephrectomy) renal infiltration diagnosed in our hospital. Clinico-radiological data were obtained from clinical history. In each case, histological as well as IHC and molecular data were reviewed.

**Results:** We identified 27 patients: 15 male/12 female; median age of 68 yrs. (range: 25-85 yrs.). Only in 6 cases, there was a previous known history of HN. Based on radiological study, 12 cases were suspected as HN, 11 cases as carcinoma (10 renal and 1 urothelial) and 4 as unspecific tumor. CT-scan patterns: solitary lesion (n=16), multiple lesions (n=5), diffuse renal enlargement (n=3), normal (n=2) and renal pelvis thickening (n=1). In 6 cases, the lesions were bilateral. 14 patients had concurrent adenopathy and 6 had hepatosplenomegaly. Histopathologically, 25 cases were mature B-cell non-Hodgkin lymphomas. The remaining cases included 1 acute myeloid leukemia and 1 T-cell lymphoblastic lymphoma. The pathological classification of all 27 HN and their prior radiological diagnosis are summarized in Table 1. Five patients had also a concurrent renal carcinoma. Twenty-five cases, but two (1 case of intravascular lymphoma and 1 case of focal capsular renal infiltration), had a diffuse parenchymal infiltration by the HN. During the staging work-up 15 patients were found to have single or multiple extranodal involvement (bone marrow n=11; bone/soft tissues n=4; lung n=3; CNS n=2; adrenal n=1; uterus n=1). Follow-up was available in 24 patients: 13 died of disease (1-117 mos.; median: 72 mos.), 8 were alive free of disease (7-161 months; median: 72 mos.) and 3 alive in progression (follow-up time 1, 5 and 18 mos).

| **Pathological diagnosis** | **Radiological diagnosis prior to pathological examination** | | **Concomitant** |
|---|---|---|---|
| | Renal carcinoma and other (n=15) | Lymphoma (n=12) | **Renal carcinoma (n=5)** |
| **DLBCL** | 3 | 6 | 0 |
| • **Activated type** | 3 | 2 | 1 Clear-RCC |
| • **Germinal center type** | | | |
| • **T-cell rich** | 1 | 0 | 0 |
| • **Intravascular** | 0 | 1 | 0 |
| **Waldenström Macroglobulinemia** | 1 | 2 | 0 |
| **LLC/SLL** | 1 | 0 | 1 Clear-RCC |
| **Follicular lymphoma** | 2 | 0 | 1 Clear-RCC<br>1 Chromophobe-RCC |
| **MALT lymphoma** | 1 | 0 | 1 Clear-RCC |
| **Burkitt lymphoma** | 1 | 0 | 0 |
| **PTLD** | 0 | 1 | 0 |
| **AML** | 1 | 0 | 0 |
| **T-cell lymphoblastic lymphoma** | 1 | 0 | 0 |

DLBCL: diffuse large B-cell lymphoma; LLC/SLL: chronic lymphocytic leukaemia/small lymphocytic lymphoma; PTLD: post-transplant lymphoproliferative disorder; AML: acute myeloid leukemia; RCC: renal cell carcinoma

Figure 1 - 1046

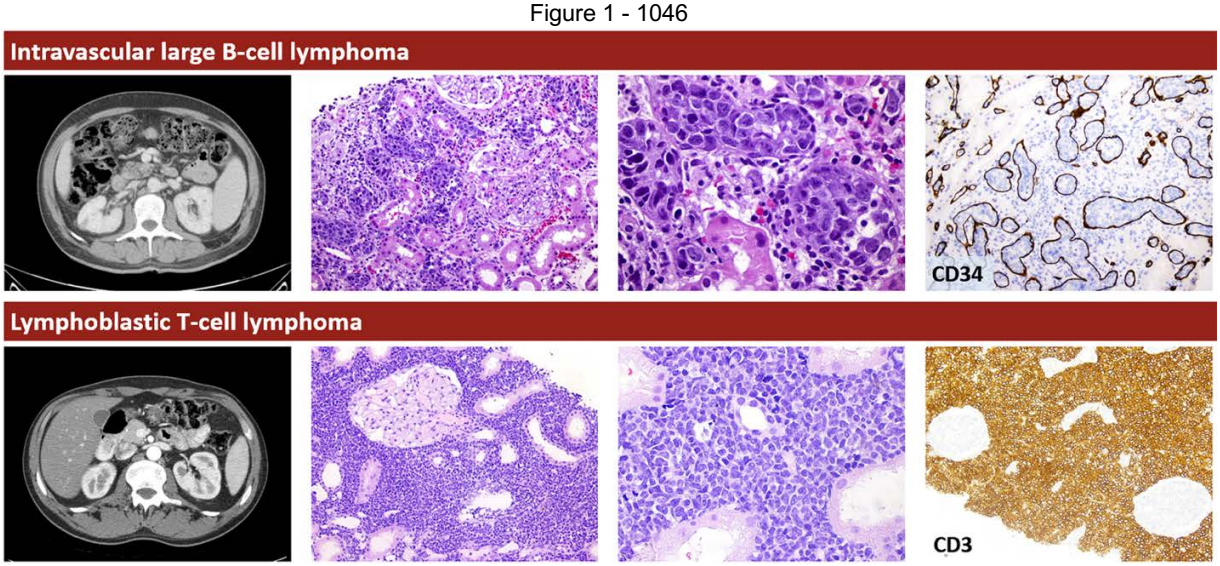

Figure 2 - 1046

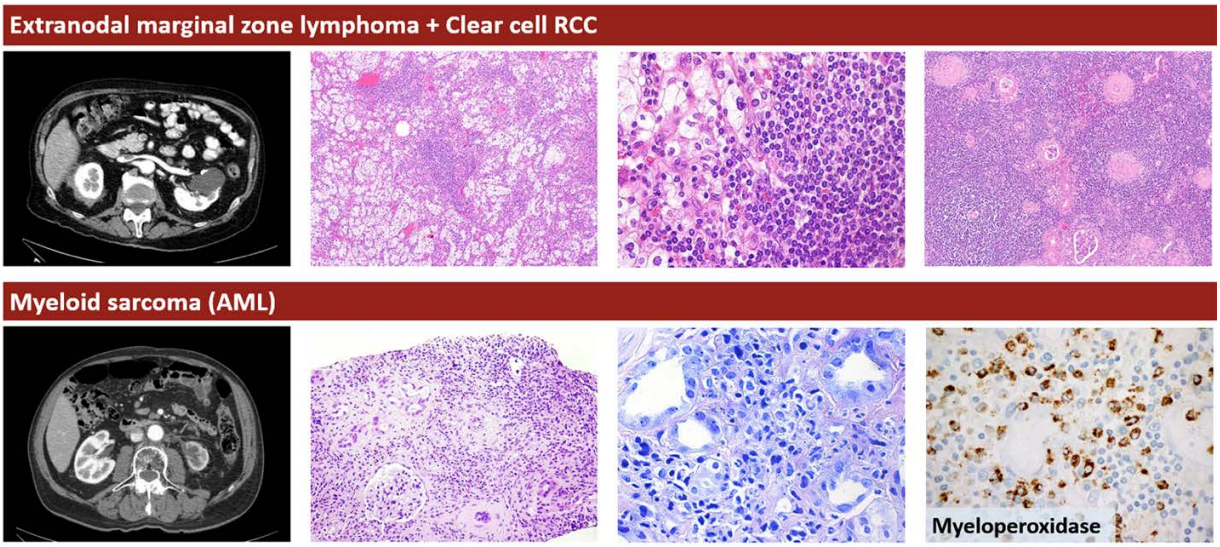


**Conclusions:** Renal involvement by HN usually occurs in disseminated disease and often silent with clinico-radiological findings that lead to an erroneous diagnosis of renal carcinoma. PKB is essential to establish the correct diagnosis in this situation. A definitive diagnosis of renal involvement by HN in limited samples, such as PKB, is possible through correlation of morphology and molecular studies. B-NHL predominated, being DLBCL the most common subtype.